UNIVERSIDADE D
COIMBRA

Lígia Vanessa Rocha Fão

ROLE OF SRC KINASE FAMILY IN HUNTINGTON'S DISEASE - IMPACT ON NEURITES AND MITOCHONDRIA

Tese no âmbito do Programa de Doutoramento em Ciências da Saúde, ramo de Ciências Biomédicas, orientada pela Professora Doutora Ana Cristina Carvalho Rego e co-orientada pela Doutora Sandra Isabel Freitas Mota e pelo Doutor Ramiro Almeida, apresentada à Faculdade de Medicina da Universidade de Coimbra.

Setembro de 2022

Lígia Vanessa Rocha Fão

Role of Src kinase family in Huntington's Disease - impact on neurites and mitochondria

Setembro de 2022

Tese de Doutoramento do Programa de Doutoramento em Ciências da Saúde, ramo de Ciências Biomédicas, orientada pela Professora Doutora Ana Cristina Carvalho Rego e co-orientada pela Doutora Sandra Isabel Freitas Mota e pelo Doutor Ramiro Almeida, apresentada à Faculdade de Medicina da Universidade de Coimbra

The research described in the present thesis was performed at the Center for Neuroscience and Cell Biology, University of Coimbra, Coimbra, Portugal.

Lígia Fão received a PhD fellowship from 'Fundação para a Ciência e Tecnologia' (FCT), Portugal, fellowship reference SFRH/BD/148263/2019. The research work was funded by the European Huntington's Disease Network (EHDN) project, reference 1159, the European Regional Development Fund (ERDF), through Centro 2020 Regional Operational Programme under project CENTRO-01-0145-FEDER-000012-HealthyAging2020, and through the COMPETE 2020 - Operational Programme for Competitiveness and Internationalisation and Portuguese national funds via 'Fundação para a Ciência e a Tecnologia' (FCT), under projects UIDB/04539/2020 and UIDP/04539/2020.

UNIÃO EUROPEIA

Fundo Social Europeu

À minha família, ao meu namorado e aos meus amigos

AGRADECIMENTOS

Escrever este capítulo “por fim”, para além de me permitir agradecer a todas as pessoas importantes que fizeram parte desde longo percurso, permite-me também perceber que chega ao fim mais um ciclo da minha vida, ao qual sou muito grata.

Em primeiro lugar quero agradecer à minha orientadora, Prof. Doutora Ana Cristina Rego, por todas as oportunidades e aprendizagens ao longo de todos estes anos. Agradeço por me ter aceitado no seu laboratório, primeiro como “aluna curiosa que queria descobrir o mundo científico”, depois como aluna oficial de mestrado e por fim como aluna de doutoramento, e por toda a confiança que depositou em mim e no meu trabalho. Sem a professora este doutoramento não teria sido possível.

No seguimento, quero agradecer aos membros do grupo que tiveram uma grande e importante contribuição ao longo destes anos. À Sandra Mota, minha co-orientadora e amiga, que me ensinou tanto, sempre com muita paciência, disponibilidade e abertura. Muito daquilo que eu sei, devo-te a ti, Sandra. À Luana Naia, que sempre me inspirou, ajudou e ensinou, obrigada por todas as ideias brilhantes. À Rita Vilaça, por tanto, que nem cabe aqui. Rita, tu mudaste a minha vida, dentro e fora do laboratório, foste um pilar fundamental nos últimos anos, foste a minha companhia em tempos de “covid” e ainda ficaste amiga para a vida. Foste um dos melhores presentes de Coimbra, sem dúvida! À Patrícia Coelho, por todos os momentos de amizade, de desabafos, de descontração, de partilha, mas também de aprendizagem e de “construção científica”, foi um prazer partilhar estes últimos anos de bancada (e fora dela) contigo. Agradeço ainda à Isabel Dantas, a melhor técnica (que virou amiga) que o CNC já teve. Obrigada pela tua pronta disponibilidade, amizade e bom humor. Obrigada a todas por tanto! Ficarão para sempre no meu coração.

Agradeço aos meus melhores e para sempre amigos. À Sara, à Eduarda e ao Rui. Vocês foram a minha casa, o meu refúgio, o meu pilar, não só ao longo destes 5 anos, mas ao longo dos últimos anos da nossa existência. Sem vocês, nada disto teria piada, e arrisco-me até a dizer, que tudo isto seria difícil de acontecer sem vocês. Obrigada por estarem sempre desse lado, por todos os momentos, por todas as rizadas, por todas as memórias. Eu sei que “como nós” existe pouco por aí, e que grata sou por isso.

Agradeço ao Sergii, o namorado mais paciente e amoroso da história. Obrigada por me permitires partilhar vida contigo e obrigada por acreditares em mim tanto como eu, obrigada por lutares ao meu lado pelos “nossos” sonhos, obrigada por todos os “estás bem?”, obrigada por todos os “tu consegues, não duvido de ti!”, obrigada por todos os abraços, mimos e palavras de compreensão quando a frustração e o cansaço abalaram a minha motivação. Foste mais do que “a mão”, foste a energia, o corpo e alma que me ajudou a evoluir nestes últimos dois anos. Para ti, um “Universo de Obrigadas”, por tudo!

Por fim, agradeço aos meus pais. As pessoas que me permitiram chegar até aqui. Obrigada por todos os valores e ensinamentos que me passaram. Em especial, o maior “obrigada” do mundo é para ti mãe, obrigada por seres um exemplo de mãe, a mesma mãe que eu quero ser para os meus filhos, obrigada por acreditares em mim mais do eu mesma, obrigada por nunca duvidares das minhas escolhas, por confiares nas minhas capacidades e, acima de tudo, por quereres a minha felicidade, quase mais do que queres a tua. Simplesmente, Obrigada!

TABLE OF CONTENTS

LIST OF FIGURES

LIST OF TABLES

In accordance with the terms of the article 8 paragraph 2 of the Portuguese Decree-Law No. 388/70, the author certifies that this thesis includes total or partial results/revisions of the following peer-reviewed publications. In regards to the provisions of the Decree-Law, the author of this PhD thesis declares that intervened in the design and implementation of the experimental work, analysis and interpretation of the data and in the writing of the manuscripts published under the name of **Fão L**.

Originals:

Fão L, Mota SI, Rego AC. c-Src regulates Nrf2 activity through PKCδ after oxidant stimulus. *Biochim Biophys Acta Mol Cell Res*. 2019 Apr;1866(4):686-698. [Epub 2019 Jan 24] doi: 10.1016/j.bbamcr.2019.01.011.

Fão L, Coelho P, Duarte L, Vilaça R, Hayden MR, Mota SI, Rego AC. Restoration of c-Src/Fyn Proteins Rescues Mitochondrial Dysfunction in Huntington's Disease. *Antioxid Redox Signal*. 2022 Aug 5. [Epub ahead of print] doi: 10.1089/ars.2022.0001.

Fão L, Coelho P, Rodrigues R, Rego AC. Restored Fyn levels in Huntington's Disease contributes for enhanced synaptic GluN2B-composed NMDA receptors and CREB activity. (Submitted to *Cells*, Manuscript ID: cells-1925584).

Reviews:

Fão L, Mota SI, Rego AC. Shaping the Nrf2-ARE-related pathways in Alzheimer's and Parkinson's diseases. *Ageing Res Rev.* 2019 Sep;54:100942. [Epub 2019 Aug 12] doi: 10.1016/j.arr.2019.100942.

Fão L, Rego AC. Mitochondrial and Redox-Based Therapeutic Strategies in Huntington's Disease. *Antioxid Redox Signal*. 2021 Mar 10;34(8):650-673. [Epub 2020 Jun 4] doi: 10.1089/ars.2019.8004.

Magalhães JD*, **Fão L*,** Vilaça R*, Cardoso SM, Rego AC. Macroautophagy and

Mitophagy in Neurodegenerative Disorders: Focus on Therapeutic Interventions. *Biomedicines*. 2021 Nov 5;9(11):1625. doi: 10.3390/biomedicines9111625. (*equal contribution)

Moraes BJ*, Coelho P*, **Fão L*,** Ferreira IL, Rego AC. Modified Glutamatergic Postsynapse in Neurodegenerative Disorders. *Neuroscience* 2021 Feb 1;454:116-139. [Epub 2019 Dec 27] doi: 10.1016/j.neuroscience.2019.12.002. (*equal contribution)

LIST OF ABBREVIATIONS

$^{\bullet}$NO - Nitric oxide

$^{\bullet}$OH - Hydroxyl radical

$^{1}O_2$ - Singlet oxygen

3-NP - 3-Nitropropionic acid

8-OHdG - 8-Hydroxy-2'-deoxyguanosine

β-TrCP - β-tTansducin repeat-containing protein

$\Delta\psi$m - Mitochondrial transmembrane potential

aa - aminoacids

AD - Alzheimer's disease

AKAP121 - A-kinase anchor protein 121

AKT - Protein kinase B

ALFY - Autophagy-linked FYVE protein

ANT1 - Adenine nucleotide translocase 1

ARE - Antioxidant Response Element

ATG - Autophagy-related

ATP - Adenosine triphosphate

BDNF - brain-derived neurotrophic factor

BiP - immunoglobulin protein

BTB - bric-a-brac domain

Ca^{2+} - Calcium ion

CAG - Cytosine-Adenine-Guanine

CaMKII - Calcium/calmodulin-dependent protein kinase II

CBP - (CREB)-binding protein

CHD6 - Chromo-ATPase/helicase DNA-binding protein

CMA - Chaperone-mediated autophagy

CNS - Central nervous system

CREB - cAMP response element-binding protein

CTR - C-terminal region

Cul3 - Cullin3

DA – Dopamine

DG - Dentate gyrus

DGR - Kelch domain, by Keap1 protein

DMF – Dimethylfumarate

Drp1 - Dynamin-related protein 1

E1 - Ubiquitin-activating enzyme

E2 - Ubiquitin-conjugating enzyme

E3 - Ubiquitin-ligase

ETC - Electron transport chain

ER – Endoplasmic reticulum

ERK - Extracellular signal-regulated kinase

Fe^{2+} – Iron ion (reduced form)

FEA - Fumaric acid ester

Fis1 - Mitochondrial fission 1

FL - Full-length

FUNDC1 - Fun14 domain-containing protein 1

G6PD - Glucose-6-phosphate dehydrogenase

GABA - Gamma-aminobutyric acid

GCLc - Glutamate-cysteine ligase catalytic subunit

GCLM - Glutamate-cysteine ligase modifier subunit

GLT1 - Glutamate transporter 1

GPe - Globus pallidus, internal segment

GRP75,78 - Glucose-regulated protein 75, 78

GSH-Px - Glutathione peroxidase

GSH-R - Glutathione reductase

GSK-3β - Glycogen synthase kinase-3β

GST - Glutathione S-transferase

H_2O_2 - Hydrogen peroxide

HD - Huntington's disease

HO-1 - Heme oxygenase-1

$HO_2^{\bullet}$ - Hydroperoxyl radical

HOBr - Hypobromous acid

HOCl - Hypochlorous acid

HONOO - Peroxynitrous acid

Hsc70 - Heat shock cognate 70

HTT, Htt – Huntingtin

IGF-1 - Insulin-like growth factor 1

IP3R - Inositol-1,4,5-trisphosphate (IP3) receptor

IVR - Intervening region

K – Lysine

K^+ - Potassium ion

kb - Kilobase

Keap1 - Kelch-like ECH-associated protein 1

KI - Knock-in

KO – Knockout

LAMP2A - Lysosomal-associated membrane protein 2A receptor

LC3 - Microtubule-associated protein 1A/1B-light chain 3

LTD - Long-term depression

LTP - Long-term potentiation

Maf - Musculoaponeurotic fibrosarcoma

MAMs - Mitochondria-associated membranes

MAPK - Mitogen-activated protein kinase cascades

MCU - Mitochondrial calcium uniporter

Mff - Mitochondrial fission factor

Mfn - Mitofusin(s)

Mg^{2+} - Magnesium ion

mHTT, mHtt - Mutant huntingtin

MOM - Mitochondrial outer membrane

MRI - Magnetic resonance imaging

MSNs - Medium spiny neurons

mtDNA – Mitochondrial DNA

mTORC1 - Mammalian target of rapamycin complex 1

Na^+ - Sodium ion

ND2 - NADH dehydrogenase subunit

NDD - Neurodegenerative disorders

Neh - Nrf2-ECH homology

NES - Nuclear export signal

NF-κB - Nuclear factor kappa B

NMDAR - *N*-methyl-D-aspartate receptor(s)

NOX - NADPH oxidase

NQO1 - NAD(P)H:quinone dehydrogenase 1

NTR - N-terminal region

Nrf2 - Nuclear factor erythroid 2-related factor 2

$O_2^{\bullet-}$ - Superoxide anion

O_3 – Ozone

ONOO- - Peroxynitrite

OPA1 - Optic atrophy 1

OPTN - Optineurin

OXPHOS - Oxidative phosphorylation

p90RSK - p90 Ribosomal S6 kinase

PARL - Presenilin-associated rhomboid-like

PKA - Protein kinase A

PD - Parkinson's disease

PDGF - Platelet-derived growth factor

PDR - Proline-rich domain

PI3K -Pphosphatidylinositol-3-kinase

PINK1 - PTEN-induced kinase 1

PGC-1α - Peroxisome proliferator-activated receptor (PPAR)γ coactivator 1α

PKC - Protein kinase C

PolyQ - Polyglutamine

PSD - Post-synaptic density

PTP - Permeability transition pore

PTP1B - Protein-tyrosine phosphatase 1B

PTPN - Protein tyrosine phosphatase non-receptor

Q – Glutamine

RARα - Retinoic acid receptor α

RNS - Reactive nitrogen species

$RO_2^{\bullet}$ - Peroxyl radical

ROS - Reactive oxygen species

S – Serine

SQSTM1 - Sequestosome 1 (p62)

Sig-1R - Sigma-1 receptor

SHP-2 - Homology 2 domain-containing tyrosine phosphatase-2

SFN - Sulforaphane

SKF - Src kinase family

SN - *Substantia nigra*

SNpc - *Substantia nigra pars compacta*

SNpr - *Ssubstantia nigra pars reticulata*

SOD1,2,3 - Superoxide dismutase(s) 1,2,3

STEP - Striatal-enriched protein tyrosine phosphatase

STN - Subthalamic nucleus

SULFs – Sulfotransferases

Tfam - Mitochondrial transcription factor A

TIM23 - Translocase of the mitochondrial inner membrane 23

TMRM - Tetramethylrhodamine methyl ester

TR - Thioredoxin reductase

UGDH - UDP-glucose dehydrogenase

UHDRS - Unified Huntington's Disease Rating Scale

ULK1 - Autophagy activating kinase 1

UPS - Ubiquitin-proteasome system

VDAC1 - Voltage-dependent anion channel isoform 1

vs - Versus

WT – Wild-type

YAC - Yeast artificial chromosome

SUMMARY

Huntington's Disease (HD) is an autosomal-dominant neurodegenerative disorder with no cure or effective therapies. The disease is caused by the extension of cytosine-adenine-guanine (CAG) repeats at the exon 1 of the huntingtin (*HTT*) gene. Mutant HTT (mHTT), the main HD proteinaceous hallmark, participates in reactive oxygen species (ROS) formation, reduced antioxidant proteins, altered protein degradation pathways, mitochondrial dysfunction and modified *N*-methyl-D-aspartate receptors (NMDAR) activity. Importantly, two members of the Src Kinase Family (SKF), c-Src and Fyn, are activated by ROS, modulate pathways involved in antioxidant defense, have important roles in mitochondrial normal function and regulate NMDARs activity and localization. However, c-Src/Fyn involvement in HD is largely unexplored. In the present work, we investigate the involvement of SKF proteins in HD ethiopatogenesis in human and mouse models, as well as its possible involvement on redox changes, mitochondrial function and NMDAR postsynaptic density (PSD) location and related signaling.

Previous studies in HD striatal cells showed increased ROS levels and reduced nuclear factor erythroid 2-related factor 2 (Nrf2) protein levels despite increased phosphorylation/activation, being Nrf2 the main transcription factor involved in the expression of cell defense enzymes. Thus, in **Chapter 3** we report increased Nrf2 phosphorylation at Ser40 along with enhanced SKF levels and phosphorylation/activation at Tyr416 following acute exposure of HT22 neural cells to hydrogen peroxide (H_2O_2). Cytosolic Nrf2 activation is modulated through phosphorylation by PKCδ, an enzyme controlled by SKF. Of relevance, Nrf2 phosphorylation at Ser40, its nuclear accumulation and transcriptional activity involving expression of heme oxygenase-1 (HO-1) are shown to be dependent on SKF activation. Moreover, modulation of Nrf2 activity by c-Src occurs through protein kinase C (PKC)δ phosphorylation at Tyr311. We demonstrate SKF-mediated regulation of Nrf2 transcriptional activity, via PKCδ activation, following an acute H_2O_2 stimulus. These data demonstrate the role of SKF, namely c-Src,

in controlling Nrf2 activity and transcriptional activity under cellular oxidant conditions, common to several neurodegenerative disorders, as in HD. Thus, further studies were conducted to investigate SKF involvement in HD pathogenesis.

In **Chapter 4**, we clearly show that c-Src and Fyn proteins are reduced in HD models, including *postmortem* human brain caudate, YAC128 mouse brain striatum and cortex at early stages, YAC128 striatal neurons and Q111/ ST*Hdh*^{Q111} striatal cell lines. Reduced c-Src and Fyn protein levels in HD result from augmented degradation through autophagy in Q111 cells, and is accompanied by a decrease in c-Src/Fyn active form(s). Moreover, decreased Fyn mitochondrial co-localization correlates with HD-related mitochondrial dysfunction and altered morphology, and increased levels of reactive/oxidant species. Importantly, expression of constitutive active c-Src/Fyn aimed to restore active SKF levels improves mitochondrial morphology and function, namely through improved mitochondrial transmembrane potential, mitochondrial basal respiration and ATP production, but does not affect mitophagy. Additionally, constitutive active c-Src/Fyn expression diminishes the levels of reactive species in HD cells and reduces the number of apoptotic cells through reduced levels of active caspase-3.

Since SKF have important roles in the modulation of NMDARs activity and localization, we next analyzed the impact of HD-mediated altered SKF levels on synaptic and extrasynaptic NMDARs (**Chapter 5**). Therefore, we explore the impact of HD-mediated altered Fyn levels at post-synaptic density (PSD), and its role in distorted NMDARs function and localization, as well as in intracellular neuroprotective pathways in YAC128 mouse striatal neurons. We show that reduced synaptic Fyn levels and activity in HD striatal neurons is related with decreased phosphorylation of synaptic GluN2B-composed NMDARs; this occurs concomitantly with augmented extrasynaptic NMDARs activity and currents and reduced cAMP response element-binding protein (CREB) activation, along with induction of cell death pathways. Importantly, expression of the constitutive active form of SKF reestablishes NMDARs localization, phosphorylation and function at PSD in YAC128 mouse neurons. Enhanced SKF levels and activity also promotes CREB activation and reduces caspase-3 activation in YAC128 mouse striatal neurons.

Overall, this work provides important insights about c-Src/Fyn kinases involvement in regulating the transcription factor Nrf2 and in HD pathogenesis, namely by controlling mitochondrial function and NMDARs activity, and potentially influencing disease progression. Based on these findings, this thesis provides support for SKF as possible novel HD therapeutical targets.

Keywords: Src, Fyn, mitochondria, NMDA receptors, Huntington's disease

RESUMO

A doença de Huntington (HD, do inglês 'Huntington's disease') é uma doença neurodegenerativa autossómica dominante, sem cura ou terapias eficazes. A doença é causada pela extensão de repetições do trinucleótido citosina-adenina-guanina (CAG) no exão 1 do gene da huntingtina (*HTT*). A expressão de HTT mutante (mHTT), a principal alteração proteica na DH, influencia a formação de espécies reativas de oxigénio (ROS, do inglês 'reactive oxygen species'), os níveis de antioxidantes, e altera as vias de degradação proteica, a atividade mitocondrial e a atividade e localização dos recetores *N*-metil-D-aspartato (NMDAR, do inglês "*N*-methyl-D-aspartate receptors"). De forma interessante, dois membros da família das proteínas Src cinase (SKF, do inglês "Src family kinases"), c-Src e Fyn, são ativados por ROS, modulam vias envolvidas na defesa antioxidante, possuem papéis importantes na função mitocondrial e regulam a atividade e localização dos NMDARs. No entanto, o envolvimento de c-Src/Fyn na HD não se encontra suficientemente explorado. No presente trabalho, investigámos o envolvimento das proteínas SKF na patogénese da HD em modelos humanos e de murganho, bem como o seu possível envolvimento em alterações redox, função mitocondrial e sinalização relacionada com a ativação dos NMDAR na HD.

Estudos prévios, do nosso grupo de investigação, mostraram que células estriatais da HD apresentam um aumento dos níveis de ROS e uma diminuição dos níveis proteicos de Nrf2 (do inglês "nuclear factor erythroid 2-related factor 2"), apesar de um aumento da sua fosforilação/ativação, sendo Nrf2 o principal fator de transcrição envolvido na expressão de enzimas de defesa celular. Assim, no **Capítulo 3** desta tese mostramos um aumento da fosforilação de Nrf2 no resíduo Ser40 e a fosforilação/ativação da SKF no resíduo Tyr416 após exposição aguda de células neurais HT22 a peróxido de hidrogénio (H_2O_2). Mostramos ainda que a ativação citosólica do Nrf2 é modulada através da fosforilação por PKCδ (do inglês "protein kinase C"), uma enzima controlada por SKF. De forma relevante, a fosforilação do Nrf2 no resíduo Ser40, assim como

a sua migração para o núcleo e atividade transcricional envolvendo a expressão da heme oxigenase-1 (HO-1) são dependentes da ativação da SKF. Para além disso, a modulação da atividade de Nrf2 pela c-Src ocorre através da fosforilação de PKCδ no resíduo Tyr311. Assim, neste capítulo demonstramos que a regulação da atividade transcricional de Nrf2, via ativação de PKC, é mediada pela SKF, após um estímulo agudo de H_2O_2. Estes resultados indicam um papel de SKF, nomeadamente da c-Src, no controlo da atividade transcricional de Nrf2 em condições de oxidação celular, comuns a diversas doenças neurodegenerativas, tais como a HD. Assim, os estudos subsequentes foram conduzidos de forma a investigar o envolvimento da SKF na patogénese da HD.

No **Capítulo 4** demonstramos claramente que os níveis das proteínas c-Src e Fyn se encontram reduzidos em diferentes modelos de HD, nomeadamente no núcleo caudado obtido de cérebro humano *postmortem*, estriado e córtex cerebral do murganho YAC128 em estádios iniciais, neurónios estriatais YAC128 e linhas de células estriatais Q111/ ST*Hdh*^{Q111}. Os resultados mostraram que a diminuição dos níveis das proteínas c-Src e Fyn era acompanhada por uma diminuição da sua forma ativa, e resultava de um aumento da sua degradação por autofagia. A co-localização diminuída da Fyn com a mitocôndria correlacionou-se com a disfunção mitocondrial, morfologia alterada, e níveis aumentados de espécies reativas/oxidantes em diferentes modelos da HD. De forma importante, a expressão de SKF constitutivamente ativa, com o objetivo de restaurar os níveis ativos de SKF, melhorou a morfologia e a função mitocondrial, nomeadamente através de um aumento do potencial transmembranar mitocondrial, da respiração basal mitocondrial e produção de ATP, sem alterar a mitofagia. Além disso, a expressão ativa da SKF diminuiu os níveis de ROS em células que expressam mHtt e reduziu o número de células apoptóticas, associado a uma diminuição dos níveis de caspase-3 ativa.

Uma vez que a SKF apresenta um papel importante na modulação da atividade e localização dos NMDARs, analisámos ainda o impacto dos níveis alterados da SKF, no contexto da HD, nos níveis sinápticos e extrassinápticos dos NMDARs (**Capítulo 5**). No presente estudo, explorámos o impacto dos níveis de Fyn na densidade pós-sináptica (PSD), e o seu papel na função e localização dos NMDARs, assim como a ativação de vias neuroprotetoras intracelulares, em neurónios estriatais obtidos do murganho YAC128. Assim,

neste capítulo da tese mostramos que os níveis sinápticos reduzidos de Fyn estão relacionados com a diminuição da fosforilação dos NMDARs sinápticos, que contêm a subunidade GluN2B. Concomitantemente, a atividade e correntes dos NMDARs extrassinápticos aumentou, à qual se associou uma diminuição da ativação de CREB (do inglês “cAMP response element-binding protein”) e a indução de vias de morte celular. A expressão da forma constitutivamente ativa da SKF restabeleceu a localização, fosforilação e função de NMDARs na PSD em neurónios do murganho YAC128. A reposição dos níveis ativados da SKF promoveu ainda a ativação do CREB e reduziu a ativação de caspase-3.

De uma forma geral, este trabalho fornece informação importante sobre o envolvimento das cinases c-Src/Fyn na regulação do fator de transcrição Nrf2 e na patogénese da HD, através do controlo da função mitocondrial e atividade de NMDARs na HD, potencialmente influenciando a progressão da doença. Desta forma as SKF poderão constituirnovos alvos terapêuticos para a HD.

Palavras-chave: Src, Fyn, mitocôndria, recetores NMDA, doença de Huntington.

CHAPTER I

STATE OF THE ART

1.1. HUNTINGTON'S DISEASE

1.1.1. AN OVERVIEW AND GENETIC BACKGROUND

George Huntington was the first clinician to accurately describe the main clinical features of a familial-based disorder that is nowadays named Huntington's disease (HD). At the age of 21, George Huntington published in *Medical and Surgical Reporter of Philadelphia* (1872) the main clinical aspects of a hereditary chorea, a motor symptom characterized by abnormal and involuntary "dance-like" movements. Although the disease had already been noted since the seventeen century by other physicians, including his father and grandfather, this first detailed publication allowed to distinguish this hereditary chorea from other forms of chorea. After this description, the disease was named Huntington's Chorea, and later as HD since not all patients develop chorea, while other movement disturbances as well as cognitive and behavioral symptoms are also present (Lanska, 2000).

HD is an autosomal dominant progressive neurodegenerative disorder caused by the extension of cytosine-adenine-guanine (CAG) repeats at the exon 1 of the huntingtin (*HTT*) gene, located in the short arm of chromosome 4 (4p16.3). The unstable CAG trinucleotide expansion encodes for a polyglutamine (polyQ) tract at the N-terminus of mutant huntingtin (mHTT in humans; mHtt in non-human animals) that makes it prone to misfold and aggregate (Ayala-Peña, 2013). This polyQ expansion leads to conformational changes and abnormal cytoplasmic (mainly perinuclear) and nuclear accumulation of mHTT (Scherzinger et al., 1997). Healthy individuals, or general population, have approximately 16 to 25 CAG repeats in the *HTT* gene, whereas 40–50 CAG repeats cause the adult-onset form, with motor symptoms manifesting in the third or fourth decade of life; more than 60 CAG repeats cause juvenile-onset HD, with initial symptoms starting before 20 years of age (MacDonald et al., 1993). Thirty-six to 39 CAG repeats correspond to a range of HD alleles with reduced penetrance and since they are meiotically unstable, individuals may manifest the disease at older age (e.g. at 60 years of age or older), presenting only mild

chorea, and without the cognitive, psychiatric and behavioral abnormalities usually associated with longer repeat tracts, or even showing no clinical or neuropathological HD phenotypes (Langbehn et al., 2004). Chorea is not a major manifestation of juvenile-onset HD, whereas rigidity and seizures are the predominant characteristics of this HD form, occurring after abnormal behavior (Nance and Myers, 2001). Genetic anticipation can explain the occurrence of this highly polymorphic genotype since CAG length is instable due to intergenerational transmission (Ranen et al., 1995). This phenomenon explains the risk of transmitting the disease to offsprings, from individuals with no symptoms, who have CAG repeats ranging from 27 to 39; indeed, about 10-15% of all HD cases appear in individuals with non-affected parents whose repeat length fall within this normal borderline range (Semaka et al., 2009). During transmission, the expanded repeat is only mildly altered by one or a few CAG repeats, eventually decreasing if transmitted maternally, and increasing if transmitted paternally (Bates et al., 1997). Some studies indicate that 27 to 35 range of CAG repeats can be meiotically unstable during paternal transmission, leading to descendants with HD and carrying CAG expansions of 40 or more repeats (Myers, 2004). Therefore, juvenile-onset HD is usually associated with paternal transmission in the majority of the cases. Until now, the longest CAG expansion reported is 250 CAG repeats, interestingly of probable maternal inheritance (Nance et al., 1999).

The size of CAG trinucleotide expansion is the major determinant and inversely correlates with the age of clinical onset, further leading to an increased disease severity (Ayala-Peña, 2013; Kumar et al., 2010). Although the influence of CAG repeats length on rate of disease progression is not the strongest factor, it is still significant (Rosenblatt et al., 2012). Of relevance, a CAG repeat expansion in a second allele does not seem to have an effect on the age of motor onset, which reflects the dominant effect of a single mutant allele, and shows that HD pathogenesis is not HTT dosage-dependent (Lee et al., 2015). Moreover, the CAG repeat length cannot explain the total variance of the age at onset; indeed, a large set of genes in the chromosomal region of HTT harbor variations, which can alter disease onset and progression (Farrer et al., 1993; Lee et al., 2012; Lee et al., 2015). Additionally, motor, cognitive and other symptoms found in HD can be modulated by environmental factors (Mo et al., 2015).

HD affects 5 to 10 per 100,000 individuals in North America and Europe (Bates et al., 2015). In Europe, there is an evident heterogeneity with ranges from 0.53 per 100,000 in Finland (Palo et al., 1987) to 10.85 per 100,000 in Italy (Squitieri et al., 2016) and 12.3 per 100,000 in United Kingdom (Evans et al., 2013). In 2016, Kay and colleagues concluded that HD alleles with a CAG repeat in the 36 to 38 range occur at high frequency in general population with approximately 1 in 400 individuals (Kay et al., 2016). Moreover, European descents, with high prevalence of the disease, have a higher average of CAG repeat length, when compared to East Asian and African populations (Morrison, 2012).

1.1.2. AFFECTED CIRCUITS AND NEUROPATHOLOGICAL FEATURES

HD pathology has been witnessed in peripheral tissues (van der Burg et al., 2009), like other polyQ disorders, however HD is predominantly a central nervous system (CNS) disorder, characterized, most of all, by cell loss and atrophy (Sathasivam et al., 1999). Several evidences from neuropathological and imaging studies show that HD brain abnormalities appear before evident symptoms and they can be progressive, resulting in about 25% brain weight loss in advanced HD (Halliday et al., 1998). In this way, gradual and prominent cell loss and atrophy of the neostriatum (caudate nucleus, mainly, and also putamen), in basal ganglia, followed by astrogliosis, is the main pathological hallmark of HD (Sieradzan and Mann, 2001).

The synchronized action of several cortical and subcortical brain structures, namely the spinal cord, brainstem, basal ganglia, and cerebellum, are responsible for movement coordination under normal conditions (Ferreira-Pinto et al., 2018). Specifically, the basal ganglia is composed by a group of subcortical nuclei, that together with the primary motor cortex and the thalamus, form the motor circuit responsible for the control of voluntary movement. The basal ganglia includes the striatum (caudate and putamen), internal globus pallidus (GPi) and external globus pallidus (GPe), *substantia nigra* (SN) *pars reticulata* (SNpr) and *compacta* (SNpc), and subthalamic nucleus (STN) (Calabresi et al., 2014; Obeso

et al., 2008). The striatum is made up mostly by medium spiny neurons (MSNs, ~95%), a type of gamma-aminobutyric acid (GABA)ergic neurons (Dubé et al., 1988), but also by cholinergic and GABAergic interneurons (Lapper and Bolam, 1992). MSNs contain GABA and express either enkephalin or substance P as co-transmitters and are innervated by excitatory glutamatergic inputs from the cortex (mainly) and thalamus, together with dopaminergic inputs from the SN and cholinergic or GABAergic inputs from striatal interneurons (Pickel et al., 1992). MSNs can participate in the two motor circuits, the direct or indirect pathways, due to their differentially expression of dopamine (DA) D1 or D2 receptors. In the direct pathway, the striatum, GPi, SNpr, thalamus, and motor cortex, promote the movement activation due to the inhibition of the GPi and consequent thalamus disinhibition. In the indirect pathway, the striatum, GPe, STN, SNpr, thalamus, and motor cortex activate the STN and inhibit the thalamus to favor movement inhibition (Calabresi et al., 2014) **(Figure 1.1).**

HD striatal pathology in both caudate and putamen is more prominent in the dorsal and rostral regions, which are more affected than the ventral one, in early disease, and further, striatal degeneration occurs in a dorsomedial to ventrolateral direction, since the tail of the caudate nucleus initially shows more degeneration than the body and head or the ventral putamen (Vonsattel, 2008; Vonsattel and DiFiglia, 1998). Interestingly, this caudate atrophy is related with CAG repeats and with a worsening of the Unified Huntington's Disease Rating Scale (UHDRS) motor score, as detected by magnetic resonance imaging (MRI) or computed tomography (Culjkovic et al., 1999; Jech et al., 2007). In this way, in HD early stages, the balance between the direct and indirect pathways is affected, leading to motor dysfunction. In both early symptomatic and presymptomatic stages, MSNs enkephalin-containing (and D2 receptor-expressing) neurons projecting to the GPe, of the indirect pathway, appear to be affected before the MSNs of the direct pathway, inducing a reduced release of GABA from caudate/putamen to GPe and consequently, a decrease in the inhibition of GPe neurons that also express GABA, leading to more GABA release to STN and GPi. In turn, glutamatergic STN neurons projecting to GPi/SNr release less glutamate, becoming hypofunctional, which causes the loss of inhibitory activity of the GPi/SNpr over thalamic neurons that project to the cortex. Ultimately, this leads to an increase in excitatory stimulation in the cortex,

resulting in the appearance of choreic-like or exacerbated movements (Vonsattel, 2008). Additionally, in the later stages, additional loss of striatal neurons projecting to the GPi, of the direct pathway, may occur. A decrease in the release of GABA into GPi/SNpr results in increased inhibition of thalamus and consequently decrease cortex stimulation and uncontrolled movements (Albin et al., 1990) **(Figure 1.1).**

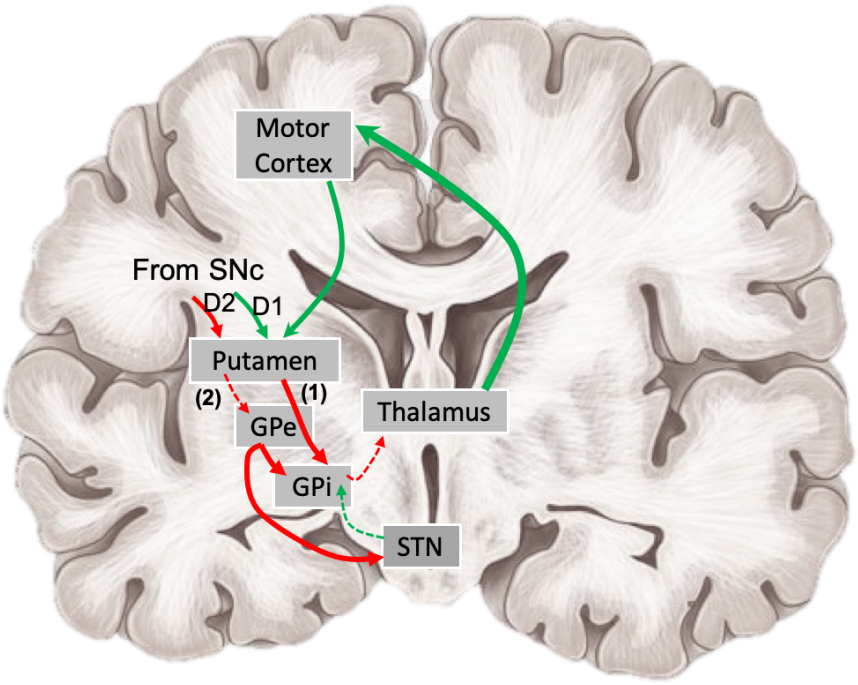

Figure 1.1 | Schematic representation of basal ganglia circuitries in human brain coronal sections. The inhibitory striatal indirect pathway (2) suffers a preferential degeneration, which leads to altered stimulation of the direct pathway (1) and changed thalamo-cortical inputs, resulting in excessive movement generation. Succinctly, the communication between putamen and GPe is altered, reducing GABA release, which increases the inhibition into STN from GPi, reducing the excitation from the STN to GPi. Since GPi has decreased excitatory inputs, the thalamus is less inhibited, resulting in augmented excitation in cortical receiving areas. Excitatory outputs are represented in green, while the inhibitory outputs are represented in red.

Aylward and coworkers revealed that caudate shrinkage is significant 10 years before estimated disease onset, whereas putamen and globus pallidus shrinkage is not significant until 3 years from estimated disease onset (Aylward et al., 1996). Indeed, caudate is highly affected in HD, and although cerebral cortex alterationsss may not be uniform in HD, marked neuronal loss and shrinkage is also seen in deep layers of the cerebral cortex. Other regions,

including globus pallidus, hippocampus, amygdala, thalamus, subthalamic nucleus, *substantia nigra*, and cerebellum, show varying degrees of atrophy and neuronal loss, which depends on disease stage (Rosas et al., 2003). In accordance with that, late in disease, volumetric losses are observed in cortex (20%), cerebral white matter (30%), striatum (60%), globus pallidus (55%), and thalamus (30%) (De La Monte et al., 1988; Heinsen et al., 1994). The severity of HD degeneration can be classified in five grades (0–4), nominated in ascending order of severity, base in a large number of post-mortem tissues and classifies HD cases (Vonsattel et al., 1985). Grade 0, also termed presymptomatic, comprises less than 1% of all HD brains and despite its appearance it is indistinguishable from normal brains at first examination, while histological examination shows 30–40% neuronal loss in caudate nucleus head. Grade 1 comprises 4% of all HD brains. In this stage neuronal loss appears in caudate nucleus tail and body, and dorsal portion of putamen. While caudate nucleus head already shows 50% or greater loss of neurons. Grade 2 comprises 16% of HD cases. In this stage, the ventricular profile of the caudate remains convex, but less than in normal brain, and striatal atrophy is present. The lateral half of the striatum shows relative preservation in both grades 1-2. Grade 3 comprises 53% of HD cases and displays severe striatal atrophy, and the ventricular profile of the caudate is flat. In grade 4, 95% caudate neurons are loss and the striatum presents severely atrophic; at this stage the ventricular surface of the caudate is concave (Vonsattel et al., 1985, 2011). The degree of striatal atrophy is also correlated with the degeneration of other brain structures. In grades 1 and 2 nonstriatal structures are generally preserved or can show a slight atrophy, while in grades 3 and 4, the other structures that comprise the basal ganglia, cerebral cortex, cerebellum and white matter can be markedly affected (Vonsattel et al., 1985, 2011).

1.1.3. SYMPTOMS AND NEUROPATHOLOGICAL MANIFESTATIONS

In the majority of HD cases, symptoms onset occurs between 30-50 years of age. Each HD patient is clinically unique, however chorea is the most prevalent and manifested symptom in HD (Berardelli et al., 1999). Chorea is characterized by abnormal and involuntary rapid “dance-like” movements of hands and/or feet with an extension to other parts of the body along disease progression. Involuntary movements are an early manifestation of the disease and they can occur in the face, fingers, feet or thorax, or they can manifest as abnormal fast movements of the eyes (saccades) (Berardelli et al., 1999), the latter also occurring in spinocerebellar ataxias. Moreover, additional “motor impairment” is described in HD patients, which consists of voluntary movement deficits, including incoordination, orofacial dyskinesia, bradykinesia, motor sequencing difficulties and apraxia (Ross et al., 2014a).

In adult-onset HD, patients show a progressive deterioration of motor and cognitive function that follows three well-defined stages spread over 15–20 years after diagnosis (Harris et al., 2019). The initial stage starts before the appearance of prominent motor alterations, and is characterized by psychiatric symptoms that include apathy, irritability, depression, and other mood alterations (Julien et al., 2007; Thompson et al., 2012). Indeed, cognitive impairments emerge years before HD diagnosis and the progression is gradual, later evolving to dementia; it can include affected learning and memory, motor planning and working memory. Patients with HD can present problems in sustained attention and retrieval of established memory rather than formation of new memories, being generally classified as subcortical dementia syndrome (Ross et al., 2014b). Additionally, slight motor abnormalities, such as motor tics and jerky voluntary movements, can also be present (Beste et al., 2009). The second stage is characterized by a dramatic increase in involuntary movements, which become generalized, abrupt, and uncontrolled. With choreic movements becoming more prominent, daily activities such as walking, eating, speaking, and swallowing start to deteriorate. In some cases, bradykinesia may coexist with choreic movements (Thompson et al., 1988). In this second stage another hallmark that can occur is the loss of body weight, despite efforts to maintain a high caloric diet (Marder et

al., 2009). In fact, a well-recognized statement in HD patients is the relatively severe muscle wasting and progressive inability to maintain body weight (Hamilton, 2004). In general, health progressively deteriorates by the third stage, which typically occurs 10–15 years after diagnosis, and cognitive capacities progressively decline and finally culminate in dementia. In this final stage, choreic movements are replaced by bradykinesia and rigidity (Julien et al., 2007; Thompson et al., 2012). Death becomes imminent, and the most common causes are pneumonia and heart disease.

1.1.4. HUNTINGTIN PROTEIN

The *HTT* gene encodes a polymorphic stretch of glutamines (Q) at the N-terminal of a soluble and high molecular weight protein, huntingtin (HTT), with approximately 3144 amino acids (~348 kDa), which has no similar sequence with other proteins (Faber et al., 1998).

The broadly studied N-terminal region of HTT is preceded by 17 amino acids and followed by a proline-rich domain (PRD). Both the polyQ stretch and the PRD are polymorphic in the human population. This N-terminal 17 amino acids consists of an amphipathic α-helix (Atwal et al., 2007), which structure is important for retention in the endoplasmic reticulum (Atwal et al., 2007; Rockabrand et al., 2007). It further functions as a nuclear export signal (NES) and it may undergo post-translational modifications, which includes phosphorylation, acetylation, palmitoylation, ubiquitylation, and sumoylation. (Atwal et al., 2007; Maiuri et al., 2013). Under normal conditions, HTT ubiquitination at lysines 6, 9, and 15 and phosphorylation at serines 13 and 16, are important for HTT clearance and its subcellular localization. However, post-translational modifications have been mostly studied in the context of the mutant polyQ HTT. S434 or S536 phosphorylation of mHTT reduces HTT proteolysis by caspase 3 and calpain, respectively, and decreases polyQ-HTT toxicity (Schilling et al., 2006). mHHT can be acetylated, which is important for its clearance by the autophagic-lysosomal pathway, however wild-type HTT is comparatively less acetylated (Jeong et al., 2009). Indeed, it is still unknown if these mechanisms

are relevant for the regulation of normal HTT functions. In this way, both S13 and S16 phosphorylation promotes wild-type and mutant HTT clearance, thus reducing toxicity (Thompson et al., 2009). Phosphorylation at S13 and S16 is important for mediating HTT nuclear localization (Maiuri et al., 2013). Additionally, HTT phosphorylation/dephosphorylation at S421 and S1181/S1201 regulate microtubule-dependent intracellular organelles transport, and HTT phosphorylation at S1181/S1201 increases both anterograde and retrograde transport, whereas S421 phosphorylation selectively promotes in anterograde direction (Ben M'Barek et al., 2013; Colin et al., 2008; Humbert et al., 2002) **(Figure 1.2).**

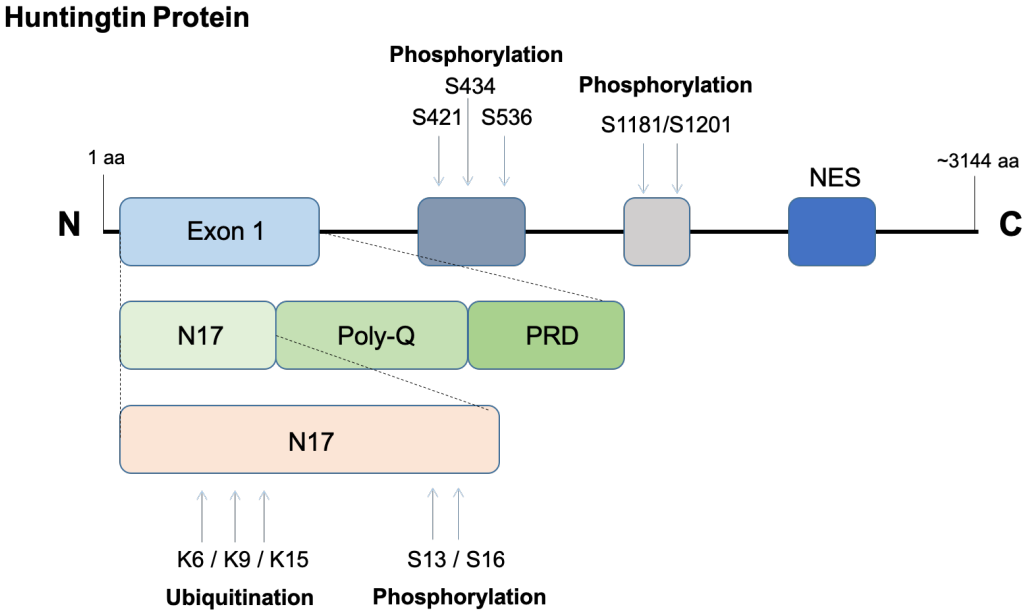

Figure 1.2 | Schematic representation of Huntingtin protein. Huntingtin is a large protein with composed by ~3144 aminoacids (aa) and a few known domains with various sites of post-translational modifications, as described. Huntingtin contains a Exon 1 with a N17 domain, a polyQ and a Proline-rich domain (PDR) domains repeats. At the N17 domain ubiquitination can occur at lysines K6, K9 and K15, and phosphorylation at serines S13 and S16. The polyQ region can include 10 to 35Q in normal individuals, between 36 and 39Q, individuals may not develop symptoms but are at risk to develop HD and above 39Q, individuals develop HD symptoms and the disease manifestation occurs.

HTT protein can be found at different levels throughout most human and murine tissues and it is ubiquitously expressed, not only in the brain but also in peripheral tissues (Marques Sousa and Humbert, 2013). Although, HTT expression is higher in the nervous system than in other tissues, human HTT

transcripts are not restricted to the brain regions that degenerate in cases of HD, since HTT can be found in several types of striatal projection neurons and interneurons, as well as in the cortex, hippocampus, and cerebellum (Marques Sousa and Humbert, 2013). Expression of HTT during development is vital because its knockout (KO) is lethal at embryonic day 8 (Duyao et al., 1995).

At intracellular level, mHTT is mainly found in the nucleus (as nuclear inclusions) and in perinuclear regions, which promotes nuclear changes, including invagination of the nuclear membrane, as observed in postmortem HD patient's and symptomatic transgenic mouse brains (Cooper et al., 1998; Davies et al., 1997). mHTT can also be associated with different membranous organelles, namely endosomes (Nath et al., 2015), endoplasmic reticulum (Atwal et al., 2007), synaptic vesicles (Suopanki et al., 2006), and mitochondria (Panov et al., 2002).

Different studies have described HTT protein-protein interactions, with more than 350 partners of wild-type HTT protein (Ratovitski et al., 2012). Normal HTT has been described to have anti-apoptotic properties (Rigamonti et al., 2000), participate in cell division (Lopes et al., 2016) and endocytosis (DiFiglia et al., 1995), act as a general facilitator of transcription (Zuccato et al., 2001), in intracellular vesicle trafficking (Caviston and Holzbaur, 2009), mitochondrial bioenergetics (Ismailoglu et al., 2014), selective macroautophagy (Rui et al., 2015) and/or membrane recycling (Hilditch-Maguire et al., 2000). Wild-type HTT has been also described to be important in embryonic development and differentiation, tissue maintenance and cell morphology and survival. Significantly, the stretched HD polyQ domain changes some of these interactions. In fact, the most debated HD hypothesis nowadays is that the disease arises from the combined effect of loss-of-function of wild-type HTT with a gain-of-function of mHTT. Proteases can cleave mHTT, which produce N-terminal fragments with the abnormal polyQ domain that translocate and accumulate in the nucleus, causing neuronal cell death, namely by interfering with gene transcription (Davies et al., 1997; DiFiglia et al., 1997). Moreover, the wild-type HTT can also be cleaved by these proteases, inducing its degradation (Goffredo et al., 2002). mHTT can further form aggregates and interfere with cellular functions, thereby causing cell death and neurotoxicity (Bates, 2003; Chan et al., 2002). However, mHTT inclusions have been also described as being

protective, since they can sequester toxic soluble mHTT oligomers (Leitman et al., 2013). These studies reveal a toxic gain-of- function of mHTT. Alterations in normal endogenous HTT levels may also play a role in HD pathogenesis, since wild-type HTT can co-aggregate with mHTT (Busch et al., 2003). In accordance with this hypothesis, a large portion of chromosome 4 deletion, including the HTT locus, does not cause HD (Cattaneo et al., 2001). Additionally, homozygous and heterozygous HD patients are indistinguishable, since the normal allele in pathological conditions does not improve the phenotype (Squitieri et al., 2003). Altogether, these studies suggest both gain-of-function and loss-of-function mechanisms contributing to HD pathology.

1.5.1. MODELING HUNTINGTON'S DISEASE

Different HD models have been developed throughout time, either expressing full-length or truncated mouse mHtt or human mHTT, revealing distinct degrees of similarity to the human condition. This section describes the most commonly used HD models and their main characteristics.

1.5.1.1. ANIMAL MODELS

Transgenic mouse models can be described in three major types: truncated (expressing, for example, the first exon of the mutant *HTT* gene), full-length (expressing the complete mutant *HTT* gene), and knock-in (KI) models (with direct insertion of the CAG repeat expansion into the mouse *Htt* gene).

The two most widely used truncated models are R6/1 and R6/2, which belongs to the R6 line. This line holds 1 kilobase (kb) of the human *HTT* promoter region followed by the exon 1 of the *HTT* gene, with 115 to 150 CAG repeats (Davies et al., 1997; Mangiarini et al., 1996). R6/1 mice hold 115 CAG repeats with a late age of onset and slow disease progression, with symptoms appearing around 4.5 months of age and mice living around 9 months (Davies et al., 1997; Hodges et al., 2008; Mangiarini et al., 1996), while R6/2 mice hold 150 CAG repeats, showing a very early disease onset with rapid symptom progression (symptoms appearing as early as at 4 or 5 weeks of age) and an extremely short

lifespan, between 13 to 18 weeks (Mangiarini et al., 1996; Sawiak et al., 2009). Indeed, the R6/2 mice is the most extensive studied model in the R6 line. By 5 weeks of age, R6/2 mice already exhibit behavioral deficits with progressive brain and striatal atrophy (nearly 40% reduction) and by 12 weeks of age, this model shows substantially reduced striatal neuron number (Mangiarini et al., 1996; Sawiak et al., 2009). Moreover, postnatal day 1 mice already display nuclear inclusions in striatum and somatosensory cortex (Morton et al., 2000). R6/2 and other truncated mouse model, such as the N171-82Q (Schilling et al., 1999), have an aggressive phenotype, being useful for therapeutic research, although it does not exactly simulate HD genetic or neuropathological adult-onset.

Regarding the full-length mouse models that express the full-length human mutant *HTT* gene with a varying number of CAG repeats, the two most used models are the yeast artificial chromosome (YAC) mice and the bacterial artificial chromosome (BAC) mice. These models exhibit a slower disease progression when compared to truncated models, however, the YAC model is one of the most used to study HD pathological mechanisms and therapeutic interventions. Several YAC transgenic mouse models were created by the Hayden laboratory, expressing human full-length HTT with 18, 46, 72 and 128 CAG repeats (Hodgson et al., 1999; Slow, 2003). A microinjection of YAC DNA construct was introduced into the friend leukemia virus B NIH strain (FVB/N) pronuclei and maintained on an inbred FVB/N background strain to generate the YAC models (Hodgson et al., 1999; Slow, 2003). The YAC128 mouse model is especially interesting since they mimic some features of the human motor phenotype, such as hyperkinesia at early stages, followed by hypokinesia at later stages (André et al., 2011), as well as some mild cognitive alterations, with neuronal loss mainly confined to the striatum, closely resembling the human disease. In YAC128 mice motor abnormalities are progressive, showing augmented open field activity (hyperkinetic state) at 3 months of age, rotarod performance abnormalities at 6 months and open field activity significantly diminished (hypokinetic state) at 12 months of age (Slow, 2003; Van Raamsdonk et al., 2005b). Although HD patients and other transgenic models, such as R6/2, present body weight loss, YAC128 mice have increased body weight represented by an increase in both fat mass and fat-free (lean) mass (Van Raamsdonk et al., 2006). The BACHD model has 97 CAG repeats and, similarly to YAC mice, exhibits late-onset motor deficits

(Gray et al., 2008); however, mHTT aggregates are almost entirely detected in the cortex rather than in the striatum, showing corticostriatal dysfunction (Gray et al., 2008). These full-length mouse models are good models to study neuropathology and neurophysiological HD features at both pre- and post-symptomatic stages (André et al., 2011; Hodgson et al., 1999).

The third HD mouse model are the KI mice, which appear to improve previous models in reproducing the human pathology, while replicating the genetic mutation with fidelity, being the mouse model that most closely resemble the genetic human condition, since transgenic models with exogenous promoters can overexpress the transgene resulting in multiple copies. Indeed, HD KI models have normal life span, show more vigorous behavioral abnormalities at later stages and express mHTT aggregates more selectively in striatal neurons; nevertheless, KI mice show late-onset symptoms that, although progressive, are relatively mild (Heng et al., 2008). Several HD KI mice have been generated, most of them developed based on a gene target replacement of exon 1 of the mouse *Htt* homologue, *Hdh*, with a chimeric mouse/human exon 1 coding for different CAG repeats. These models are denoted as HdhQ followed by a number, which specifies the length of CAG repeats, such as the *Hdh*Q111 (Wheeler et al., 1999), HdhQ140 (Menalled et al., 2003), HdhQ150 (Heng et al., 2007) and HdhQ175 (Menalled et al., 2012). The greater the number of CAG repeats, the earlier the symptoms appear. For example, no motor phenotype emerged up to 1.5 years-old in HdhQ140 mice (Menalled et al., 2003), while HdhQ175 mice (Menalled et al., 2012) presented a robust phenotype at 6 months of age. Similarly to HD human condition, KI mice present weight loss, striatal neuropathology, and molecular alterations, as early as two months of age.

1.5.1.2. CELLULAR MODELS

Several cell lines have been used to study HD pathological features, such as the non-neuronal human HeLa cells and the human embryonic (HEK293T), as well as neuron-like PC12 (derived from rat) cells, the Neuro2a (N2a) neuroblastoma (derived from mouse) and ST14A (derived from embryonic day 14 rat striatal primordia by retroviral transduction of the temperature-sensitive SV40 large T antigen), and still SK-N-SH and SH-SY5Y (human neuroblastoma),

rat and mouse primary striatal neurons, ST*Hdh*$^{Q111/Q111}$ or ST*Hdh*$^{Q7/Q111}$ striatal cells (derived from HD KI mice), and HD cybrids (Cisbani and Cicchetti, 2012). Cellular models can be very useful to investigate the molecular mechanisms underlying the disease, even being limited in biological complexity for drug discovery, thus requiring further validation in more complex models. However, these models are widely used to provide a cost and time-effective models to investigate pathways associated with HD.

PC12 cells expressing the N-terminal portion of the human HTT, containing 20Q or 150Q, was the first cellular model not based on transient transfections. In the presence of nerve growth factor, PC12 cells can differentiate into neuronal-like cells, and the HTT-150Q protein is predominantly present in the nucleus, showing an effect on gene transcription, making mutant cells more susceptible to apoptotic stimulation (Li et al., 1999).

HD modeling continued to evolve, and the conditional immortalization of striatal cells obtained from murine HD models emerged. The immortalized wild-type or homozygous mutant progenitor striatal cells were created from expressing endogenous wild-type Htt (expressing 7Q, the normal mouse CAG repeats) or mHtt with 111Q derived from E14 striatal primordia of wild-type or HdhQ111 KI embryos (Trettel, 2000). These cells were obtained from embryonic day 14 striatal primordia by retroviral transduction of the temperature-sensitive SV40 large T antigen (Trettel, 2000). In heterozygous ST*Hdh*$^{Q7/Q111}$ or homozygous ST*Hdh*$^{Q111/Q111}$ striatal cells the expression of mutant protein occurs at physiological level; these striatal cells also represent early phases of HD pathogenesis, since they are derived from the embryonic phase of the *Hdh* KI mice and they are proliferative cells, with no visible Htt aggregates, being one of the most attractive cell line model in HD (Trettel, 2000). ST*Hdh*$^{Q111/Q111}$ striatal cells have diminished Htt protein and mRNA levels, when compared to control cells (Naia et al., 2016, in supplementary data), they are selectively vulnerable to 3-nitropropionic acid (3-NP), used as an irreversible inhibitor of mitochondrial complex II, and to staurosporine, kinase inhibitor and apoptotic inducer (Rosenstock et al., 2011). These mHtt expressing cells show different apoptotic features, namely increased caspase-3 activation and DNA fragmentation (Rosenstock et al., 2011). STHdh$^{Q111/Q111}$ striatal cells represent a consistent HD model to study mHtt-induced cytotoxicity in the striatum in early stages of the

disease since they present high levels of reactive oxygen species (ROS), and decreased mitochondrial function, and reduced intracellular antioxidant response (Naia et al., 2014, 2011; Ribeiro et al., 2013).

1.2. OXIDATIVE STRESS AND MODULATION

Reactive species include both free radical and non-free radical intermediates and it can be classified into four groups: a) Reactive oxygen species (ROS), b) Reactive nitrogen species (RNS), c) Reactive sulfur species (RSS) and d) Reactive chloride species (RCS) (Sosa et al., 2013). ROS and RNS are the most present and studied reactive species and are physiologically formed as byproducts of normal metabolism, having important roles in cell signaling, homeostasis, autophagy and cell division (Obuobi et al., 2016). Under physiological conditions, low levels of ROS are damned due to fast production and elimination, and are tightly regulated through a process designated as “redox homeostasis” (Droge, 2002). However, aging, genetic and/or environmental factors may impair this homeostasis, leading to oxidative/nitrosative stress through increased ROS/RNS formation and failure of repair and detoxifying systems (Barnham et al., 2004). This causes impaired DNA structure, membrane disturbance and altered protein structure and function, leading to cellular damage (Schieber and Chandel, 2014).

ROS half-lives can vary from a few nanoseconds to hours, depending on its molecules stability, which include superoxide anion ($O_2^{\bullet -}$), hydrogen peroxide (H_2O_2), hydroxyl radical ($^{\bullet}OH$), peroxyl radical ($RO_2^{\bullet}$), alkoxyl radical ($RO^{\bullet}$), hydroperoxyl radical ($HO_2^{\bullet}$), hypochlorous acid (HOCl), hypobromous acid (HOBr), singlet oxygen ($^1O_2$) and ozone (O_3) (Sosa et al., 2013). H_2O_2 is a non-radical and relatively stable ROS that act as a cellular signaling molecule (Obuobi et al., 2016), showing a rapid but limited permeation across biomembranes (Bienert et al., 2006); however, it may cause several harmful effects and alteration of cellular homeostasis, since it can be converted into highly reactive $^{\bullet}OH$, through the Fenton reaction, in the presence of iron II (Fe^{2+}) (Grant, 2011). The most abundant RNS is nitric oxide ($^{\bullet}NO$), which is able to react with certain ROS (Sosa et al., 2013). The reaction between the $O_2^{\bullet -}$ and $^{\bullet}NO$ allows the spontaneous formation of peroxynitrite (ONOO-), which in turn is a precursor of other RNS, such as peroxynitrous acid (HONOO) (Sosa et al., 2013).

In the brain, redox signaling is involved in memory consolidation, neuronal differentiation and plasticity (Bórquez et al., 2016). Indeed, redox signaling is essential for normal brain function, however, excessive generation and long-term exposure to high levels of ROS can produce toxic effects, such as loss of enzyme activity, protein cross-linking and loss of function, protein synthesis inhibition, and DNA damage, leading to apoptotic or necrotic cell death (Koppula et al., 2012). The brain is one of the most metabolically active organs in the body, consuming about 20% of all oxygen (Gadoth and Goebel, 2011). In particular, neurons quickly undergo oxidation not only because they retain low levels of antioxidants, but also because they have localized high levels of iron, auto-oxidizable catecholamines and high levels of membrane polyunsaturated fatty acids and high metabolic rates and thus constant oxygen consumption. Additionally, neurons are post-mitotic cells that accumulate non-degradable oxidized molecules (Bórquez et al., 2016). Endogenously, two important sources of ROS are mitochondria during electron transfer (Sabharwal and Schumacker, 2014) and NADPH oxidase (NOX), an enzymatic complex located at the plasma membrane that produces ROS to the cytoplasm or can catalyze the transfer of an electron from NADPH to O_2, generating $O_2^{\bullet-}$ in the extracellular space, which is then rapidly dismutated into H_2O_2 by superoxide dismutase 3 (SOD3) that freely diffuses across the plasma membrane (Valencia et al., 2013). In this way, large amounts of ROS lead to neuronal death and altered brain function, as observed in neurodegenerative disorders (NDD) (Anderson and Maes, 2014). Thus, increased oxidative markers and deficient enzymatic antioxidant systems are common pathological hallmarks in NDD, as Alzheimer's disease (AD) (Aslan and Ozben, 2004), Parkinson's disease (PD) (Jenner, 2003) and HD (Ribeiro et al., 2013).

1.2.1. NRF2 AS AN ANTIOXIDANT TARGET TO OXIDATIVE STRESS

One of the main (neuro)protective mechanism is the activation of Nuclear factor erythroid 2-related factor 2 (Nrf2), a ubiquitous transcription factor that modulates oxidative stress response. Nrf2 regulates the antioxidant, anti-

inflammatory and detoxifying genes, through binding to the Antioxidant Response Element (ARE), enhancer sequences present in the regulatory regions of Nrf2 target genes (Gan and Johnson, 2014; Yamazaki et al., 2015). Moreover, Nrf2 has been described to contribute for normal mitochondria structure and function, with a specific important role under stress conditions. Several evidence show Nrf2 expression in both glial cells and neurons in human and mouse brain. Although Nrf2 is more commonly expressed in astrocytes, endogenous Nrf2 expression and activation are evident in neurons in aging and neurodegeneration (Liddell, 2017). Nrf2 activation protects against mitochondrial toxins in primary neuronal cultures (Lee et al., 2003), while Nrf2 knockout mice showed increased susceptibility to common neurotoxins, general neurodegeneration and astrogliosis (Hubbs et al., 2007) and dopaminergic neuronal dysfunction (Rojo et al., 2010).

Structurally, Nrf2 is formed by seven functional regions, also known as Nrf2-ECH homology (Neh) domains, from Neh1 to Neh7 (ECH, erythroid cell-derived protein with CNC homology with chicken Nrf2). The Neh1 domain belongs to the C-terminal half of Nrf2 and encloses the CNC-bZIP region, which allows the dimerization with a small musculoaponeurotic fibrosarcoma (Maf) proteins (MafF, MafG or MafK, in vertebrates) in the nucleus and the binding of Nrf2 to DNA (Hirotsu et al., 2012; Motohashi et al., 2004). Neh2 domain, at the N-terminal region, contains two degrons commonly known as the DLG (Leu23 to Arg43, low affinity) and ETGE (Gln73 to Ile86, high affinity) motifs (Fukutomi et al., 2014), which allows the interaction with Kelch-like ECH-associated protein 1 (Keap1) protein, mainly responsible for Nrf2 regulation in the cytosol (Kit I Tong et al., 2006). The Neh3 domain, present in the extremity of Nrf2 C-terminal, can recruit the chromo-ATPase/helicase DNA-binding protein (CHD6) and modulates its transcriptional activation (Nioi et al., 2005). Neh4 and Neh5 domains are involved in transactivation activity, allowing the recruitment of cAMP response element-binding protein (CREB)-binding protein (CBP) (Katoh et al., 2001; Kwok et al., 1994). The Neh6 domain has the DSGIS (Asn329 to Ser342) and DSAPGS (Ser363 to Glu379) motifs (Chowdhry et al., 2013), involved in recruitment of β-transducin repeat-containing protein (β-TrCP), which negatively controls Nrf2 (Rada et al., 2012, 2011). Wang and colleagues, identified the Neh7 domain as

a region that interacts with the retinoic acid receptor α (RARα), responsible for reducing the expression of Nrf2 target genes (H. Wang et al., 2013).

In general, Nrf2 is ubiquitously expressed in most eukaryotic cells and is maintained at low levels in the cytosol under normal conditions due to its binding to Keap1 and constant targeting for poly-ubiquitination and proteasomal degradation (Kansanen et al., 2013; Nguyen et al., 2003). Keap1 is a cytosolic protein (Watai et al., 2007) that regulates Nrf2 activity. Keap1 is a five-domain protein composed by a C-terminal region (CTR) and a N-terminal region (NTR), combined with three functional domains: a Kelch domain (DGR) (Li et al., 2004), an intervening region (IVR) (Mai et al., 2004) and a bric-a-brac domain (BTB) (Zipper and Timothy Mulcahy, 2002). Ubiquitin, a 76 amino acid protein, tags proteins to degradation by proteolytic activity, which depends upon three enzymes, ubiquitin-activating (E1), ubiquitin-conjugating (E2) and ubiquitin-ligase (E3) (Finley, 2009). By using BTB domain, Keap1 can form homodimers to bind Cullin3 (Cul3), an adaptor to Cul3-type E3 ubiquitin ligase complex, resulting in Nrf2 ubiquitination (Cullinan et al., 2004), while by using the DGR domain, two Keap1 proteins can bind one Nrf2 protein (Kit I. Tong et al., 2006).

Under physiological conditions, Nrf2 is mostly located in the cytosol due to its interaction with Keap1 protein (Itoh et al., 1999). Under oxidative stress conditions, as excessive ROS production, Nrf2 disconnects from Keap1 and migrates to the nucleus, where it can dimerize with small Maf family members and bind to Antioxidant Response Element (ARE) (Itoh et al., 1997). When Nrf2 levels are increased in the nucleus, the Nrf2-Maf heterodimer can bind to ARE and recruit transcriptional co-activators, such as CBP or p300 (Zhu and Fahl, 2001), to promote transcription by intrinsic histone acetyltransferase activity (Kalkhoven, 2004) **(Figure 1.3).**

ARE is defined as a cis-acting DNA enhancer motif and is positioned in the promoter of antioxidant genes, responsible for cell defense (Nioi et al., 2003), as well as metabolic genes (Hirotsu et al., 2012) and enzymes that metabolize xenobiotics (Malhotra et al., 2010). Thus, binding of Nrf2 to ARE regulates the transcriptional activation of important antioxidant enzymes such as NAD(P)H:quinone dehydrogenase 1 (NQO1), superoxide dismutase 1 (SOD1, Cu/Zn-SOD), glutathione peroxidase (GSH-Px), glutathione reductase (GSH-R), glutathione S-transferase (GST), heme oxygenase-1 (HO-1), glucose-6-

phosphate dehydrogenase (G6PD), glutamate-cysteine ligase catalytic subunit (GCLc), glutamate-cysteine ligase modifier subunit (GCLM), sulfotransferases (SULFs), thioredoxin reductase (TR) or UDP-glucose dehydrogenase (UGDH) (Keum and Choi, 2014; Loboda et al., 2016). Of relevance, Nrf2 basal activity, as well as Keap1 detachment and nuclear accumulation are tightly controlled and regulated by different chemical and molecular mechanisms, in accordance with the cell environment, in a Keap1-dependent and –independent manner.

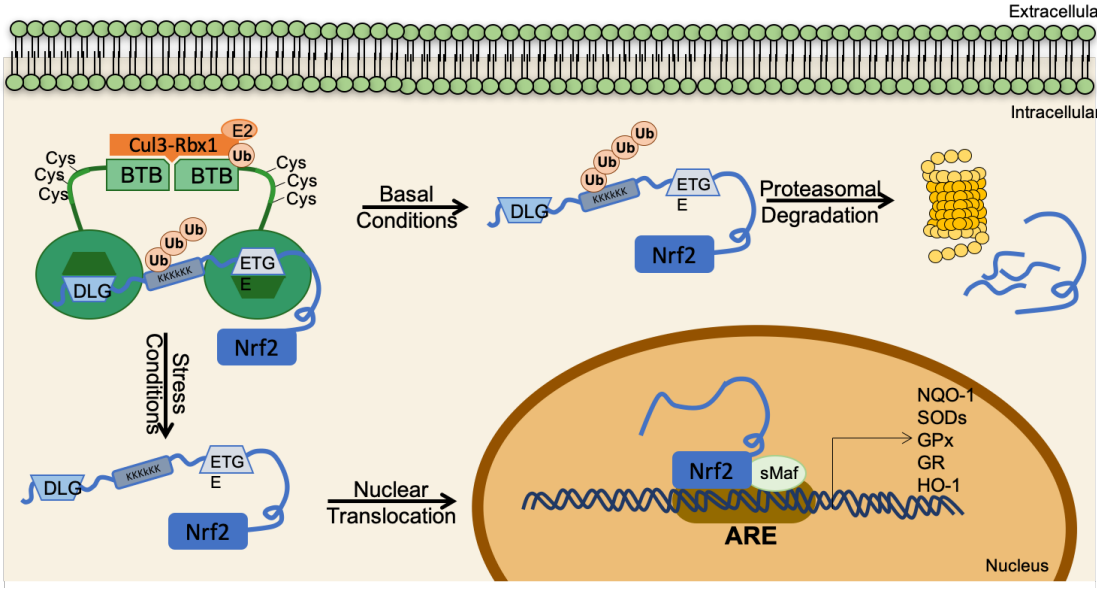

Figure 1.3 | Schematic representation of Nrf2 activation. Under basal/unstressed conditions Nrf2 is constantly ubiquitinated by Keap1–Cul3 complex resulting in Nrf2 recruitment for proteasomal degradation. Under stress conditions, Nrf2 can dissociate from Keap1, translocates into the nucleus and promotes the transcription of antioxidant and detoxifying enzymes after binding to ARE. Adapted from (Fão et al., 2019a)

1.2.1.1. NRF2 REGULATION BY PROTEIN KINASE C

Nrf2 accumulation and its nuclear activity are regulated by several chemical and molecular mechanisms, depending on cell environment. Apart from Keap1-dependent regulation, Nrf2 activation is also influenced by different kinase proteins, such as protein kinase C (PKC), mitogen-activated protein kinase cascades (MAPK), glycogen synthase kinase-3β (GSK-3β), phosphatidylinositol-3-kinase (PI3K)/ Protein kinase B (Akt), among others, favoring Nrf2 serine or threonine phosphorylation (Bryan et al., 2013; Jaramillo and Zhang, 2013). PKC,

a family of signal-regulated enzymes, is responsible for modulating numerous physiological, such as apoptosis, survival, growth and differentiation (Numazawa et al., 2003); PKC can be also activated by oxidative stress (Jung et al., 2004). PKC was the first protein family described to regulate Nrf2 phosphorylation at Ser40, in its Neh2 domain, inducing dissociation from Keap1 and consequent Nrf2 nuclear translocation, which modulates its cytosolic and nuclear accumulation (Huang et al., 2002). Later, Niture and colleagues (Niture et al., 2009), followed by others (Bang et al., 2017), described the PKCδ isoform as the main kinase responsible for this phosphorylation. Interestingly, Nrf2 phosphorylation at Ser40 is necessary for its translocation, but not for its nuclear accumulation (Bloom and Jaiswal, 2003), suggesting that other mechanisms are necessary for Nrf2 stabilization and accumulation in the nucleus, besides Keap1 decoupling.

In AD, several studied evidenced the positive influence of PKC activation on amyloid pathology (Etcheberrigaray et al., 2004; Garrido et al., 2002; Han et al., 2004) and tau pathology (Isagawa et al., 2000), although with no direct relation with the Nrf2 pathway. AD brains presented reduced PKC protein levels and activity, as well as attenuated translocation of the enzyme to the cell membrane (Wang et al., 1994). Similarly, in *in vitro* studies, Aβ induced direct PKC inhibition (Lee et al., 2004), whereas PKC activation prevented hippocampal neuronal death induced by Aβ (Tyszkiewicz and Yan, 2005). Hypothetically, decreased PKC activity may be related with decreased Nrf2 phosphorylation and nuclear migration. Thus, and considering that PKC is involved in memory processes, activation of PKC should be a potential therapeutic strategy for treating AD pathogenesis.

1.2.2. OXIDATIVE STRESS IN HUNTINGTON'S DISEASE

In HD, augmented oxidative stress, defined as an imbalance between oxidants (as explained before) and antioxidant molecules responsible for their elimination and/or reduction, is a well-recognized pathological feature, closely linked to neurodegeneration.

Accumulation of ROS in neurons, which have low levels of antioxidants, cause altered protein structure and increased oxidation, impaired DNA structure and lipid peroxidation (Schieber and Chandel, 2014), contributing to the pathogenesis of many diseases, including HD. In fact, the main HD affected area, the striatum, is highly susceptible to dysfunction of mitochondrial oxidative phosphorylation (Pickrell et al., 2011). Additionally, acute use of mitochondrial toxins, such as cyanide, sodium azide, and 3-NP can lead to striatal degeneration (Brouillet et al., 1999). Moreover, when compared to the cortex or other related areas, the striatum of young rats showed decreased antioxidant capacity (Balu et al., 2005).

In this section, we describe the evidence for ROS production in the presence of mHTT and its toxic effects related with impaired antioxidant defenses.

1.2.2.1. mHTT-MEDIATED OXIDATIVE STRESS

Numerous reports have associated HD with an imbalance in ROS and RNS production and/or of their degradation/reduction by enzymatic and non-enzymatic antioxidants (Gil and Rego, 2008, for review). Hands and colleagues previously reported that polyQ oligomerization in HeLa and PC12 cells leads to early hydrogen H_2O_2 generation (Hands et al., 2011). As described before, NOX is one of the main sources of ROS, which activity has been used as an indicator for ROS generation *in vivo*. Cortical and striatal samples from HD post-mortem patients showed augmented levels of brain NOX activity, more specifically, NOX2, shown to colocalize at plasma membrane lipid rafts and to be directly responsible for increased ROS levels in HD mice (Valencia et al., 2013). Treatment with NOX inhibitors reduced NOX activity, ROS production and neuronal cell death in HD 140Q/140Q mice (Valencia et al., 2013). In addition, mitochondrial complexes II, III and IV deficiency was reported in post-mortem HD striatum (Brennan et al., 1985; Gu et al., 1996), and related with enhanced ROS and oxidative stress in human HD samples (Browne and Beal, 2006). In YAC128 mouse-derived embryonic fibroblasts, $O_2^{\bullet-}$ formation was increased (Wang et al., 2013). Exposure to 3-NP, which damages striatal medium spiny neurons through mitochondrial impairment (Gao et al., 2015), increased ROS levels in HD cybrids, a cell model in which the contribution of mitochondrial defects from patients is isolated, relatively to control cells (Ferreira et al., 2010a). ST*Hdh*$^{Q111/Q111}$ striatal

cells, derived from HD knock-in mice, also showed increased ROS production, lesion in mtDNA and a lower spare respiratory capacity (Siddiqui et al., 2012). Moreover, using the same cellular model, our group previously showed augmented intracellular (Oliveira et al., 2015a; Ribeiro et al., 2013) and mitochondrial (Ribeiro et al., 2014) ROS production due to mHtt expression.

Analysis of protein oxidative modifications is one way of measuring ROS-mediated cytotoxicity *in vivo*. Sorolla and colleagues identified 13 oxidatively modified proteins in striatal human HD brain samples, when compared to controls, including mitochondrial enzymes, with reduced catalytic activity, concordantly with energy deficiency seen in HD (Sorolla et al., 2010). In HD patients, levels of 8-hydroxy-2'-deoxyguanosine (8-OHdG), a DNA oxidation biomarker, were also increased in caudate tissue (Browne et al., 1997), as well as in serum and leukocytes (Long et al., 2012), indicating that both nuclear and mitochondrial DNA are more oxidized in HD patients samples. In this respect, progressive mtDNA damage was observed in the striatum and cerebral cortex of 7-12-week-old R6/2 mice (Acevedo-Torres et al., 2009). Concordantly, urine, plasma and striatal microdialysates from the R6/2 mouse model evidenced increased levels of 8-OHdG (Bogdanov et al., 2001). Increased lipid peroxidation markers, such as malondialdehyde and 4-hydroxynonenal, were also observed in blood samples of HD patients (Stoy et al., 2005). Furthermore, the R6/2 transgenic mice evidenced striatal lipid peroxidation (Pérez-Severiano et al., 2000). Increased ROS, including $O_2^{\bullet -}$ formation, were also found in the brain striatum and cortex of symptomatic R6/1, R6/2, and N171-82Q HD mouse models (Ellrichmann et al., 2011; Sadagurski et al., 2011; Stack et al., 2010), and in YAC128 HD mouse embryonic fibroblasts (Wang et al., 2013) and striatal primary neurons (Naia et al., 2021). Moreover, mitochondrial ROS formation, including $O_2^{\bullet -}$, was verified in several HD models, such as fibroblasts from HD patients (Wang et al., 2013) and HD cybrids and further potentiated in the presence of 3-NP or STS treatment, the latter an inducer of apoptosis (Ferreira et al., 2010a). Additionally, H_2O_2 treatment augmented ROS levels induced by mHtt, resulting in mHtt aggregation, which in turn directly induced ROS production, cell death and impairing proteasomal function in neuronal and non-neuronal cell models (Goswami et al., 2006; Hands et al., 2011; Wyttenbach et al., 2002).

These results suggest that mHTT can exert its toxic effect by promoting ROS generation. Although controversial when considering oxidative modifications as late events in HD progression, antioxidants have been demonstrated to be beneficial in several HD models, suggesting that antioxidant therapy might slow down the rate of motor decline early in the course of HD.

1.2.2.2. ALTERED ANTIOXIDANT MOLECULES IN HUNTINGTON'S DISEASE

Oxidative damage in neurons can be counteracted with a large variety of molecules, mostly deriving from glial cells. As explained before, Nrf2 is known to upregulate the expression of cytoprotective and antioxidant enzymes/proteins by binding to ARE, enhancing sequences present in the regulatory regions of Nrf2 target genes (Gan and Johnson, 2014; Yamazaki et al., 2015). However, involvement of Nrf2 in HD progression remains poorly investigated. Malonate, a reversible complex II inhibitor, and 3-NP induced higher toxicity in Nrf2 knockout mice and Nrf2-deficient cells (Calkins et al., 2005), suggesting the involvement of Nrf2 activity in neuronal degeneration in HD. In addition, intrastriatal transplantation of astrocytes overexpressing Nrf2 in wild-type mice was shown to have an important neuroprotective effect after exposure to malonate (Calkins et al., 2005). Moreover, ST*Hdh*$^{Q111/Q111}$ striatal cells presented decreased Nrf2 levels (Oliveira et al., 2015b) and activity (Jin et al., 2013). Overall, these studies suggest that Nrf2 positive modulation should have neuroprotective effects in HD pathogenesis. Indeed, treatment of R6/2 and YAC128 HD transgenic mice with fumaric acid ester dimethylfumarate (DMF), an orally bioavailable fumaric acid ester (FAE), which is metabolized to methyl hydrogen fumarate, attenuated motor impairment and preserved striatal and motor cortical neurons by inducing Nrf2 nuclear migration and activation (Ellrichmann et al., 2011). Moreover, cystamine, an inhibitor of transglutaminase activity with additional potentially beneficial effects, protected against neurodegeneration in R6/2 (Fox et al., 2004) and YAC128 (Van Raamsdonk et al., 2005a) HD models. Systemic cystamine administration led to Nrf2-dependent ARE activation in the striatum. In order to test whether the induction of neuroprotection via cystamine occurred through Nrf2 activation, Nrf2 deficient (Nrf2$^{-/-}$) animals were treated with cystamine following

3-NP-induced neurotoxicity. Additionally, our group previously showed that creatine and cystamine increased HD mutant cells viability and prevented ROS formation in HD cells subjected to H_2O_2 (Ribeiro et al., 2013). Cystamine induced a positive effect in 3-NP-treated mice, reducing lesion volume in striatal brain mice, but more effectively in wildtype littermates, confirming that Nrf2 is essential for cystamine protection from 3-NP-induced striatal lesioning (Calkins et al., 2010). Furthermore, sulforaphane (SFN) stimulated the Keap1-Nrf2-ARE pathway and inhibited mitogen activated protein kinases (MAPKs) and factor nuclear kappa B (NF-κB) pathways to mitigate 3-NP-induced neurotoxicity, including suppression of the lesion area, apoptosis, microglial activation, and mRNA or protein expression of inflammatory mediators, suggesting that SFN is an appellative therapeutic approach (Jang and Cho, 2016).

GSH is the main endogenous antioxidant involved in the maintenance of cellular redox homeostasis. Different studies showed altered GSH metabolism in HD, which can contribute to redox imbalance during disease progression. Indeed, cortical samples from post-mortem HD patients showed reduced levels of GSH (Flint Beal et al., 1992). Decreased levels of both GSH and GSH-R in plasma were associated with caudate atrophy in HD patients (Peña-Sánchez et al., 2015), and studies in peripheral tissues of HD patients reported decreased GSH levels in plasma (Klepac et al., 2007) and reduced GSH-Px activities in HD leukocytes (Chen et al., 2007). In addition, polyQ oligomerization in HeLa and PC12 cells induced early disturbance in GSH levels (Hands et al., 2011). Conversely, other studies showed that, in some cellular (ST*Hdh*$^{Q111/Q111}$ striatal cells) and animal (R6/2) HD models, GSH levels are increased, although these augmented levels were not enough to ameliorate HD-associated oxidative imbalance (Ribeiro et al., 2012; Yeun et al., 2005). Tolfenamic acid, a nonsteroidal anti-inflammatory drug with neuroprotective properties, also exhibited antioxidant effects in both R6/1 mice and PC12 cell models, increasing GSH levels and reducing ROS accumulation, respectively, suggesting that tolfenamic acid has a good therapeutic effect in HD models (Liu et al., 2019).

HD patients showed reduced SOD1 activity in cytosol of parietal cortex and cerebellum (Browne et al., 1997), but increased immunoreactive staining for HO-1 in cortex and striatum (Browne et al., 1999). Concordantly, decreased SOD1 activity was detected in erythrocytes derived from HD patients (Chen et

al., 2007). These studies are in accordance with data from transgenic HD mice, which showed reduced SOD1 activity in older mice (at 35 weeks of age), suggesting that the antioxidant mechanism to protect cells fails with advanced disease stage (Santamaría et al., 2001). Importantly, Mason and co-workers, demonstrated that augmented GSH-Px activity (by genetic or pharmacological approaches), was neuroprotective in different HD models, namely in yeast, mammalian cells and Drosophila (Mason et al., 2013). Furthermore, overexpression of SOD1 in mHtt expressing cells (HD 150Q cells) decreased mHtt aggregation and proteasome malfunction induced by oxidative stress (Goswami et al., 2006).

PC12 cells overexpressing the N-terminal fragment of Htt protein with either a nonpathogenic or pathogenic polyQ repeat (Htt-103Q), showed reduced expression of the antioxidant protein Prx1. Treatment of these cells with dimercaptopropanol, a thiol-based antioxidant, alleviated the cytotoxicity induced by mHTT and the expression level of Prx1 (Pitts et al., 2012). This study suggests the involvement of mHTT in ROS production and reveal the importance of thiol-based antioxidants as potential drugs for HD treatment.

1.3. MITOCHONDRIAL DYSFUNCTION IN HUNTINGTON'S DISEASE

Mitochondrial bioenergetics and dynamics are significantly linked with neuronal physiology and homeostasis. Neurons are extremely dependent on mitochondria since they are highly energy requiring cells. Indeed, mitochondria have an important role in generating adenosine triphosphate (ATP) through oxidative phosphorylation (OXPHOS). Electron leakage at complexes I and III generates $O_2^{\bullet-}$; thus, altered mitochondrial function due to complexes inhibition induces oxidative stress. Mitochondria also have an important role in intracellular Ca^{2+} homeostasis, namely through the crosstalk with endoplasmic reticulum, and further regulate oxidative and nitrosative stress, neuronal survival, and cellular metabolism, including heme synthesis and iron usage.

Several evidence showed that mitochondrial dysfunction is closely related with HD pathogenesis. Previous studies reported ultrastructural defects in mitochondria isolated from post-mortem HD cortical tissue and compromised oxidative function and ATP synthesis in pre-symptomatic HD carriers (Saft et al., 2005), suggesting mitochondrial dysfunction as an early relevant pathogenic mechanism. Moreover, post-mortem HD patient's brain specimens and human HD lymphoblasts showed abnormal mitochondrial morphology and trafficking (Napoli et al., 2013). Concordantly, isolated brain mitochondria from caudate nucleus of HD patients (Yano et al., 2014) and different HD cellular (human neuroblastoma cells; ST*Hdh*$^{Q111/Q111}$) and animal models (Hdh(CAG)150 knock-in mouse) showed HTT fragments in close contact with mitochondria (Choo, 2004; Orr et al., 2008), suggesting a direct effect of mHTT on mitochondrial function.

Considering these observations, in this section we highlight the major findings regarding the role of mitochondrial dysfunction in HD pathogenesis, by describing mHTT-mediated altered mitochondrial membrane potential and respiration, Ca^{2+} buffering, mitochondrial bioenergetics and dynamics, and potential therapeutic targets for mitochondrial malfunction in HD.

1.3.1. ALTERED MITOCHONDRIAL MEMBRANE POTENTIAL AND ELECTRON TRANSFER FUNCTION

Normal mitochondrial activity creates an electrochemical proton gradient and thus a mitochondrial transmembrane potential ($\Delta\psi m$) of -150 to -180 mV, allowing ATP synthesis. Studies with caudate and putamen of post-mortem symptomatic HD patients, and striatal mHtt-expressing cells, brains of HD animal models (Htt171-82Q and 3-NP rat HD mice, with 20 weeks) and peripheral cells derived from HD patients (pre-symptomatic and symptomatic) showed a dramatic decrease in the activity of complexes II, III and mildly of complex IV (Benchoua et al., 2006; Browne, 2008; Gu et al., 1996; Pandey et al., 2008; Silva et al., 2013a). Different reports showed altered electron transfer chain activity, which cause impaired ΔΨm in HD. Mitochondria isolated from HD patients and HD transgenic mouse brains (with 72 or 150 polyQ repeats, respectively) showed increased depolarized mitochondrial membrane (Panov et al., 2002). Several studies also reported that HD lymphoblasts are highly susceptible to decreased $\Delta\psi m$, showing correlation with increased polyQ repeats (Naia et al., 2014; Panov et al., 2002). We previously showed significant changes in $\Delta\psi m$ associated with apoptotic events in symptomatic HD cybrids (an *ex-vivo* peripheral model obtained from the fusion of HD human platelets with mtDNA-depleted rho0 cells) and in HD human B-lymphocytes (Almeida et al., 2008; Ferreira et al., 2010a). Concordantly, when compared with wild-type cells, striatal ST*Hdh*$^{Q111/Q111}$ cells showed significant $\Delta\psi m$ reduction after increasing Ca^{2+} concentrations (Milakovic et al., 2006) **(Figure 1.4).** Of relevance, the ΔΨm defect in ST*Hdh*$^{Q111/Q111}$ cells was attenuated in the presence of ADP and the reduced Ca^{2+} uptake capacity was improved in the presence of inhibitors of the permeability transition pore (PTP) (Milakovic et al., 2006). Melatonin (endogenously produced by the pineal gland and the retina) has been described to be protective in HD context, preventing toxicity induced by 3-NP. Indeed, melatonin inhibited mutant Htt-induced ΔΨm loss in ST14A cells (Wang et al., 2011); this further inhibited the release of mitochondrial proapoptotic factors, making melatonin a therapeutic strategy for counteracting cell death and improve HD-related mitochondrial features (Wang et al., 2011). Moreover, HTT phosphorylation at Ser421 improved

Δψm in HD human lymphoblasts (Humbert et al., 2002; Naia et al., 2014). Moreover, striatal mitochondria isolated from R6/1 HD transgenic mice showed reduced activity of complexes II, III, IV and altered oxygen consumption rates. Similarly, 3-NP treatment reduced the activity of complexes II, IV and V in mice (Sandhir et al., 2012). Moreover, our group previously demonstrated that insulin-like growth factor 1 (IGF-1) alleviated HD symptoms through improvement of mitochondrial function; HD models (YAC128 and R6/2 mice, human HD lymphoblasts and ST*Hdh*$^{Q111/Q111}$ cells) exhibited reduced ATP/ADP ratio, decreased O_2 consumption, increased mitochondrial ROS and fragmentation, aberrant lactate/pyruvate levels and decreased mitochondrial membrane potential, and each of these parameters was shown to be rescued by IGF-1 treatment *via* upregulation of PI3K/AKT signaling in cellular and mouse models of HD (Naia et al., 2016, 2014; Ribeiro et al., 2014).

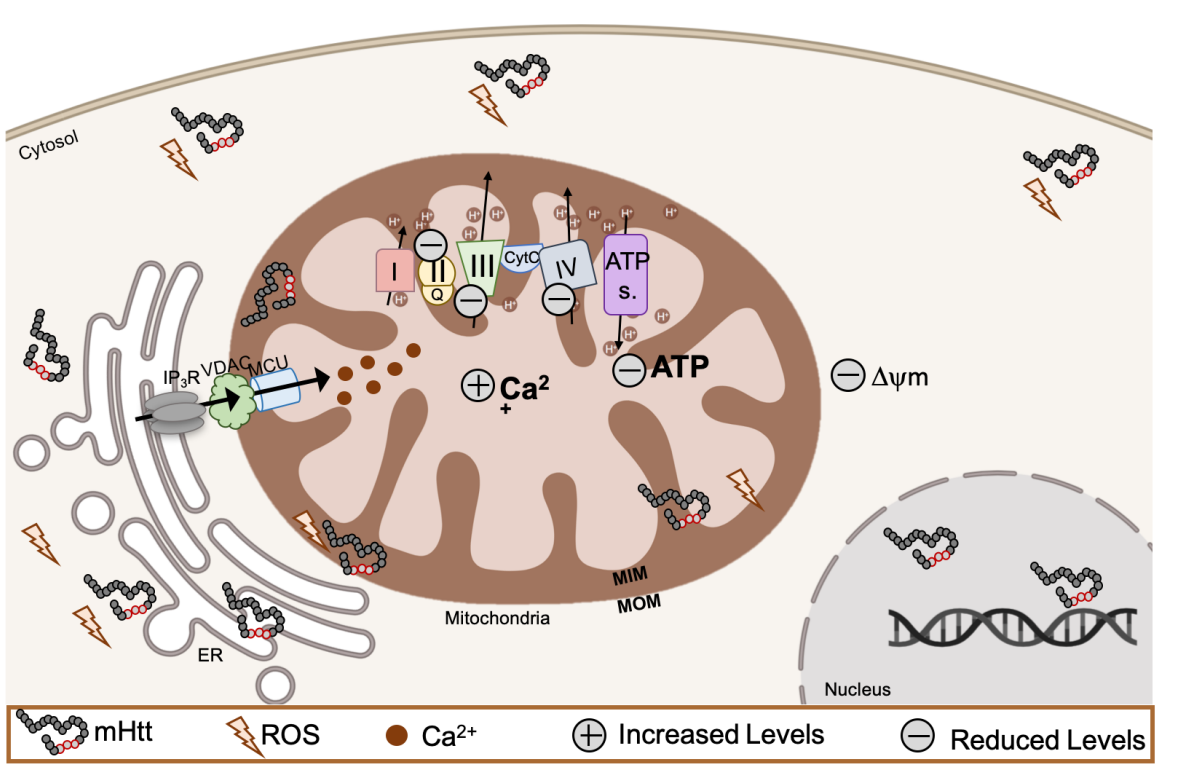

Figure 1.4 | Effect of mHtt expression on mitochondrial complexes function and Δψm. mHTT can associate with the MOM and MIM leading to decreased complexes II, III and IV function, as well as decreased ATP production, which results in decreased Δψm. Adapted from (Fão and Rego, 2021)

1.3.2. IMPAIRED MITOCHONDRIAL BIOGENESIS IN HUNTINGTON'S DISEASE

Mitochondrial biogenesis is a complex multi-step process where transcription and translation of mtDNA and nuclear-encoded mitochondrial-related transcripts associate to control mitochondrial protein import and general assembly of a mitochondrial network. mtDNA is a ~16-kb genome that encodes for 13 protein subunits of the mitochondrial electron transport chain and ATP synthase (Anderson et al., 1981). Most of the mitochondrial proteins are nuclear encoded, then synthesized in the cytosol, and imported into the mitochondria. Thus, an imbalance in nuclear- and/or mitochondrial-encoded proteins synthesis, import and folding, or mutations in mtDNA, can disturb mitochondrial integrity and functionality.

Different studies provided evidences that mtDNA damage is implicated in the pathogenesis of HD (Gemba et al., 1999; Yang et al., 2008) since mtDNA is a major target of the oxidative stress associated with mHTT. In line with that, some authors showed that the abundance of mtDNA decreases dramatically in striatal cells expressing mHtt (ST*Hdh*$^{Q111/Q111}$)(Siddiqui et al., 2012). Additionally, HD patients showed mtDNA depletion in leukocytes, which was negatively correlated to the number of mHTT polyQ repeats (Liu et al., 2008). Moreover, human peripheral HD leukocytes and striatum from transgenic HD R6/2 mice showed significantly reduced mtDNA copy number (Hering et al., 2015; Petersen et al., 2014).

Mitochondrial proteins encoded in nucleus are synthesized as precursors and maintained in the cytosol with an unfolded conformation, existing in complexes with cytosolic chaperones, such as HSP70 and HSP90, to avoid their degradation and aggregation (Young et al., 2003). Most of these precursors contain N-terminal mitochondrial targeting sequences (MTS), which are 10–80 amino acid residues with no sequence identity, in order to direct them to the mitochondria and into the correct mitochondrial compartment. Several mitochondrial proteins are located to the matrix. Once in the mitochondrial matrix, MTS are cleaved generating mature polypeptides. Moreover, cooperation between the two main mitochondrial translocases, the translocase of the outer membrane (TOM)

complex at MOM and the translocase of the inner membrane (TIM23) complex, is needed for these proteins to be imported (Bausewein et al., 2017; Mokranjac and Neupert, 2010). In addition, an intact mitochondrial membrane potential and the hydrolysis of ATP are essential for protein translocation through the TIM23 complex.

Highly purified synaptosomal mitochondria from presymptomatic R6/2 mice showed mitochondrial import defects. Indeed, mHTT can interact with TIM23 complex, while wild-type HTT does not associate with this translocase complex, suggesting a role of polyQ domains in these interactions (Yano et al., 2014). Interestingly, the delivery of Tim23, Tim50, and Tim17a (subunits of TIM23 complex) by lentiviral to rescue mitochondrial protein import, improved mitochondrial function and reduced cell death in mHTT-expressing neurons (Yano et al., 2014), suggesting a possible therapeutic approach against impaired mitochondrial import in HD.

Mitochondrial network is constantly renewed through nuclear- and mtDNA-encoded proteins. However, mHTT can interact and affect the function of several transcription factors involved in maintenance of mitochondrial function and biogenesis. Peroxisome proliferator-activated receptor (PPAR)γ coactivator 1α (PGC-1α) is a regulator of several metabolic processes including mitochondrial respiration and biogenesis (Cui et al., 2006), expression of nuclear-encoded subunits of each of the electron transport-chain complexes, and antioxidant defense proteins, suppressing cellular ROS formation (St-Pierre et al., 2006). PGC-1α also regulates the expression of the mitochondrial transcription factor A (Tfam), the major transcriptional regulator of mtDNA (Palikaras and Tavernarakis, 2014). Striatum of early-stage HD patients showed diminished Tfam and PGC-1α levels and decreased expression of 24 out of 26 PGC-1α target genes, increasing disease severity and loss of mitochondrial function (Cui et al., 2006; Weydt et al., 2006) **(Figure 1.5).** Additionally, a PGC-1α coding variant was described to be associated with the age of onset of motor symptoms in HD patients (Weydt et al., 2014). Moreover, spongiform lesions predominantly in the striatum were seen in PGC-1α null mice, which developed a neurological phenotype consistent with neurodegeneration, suggesting an increased susceptibility of striatal neurons to altered PGC-1α expression (Lin et al., 2004). mHTT can further interact with the PGC-1α promoter, interfering with the

transcriptional activation functions of promoter-bound transcription factors, cAMP response element CREB and TAF4, which results in decreased PGC-1α expression and augmented mitochondrial abnormalities.

SIRT1 is a deacetylase of the sirtuin family that deacetylates PGC-1α. Our group showed that resveratrol, a SIRT1 activator with antioxidant properties, increased mtDNA copies and mitochondrial-related transcription factors (TFAM and nuclear PGC1α) in HD human lymphoblasts, as well as increased expression of mitochondrial electron transport chain proteins and improved motor function in YAC128 mice (Naia et al., 2017b).

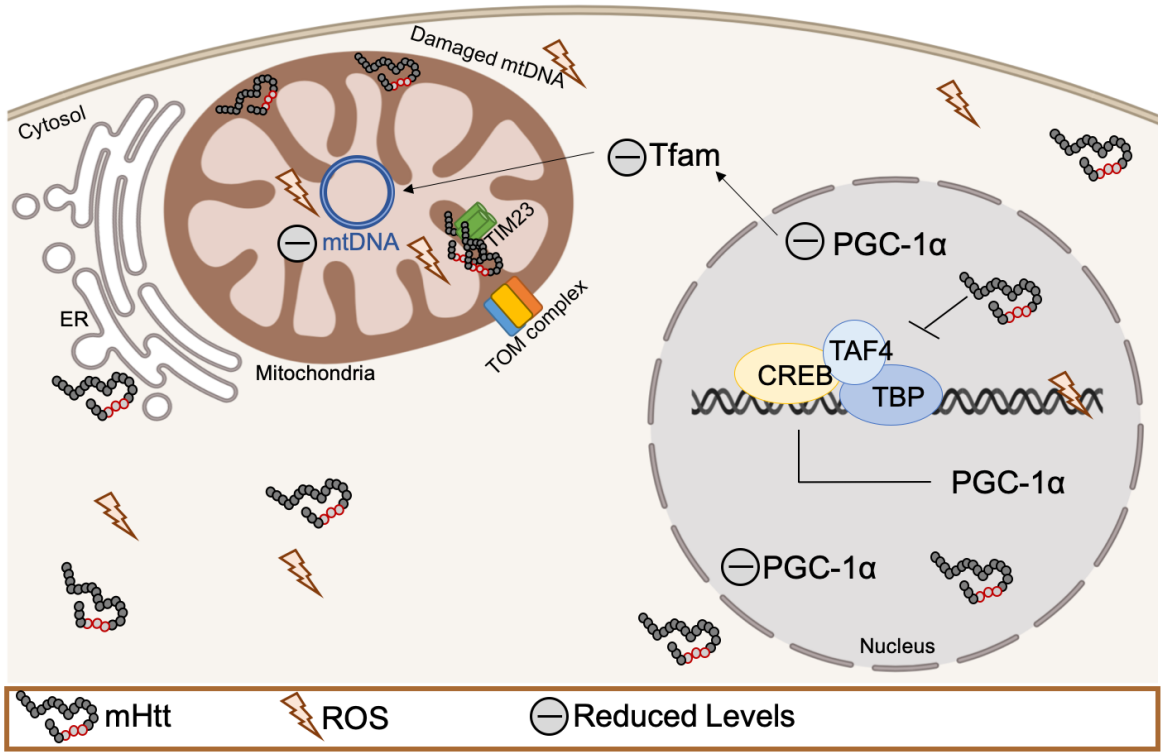

Figure 1.5 | Effect of mHtt expression on mitochondrial biogenesis. mHTT expression disturbs CREB/TAF4 signaling leading to decreased PGC-1α levels and activity, which in turn results in decreased TFAM activation and reduced mitochondrial biogenesis. HTT expression increases ROS production, resulting in decreased mtDNA. Adapted from (Fão and Rego, 2021)

1.3.3. ABNORMAL Ca^{2+} HOMEOSTASIS AND MITOCHONDRIA-ASSOCIATED MEMBRANE (MAM) COMMUNICATION

Mitochondria is an important organelle in the regulation of intracellular Ca^{2+} homeostasis, due to mitochondrial calcium uniporter (MCU) channel, which is located at MIM and allow mitochondrial Ca^{2+} buffering. Altered mitochondrial Ca^{2+} handling may participate in HD neurodegeneration. Indeed, mHTT can interact with MOM, which may induce the opening of the mitochondrial PTP. PTP opening can be stimulated by increased Ca^{2+}, ROS or decreased adenine nucleotide levels, which can induce mitochondrial swelling, depolarization, diminished ATP levels within the organelle and cell death (Milakovic et al., 2006; Panov et al., 2002). Isolated mitochondria from liver of homozygous knock-in Hdh150/150 mice also demonstrated increased predisposition to PTP induction by Ca^{2+} (Choo, 2004). Lower Ca^{2+} retention were shown in isolated mitochondria from brains of transgenic YAC72 and HD patients lymphoblasts (Panov et al., 2002). In addition, HD human lymphoblasts exposed to H_2O_2 displayed decreased mitochondrial Ca^{2+} retention (Naia et al., 2014). In contrast, our group showed increased Ca^{2+} uptake in isolated mitochondria from pre-symptomatic R6/2 and YAC128 brain mice (Oliveira et al., 2007). Additionally, in a study using synaptic and non-synaptic mitochondria from YAC128 mice brain, augmented Ca2+ uptake could be directly correlated with mHTT levels associated with the mitochondrial membrane (Pellman et al., 2015).

Mitochondrial-associated membrane (MAM) is the connection between mitochondria and a specialized domain of the endoplasmic reticulum (ER), the best-characterized inter-organelle connection. ER-mitochondria contact sites are important regulators of lipid metabolism and Ca^{2+} homeostasis, and consequently modulate fundamental cellular processes such as mitochondrial morphology, cell stress induced by ROS, autophagy and apoptosis (Hamasaki et al., 2013; Verfaillie et al., 2012). MAMs regulate Ca^{2+} transfer from the ER to mitochondria in order to maintain cellular bioenergetics and mitochondrial dynamics or to induce cell death (Boehning et al., 2003). Ca^{2+} transfer in MAMs can occur through the Ca^{2+} channel inositol-1,4,5-trisphosphate (IP3) receptor (IP3R), which contacts with outer mitochondrial membrane (OMM) protein voltage-

dependent anion channel isoform 1 (VDAC1) through the molecular chaperone glucose-regulated protein 75 (GRP75) (Szabadkai et al., 2006). Thus, IP3R is highly concentrated in ER-mitochondrial contact sites. Importantly, Tang and colleagues showed that mHTT can interact with type 1 IP3R (IP3R1), suggesting an important role of this ER Ca^{2+} channel in HD Ca^{2+} deregulation and neurodegeneration (Tang et al., 2003) **(Figure 1.6).**

The ER protein sigma-1 receptor (Sig-1R) is further localized at the ER-mitochondria junction and is usually used as a MAM marker (Hayashi and Su, 2007). Sig-1R forms a Ca^{2+}-sensitive chaperone complex with immunoglobulin protein/glucose-regulated protein 78 (BiP/GRP78), prolonging Ca^{2+} signaling from the ER to the mitochondria by stabilizing IP3R at MAMs (Hayashi and Su, 2007). Hyrskyluoto and coworker showed that mHTT expression (N-terminal HTT fragment with 120 polyQ repeats or full-length HTT with 75 repeats) diminished S1R expression in neuronal PC6-3 cells. Importantly, selective S1R agonist PRE-084 treatment improved S1R, SOD1, SOD2 and thioredoxin 2 expression in these cells (Hyrskyluoto et al., 2013). PRE-084 administration also diminished caspase-3 cleavage and oxidative stress and increased calpastatin (endogenous calpain inhibitor), activating the NF-κB pathway, suggesting a protective effect of S1R augmented function in HD (Hyrskyluoto et al., 2013). In accordance, S1R downregulation with antisense RNA amplified the amount of mHTT aggregates in both the cytoplasm and nucleus. Pridopidine, which was first described as a dopamine stabilizer (Ponten et al., 2010; Waters et al., 2014), was recently shown to interact with S1R (Sahlholm et al., 2015). Several clinical trials using pridopidine showed its efficacy in treating motor symptoms of HD (Karl et al., 2013; Lundin et al., 2010; Reilmann et al., 2019), suggesting that S1R may be involved in the therapeutic effects of pridopidine.

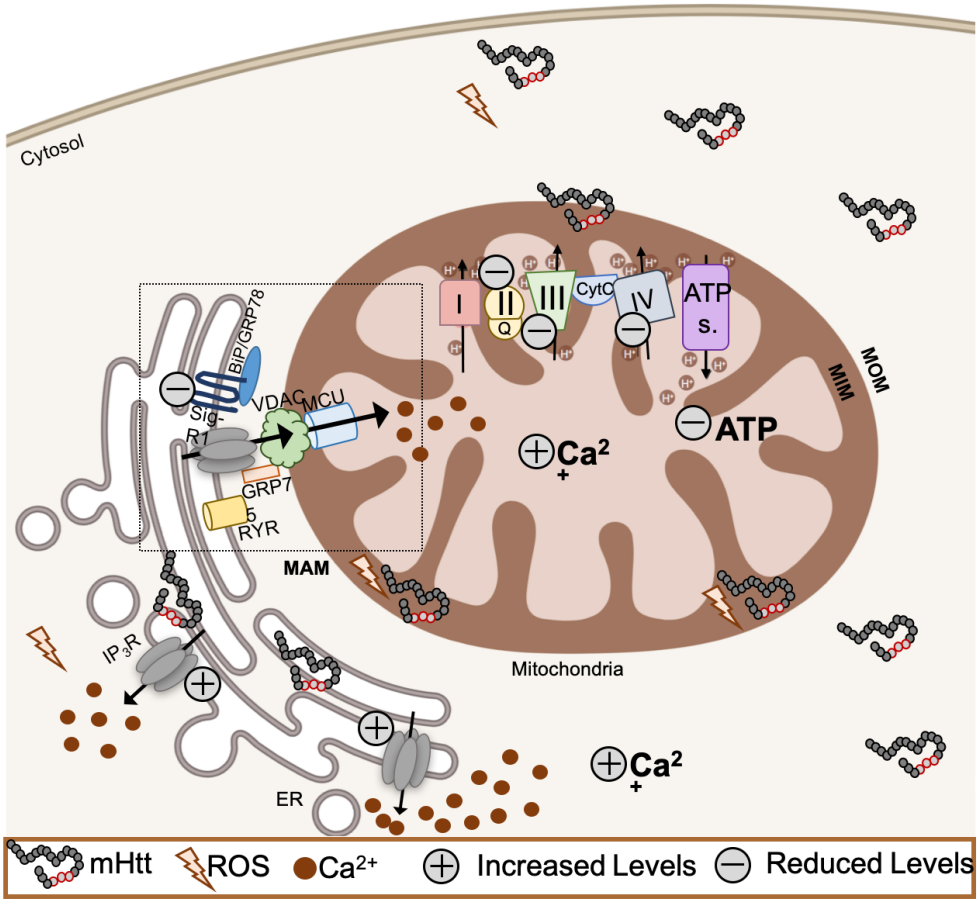

Figure 1.6 | Influence of mHtt expression on MAMs and calcium altered levels. In MAMs (ER-mitochondria contact sites) mitochondria can take up Ca^{2+} into the matrix through the interaction between IP_3R and VDAC (at the MOM) and MCU (at the MIM). GRP75 localizes in MAMs and acts as a bridging molecule between the two organelles by assembling the IP3R-GRP75-VDAC complex, which is involved in the transport of Ca^{2+} from the ER to mitochondria. Adapted from (Fão and Rego, 2021)

1.3.4. mHTT-INDUCED MITOCHONDRIAL DYNAMICS CHANGES

Mitochondria are dynamic organelles and thus their structure varies constantly from a tubular network to individual mitochondria. Mitochondrial dynamics (including mitochondrial fusion and fission), mitochondrial biogenesis and elimination of unwanted mitochondria, by mitophagy (described in 1.4 section), and movement are processes that must coexist in balance for normal mitochondrial network and function. Indeed, mitochondria can divide (fission) and unite (fusion) in response to several stimuli. Both dynamic processes make

possible the exchange of membranes and intra-mitochondrial content or mobility of the organelle to specific subcellular locations.

Altered mitochondrial morphology and consequently neuronal dysfunction have been described in HD models, complemented with altered expression of genes involved in fission/fusion balance (Reddy and Shirendeb, 2012). Mitochondrial fission is regulated by dynamin-related protein 1 (Drp1), which have an effector guanosine triphosphate (GTP)ase domain and can translocate from cytosol to MOM, after a fission stimulus (Knott et al., 2008). Additionally, mitochondrial fission 1 (Fis1) and mitochondrial fission factor (Mff), located at MOM, serve as adaptors for Drp1, which allows the recruitment of Drp1. The GTPases mitofusins (Mfn) 1 and 2, present at MOM, mediate the fusion of MOMs of juxtaposing mitochondria. Moreover, mitochondrial fusion is regulated by optic atrophy 1 (OPA1), which is located in MIS and shows association with the MIM. Striatum and cortex of several HD animal models further showed reduced levels of Mfn1, Mfn2 and OPA1 and augmented levels of Drp1 and Fis1, revealing excessive mitochondrial fragmentation (Costa et al., 2010; Shirendeb et al., 2011) . Moreover, mHTT can interact with Drp1, resulting in increased GTPase activity and consequently less efficient mitochondria and reduced energy production for neuronal function (Song et al., 2011) **(Figure 1.7).** Interestingly, although mitochondrial fission has been associated with HD, the phenotype analyses of HD mice with and without Mff, which greatly reduces mitochondrial fission, showed that R6/2 HD mice lacking Mff exhibit more severe neurological phenotypes and have shortened lifespans (Cha et al., 2018). This recent study suggests a protective role for mitochondrial fission in HD and emphasize the idea that manipulation of mitochondrial dynamics can be applied to HD therapy. Recently, Aladdin and co-workers demonstrated that skin fibroblasts from juvenile HD patients had significantly lower levels of mitochondrial fusion and fission proteins and reduced branching in the mitochondrial network. Moreover, juvenile HD fibroblasts exhibited higher proteasome activity, which was associated with elevated gene and protein expression of parkin, as well as augmented proteasomal degradation of the mitochondrial fusion protein Mfn1 in diseased cells (Aladdin et al., 2019). These data suggest that expansion of mHtt is linked to increased proteasome activity and faster turnover of specific substrates of ubiquitin-proteasome system in order to protect cells, which could

contribute to altered mitochondrial dynamics in early phases of the disease. However, mitochondrial fusion also seems to be positive in HD models. Metformin, an antidiabetic drug, mimics caloric restriction by acting on cell metabolism at multiple levels. In HD context, metformin restored ATP levels in ST*Hdh*$^{Q111/Q111}$ cells, and prevented mitochondrial membrane depolarization, excess fission and modulated the disturbed mitochondrial dynamics in HD cells (Jin et al., 2016). Additionally, 3-NP-mediated HD model mitochondria showed increased cholesterol to phospholipid ratio, suggesting decreased mitochondrial membrane fluidity, as well as ultrastructural mitochondrial changes, accompanied by organelle swelling.

Mitochondria are present in different subcellular locations where high energy is required through mitochondrial trafficking, which has been shown to be deregulated in neurodegenerative diseases as HD. In neurons expressing mHTT, mitochondria are mainly localized in the cell body and less transported to dendrites, axons or synapses (anterograde movement), resulting in reduced ATP levels at these sites, followed by synaptic degeneration (Shirendeb et al., 2012). Both N-terminal fragments and full-length mHTT can directly disturb mitochondrial trafficking in either anterograde or retrograde movement (Orr et al., 2008; Shirendeb et al., 2012; Trushina et al., 2004). In striatal and cortical neurons overexpressing mHTT protein aggregates can sequester and block mitochondrial transport machinery, hindering mitochondrial movement through neuronal projections (Trushina et al., 2004), suggesting that improvement of mitochondrial movement could be a possible therapeutic strategy in HD.

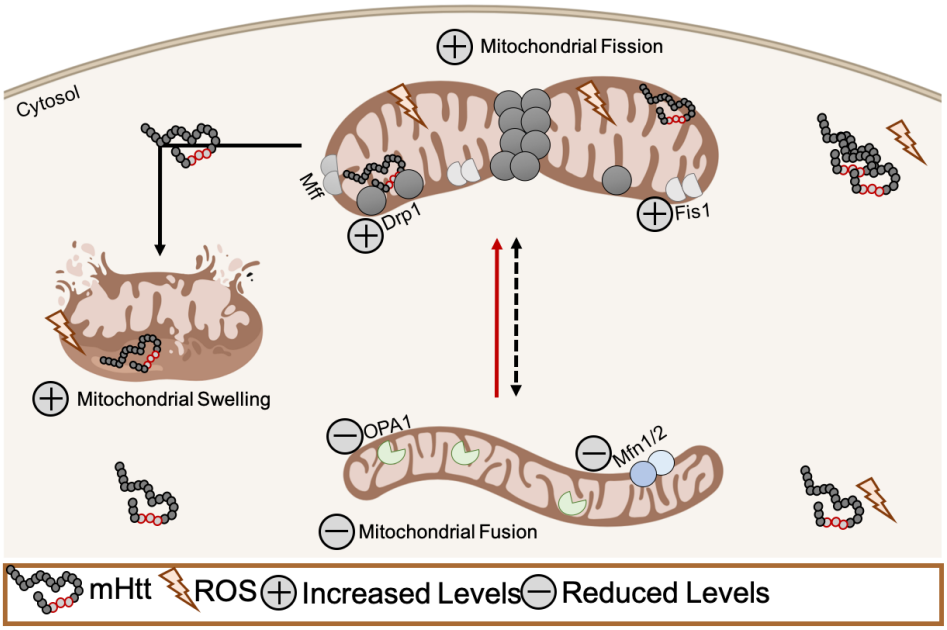

Figure 1.7 | Effect of mHtt expression on mitochondrial morphology. mHTT disrupts the balance between fission and fusion, with increased mitochondrial fragmentation resulting from increased levels of Drp1 and Fis1 as well as decreased levels of Mfn1, Mfn2 and OPA1. mHTT can further interact with and increase Drp1's GTPase activity. Furthermore, mHTT expression leads to increased mitochondrial swelling. Adapted from (Fão and Rego, 2021)

1.4. PROTEIN DEGRADATION IN HUNTINGTON'S DISEASE

1.4.1. AN OVERVIEW OF PROTEIN DEGRADATION PATHWAYS

Intracellular protein degradation is an important intracellular degradative process that maintains intracellular homeostasis through degradation and recycling of toxic macromolecules and damaged organelles (Klionsky and Emr, 2000). Impairment of the protein quality control mechanisms in neuronal cells are a common feature in several NDD, such as AD, PD and HD (Harding and Tong, 2018). In NDD, clearance of misfolded proteins by the proteasome, autophagy pathways and exocytosis is impaired, which leads to accumulation of toxic protein oligomers and aggregates in neurons (Harding and Tong, 2018). Toxic protein species affect various cellular functions resulting, lately, in cell death. In HD the ubiquitin-proteasome system (UPS) and macroautophagy pathways are particularly altered, which favors the accumulation of protein aggregates (Harding and Tong, 2018). These processes occur at basal levels in almost all mammalian cells and can be stimulated in response to starvation, providing the cell with the building blocks for new proteins and lipids. UPS is one major pathway for intracellular monomeric protein degradation. On the other hand, autophagy plays an important role in the clearance of protein aggregates, pathogens and in the regulation of inflammation and immunity, as well as during starvation (Deretic et al., 2013; Okamoto, 2014). Autophagy pathways assume a critical role in neurons, as they are unable to dilute the accumulation of toxic components by cell division, and so may activate programmed cell death in response to the accumulation of misfolded proteins. Therefore, this section summarizes the most important protein degradation pathways and their alterations in HD models.

1.4.1.1. UBIQUITIN PROTEASOME SYSTEM

The UPS is the major pathway in the regulation of intracellular protein degradation. Monomeric proteins are tagged for degradation by the conjugation of a minimum of four ubiquitins in a polyubiquitin chain (Pickart and Fushman, 2004). Ubiquitin, a 76 amino acid protein, tag proteins to degradation by

proteolytic activity, which depends upon the three enzymes E1, E2 and E3 (Finley, 2009). Additional ubiquitins are added to the already conjugated ubiquitin, resulting in a polyubiquitin chain. Lysine residues within ubiquitin are used as sites for additional ubiquitin conjugation (Pickart and Fushman, 2004). The recognized targeting signal is a chain with at least four ubiquitin molecules linked through isopeptide bonds between the C terminus of one ubiquitin and lysine 48 (K48) of the next (Thrower et al., 2000). Beyond K48, ubiquitin chains can be linked through other linkage sites, being K48, K63, and K11 the most common (Xu et al., 2009). After being poly-ubiquitinated, proteins can be delivered to the proteasome in order to be degraded. The 26S proteasome is a multicatalytic protease complex, localized both in the nucleus and the cytoplasm, composed of 19S regulatory and 20S core particles. The 20S core is organized in four heptameric rings, with tryptic, chymotryptic, and peptidylglutamyl proteolytic activities contained in the inner β rings (Pickart and Cohen, 2004). The 19S regulatory cap binds the polyubiquitin chain, removes the ubiquitins, unfolds the substrate, and activates the 20S proteolytic core in an ATP-dependent manner (Smith et al., 2007). The 11S regulatory complex performs an analogous role to the 19S complex, but in a ubiquitin and ATP-independent manner (Rechsteiner and Hill, 2005).

1.4.1.2. MACROAUTOPHAGY

Autophagy can be divided into three main types, according to the delivery of cargo to the lysosome: macroautophagy, microautophagy and chaperone-mediated autophagy (CMA). In macroautophagy, cytoplasmic cargo is engulfed by a growing double-membrane vesicle that after closure (autophagosome) fuses with the lysosome for degradation (autolysosome) (Mizushima, 2007). The process is complex and involves a group of specific autophagy-related proteins acting in a concerted flux, and it can occur randomly (bulk macroautophagy) or selectively through specific adaptors. In microautophagy, the cargo (mostly proteins) is directly internalized through invagination of the lysosome membranes and endosomal vesicles (Ahlberg et al., 1982). Chaperone-mediated autophagy (CMA) is a selective process by which proteins with a specific targeting motif (the pentapeptide KFERQ motif) are recognized by cytosolic chaperone heat shock

cognate 70 (Hsc70) and its co-chaperones, assisting the translocation of cargo into the lumen of lysosomes through lysosomal-associated membrane protein 2A receptor (LAMP2A) (Kaushik and Cuervo, 2012). CMA constitutes an alternative lysosome-mediated degradation pathway that can be upregulated when blockage of macroautophagy occurs (Kaushik et al., 2008). For the scope of this review, macroautophagy and selective autophagy of mitochondria, known as mitophagy, will be further detailed and explored in the context of neuronal function and neurodegeneration **(Figure 1.8).**

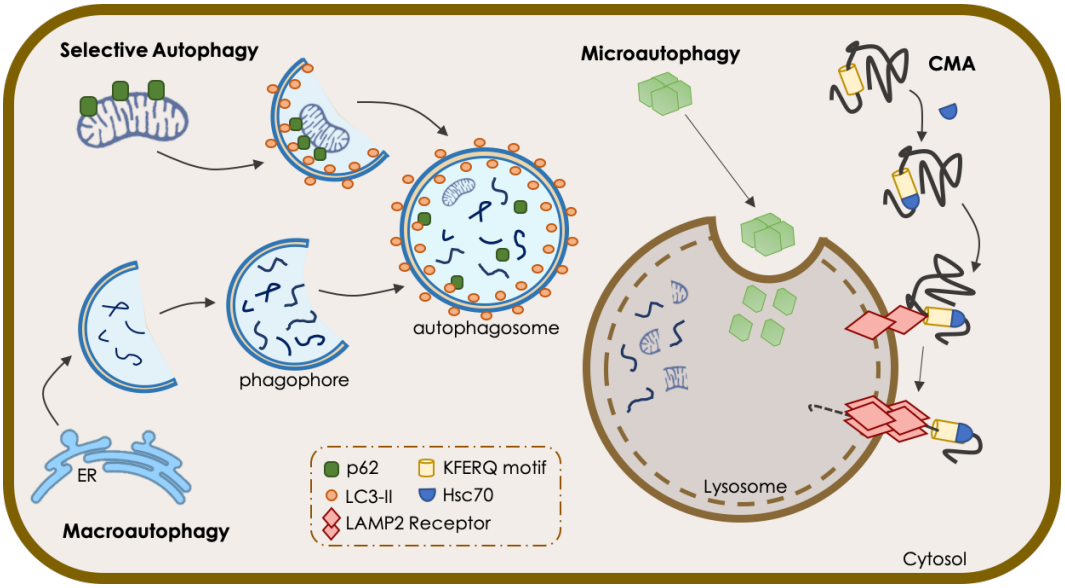

Figure 1.8 | Different types of autophagy. Selective autophagy and macroautophagy initiates with isolation membrane formation and later the phagophore. Through a series of chain reactions, the phagophore sequesters its materials into a double-membraned to form the autophagosome, which, in turn, docks and fuses with the lysosome. In microautophagy the cargo is directly internalized through invaginations in the membranes of lysosomes and endosomes. The chaperone-mediated autophagy (CMA) initiates with recognition of cytosolic proteins carrying KFERQ consensus pentapeptide motifs by the cytosolic HSC70 chaperone and translocated to the lysosome membrane through binding with lysosomal-associated membrane protein type-2A (LAMP-2A), resulting in their internalization and degradation. Adapted from (Magalhães et al., 2021)

Macroautophagy is a complex and sequentially process starting with autophagosome formation and engulfment of cargo, followed by closure and maturation and finally fusion with the lysosome for degradation. Each of these steps involves distinct autophagy-related (ATG) proteins that mechanistically coordinate the autophagic flux along autophagosome biogenesis and fusion with the lysosome (Klionsky, 2007). The initiation of autophagy is regulated by the

phosphorylation status of unc-51 like autophagy activating kinase 1 (ULK1), which is regulated by the upstream mammalian target of rapamycin complex 1 (mTORC1) (Kim et al., 2011). mTORC1 is active in nutrient-rich conditions or when PI3K/Akt pathway is stimulated by growth factors (e.g. IGF1). Active mTORC1 phosphorylates ULK1 and ATG13, components of the ULK1 initiation complex (also composed by ATG101 and FAK family kinase-interacting protein with 200 kDa, FIP200) (Zachari and Ganley, 2017) suppressing autophagy. In nutrient-depleted conditions, mTORC1 is inactivated, facilitating ULK1 autophosphorylation (Hosokawa et al., 2009). Moreover, when the cellular energetic status is low, AMP activates AMPK, which in turn inhibits mTORC1 and phosphorylates ULK1, promoting autophagy (Egan et al., 2011; Hosokawa et al., 2009). Once ULK1 is activated it phosphorylates ATG13 and FIP200, thus activating the entire ULK1 initiation complex (Mercer et al., 2009). After ULK1 complex activation, it translocates to omegasomes (specific regions at the endoplasmic reticulum (ER), initiating phagophore membrane assembly for autophagosome biogenesis (Axe et al., 2008). At omegasomes, ULK1 promotes the recruitment and activation of class III phosphatidylinositol 3-kinase complex (PI3PK, composed by vacuolar protein sorting 34, beclin-1, phosphoinositide-3-kinase regulatory subunit 4 and ATG14L), through phosphorylation of Beclin-1 (Axe et al., 2008; Lamb et al., 2013). PI3PK is responsible for generation of phosphatidylinositol-3 phosphate (PI3P) for phagophore expansion (Russell et al., 2013). The generation of PI3P is essential for the nucleation of the phagophore vesicle, recruitment of PI3P-binding proteins that are involved in phagophore expansion and curvature shaping and recruitment of downstream ATG proteins (Dooley et al., 2014). The recruitment of PI3P effectors like WD-repeat domain phosphoinositide-interacting proteins (WIPIs) to the omegasome is essential for autophagosome biogenesis and autophagic flux (Dooley et al., 2014; Polson et al., 2010). Alfy, a large scaffolding FYVE domain-containing protein, is a PI3P effector that targets ubiquitinated aggregates to the autophagosome thus participating in selective autophagy (Simonsen et al., 2004). The next step is the recruitment of microtubule-associated protein 1A/1B-light chain (LC3) to the phagophore, assisted by ubiquitin-like conjugation systems. Initially, the E1 ubiquitin ligase ATG7 and E2 ubiquitin ligase ATG10 are involved in conjugation of ATG12 to ATG5 that further binds to ATG16L1.

The complex ATG12-ATG5-ATG161L is essential for the recruitment of the LC3 to the PI3P positive membranes (Dooley et al., 2014). First, LC3 is proteolytically cleaved at C-terminal by ATG4 protease forming LC3-I which in turn, through the action of ATG3 and ATG7 and ATG12-ATG5-ATG161L, generates LC3-II through its binding to the amine headgroup of phosphatidylethanolamine (PE) in the phagophore membrane (Fujita et al., 2008b; Kirisako et al., 2000). Such lipidation of LC3 is essential to the expansion and closure of the phagophore and further maturation of the autophagosome (Kabeya et al., 2004). Moreover, lipidated LC3 is involved in specific cargo-recognition via the LIR (LC3 interaction region) domain through selective adaptor proteins (Wild et al., 2014). The phagophore expansion and elongation is poorly defined but the interaction of WIPI2 with ATG9 enriched vesicles is essential for the process (Orsi et al., 2012). Recent work showed that additional ATG proteins are involved in the final steps of autophagosome biogenesis, but their exact roles are not clearly defined yet. Studies showed that defects in LC3 ubiquitin-conjugation systems impaired autophagosome closure (Fujita et al., 2008a; Mizushima et al., 2001) implying these complexes in the final steps of autophagosome biogenesis. The closure of autophagosome vesicle is mediated by the endosomal sorting complex required for transport (ESCRT) machinery (Yu and Melia, 2017). After the closure, autophagosome dissociates from ER and its maturation proceeds through interaction with multiple endocytic vesicles. Dephosphorylation of PI3P at the autophagosome membrane by phosphoinositide 3-phosphatases of the myotubularin protein family is required prior to their fusion with lysosomes (Taguchi-Atarashi et al., 2010) **(Figure 1.9).**

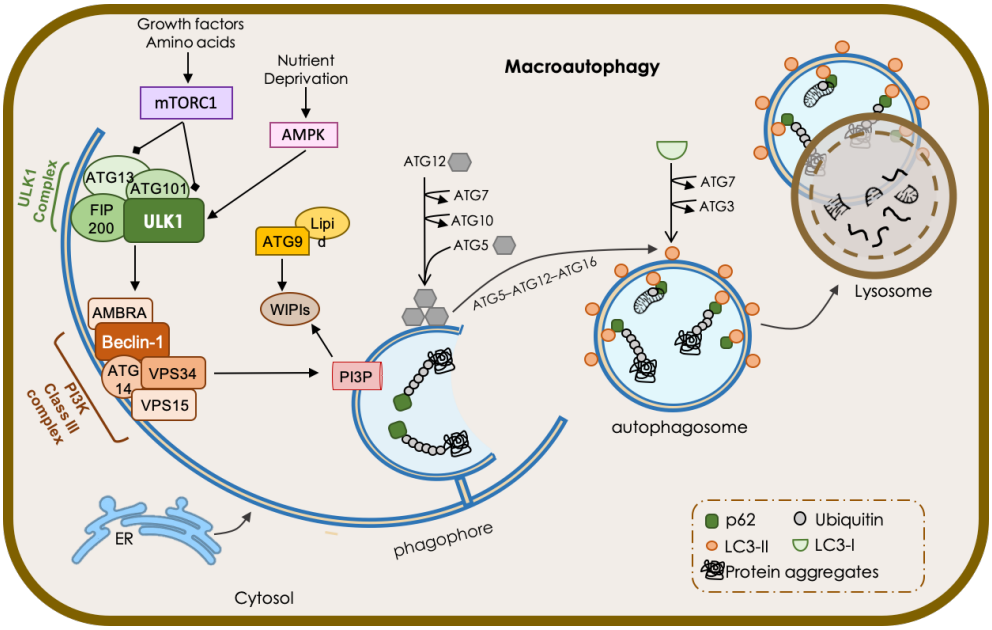

Figure 1.9 | Overview of macroautophagy machinery. Nutrient deprivation and cellular stresses induce mTORC1 inhibition and AMPK activation, which, in turn, activate the ULK1 complex. ULK1 complex positively regulation subsequently activates phosphatidylinositol 3-kinase (PI3K), which leads to PI3P synthesis in phagophore and initiates autophagy. The sources of membrane for phagophore nucleation and expansion can be varied, from ER membrane, Golgi apparatus, trans-Golgi network (TGN), plasma membrane, endosomal compartment to mitochondria. Two ubiquitin-like conjugation systems, the Atg12–Atg5–Atg16L1 complex and LC3-II, participate in the expansion and closure of the phagophore. Once it is completed, the autophagosome can fuse with lysosome to form an autolysosome, resulting in the degradation of autophagic substrates. Adapted from (Magalhães et al., 2021)

1.4.1.3. MITOPHAGY

The elimination of defective mitochondria is an essential quality control mechanism to sustain a healthy pool of mitochondria and maintain a viable network in neuronal cells (Martinez-Vicente, 2017). These cells are more sensitive to mitochondrial defects due to their high metabolic demands; thus, the selective elimination of dysfunctional organelles is vital for reliable neurotransmission. Mitochondria that are irreversibly damaged or become no longer efficient are eliminated by mitophagy, a selective mechanism where specialized receptors recognize flawed mitochondria and mediate cargo targeting to autophagic vesicles (Pickles et al., 2018).

Cells make use of different methods to recycle defective mitochondria, namely ubiquitin-dependent and independent pathways. Majorly, neuronal cells resort to the ubiquitin-dependent mechanism system controlled by PTEN-induced

kinase 1 (PINK1)/Parkin to preserve an active and dynamic pool of mitochondria. PINK1 is a mitochondrial protein whose accumulation in the OMM acts as a sensor for maintaining mitochondrial function, since it flags damaged mitochondria for degradation (Pickrell and Youle, 2015). PINK1 exhibit a mitochondrial-targeting sequence thus being systematically imported to the IMM by complexing with translocases of the outer membrane 20 and 40 (TOM20 and TOM40) (Lazarou et al., 2012), where it is cleaved by the intramembrane serine protease presenilin-associated rhomboid-like (PARL) (Deas et al., 2011) and therefore maintained at low levels under physiological conditions. Upon a given damage, the molecular interactions between TOM20/40 and PINK1 decrease and PINK1 clusters in the OMM of damaged mitochondria, promoting Parkin phosphorylation and its subsequent recruitment (Kondapalli et al., 2012). Parkin, a cytosolic E3 ubiquitin ligase, ubiquitinates a myriad of proteins of the OMM, which are recognized by receptors such as p62, also denominated sequestosome 1 (SQSTM1). p62/SQSTM1 is the ubiquitin-binding receptor responsible for driving ubiquitinated mitochondria to the autophagosome assembly site by interacting with the ATG8 family LC3/GABARAP receptors (Pankiv et al., 2007). These receptors also recognize LIR motifs of many OMM proteins for specific targeting of damaged mitochondria to the autophagosome assembly site (Birgisdottir et al., 2013) **(Figure 1.10).**

In neuronal cells, ubiquitin-independent mitophagy orchestrated by two bi-functional proteins, BCL2 and adenovirus E1B 19 kDa-interacting protein 3 (BNIP3L) and BNIP3-like protein X (NIX), is also responsible for the differentiation of retinal ganglion cells (RGCs). BNIP3 and NIX contain a BH3 domain and are mainly located at the OMM. These proteins have a WXXL-like motif with affinity for LC3 and its homologue GABARAP, driving mitochondria to autophagic vesicles. During retinal neurogenesis, a metabolic shift takes place, accompanied by an increase in the expression of both proteins (Esteban-Martínez and Boya, 2018). NIX activity can be mediated by increasing ROS levels in several cell lines (Ding et al., 2010) adding a new layer of complexity apart from developmental functions. Indeed, ROS production increases as a consequence of damaged mitochondria (Stefanatos and Sanz, 2018) and can induce mitophagy (Shefa et al., 2019). NIX can also regulate the translocation of Parkin to mitochondria upon a depolarizing stimulus, such as CCCP (Ding et al., 2010). In addition, BNIP3L

and NIX-regulated mitophagy has neuroprotective functions. In a model of brain ischemia, the selective degradation of mitochondria mediated by these proteins was crucial for neuronal survival and function (Yuan et al., 2017). Also, NIX overexpression alone is sufficient to restore mitophagy defects observed in cell lines derived from PD patients (Koentjoro et al., 2017).

Fun14 domain-containing protein 1 (FUNDC1) is an OMM protein that interacts with LC3 and GABARAP and mediates mitophagy in hypoxic conditions. At homeostatic levels, FUNDC1-dependent mitophagy is repressed by Src kinase-mediated phosphorylation in the moiety of the LIR motif at Tyr18. In a hypoxic state, reduced Src activity results in FDUNC1 Tyr18 dephosphorylation, facilitating its interaction with LC3 and subsequent mitophagy (Liu et al., 2012). Moreover, hypoxia-driven phosphorylation of ULK1 by AMPK at Ser555 favours ULK1 translocation to the mitochondria, enhancing FUNDC1 activity (Shefa et al., 2019). Additionally, Optineurin (OPTN) is a cytosolic receptor located at the OMM that promotes mitophagy through its interaction with LC3 (Wong and Holzbaur, 2014a). Interestingly, OPTN dysfunction is associated with neurodegenerative diseases, as well as other pathologies (Weil et al., 2018). Overall, mitophagy constitutes an essential quality control mechanism for maintaining neuronal metabolism and homeostasis. The transport of mitochondria within neurons relies on anterograde and retrograde movements and is essential to fulfil the energetic and metabolic requirements along the neuronal structure. These movements are also essential for mitochondrial repair and degradation and are assisted by transport adaptor proteins.

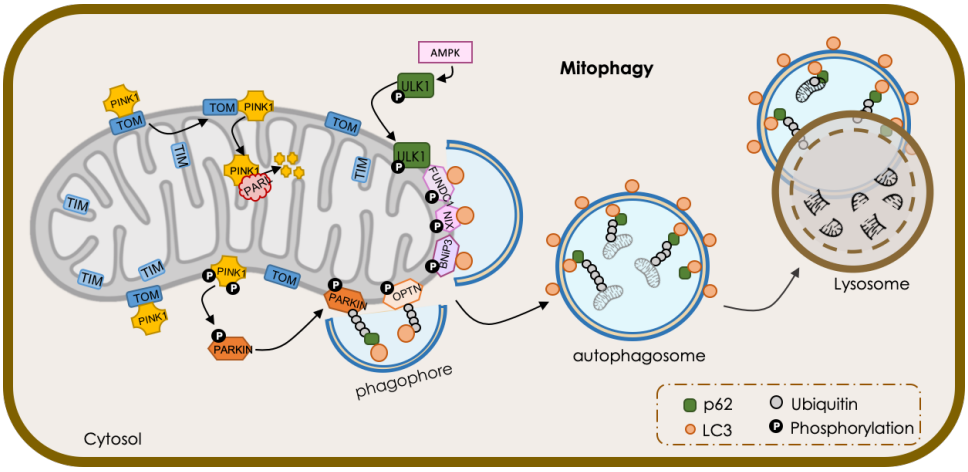

Figure 1.10 | Overview of mitophagy machinery. Dysfunctional mitochondria stabilize PTEN-induced kinase 1 (PINK1) in the outer mitochondrial membrane (OMM) while its proteolytic cleavage through presenilin-associated rhomboid-like (PARL) proteases is blocked. Concurrently, PINK1 recruits Parkin through a series of modifications, such as phosphorylation of both Parkin and ubiquitin. Polyubiquitinated proteins are recognized by several adaptor molecules, including p62 and optineurin (OPTN), anchoring mitochondria to nascent phagophore through microtubule associated light chain 3 (LC3) binding. Receptor-mediated mitophagy relies on various OMM proteins such as BCL2 Interacting Protein 3 (BNIP3), BNIP3-like protein X (NIX), and FUN14 domain-containing protein 1 (FUNDC1). After elongation is completed, autophagosome fuses with lysosome for degradation of dysfunctional mitochondria. Adapted from (Magalhães et al., 2021)

1.4.2. UBIQUITIN PROTEASOME SYSTEM IN HUNTINGTON'S DISEASE

UPS involvement in HD pathology was initially proposed when nuclear polyQ inclusions were positively labeled by antibodies against ubiquitin in post-mortem brains of HD patients and in different cellular and animal HD models (DiFiglia et al., 1997; Gutekunst et al., 1999). In subsequent studies, it was found that the proteasome could not digest expanded polyglutamine sequence efficiently, but only cut the flanking basic residues (Venkatraman et al., 2004), suggesting that expanded polyQ tracts or aggregated proteins could not be digested by the UPS, resulting in an impairment of the function of the UPS. Transfected PC12 cells that co-express N-terminal Htt with a normal (23Q) and expanded (76Q) polyQ showed N-terminal mHtt fragments accumulated via inhibition of the UPS (Li et al., 2010). Moreover, Bennett and coworkers showed that production of protein aggregates specifically targeted to either the nucleus or cytosol led to global impairment of UPS function in both cellular compartments,

which was independent of sequestration of protein aggregates (Bennett et al., 2005). Concordant results were obtained in HD mouse models. Despite whole cell homogenates of brain tissues did not detect reduced UPS activity in HD mouse brains (Díaz-Hernández et al., 2003; Wang et al., 2008), Lys 48-linked polyubiquitin chains accumulated early in HD mouse brains (Bennett et al., 2007). Additionally, as referred before, mHtt can induce mitochondrial dysfunction, leading to reduced ATP levels in HD synapses and contributing to reduced activity of synaptic UPS seen in HD mouse brains (Orr et al., 2008; Wang et al., 2008).

1.4.3. AUTOPHAGY IN HUNTINGTON'S DISEASE

Two putative KFERQ-like CMA-targeting motifs were identified in the HTT protein: one at amino acids 99–103 (KDRVN), and one at amino acids 248–252 (NEIKV). Upon phosphorylation at Ser16, the very N-terminus (14-LKSFQ-18) is considered a KFERQ-like third motif (Qi et al., 2012). While normal HTT is degraded by the UPS, polyQ-HTT is a target for CMA-degradation, since purified intact lysosomes showed mHTT fragments in a LAMP2A-dependent manner (Qi et al., 2012). However, CMA-dependent mHTT degradation is less efficient. This may be explained by polyQ expansion-mediated delay of mHTT CMA transport across the lysosomal membrane, leading to accumulation in the cytosol. Furthermore, LAMP2A and Hsc70 can strongly interact with polyQ-HTT, which results in CMA pathway traffic blockage (Qi et al., 2012). However, LAMP2 mRNA expression is increased in the caudate nucleus of HD patients (Koga et al., 2011), which is consistent with increased levels of LAMP2 protein and concomitant induction of CMA in HD patient cells and mouse models (Koga et al., 2011), suggesting an attempt to increase the activity of this system. Indeed, full-length polyQ-HTT is primarily targeted to macroautophagy, whereas N-terminal fragments of HTT can be selectively targeted to CMA (Müller et al., 2015). Interestingly, R6/2 HD mice showed diminished inclusion formation and improved HD phenotypes after N-terminal mHTT fragment target to the CMA pathway. Furthermore, clearance of phosphorylated N-terminal fragments of polyQ-HTT

depends on LAMP2A and Hsc70 proteins (Thompson et al., 2009). Fibroblasts from HD patients, striatal *Hdh* knock-in cells and pre-symptomatic HTT Q111 knock-in mice showed augmented CMA activity (Koga et al., 2011). This increase in CMA activity was not sustained when aged mice became symptomatic. Moreover, a significant decrease in LAMP-2A staining was detected in older HTT Q111 knock-in mice (Koga et al., 2011). Since LAMP-2A localization and CMA activity is regulated by lipid composition at the lysosomal membrane, and altered lipid metabolism occurs in HD (Martinez-Vicente et al., 2010), modifications in lipid homeostasis might contribute to HD dysfunction in CMA. Thus, to compensate for malfunctioning macroautophagy pathway, HD neurons might upregulate CMA. However, CMA-competent lysosomes are less efficient at degrading substrates over time, while polyQ-HTT interferes with LAMP-2A and Hsc70 cargo uptake.

As an attempt to maintain the normal proteostasis, since UPS-mediated protein degradation and CMA fails, macroautophagy may be upregulated in HD (Pandey et al., 2007). PolyQ-HTT is targeted for autophagic clearance, suggesting selectivity of macroautophagy towards pathogenic HTT (Ravikumar, 2002). However, UPS and autophagy degradation pathways are significantly compromised in HD, which results in polyQ-HTT aggregates accumulation, ultimately leading to neuronal dysfunction and death (Cortes and La Spada, 2014). Furthermore, progressive failure of degradation pathways and proteostasis lead to accumulation of damaged organelles such as mitochondria and ER. Interestingly, in addition to polyQ-HTT aggregates being a substrate for autophagy-mediated degradation, HTT protein is further involved in autophagy pathway regulation (Kegel et al., 2000), as described below in this section. Moreover, HTT has a role in axonal transport of autophagosomes, as suggested by live-cell imaging studies in striatal neurons. After both loss of HTT or expression of mHTT, decreased autophagosome transport and subsequent inhibition of substrate degradation were observed (Wong and Holzbaur, 2014b).

Brain biopsies from HD patients showed significant abnormalities in compartments of the vesicular-endocytic pathway, with abnormal proliferation of multivesicular bodies, endosomes and lysosomes, accompanied by disruption of the Golgi apparatus and disorganization of the ER (Tellez-Nagel et al., 1974). Concordantly, striatal neurons in brains from HD patients stained for HTT,

showed significant increases in endosome-lysosome-like organelles and HTT-positive tubulovesicular structures (Sapp et al., 1997).

Normal HTT acts as a scaffold protein to selective autophagy, since HTT can physically interact with p62 in order to facilitate its association with LC3-II and ubiquitinated substrates. HTT can also bind to ULK1, releasing ULK1 from negative regulation by mTOR (Rui et al., 2015). Indeed, ULK1 was shown to have reduced activity in HD cellular and animal models (Q175) (Antonioli et al., 2017; Wold et al., 2016). Moreover, HTT can contribute to microtubular transport of autophagosomes that is essential for autophagosome-lysosome fusion (Wong and Holzbaur, 2014b). Indeed, different cell types, such as primary neurons, striatal cell lines, fibroblasts and hepatocytes from two HD mouse models, and lymphoblasts derived from HD patients showed increased number of autophagic vacuoles without an augmented autophagy-mediated degradation (Martinez-Vicente et al., 2010). Additionally, two HD mouse models, R6/2 and YAC128 mice (described in section 1.1.5.1) showed specifically increased levels of the autophagy markers p62 and LC3-II in the striatum at later age (18 months) (Lee et al., 2012), suggesting deficit(s) in autophagy-mediated protein degradation. Conversely, polyQ-HTT aggregates can sequester mTOR, leading to autophagy induction (Ravikumar et al., 2004). One possible explanation for this contradiction is a substantial alteration in macroautophagy cargo recognition in HD cells, which results in ‘empty’ autophagosomes formation (Martinez-Vicente et al., 2010). Autophagosomes have reduced amount of cytosolic cargo inside, possibly due to abnormal p62–polyQ-HTT interaction, leading to reduced protein degradation rate in HD samples (Martinez-Vicente et al., 2010), which can result in serious deleterious effects on cell homeostasis and consequent neuronal loss. Compensatory activation of macroautophagy in response to polyQ-HTT aggregates may be an important approach to HD neuron survival. Definitely, organelles are turned over by macroautophagy, requiring the recognition of targeted membranes by the autophagy machinery. Because polyQ-HTT can interact with different organelle membranes (Kegel et al., 2000; Ravikumar et al., 2004), it is possible that polyQ-HTT interferes with organelle recognition by autophagic vacuoles. Concordantly with this hypothesis, HD cells show accumulation of defective mitochondria, which suggest that compromised mitochondria are not efficiently recognized or marked up to autophagy.

Furthermore, polyubiquitination is another way for protein aggregates to be degraded by macroautophagy and polyQ-HTT can bind to polyubiquitinated protein aggregates, which can restrict their recognition by the autophagy system (Ravikumar, 2002).

Several studies revealed that HTT interacts with autophagy-associated proteins indirectly influencing the autophagy pathway. Clearance of polyubiquitinated inclusions are mediated by the selective autophagy receptor, p62, which can exist in polyubiquitinated mHTT aggregates (Nagaoka et al., 2004). A shell of p62 and LC3 proteins can surround mHTT aggregates to promote recruitment to autophagosomes, whereas p62 knock-down leads to augmented cell death in the presence of mHTT (Bjørkøy et al., 2005). p62 expression levels are diminished in the HD R6/1 mouse model brain, as a result of decreased protein synthesis, at the early stage of the pathology. However, at late stages, p62 accumulates in the striatum and hippocampus (Rué et al., 2013). ST*Hdh*$^{Q111/Q111}$ striatal cells, derived from HD knock-in mice, also showed increased p62 levels, in response to proteotoxic stress (Huang et al., 2018). Thus, p62 can bind mHTT aggregates and progressively accumulate in HD mice and patient's cell nuclei, contributing to the onset of HD symptoms. Previously, Kurosawa and colleagues, revealed that genetic p62 depletion in three HD mouse models (R6/2, HD190QG and HD120QG mice) improved HD phenotypes and life expectancy, showing reduced nuclear inclusions and increased cytoplasmic inclusions of mHTT. These data suggest that p62 genetic ablation in HD mice interrupts autophagic clearance of polyQ inclusions, reducing polyQ nuclear influx and ameliorating disease phenotypes by decreasing toxic nuclear inclusions (Kurosawa et al., 2015).

The selective autophagy receptor NBR1, which sequestrates protein aggregates, shares similar function and structure with p62 and has been shown to interact with p62 (Lamark et al., 2003). As explained before, mHTT forms nuclear inclusions with p62, leading to neurotoxicity. In contrast to what happens with p62, NBR1 does not accumulate within neuronal nuclei or at late stage of HD in mice or patients (Rué et al., 2013), suggesting that NBR1 may take over p62 nuclear accumulation, to maintain some basic rate of selective macroautophagy. The adaptor protein autophagy-linked FYVE protein (ALFY) acts as a scaffold for aggregates, p62, and the autophagosome and has a central

role in the autophagic degradation of mHTT aggregates (Filimonenko et al., 2010). Concordantly, ALFY mRNA expression is decreased in the caudate nucleus of HD patients (Isakson et al., 2013). The autophagy adaptor OPTN can also act as an autophagy receptor, which recognises and promotes autophagic clearance of protein aggregates (Ryan and Tumbarello, 2018). OPTN enables intranuclear mHTT inclusion clearance via selective autophagy (Mori et al., 2012). Intriguingly, OPTN shows a cell-specific expression pattern in striatum, which is related with the neuronal loss pattern in this HD brain region (Okita et al., 2012). Moreover, OPTN overexpression reduced mHTT aggregation via increased selective autophagy (Shen et al., 2015). Toll-interacting protein (Tollip) is another selective autophagy cargo receptor protein with protein aggregate clearance function (Lu et al., 2014a). A study using the stable Neuro2a cell line expressing mHTT (HD60Q and HD150Q) showed that Tollip associate with mHTT derived N-terminal peptides, stimulating their aggregation and enhancing their clearance via autophagy, protecting the cells from proteotoxicity (Oguro et al., 2011). Additionally, R6/2 mouse striatum and cortex showed Tollip protein in nuclear inclusions (Doi et al., 2004). As estimated, Tollip depletion led to cell death, while Tollip overexpression enhanced aggregate clearance (Lu et al., 2014b). Thus, by acting as a mediator of selective autophagy associated with HD, Tollip might be a good candidate for a HD therapeutic strategy.

Beclin 1 is a major autophagy regulator, which levels are reduced with aging. Beclin 1 can be recruited to mHTT aggregates, reducing its activity, further contributing to autophagy dysfunction in HD (Shibata et al., 2006). A study from Ashkenazi and colleagues, using the HD-N171-82Q mice (expressing the first 171 amino acids of human HTT) and primary fibroblasts from HD patients, showed that mHTT outcompetes ataxin 3 in binding Beclin 1, avoiding its activation (Ashkenazi et al., 2017). Rhes is a striatal-specific protein and a Beclin 1 activator that recruits Beclin 1 away from Bcl-2, preventing its inhibitory action. However, mHTT can inhibit Rhes interaction with Beclin 1, reducing its role in promoting autophagy (Mealer et al., 2014). Conversely, Beclin 1 overexpression increased mHTT aggregates clearance and reduced neuronal damage (Shibata et al., 2006). Expression of Beclin-1 show an age-dependent decrease in human brain (Shibata et al., 2006) and in HD patient's fibroblasts (Ashkenazi et al., 2017), as well as age-related decreased trafficking of the lysosomal protein

LAMP2 (Kaushik et al., 2008). Remarkably, R6/2 HD transgenic mice and HD patients brains showed Beclin-1 accumulation into polyQ-HTT inclusions (Shibata et al., 2006).

PolyQ-HTT aggregates also sequestered mTOR, as observed in COS-7 cells expressing mutant (Q74) huntingtin exon 1, brain tissue of mice expressing mHTT (Q82) and brain tissue from HD patient's caudate and putamen (Ravikumar et al., 2004). Additionally, ULK1 activity was decreased in the brains of zQ175 HD mice, since ULK1 substrates such as Beclin-1 and ATG14 are less phosphorylated, together with the redistribution of ULK1 to an insoluble fraction where aggregated mHTT was found (Wold et al., 2016). Moreover, Metzger and coworkers showed that the V471A polymorphism in ATG7 is related to an earlier onset form of HD (Metzger et al., 2010).

TFEB is a master regulatory transcription factor of the autophagy-lysosome pathway (lysosomal biogenesis and autophagy), which was shown to be upregulated by peroxisome proliferator-activated receptor-gamma coactivator (PGC)-1alpha (Tsunemi et al., 2012), a member of transcription coactivators that plays a central role in the regulation of cellular energy metabolism, mitochondrial biogenesis and adaptive thermogenesis. N171-82Q HD transgenic mice showed abnormal TFEB expression and activity, suggesting that TFEB signaling is impaired in HD (Tsunemi et al., 2012). Concordantly, TFEB can promote polyQ-HTT clearance (Tsunemi et al., 2012), which emphasizes TFEB as a possible therapeutic target for HD or other diseases with protein aggregates accumulation.

1.4.4. MITOPHAGY IN HUNTINGTON'S DISEASE

Previous studies reported ultrastructural defects in mitochondria isolated from post-mortem HD cortical tissue and compromised oxidative function and ATP synthesis in pre-symptomatic HD carriers (Saft et al., 2005), suggesting that mitochondrial dysfunction is an early relevant pathogenic mechanism. HD mutant cells and striatal and cortical neurons isolated from YAC128 transgenic mice presented altered mitochondrial bioenergetics, including pyruvate dehydrogenase (PDH) dysfunction (Naia et al., 2017a), as well as $\Delta\psi$m

deregulation (Naia et al., 2017b), augmented mitochondrial ROS production (Ribeiro et al., 2014) and increased Ca^{2+} uptake in isolated mitochondria from pre-symptomatic R6/2 and YAC128 mouse forebrain (excluding the cerebellum) (Oliveira et al., 2007). Abnormal elimination of dysfunctional mitochondria observed in HD suggests an impairment in mitophagy (described in section 1.3). Levels of basal mitophagy were seen to be reduced in the dentate gyrus (DG) region of HD mice crossed with the mito-Keima mouse line (Sun et al., 2015). Moreover, a recent study showed that mitophagy is affected in ST*Hdh*$^{Q111/Q111}$ striatal cells (Franco-Iborra et al., 2020). These authors showed that mHTT affects the initiation of the mitophagy process, as well as the recruitment of mitophay receptors and its interaction with LC3-II during mitophagy (Franco-Iborra et al., 2020).

As explained earlier, PINK1-Parkin-mediated mitophagy starts with PINK1 stabilization at the OMM of damaged mitochondria to recruit Parkin. In the caudate nucleus of HD patients, mRNA expression of PINK1 is significantly decreased (Kamat et al., 2014). Augmented mitochondrial fragmentation (Costa et al., 2010) and inefficient incorporation of mitochondria into autophagosomes (Wong and Holzbaur, 2014b) are HD features, thus decreased PINK1 may exacerbate the dysfunctional autophagosome recruitment in HD cells. Concordantly, PINK1 overexpression in HD flies and ST*Hdh*$^{Q111/Q111}$ cells proved to be protective in these models (Khalil et al., 2015). Moreover, juvenile HD fibroblasts showed increased Parkin levels (Aladdin et al., 2019). Although there is some lack of information regarding the alterations in PINK1/Parkin-dependent mitophagy in HD, its activation may constitute an interesting therapeutic approach. Moreover, mHTT can interact with Drp1, resulting in increased Drp1 GTPase activity and consequently increased mitochondrial fission, causing reduced mitochondrial function (Song et al., 2011). Recently, Aladdin and co-workers showed that skin fibroblasts from juvenile HD patients had significantly lower levels of mitochondrial fusion and fission proteins and reduced branching in the mitochondrial network. Furthermore, juvenile HD fibroblasts revealed higher proteasome activity, which was associated with elevated gene and protein expression of Parkin, as well as increased proteasomal degradation of the mitochondrial fusion protein Mfn1 in diseased cells (Aladdin et al., 2019). These data suggest that expansion of mHTT is linked to increased proteasomal activity

and faster turnover of specific substrates of ubiquitin-proteasome system in order to protect cells, which could contribute to altered mitochondrial dynamics in early phases of the disease.

1.5. SYNAPTIC DYSFUNCTION IN HUNTINGTON'S DISEASE

There is a clear evidence for altered dendrite morphology in MSNs of HD patients, showing recurved endings and appendages, altered spine density and abnormalities in the size and shape of spines, or even their complete absence (Graveland et al., 1985). Concordantly, some HD mouse models such as the R6/2 (Klapstein et al., 2017), YAC72 (Hodgson et al., 1999) and YAC128 (Milnerwood et al., 2010; Slow, 2003) mice show early and significant changes in striatal somato-dendritic morphology, reduced dendritic fields and somatic areas, decreased dendritic spine density and length in striatal MSNs and cortical pyramidal neurons, indicating dysfunctional synaptic connections and neurons, possibly contributing for striatal neuronal loss. Murmu and coworkers showed that mHTT in R6/2 mice causes a progressive loss of persistent-type spines, important for neuronal circuitry and long-term memory in the brain (Murmu et al., 2015, 2013). Interestingly, HD knock-in mice with 140Q presented reduced number of thalamo-striatal synapses as early as 1 month of age and impaired cortico-striatal synapse at 12 months of age (Deng et al., 2013). However, the mechanism by which mHTT drives initial selective neurodegeneration remains so far elusive.

N-methyl-D-aspartate receptor (NMDAR) are important postsynaptic receptors that contribute to normal synaptic function and cell survival. In this section we discuss, in more detail, NMDARs involvement in HD and synaptic dysfunction.

1.5.1. NMDA RECEPTORS IN HUNTINGTON'S DISEASE

1.5.1.1. NMDA RECEPTORS FUNCTION

NMDARs are cationic channels stimulated to open by the neurotransmitter glutamate. After glutamate binding, it requires a sufficient postsynaptic

depolarization (favored by pre-activation of high-affinity and Na^+-permeable α-amino-3-hydroxy-5-methyl-4-isoxazolepropionic acid (AMPA) receptors) to remove the Mg^{2+} blocker ion from the channel, resulting in mostly Ca^{2+} entry, but also sodium (Na^+) and potassium (K^+) (MacDermott et al., 1986) (**Figure 1.11).** NMDARs are crucial ionic channels for several events, namely excitatory transmission, synaptic integration, learning and memory in the CNS (Mota et al., 2014, for review). NMDARs are hetero-tetramer channels comprised by two required GluN1 subunits and two modulatory GluN2 or GluN3 subunits (Cull-Candy et al., 2001). GluN2 subunit has different subtypes, namely GluN2A, B, C or D, with different spatial and temporal patterns of expression (Zhang et al., 2016) **(Figure 1.11).** Reduced expression and activity of GluN2B subunits contributes to cognitive decline, exhibiting impaired long-term potentiation (LTP) and memory (Brigman et al., 2010).

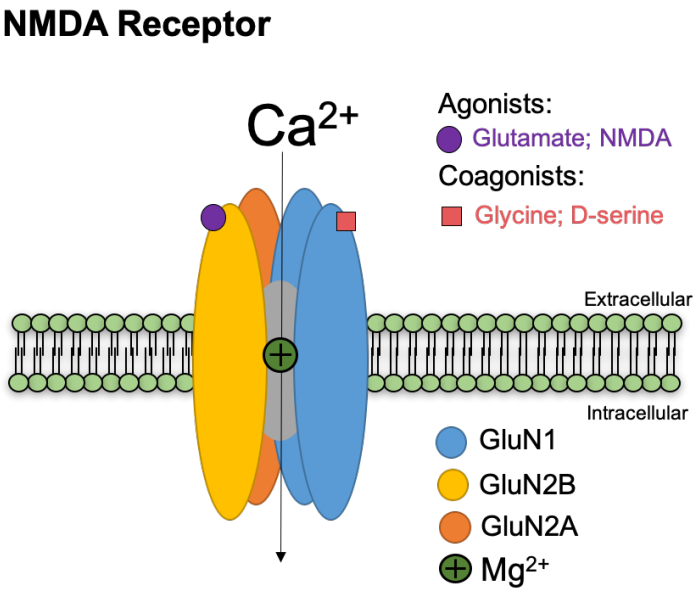

Figure 1.11 | Scheme of the NMDA receptor. NMDARs are composed by two obligatory GluN1 subunits and two modulatory GluN2(A-D) or GluN3(A-B) subunits – the scheme shows the most frequent GluN2A,B composition. When stimulated by glutamate, or NMDA (selective pharmacological agonist), in the presence of glycine or D-serine (co-agonists), the Mg^{2+} ion is removed if under depolarized conditions, which results in the opening of the channel, allowing the Ca^{2+} (mainly) and Na+ influx and K^+ outflux.

NMDARs can have both synaptic or extrasynaptic localization. The activation of extrasynaptic NMDARs requires higher glutamate concentrations and these receptors are located on dendrites or the sides/neck of spines (Oliet and Papouin, 2014). Synaptic NMDARs are inhibited by D-serine degradation,

decreasing LTP, while glycine degradation has no effect on LTP, suggesting that synaptic NMDARs play a key role on LTP, in contrast with extrasynaptic receptors (Papouin et al., 2012). Nevertheless, both synaptic and extrasynaptic NMDARs are crucial for long-term depression (LTD) (Newpher and Ehlers, 2009; Papouin et al., 2012). In this way synaptic NMDARs seem to be neuroprotective, whereas stimulation of extrasynaptic NMDARs cause loss of mitochondrial membrane potential and cell death (Zhang et al., 2016).

Indeed, synaptic NMDAR activation is associated with augmented CREB-dependent gene expression. CREB is a signal-regulated transcription factor, important for neuronal survival with important roles in several processes, such as synaptic plasticity, addiction, neurogenesis, learning and memory, which binds to the cAMP response element (CRE) promoter sequence of its target genes, upon phosphorylation at Ser133 by protein kinase A (PKA), required to recruit CREB binding protein (CBP) and initiate transcription (Alberini, 2009). Beyond PKA, CREB can be phosphorylated at Ser133 by Akt, PKC, calcium/calmodulin-dependent protein kinase II (CaMKII), p90 ribosomal S6 kinase (p90RSK), casein kinase I, and casein kinase II (Trinh et al., 2013; Wen et al., 2010). Moreover, CBP acts as a transcriptional co-activator with histone acetyl transferase activity, and thus CBP-induced CREB acetylation also increases its transcriptional activity. Activated CREB promotes the expression of survival-related genes, including brain-derived neurotrophic factor (BDNF), which has neuroprotective properties and can rescue neurons from NMDAR blockade-induced neuronal death (Hansen et al., 2004). In contrast, extrasynaptic NMDARs activation promotes cell death pathways (e.g. dendritic blebbing, loss of mitochondrial membrane potential and CREB shutoff pathway, reducing BDNF expression) (Hardingham et al., 2002).

1.5.1.2. mHTT-INDUCED NMDA RECEPTORS ALTERED FUNCTION

Before the identification of the *HTT* gene in 1993, several studies showed that injection of quinolinic acid, a NMDAR agonist, in the striatum caused selective loss of MSNs, mimicking many behavioral and neuropathological characteristics observed in HD patients (Beal et al., 1991). Although these experiments were merely based on excitotoxic events, they were key on

identifying the susceptibility of striatal dendrites. Supporting this notion, different HD mouse models and HD patient post-mortem brains show impaired glutamate uptake (Hassel et al., 2008; Miller et al., 2012), for which reduced glutamate transporter 1 (GLT1) levels in astrocytes may contribute, enhancing extracellular glutamate levels (Estrada-Sánchez and Rebec, 2012; Faideau et al., 2010).

Studies performed by Lynn Raymond's and Michael Hayden's groups demonstrated that expression of HTT-138Q, but not HTT-15Q, in HEK293 cells transfected with cDNAs encoding GluN1, GluN2 (A or B) resulted in NMDAR activation. Interestingly, the potentiating effect of HTT-138Q was selective for the GluN1/GluN2B NMDAR subunits, but not for the GluN1/GluN2A NMDAR subunits (Chen et al., 1999). Still using HEK293 cells, it was demonstrated that HTT-138Q expressing cells were more sensitive to NMDA-induced apoptosis, particularly in the presence of GluN1/GluN2B NMDAR subunits (Zeron et al., 2001). The specificity of mHTT effects on NMDAR subtypes is specifically important since MSN express mostly GluN1/GluN2B NMDAR subunit combinations (Landwehrmeyer et al., 2018; Portera-Cailliau et al., 2010). Moreover, GluN2B-containing NMDARs present increased permeability to calcium, which can induce dramatic effects on intracellular calcium signals in MSNs (Monyer et al., 1994). We previously showed that striatal neurons from YAC128 mice, almost exclusively composed by GABAergic neurons, exhibit delayed intracellular calcium recovery and immediate calcium deregulation following NMDAR activation, which was linked to altered mitochondrial-dependent calcium handling, evidencing NMDAR-dependent HD striatal neuronal dysfunction (Oliveira et al., 2006).

Heng and colleagues demonstrated that double-mutant mice, expressing HTT-150Q and overexpressing GluN2B NMDAR subunits presented exacerbation of selective striatal neurodegeneration, evidencing the role of GluN2B-composed NMDAR-mediated excitotoxicity and striatal atrophy in HD (Heng et al., 2009). However, the available data concerning NMDAR-subunits in HD models is not consistent. In human post-mortem HD brain tissue, radioligand-binding studies showed a loss of NMDARs in the striatum of HD patients in early symptomatic or in pre-symptomatic stages of the disease, suggesting that neurons expressing high levels of NMDARs are most vulnerable and are lost during disease progression (Young et al., 1988). Furthermore, R6/2 mice in pre-

symptomatic and early symptomatic stages showed decreased GluN2A mRNA levels (Ali and Levine, 2006). Concordantly, YAC72 mice exhibited increased GluN2B/GluN2A ratio in the striatum, when compared to cortex or hippocampus (Li et al., 2003). However, GluN1 and GluN2B total expression levels were not significantly different in striatal neuronal lysates from YAC46 or YAC72 mice at 2 months of age, suggesting that mHTT does not influence transcription or translation of NMDARs at this early age (Li et al., 2003). Studies in a different model of HD (N171-82Q) showed unchanged levels of striatal GluN1 and GluN2B subunit expression at either pre-symptomatic or symptomatic stages, while a transient decrease was noted for GluN2A protein expression at the pre-symptomatic stage (Jarabek, 2003). Altered surface levels of NMDARs may provide an explanation for the enhancement of NMDAR-mediated currents and toxicity observed in HD models. In fact, Fan and colleagues performed co-immunoprecipitation experiments and showed that YAC72 mouse MSNs have an increased proportion of GluN1 C2' isoforms associated with GluN2 subunits, which may result in a faster rate of NMDAR insertion to the surface in HD YAC72 mice (Fan et al., 2007).

Likewise, Milnerwood and coworkers found that YAC128 mice have increased extrasynaptic GluN2B-containing NMDAR expression and currents (Milnerwood et al., 2010). These authors showed that application of DL-threo-beta-benzyloxyaspartate (DL-TBOA), a GLT1 transport inhibitor that enhances glutamate spillover to extrasynaptic receptors, further increased NMDA currents in YAC128 MSNs. Interestingly, those effects were ameliorated upon extrasynaptic GluN2B-containing NMDAR antagonism with application of ifenprodil. Moreover, 2- to 4-month-old YAC128 mice treated with a low dose of memantine, which appears to preferentially antagonize extrasynaptic NMDARs, induced increased CREB activation and improved motor learning, when compared to WT mice. Extrasynaptic NMDAR activation is associated with a CREB-inactivating dephosphorylation signal (Hardingham et al., 2002). Consistently, YAC128 mice present decreased CREB phosphorylation levels in the striatum, whereas extrasynaptic NMDARs are overactivated (Milnerwood et al., 2010). Concordantly, experiments *in vivo* further evidenced GluN2B-containing NMDAR-mediated excitotoxicity in HD (Heng et al., 2009). In this study, authors demonstrated that the double-mutant mice, which express Htt-

150Q and overexpress GluN2B NMDAR subunits, presented exacerbation of selective striatal neuron degeneration.

Moreover, post-translational modifications including phosphorylation, palmitoylation, and proteolytic cleavage are important mechanisms underlying NMDAR mislocalization in HD. The GluN2B-containing NMDAR Tyr1472 phosphorylation by Src family kinases or STriatal-Enriched protein tyrosine Phosphatase (STEP) is associated with enrichment of synaptic NMDAR, whereas Tyr1336 phosphorylation is associated to extra-synaptic NMDAR retention (Goebel-Goody et al., 2009), suggesting that NMDAR lateral diffusion between synaptic and extra-synaptic sites is modulated by tyrosine phosphorylation. Nonetheless, NMDAR dissociation from postsynaptic density 95 protein (PSD-95) facilitates Tyr1472-GluN2B dephosphorylation, resulting in decreased GluN2B-containing NMDARs retained synaptically (Sanz-Clemente et al., 2010). Remarkably, YAC128 striatum revealed increased synaptic STEP activity, correlating with decreased Tyr1472-GluN2B phosphorylation, which facilitates NMDAR movement to extrasynaptic sites, reducing synaptic NMDAR retention (Gladding et al., 2012). In R6/2 mice, increased GluN1 subunit levels were described in striato-nigral projections, but decreased levels were observed in large aspiny striatal interneurons. Additionally, this HD mouse model further presented enhanced GluN1 subunit phosphorylation by PKA, at Ser897, in striatal projection neurons (Ariano et al., 2005). This phosphorylation induced NMDAR mobilization to the cell surface and synaptic regions, increasing receptor-dependent activity through a rise in open channel time, along with neuronal glutamate responsiveness, which may induce excitotoxicity and selective HD neuronal vulnerability (Ariano et al., 2005).

Since synaptic targeting and trafficking of both PSD-95 and GluN2B subunits are regulated by palmitoylation, the altered interaction between mHTT and palmitoyl transferase HIP14 can also facilitate GluN2B mislocalization (Huang et al., 2004; Singaraja, 2002). In addition, STEP-induced regulation of GluN2B phosphorylation and calpain-mediated cleavage of the GluN2B C-terminus, also contribute to altered synaptic/extrasynaptic balance of striatal GluN2B-containing NMDAR in presymptomatic YAC128 mice (Gladding et al., 2012). Moreover, R6/1 mice presented hippocampal reduced total levels of GluN2A, but no change in GluN2B, and decreased tyrosine phosphorylation

levels of Tyr1246-GluN2A, Tyr1325-GluN2A and Tyr1472-GluN2B (Giralt et al., 2017).

Striatal neurons from the YAC72 mouse showed increased NMDA-evoked currents, which were selectively blocked by GluN2B-specific antagonist ifenprodil, supporting the evidence for GluN2B NMDAR subtype involvement in HD (Zeron et al., 2002). Similar results were obtained in YAC128 MSN cultures (Tang et al., 2005). Consistently, R6/2 mice presented enhanced NMDA currents specifically in the striatum, possibly reflecting an alteration of NMDAR subunit composition, in a pre-symptomatic phase (Starling et al., 2005). Together, these results demonstrate that striatal neurons expressing mHTT have an altered NMDAR function and location.

1.6. SRC KINASE FAMILY PROTEINS

1.6.1. A GENERAL OVERVIEW OF SRC KINASE FAMILY PROTEINS

Src kinase family (SKF) is a non-receptor tyrosine kinases family with eleven members: c-Src, Fyn, Yes, Brk, Lyn, Fgr, Frk, Hck, Lck, Srm and Blk. c-Src, Fyn and Yes were shown to be expressed ubiquitously (Parsons and Parsons, 2004; Roskoski, 2004). SKF members have a similar structure with six functional regions: i) N-terminal Src homology domain (SH) 4 (SH4) that holds a myristic acid, essential for SKF stabilization at the cell membrane inner surface; ii) between the SH4 and SH3 domains, SKF members have an unique domain of each element; iii) the SH3 domain, with a proline rich sequence functioning as mediator to intra- and intermolecular interactions; iv) a SH2 domain, responsible for binding phosphorylated tyrosine residues on Src and other proteins; v) a SH1 domain, in charge of catalytic capacity; and vi) the C-terminal tail holding the negative regulatory Tyr530 residue (Chojnacka and Mruk, 2015) **(Figure 1.12).**

Phosphorylation and dephosphorylation of SKF tyrosine residues regulate SKF activity. SKF can be phosphorylated at Tyr530 and Tyr419, in humans, or Tyr527 and Tyr416, in mice, respectively. These tyrosine residues regulation can occur by kinases and phosphatases proteins, mentioned further ahead, leading to structural changes by intramolecular interactions (Roskoski, 2015). In this way, SKF proteins conformation is considered closed, and so inactive, when Tyr530 phosphorylation happens, which prevents the autophosphorylation of Tyr419, keeping these kinases unable to bind substrates. Inversely, SKF are activated when the dephosphorylation of Tyr530 opens the protein conformation, allowing Tyr419 autophosphorylation and being able to interact with substrates and be active to phosphorylate other proteins **(Figure 1.12).**

Without stimulus, SKF proteins are maintained in an inactive state, however SKF can be activated by other proteins interactions (Chojnacka and Mruk, 2015). Indeed, SKF can be inactivated by the Csk or Csk-homologous kinases, due to SKF Tyr530 phosphorylation, whereas tyrosine phosphatase non-receptor type 1, 2, 6, 11 (PTPN1, PTPN2, PTPN6, and PTPN11) and

receptor-like protein tyrosine phosphatases (alpha, gamma and type C) can dephosphorylate the SKF Tyr530 residue, leading to their activation (Hebert-Chatelain, 2013). Furthermore, SKF proteins can be activated by phosphoinositide 3-kinase (PI3K) or Akt, cyclic adenosine monophosphate (cAMP) and extracellular signal-regulated kinase (ERK), or even membrane receptors such as Platelet-Derived Growth Factor (PDGF) β-receptor, which are all signaling cascades important for SKF function (Alonso et al., 1995; Ehinger et al., 2021; Watson et al., 2016). Besides intracellular interactions, SKF members are also redox-sensitive and can be activated by H_2O_2 and peroxynitrite, while tyrosine phosphatases, which are also ROS sensitive due to the presence of SH groups, can be inhibited favoring SKF activation (Akhand et al., 1999).

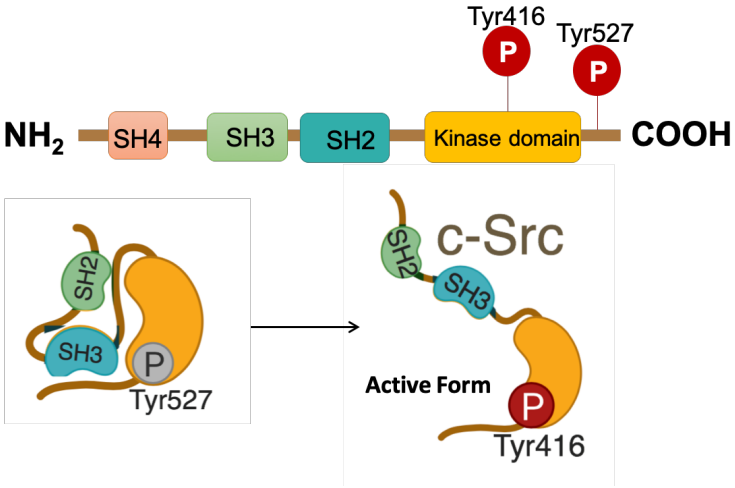

Figure 1.12 | Scheme of SKF proteins. At the structural level, SKF are composed to an N-terminal group attached to the SH4, a unique region following the SH4 domain, a SH3 domain, a SH2 domain, a kinase domain (also named SH1 domain), and a C-terminal domain. SKF members are maintained in an inactive status, which is its closed conformation, supported by an interaction between the SH3 domain and the proline-rich region. When activated by several interactions, SKF proteins are dephosphorylated at Tyr527, opening the conformation and phosphorylation at Tyr 416 occurs, thereby creating a fully activated c-Src protein.

Specially, c-Src and Fyn kinases have been extensively investigated for a long time since they may have a role in malignant transformation and oncogenesis (Levinson et al., 1972). Additionally, c-Src and Fyn can be located in several cellular compartments, such as the cytosol, mitochondria, rough endoplasmic, plasma membrane, nucleus, endosomes and lysosomes

(Sandilands and Frame, 2008). Active SKF members are mostly degraded by the UPS (Hebert-Chatelain, 2013). The brain expresses high levels of c-Src and Fyn; as such, these two kinases are involved in different processes besides cell division, as neurons are post-mitotic cells (Brown and Cooper, 1996). Indeed, c-Src/Fyn, and specially Fyn, are highly expressed in the striatum, the most affected brain area in HD (Pascoli et al., 2011).

1.6.2. C-SRC AND FYN FUNCTIONS AND INTERACTIONS

Different studies showed that SKF is involved in several intracellular processes, such as cell growth, differentiation, metabolism, signal transduction, neuronal ion channel and receptor regulation (Cao et al., 2007). These proteins can modulate and participate in several intracellular pathways, being involved in different important roles for cellular normal function (Anguita and Villalobo, 2017). One of the most studied SKF roles in the adult CNS is the regulation of different channels and receptor's activity (Wang et al., 2004), being involved in the control of learning and memory, pain, epilepsy and neurodegeneration (Salter and Kalia, 2004).

In this section we discuss c-Src and Fyn roles at the synapse and mitochondria, where they perform important roles in neurons.

1.6.2.1. c-SRC AND FYN AND SYNAPTIC ROLE

At presynaptic level, c-Src mediates synaptic vesicles recruitment to the reserve pool, regulating neurotransmitters release by synapsin-I Tyr301-phosphorylation (Messa et al., 2010). Concordantly, several studies previously showed a relevant role for c-Src and Fyn in synapse development and plasticity (Grant and Silva, 1994; Maness, 1992). Fyn-deficient mice showed impaired LTP and alteration in both short- and long-term contextual fear memory (Grant et al., 2006; Isosaka et al., 2008). Additionally, the use of PP2, a selective SKF inhibitor, further correlated with spatial memory reduction in the radial arm maze (Mizuno et al., 2003). Fyn was shown to play a relevant role in LTP, learning and memory, as well as in dendritic spine and synapse formation. Fyn knockout mice exhibited

reduced dendritic spine density of pyramidal neurons in cortical layers at 3 months of age; primary cortical neurons from this Fyn knockout mice also showed decreased spine formation (Babus et al., 2011; Morita et al., 2006). Altogether, these studies show that Fyn kinase has an important role in spinogenesis regulation, both *in vitro* and *in vivo*, as in synaptic plasticity, learning and memory, which are fundamental for normal function and maintenance of synapsis over time. Disruption of these functions may contribute to synapse and spine loss that strongly correlates with cognitive impairments observed in HD.

SKF may regulate learning and memory through phosphorylation of NMDAR subunits, which play an important role in synaptic plasticity and formation (Jiang et al., 2008). Indeed, Takasu and colleagues showed that Ca^{2+} influx mediated by NMDARs activation upon its phosphorylation by a SFK, resulted in gene transcription required for the remodeling of synaptic connections, in excitatory synapses of primary cortical neurons (Takasu et al., 2002). Hence, SKF are key NMDARs regulatory proteins. NMDARs modulation by Fyn was earlier discovered, since this kinase can phosphorylate the two NMDARs subunits (GluN2A and GluN2B) located in postsynaptic membranes in rat neurons (Suzuki and Okamuranoji, 1995). On other hand, c-Src was found to be a component of the NMDAR complex, being able to increase NMDAR currents (Brugge et al., 1985). Overexpression of c-Src or Fyn proteins potentiated NMDARs currents in HEK293 cells transiently expressing NMDARs (Köhr and Seeburg, 1996), which occurs through GluN2B phosphorylation at Tyr1472 (Ali and Salter, 2001; Lau and Huganir, 1995). c-Src or Fyn phosphorylation of GluN2B Tyr1472 residue was associated with enrichment of synaptic NMDARs (Goebel-Goody et al., 2009). Additionally, IL-1β administration in primary cortical neurons induced Src kinases activation, which led to NMDARs phosphorylation, generating a Ca^{2+} signal that results in the activation of CaMK-II and CREB, being implicated in the expression of IL-6, a key inflammatory mediator (Tsakiri et al., 2008). Moreover, PSD-95, an adaptor protein that binds NMDARs at GluN2A and GluR2B subunits, can also be phosphorylated at Tyr523 residue, by c-Src and Fyn (Du et al., 2009). Interestingly, Gingrich and coworkers showed that the interaction between c-Src and mitochondrial complex I favors c-Src anchoring to NMDARs, as along with the regulation of the activity of these receptors(Gingrich et al., 2004).

1.6.2.2. c-SRC AND FYN IN MITOCHONDRIA

Mitochondrial normal function clearly depends on protein phosphorylation (Hebert-Chatelain, 2013). Several SKF members were found in mitochondria from rat brain, namely Fgr, Fyn, Lyn and Src (Salvi et al., 2002). Additionally, several SKF regulators, such as Src Homology 2 domain-containing tyrosine Phosphatase-2 (SHP-2) and PTPN1, also known as protein-tyrosine phosphatase 1B (PTP1B), and Csk were found in rat brain mitochondria, suggesting that Src activity can be directly regulated within mitochondria (Augereau et al., 2005; Salvi et al., 2004, 2002).

The first studies about SKF in mitochondria suggested that Src, Fyn, Lyn, Fgr and Csk could be resident proteins in mitochondria (Salvi et al., 2004). Boerner and colleagues further suggested that the intramitochondrial localization of SKF members could result from continuous mitochondrial import and export (Boerner et al., 2004), since SKF members do not have a mitochondrial localization signal and they might need an adaptor protein to be translocated to mitochondria. Later, two specific proteins were shown to import SKF members to mitochondria. The first described protein was Dok-4, a member of the downstream of kinase family (Itoh et al., 2005). Dok-4 overexpression resulted in augmented c-Src mitochondrial accumulation, in endothelial cells, while downregulation of Dok-4 resulted in increased c-Src accumulation in the cytosol (Itoh et al., 2005). Likewise, Dok-4 increases the association of Src with complex IV without altering their activity (Itoh et al., 2005). The second described protein responsible for SKF mitochondrial localization is the A-kinase anchor protein 121 (AKAP121), an anchoring protein that interacts with β-tubulin targeting protein kinase A (PKA) to the MOM. Indeed, AKAP121 can bind to both PTP1B and c-Src (A Livigni et al., 2006). Livigni and coworkers showed that AKAP121 binds to mitochondria and, in a SKF-depended process, it can increase cytochrome c oxidase activity, mitochondrial membrane potential and ATP synthesis (A Livigni et al., 2006). Moreover, overexpression of AKAP121 in HEK293 cells augmented ATP mitochondrial production and mitochondrial membrane potential in a c-Src- and PKA-dependent way (A Livigni et al., 2006). So far, the mechanism or proteins responsible for SKF mitochondrial export were not identified.

Different studies showed that SKF targets mitochondria and are involved in normal mitochondrial function. c-Src was shown to bind mitochondrial complex I (NADH dehydrogenase) subunit 2 (ND2), in excitatory synapses (Gingrich et al., 2004). c-Src was shown to phosphorylate the NDUFV2 and NDUFB10 subunits of complex I, increasing the rate of respiration, electron transfer and cellular ATP levels (Hebert-Chatelain et al., 2012). As such, SKF inhibition resulted in decreased mitochondrial respiration (Ogura et al., 2012). Succinate dehydrogenase (SDH; complex II), an enzyme with important dual roles in respiratory chain and citric acid (TCA) cycle, can also be phosphorylated at Tyr215 by c-Src (Ogura et al., 2012); although this phosphorylation has no effect on mitochondrial respiratory activity, it is important for efficient electron transfer through the electron transport chain (ETC) (Ogura et al., 2012). Complex IV or cytochrome c oxidase (subunit II) can be also phosphorylated by SKF, which increases the activity of this enzyme, and is important for the normal osteoclast function (Miyazaki et al., 2006). Other studies suggested that adenine nucleotide translocase 1 (ANT1), responsible for transporting ADP from cytosol to mitochondria in exchange of ATP, is another mitochondrial SKF substrate (Feng et al., 2010). Concordantly, treatments with ATP, H_2O_2 or orthovanadate, known to augment SKF activity, resulted in augmented complex IV enzymatic activity (Hébert Chatelain et al., 2011). Overall, SKF are important proteins in the regulation of mitochondrial oxidative phosphorylation system, and consequently in maintaining cell viability (Ogura et al., 2014, 2012).

1.7. HYPOTHESIS AND SPECIFIC AIMS OF THE PRESENT WORK

As described along this chapter, HD pathological mechanisms involve synaptic changes, altered NMDAR activity, mitochondrial dysfunction and ROS production. Likewise, c-Src/Fyn kinases are regulated by ROS, influence NMDAR activity and mitochondrial function. Additionally, several studies showed that different pathways involving c-Src kinase are upregulated after specific stimulus, resulting in Nrf2 activation, an important altered antioxidant pathway altered in HD. Since c-Src/Fyn are highly expressed in striatum, the most affected brain area in HD, all of these observations favor a common interplayer between mHTT and c-Src/Fyn-regulated pathways, suggesting a relevant role for c-Src/Fyn in HD. However, its involvement in HD is largely unexplored.

We hypothesize that mHTT modifies c-Src/Fyn levels and/or activity, interfering with relevant intracellular pathways, , especially in ROS modulation, mitochondrial function and NMDARs localization and activation, thus affecting striatal neuronal function.

Thus, the present work aimed to clarify the involvement of c-Src/Fyn in HD cells and striatal neuronal dysfunctional pathways, involving HD-related ROS production, mitochondrial dysfunction and NMDARs activity, and evaluate whether targeting this kinase can ameliorate HD pathology. To achieve this objective, we used several HD models expressing full-length HTT: i) striatal cells derived from HD KI mice expressing mHtt with 111Q ($STHdh^{Q111/Q111}$; mutant cells) *versus* wild-type striatal cells ($STHdh^{Q7/Q7}$); ii) human brain post-mortem tissue (caudate and parietal cortex) from HD patients and controls; iii) human lymphoblastoid cell lines obtained from HD patients and age-matched unaffected (control) siblings; iv) primary cortical and striatal neurons isolated from YAC128 *versus* wild-type embryos at embryonic 16-17 days (E16-E17); and v) 3 and 12 month-old striatal and cortical tissue from YAC128 *versus* wild-type mice.

The study was divided into three parts.

I) Previous studies showed that Fyn is implicated in nuclear Nrf2 export and degradation, as well as, in Nrf2 regulation (Kaspar and Jaiswal, 2011). The Nrf2 pathway is altered in HD (Oliveira et al., 2015a) and c-Src can be activated by oxidative stress (Akhand et al., 1999). Thus, in this first part of the work we aimed to define whether acute H_2O_2 exposure, which is increased in HD, acts as a regulator of c-Src and Nrf2 phosphorylation, as well as the influence of c-Src activation on Nrf2 regulation.

II) Several studies have previously showed that c-Src/Fyn synapse-enriched kinases are important proteins in synaptic activity and plasticity, as well as in NMDARs regulation (Goebel-Goody et al., 2009); however, the involvement of these kinases in NMDARs and related signaling pathways in HD is mainly unexplored. Thus, in the second part of this work we aimed to analyse c-Src/Fyn levels in HD altered postsynaptic density and explore the impact of c-Src/Fyn overexpression on HD striatal NMDAR activity and associated intracellular pathways linked to CREB activation.

III) Increased ROS production and mitochondrial dysfunction are important features of HD pathology (Wang et al., 2013), while c-Src and Fyn proteins have several important roles in mitochondrial normal function and can be activated by ROS (Akhand et al., 1999). Therefore, in this last section we proposed to evaluate the role of c-Src/Fyn on HD-related mitochondrial dysfunction, altered morphology and mitophagy and ROS generation.

Data will provide a better understanding of HD-related c-Src/Fyn-mediated antioxidant defense modulation, ROS production, mitochondrial and postsynaptic alterations, and potentially define c-Src/Fyn as HD therapeutic target(s). Considering the lack of efficient therapies ought to cure or act as neuroprotective agents in HD, understanding the intracellular mechanisms compromised by HD-related c-Src/Fyn reduced activity is expected to promote a deeper knowledge about the neurodegeneration and clinical manifestations of this disease. Thus,

this study can elucidate how modulation of these kinases might constitute a potential therapeutic strategy in HD.

CHAPTER II

MATERIAL AND METHODS

2.1. MATERIALS

Fetal Bovine Serum (FBS), Opti-MEM medium (#22600), B27 supplement and penicillin/streptomycin, geneticin (G418; #11811-031) were from Gibco (Paisley, Scotland, UK). Dimethyl sulfoxide (DMSO); Mowiol 40-88, 3-(4,5-dimethylthiazol-2-yl)-2,5- diphenyltetrazolium bromide (MTT), sodium butyrate (SB), fatty-acid free albumin from bovine serum (BSA), oligomycin, carbonyl cyanide 4-(trifluoromethoxy) phenylhydrazone (FCCP), protease cocktail inhibitors, RPMI 1640 medium, Dulbecco's Modified Eagle's Medium (DMEM) medium (ref. D5648), 5-FDU (#F0503) and other analytical grade reagents were purchased from Sigma Aldrich (St. Louis, MO, USA). Enhanced ChemiFluorescence reagent (ECF), anti-rabbit IgG (from goat), anti- mouse IgG+IgM (from goat) were from GE Healthcare (Little Chalfort, UK). Anti-goat IgG-AP (from donkey) was from Santa Cruz Biotechnology (Santa Cruz, CA, USA). PureLink Genomic DNA mini kit, Tetramethylrhodamine methyl ester ($TMRM^+$), Hoechst 33342 nucleic acid stain, Propidium Iodide (PI), Lipofectamine® 3000 and Alexa Fluor-647 donkey anti-rabbit (ref. A31573) were obtained from Invitrogen/Molecular Probes (Life Technologies Corporation, Carlsbad, CA, USA). PureZOL RNA isolation reagent, iScript cDNA Synthesis kit, SsoFast EvaGree Supermix, Bio-Rad Protein Assay and Polyvinylidene fluoride (PVDF) membrane were from Bio-Rad (Hemel Hempstead, UK). Nuclear/Cytosol Extraction Kit was from BioVision (Milpitas, CA, USA). All other reagents were of analytical grade. The primary antibodies used for western blotting (WB) and immunocytochemistry (ICC) are listed in Table 2.1. For cell treatments were used: H_2O_2 (100 μM, Sigma Chemical, St. Louis, MO, USA) for 10 or 30 min and for 1, 2 or 4 h, SU6656 (5 μM, Sigma Chemical, St. Louis, MO, USA) for 1 h, 4-Amino-5-(4-chlorophenyl)-7-(t-butyl)pyrazolo[3,4-d]pyrimidine (PP2, 10 μM, Sigma Chemical, St. Louis, MO, USA), for 1 h, cycloheximide (CHX, 350 μM, Alfa Aesar J66901, United States), for 3, 6, 12, 24 h, epoxomicin (200 nM, Sigma #E3652-50UG, St. Louis, MO, USA), for 24 h, 3-methyladenine (3-MA, 5 mM, InvivoGen, #tlrl-3ma, Toulouse, France), for 4 h, bafilomycin A1 (Bafilo. A1, 50 nM, Sigma #B1793, St. Louis, MO, USA), for 24 h.

Table 2.1 | List of the primary antibodies used in this work.

ANTIBODY	REFERENCE/BRAND	DILUTION	USE
BACTIN	Sigma, A5316	1:5000	WB
BECLIN1	Cell Signaling, 3738	1:1000	WB
C-SRC	Cell Signaling, 2110	1:1000/1:250	WB/ICC
CASPASE3-CLEAVED	Cell Signaling, 9664	1:200	ICC
CREB	Abcam, ab32515	1:200	ICC
CREB (SER133)	Cell Signaling, 9196	1:200	ICC
FYN	Cell Signaling, 4023	1:1000/1:250	WB/ICC
GAPDH	Chemicon MAB374	1:2500	WB
GLUN2A	Millipore #07-632	1:1000	WB
GLUN2B	Millipore MAB #5778	1:1000	WB
GLUN2B (P-TYR1742)	Cell Signaling, 4208S	1:1000	WB
LAMIN B1	Abcam, 16048	1:1000	WB
LAMP1	Thermofisher, CD107a	1:200	ICC
LC3	Cell Signaling, 12741	1:1000/1:200	WB/ICC
NRF2	Abcam, 31163-500	1:500/1:100	WB/ICC
NRF2 (P-SER40)	Abcam, 76026	1:500/1:100	WB/ICC
P62	Sigma, P0067	1:2000	WB
PARKIN	Abcam, ab15954	1:200	ICC
PINK1	Abcam, ab23707	1:200	ICC
PKCΔ	Cell Signaling, 2058	1:1000	WB
PKCΔ (P-TYR311)	Cell Signaling, 2055	1:500	WB
PSD-95	Thermo Scientific,7E3-1B8	1:200	ICC
SRC FAM. (P-TYR416)	Cell Signaling, 6943	1:1000/1:250	WB/ICC
TFEB	Proteintech 13372-1-AP	1:200	ICC
UBIQUITIN	Dako Z0458	1:200	ICC
VDAC1	Abcam, 14734	1:1000	WB

Legend: WB_ Western Blotting; ICC_ Immunocytochemistry

2.2. HUMAN SAMPLES AND ETHICAL PERMITS

Caudate and parietal cortex samples from 5 unaffected controls and 5 HD patients (Vonsattel grade II-III) (Table 1) were obtained from German Brain Bank "Neurobiobank München" (http://www.neurobiobank.org; Neurobiobank-Munchen Control Committee approval GA 2021-06). The *postmortem* intervals did not exceed 22 h. The ethical permit to use human samples was approved by Institutional Review Board from Faculty of Medicine, University of Coimbra, by 21 December 2015 (reference no. CE-136/2015).

Table 2.2 | Human sample identification

Sample ID	Age (y)	*Postmortem* time (h)
HD2	38.58	10
HD3	54	5.5
HD5	56.92	4
HD6	57.58	12
HD8	68.75	20
CO1	53.17	14.93
CO3	59.5	11.57
CO4	73	16.65
CO5	51.58	20
CO6	58.08	21.75

Legend: HD_ Huntington's disease patient; CO_ Control individual;

2.3. EXPERIMENTAL ANIMALS

2.3.1 YAC 128 MICE

YAC128 mice, initially described previously by Slow and co-authors (2003), express full- length mutant HTT with 128 CAG repeats from a yeast artificial chromosome (YAC) transgene (RRID: MGI_MGI:3613515). YAC128 (line HD53) and wild-type mice were housed in the animal facility of the Center for Neuroscience and Cell Biology and Faculty of Medicine at the University of Coimbra (Coimbra, Portugal) under controlled temperature (22–23°C) and a 12 h light/12 h dark cycle with lights on at 07:00 h. Food and water were available *ad libitum* throughout the experiment. Animals experiences in this study were performed in accordance with the European Community directive (2010/63/EU) and protocols approved by the Faculty of Medicine, University of Coimbra (ORBEA_189_2018/11042018). All efforts were made to minimize animal suffering and to reduce the number of animals used. Animals were used at 3, 6 and 12 months of age.

2.3.2. GENOTYPING

Twenty two day-old mice were genotyped using a tail-tip DNA polymerase chain reaction (PCR) standard procedure. Primers used were LyA1 (CCT GCT CGC TTC GCT ACT TGG AGC), LyA2 (GTC TTG CGC CTT AAA CCA ACT TGG), RyA1 (CTT GAG ATC GGG CGT TCG ACT 213 CGC), RyA2 (CCG CAC CTG TGG CGC CGG TGA TGC), actin forward (GGA GAC GGG GTC ACC CAC AC), and actin reverse (AGC CTC AGG GCA TCG GAA CC). PCR protocol consisted in 35 cycles, with the following temperatures and times for each step: denaturation—94 °C for 30 s; annealing—63 °C for 30 s; and elongation—72 °C for 30 s. At the end of the cycles, DNA was left at 70 °C for 10 min. PCR products were analyzed on 1.7 % agarose gels followed by staining with ethidium bromide

and visualized under a UV trans-illuminator, Gel Doc XR system (BioRad, Hercules, USA). A 100-bp ladder (Invitrogen) was used as a size marker.

2.3.3. STRIATAL PRIMARY CULTURES

Primary striatal neurons were prepared as described previously (Naia and Rego, 2018), with some minor modifications. At 16 days of gestation, pregnant female mice were sacrificed by cervical dislocation following anesthesia using (RS)-2-chloro-2-difluoromethoxy)-1,1,1-trifluoro-ethane. Striatum were dissected out from fetal mice and cells were separated by mechanical digestion using a pipette in Ca^{2+}- and Mg^{2+}-free Hank's balanced salt solution containing 137 mM NaCl, 5.36 mM KCl, 0.44 mM KH_2PO_4, 0.34 mM $Na_2HPO_4.2H_2O$, 5 mM glucose, 1 mM sodium pyruvate and 10 mM HEPES, at pH 7.2. Cells were plated at a density of $8.4x10^4$ cells/cm^2 in poly-D-lysine coated 6-well or 96-well plates, and at a density of $4.2x10^4$ cells/cm^2 in poly-D-lysine coated glass coverslips for immunocytochemistry. Cells were cultured for 12 days in Neurobasal medium supplemented with 2% B27, 0.5 mM glutamine and 0.12 mg/mL gentamicin, at 95% air and 5% CO_2. To reduce glia growth, 10 μM of the mitotic inhibitor 5-fluorodeoxyuridine (5-FDU) was added to the culture after 72 hours in culture. One half of the medium was changed with fresh medium without 5-FDU at day 7.

2.4. CELL LINES CULTURE

2.4.1 HUMAN LYMPHOBLASTS

Human lymphoblastoid cell lines were obtained from Coriell Institute for Medical Research (USA) after NIGMS MTA agreement, and derived from HD-affected patients containing heterozygous expansion mutation, four males (43/15, 45/15, 42/18, 49/17) and one female (47/18), or from unaffected voluntary control siblings, three males and one female, defined in this work as control (Ctl) lymphoblasts.

2.4.2 STH*dh*$^{Q7/Q7}$ AND STH*dh*$^{Q111/Q111}$ *S*TRIATAL CELLS

Immortalized striatal neurons derived from knock-in mice expressing full-length normal (referred as Q7 or wild-type cells) or full-length mutant Htt (mHtt) with 111 glutamines (referred as Q111 or mutant cells) were obtained from Coriell Institute for Medical Research (USA) and maintained as previously described (Trettel, 2000). Cells were used until passage 16 by recommendation of cell line producer Dr M. MacDonald (Dept. of Neurology, Massachusetts General Hospital, Boston, USA).

2.4.3. HT22 cells

Mouse clonal hippocampal HT22 cells, a subclone of the glutamate-sensitive HT4 hippocampal cell line (Morimoto and Koshland, 1990), were obtained from Dr. Dave Schubert from The Salk Institute, La Jolla. Cells were cultivated in 95% air and 5% CO_2 at 37°C, in high glucose DMEM (Sigma D5648) containing 10% FBS, 12 mM $NaHCO_3$, 5 mM HEPES, pH 7.3, supplemented with 100 µg/mL streptomycin and penicillin. Sub-cultures were made using dissociation medium containing 140 mM NaCl, 8.1 mM Na_2HPO_4, 1.47 mM KH_2PO_4, 1.47 mM KCl, 0.55 mM EDTA, and phenol red at pH 7.3, when confluence was about 80%. When indicated, cells were pretreated with rottlerin (1 µM, Sigma Chemical, St. Louis, MO, USA) for 24 h, SU6656 (5 µM, Sigma Chemical, St. Louis, MO, USA) for 1 h, or 4-Amino-5-(4-chlorophenyl)-7-(t-butyl)pyrazolo[3,4-d]pyrimidine (PP2, 10 µM, Sigma Chemical, St. Louis, MO, USA), for 1 h.

2.5 CONSTRUCTS AND TRANSFECTION

Cells were transfected with pLNCX chick Y527F SKF (Addgene, plasmid #13660), empty pLNCX vector, GFP (Origene, GFP; #PS100010), luciferase codifying plasmid under the ARE promoter control pGL4.37[Luc2P/ARE/Hygro] (Promega), PKCδ specific siRNA (s71696; #4390771) and Control siRNA (#4390843) (Thermo Fisher Scientific), pDsRed2-Mito plasmid (MitoDsRed; ref. number 632421), obtained from Clontech (CA, USA), Mito-Keima (Addgene plasmid #131626) and mRFP-EGFP-LC3 plasmids (Addgene plasmid #21074). Empty vector pLNCX was obtained from the Y527F SKF plasmid using the restriction enzyme digestion ClaI (BioLabs, #Ro197L) according to manufacturer's protocol. Result of digestion was visualized in 1% agarose gel; the band corresponding to the empty vector was cropped and DNA was extracted using the NucleoSpin® Gel and PCR Clean-up (Macherey-Nagel, #740609) accordingly to manufacturer's protocol. Then, the blunt end and cohesive end termini of the resulting empty vector were joined using T4 DNA Ligase enzyme (BioLabs, #M0202S). Q7 and Q111 cells were transfected 24 h after plating with 0.75 μg DNA/cm^2 of growth area in opti-MEM without FBS or antibiotics, following the Lipofectamine 3000 (ThermoFisher Scientific) manufacturer instructions. Medium was changed 4 h after transfection and cells were cultured for 48 h. In primary neurons, transfection was performed at 8 DIV and in HT22 cells 24 h before experiments when at 60% of confluence, using the calcium phosphate precipitation method. Briefly, plasmid was diluted in TE (1 mM Tris-HCl pH 7.3, 1 mM EDTA), followed by the addition of $CaCl_2$ (2.5 M $CaCl_2$ in 10 mM HEPES, pH 7.2). The DNA solution was carefully added to 2 × HEBS (12 mM dextrose, 50 mM HEPES, 10 mM KCl, 280 mM NaCl and 1.5 mM $Na_2HPO_4.2H_2O$, pH 7.2) while bubbling air through the solution with a micropipete. The mixture was then incubated for 25 min at room temperature. The precipitates were added dropwise to the coverslips in Neurobasal medium and incubated for 80 min at 37°C. The DNA–Ca^{2+}-phosphate precipitates were dissolved in freshly-made dissolution medium (Neurobasal medium with 20 mM HEPES, pH 6.8) and incubated for 7 min at room temperature. The transfected neurons were then washed with Neurobasal medium and transferred back to their original dishes containing conditioned

culture medium. In HT22 cells, after 4h, transfection medium was replaced by fresh culture medium. Plasmids expression was enabled for 24 h.

2.6. TISSUE AND CELL EXTRACTIONS

2.6.1. TOTAL, MITOCHONDRIAL AND NUCLEAR-ENRICHED SUBCELLULAR PROTEIN FRACTIONS

2.6.1.1. TOTAL EXTRACTS

Total extracts were obtained from HT22, Q7 and Q111 cells, primary striatal neurons and brain areas from WT and YAC128 mice. The cells (or tissues) were scraped in Ripa buffer (containing 150 mM NaCl, 50 mM Tris HCl, 5 mM EGTA, 1% Triton X-100, 0.1% SDS, 0.5% deoxycholate, pH 7.5) supplemented with 100 nM okadaic acid, 1 mM PMSF, 25 mM NaF, 1 mM Na_3VO_4, 1 mM DTT and 1 µg/ml protease inhibitor cocktail (chymostatin, pepstatin A, leupeptin and antipain). Total homogenates were lysed in an ultrasonic bath (UCS 300 – THD; at heater power 200 W and frequency 45 kHz) during 10 s and centrifuged at 4ºC for 10 min at 20,800 *xg* to remove cell debris. The supernatant was collected and protein content was determined using the Bio-Rad protein assay reagent based on the Bradford dye-binding procedure (Bio-Rad, Hercules, CA, USA). Then, protein extracts were denaturated with 6x concentrated loading buffer (containing 300 mM Tris-HCl pH 6.8, 12% SDS, 30% glycerol, 600 mM DTT, 0.06% bromophenol blue) at 95°C, for 5 min, and a western blotting was performed.

2.6.1.2. FRESH MITOCHONDRIA ISOLATION FROM MOUSE STRIATAL TISSUE

Striatal tissue from WT and YAC128 mice (with 3, 6 or 12 months) was washed in ice-cold isolation buffer containing 225 mM mannitol, 75 mM sucrose, 1 mM EGTA, 5 mM HEPES, and pH 7.2/KOH. Striatal mitochondria were then isolated using discontinuous Percoll density gradient centrifugation, according to our

previous work with some minor modifications (Ferreira et al., 2018). For this purpose, striatal tissues were homogenized with 20 up and down strokes in Dounce All-Glass Tissue Grinder (Kontes Glass Co., Vineland, NJ, USA) using pestle A (clearance, 0.07–0.12 mm) followed by 20 up and down strokes with pestle B (clearance, 0.02–0.056 mm). After a brief centrifugation at 1100 ×*g* for 2 min at 4°C, the supernatant was mixed with freshly made 80% Percoll prepared in 1 M sucrose, 50 mM HEPES, 10 mM EGTA, and pH 7.0 in a ratio 10:1. The Mix (previous supernatant with 80% Percoll) was then carefully layered on the top of freshly made 10% Percoll (prepared from 80% Percoll) and further centrifuged at 18500×g for 10 min at 4 °C. Supernatant was discarded including the cloudy myelin containing fraction leaving the mitochondria-enriched pellet in the bottom of the tube and the pellet resuspended in 1 mL of washing buffer containing 250 mM sucrose, 5 mM HEPES-KOH, 0.1 mM EGTA, and pH 7.2 and centrifuged again at 10,000 ×*g* for 5 min at 4°C. Finally, the mitochondrial pellet was resuspended in ice-cold washing buffer and the amount of protein quantified by the Bio-Rad protein assay (BioRad, CA, USA; Cat. No. 500-0006) and a western blotting was performed.

2.6.1.3. NUCLEAR-ENRICHED FRACTIONS

Nuclear and cytoplasmic fractions from HT22 cells were obtained using the Nuclear/Cytosolic fractionation kit (Biovision, CA, USA), following the kit manufacturer protocol. Briefly, cells were scraped or resuspended in cytosol extraction buffer A containing DTT and protease inhibitors and vigorously vortex for 15 seconds to fully resuspend the cellular suspension. Extracts were then incubated on ice for 10 minutes. To isolate the cytoplasmic fraction, ice-cold cytosol extraction buffer-B was added to the extract and, after a 5 seconds vortex, centrifuged at 16,000 xg for 5 minutes. The remaining pellet (containing nuclei) was resuspended in ice-cold nuclear extraction supplemented buffer and vortex for 15 seconds for every 10 minutes, totaling 40 minutes. The final extracts were then centrifuged at 16,000 xg for 10 minutes, at 4^{o}C and a western blotting was performed.

2.7 TOTAL RNA EXTRACTION and ANALYSIS OF GENE EXPRESSION BY QUANTITATIVE qPCR

The RNA was extracted using Purezol™ (Bio-Rad, Hercules, CA, USA) reagent as described by the manufacturer's. RNA quantification was achieved using a Nanodrop apparatus. 500 ng of RNA was reverse transcribed using the iScript cDNA synthesis kit (Nzytech, Lisbon, Portugal), following the manufacturer's instructions. All specific oligonucleotides were designed using the primer design tool software from NIH (https://www.ncbi.nlm.nih.gov/tools/primer-blast/) to be used at 57ºC annealing temperature. Gene specific primers used for real time PCR reactions are described un table 2.2. PCR was performed with 50 ng of the cDNA and 400 nM of each primer using the iQ SYBR Green Supermix (Bio-Rad, Hercules, CA, USA). PCR cycles were proceeded as follow: Taq activation (95ºC, 3 min), denaturation (95ºC, 15 s), and annealing/extension (57ºC, 45 s) using the Bio-Rad CFX 96 Real-time system, C1000 Thermal cycler (Bio-Rad, Hercules, CA, USA). Melting curve was obtained under 0.5°C increments every 5 s, from 65°C to 95°C, with fluorescence recording after each temperature increment to verify the specificity of the amplification. The relative mRNA levels were estimated using Actin as a reference gene. The primers used for real-time PCR (qPCR) are listed in Table 2.3.

Table 2.3 | Sequence (5’ ☾3’) of primers used for qPCR experiments.

Gene	Forward primer	Reverse primer
Actin	GGAGACGGGGTCACCCACAC	AGCCTCAGGGCATCGGAACC
ATP6v0A1	CTGTTATCCTCGGCATCATCCAC	CAGGTAGCCAAACAACGAGGAC
c-Src	GCCTCACTACCGTATGTCC	TTTTGATGGCAACCCTCGTG
CTSD	CCTGGGCGATGTCTTTATTG	CCTGGGCGATGTCTTTATTG
Fyn	AAGCACGGACGGAAGATGAC	ATGGAGTCAACTGGAGCCAC
GAPDH	CGGCCTTCCGTGTTCCATC	GAGTTGCTGTTGAAGTCGCA
HO-1	GCTAGCCTGGTGCAAGATAC	TGTCTGGGATGAGCTAGTGC
Prdx1	TATCAGATCCCAAGCGCACC	AAGGCCCCTGAAAGAGATACC
SOD1	CACTTCGAGCAGAAGGCAAG	CCCCATACTGATGGACGTGG

2.8. PROTEIN EXPRESSION QUANTIFICATION

2.8.1. WESTERN BLOTTING

Total, mitochondrial and nuclear extracts, obtained as described previously, were denatured with denaturing buffer (50 mM Tris-HCl pH 6.8, 2% SDS, 5% glycerol, 600 mM DTT, 0.01% bromophenol blue) at 95oC, for 5 min. Equivalent amounts of protein samples (15 µg-30 µg) were separated by 8%-12% SDS-PAGE and electroblotted onto polyvinylidene difluoride (PVDF) membrane (Millipore, MA, USA). Membrane was further blocked with 5% (w/v) BSA (Santa Cruz Biotechnology, PA, USA) in Tris Buffered Saline (TBS, containing 250 mM, 150 mM NaCl, pH7.6) plus tween 0.1% before incubation with the specific antibody against: described in table 2.1, overnight, at 4°C. An anti-rabbit (1:20,000; Thermo Fisher Scientific, 31340) or anti-mouse (1:20,000; Thermo Fisher Scientific, 31340 and 31320, respectively) IgG secondary antibodies conjugated to the alkaline phosphatase, prepared in 1% (w/v) BSA in TBS-T, were used for 1 hour, at room temperature. Immunoreactive bands were visualized by alkaline phosphatase activity after incubation for 5 min with ECF reagent on Bio-Rad ChemiDoc Touch Imaging System and quantified using Image Lab analysis software.

2.8.2. IMMUNOCYTOCHEMISTRY

To assess total, nuclear and mitochondrial protein levels, HT22, Q7 and Q111 cells or primary neurons from WT and YAC128 mice were cultured on glass coverslips. Twenty-four h after transfection (transfection method in section 2.5), cells were fixed with 4% paraformaldehyde (pre-warmed at 37^{O}C) for 20 min and permeabilized in 0.1% Triton X-100 in PBS, for 2 min. Then, cells were blocked for 1 h at room temperature with 3% (w/v) BSA in PBS and further incubated with the primary antibody prepared in blocking solution, overnight, at 4°C (antibodies described in table 2.1). Cells were then washed with PBS and incubated with the adequate secondary antibody (Alexa Fluor-594 goat anti-rabbit (Invitrogen, R37117), Alexa Fluor-488 donkey anti-rabbit (Invitrogen, R37118) and Alexa Fluor-488 donkey anti-mouse (Invitrogen, R37114)) at 1:300 in blocking solution

for 1 h at room temperature. Nuclei were stained with 1 µg/mL Hoechst 33342 in PBS (Invitrogen, CA, USA) for 10 min and coverslips were mounted using Mowiol 40-88 (Sigma Chemical, St. Louis, MO, USA). Confocal images were obtained using a Plan-Apochromat/1.4NA 63x lens on an Axio Observer.Z1 confocal microscope (Zeiss Microscopy, Germany) with Zeiss LSM 710 software.

2.9. CELL VIABILITY AND APOPTOSIS MEASUREMENT

2.9.1. MTT REDUCTION ASSAY

The reduction status of the cells was measured by a colorimetric assay for cell survival, using 3-(4,5-dimethylthiazol-2-yl)-2,5-diphenyltetrazolium bromide (MTT). MTT (0.5 mg/ml) in sodium-based medium (containing 140 mM NaCl, 5 mM KCl, 1 mM $CaCl_2$, 1 mM $MgCl_2$, 10 mM Glucose, 10 mM Hepes, pH 7.4/NaOH) was added to the HT22 cell cultures and incubated for 2 h at 37ºC in the dark. When taken up by living cells, MTT is converted to a water-insoluble blue product (formazan) (Mosmann, 1983). The precipitated dye was dissolved with DMSO and colorimetrically measured at 540 nm. Values were expressed relatively to control conditions.

2.9.2. APOPTOTIC CELL DEATH

The nuclear morphology of the transfected striatal wild-type and mutant cells was analyzed by live fluorescence microscopy using Hoechst 33342 nucleic acid stain, a cell-permeant nuclear counterstain that emits blue fluorescence when bound to DNA. Cells mounted on 18-mm coverslips were washed with PBS and then incubated with 2 µg/ml Hoechst 33342 for 10 min, at 33^{o}C. Cells were then washed 5 times in saline medium to remove extracellular dye, and further examined in an Axioskop 2 plus upright epi-fluorescence microscope (Zeiss, Jena, Germany) with PlanNeofluar/0.75NA 40x lens.

2.9.3 CELL PROFILERATION

HT22 cells were plated on 6-well plates (35,000 cells/well) and cell counting was started 24 h after plating. Cells were exposed to 1 mM H_2O_2 for 30 min, 2, 4 and 6 h and the number of cells was counted after each time point using a hemocytometer in trypan blue-treated cell suspension.

2.10 TOTAL H_2O_2 AND REACTIVE SPECIES LEVELS DETERMINATION

H_2O_2 levels were determined using Amplex® Red assay. Amplex® Red reagent (10-acetyl-3,7-dihydroxyphenoxazine) is a substrate that reacts with H_2O_2 in a 1:1 stoichiometry to produce the red-fluorescent oxidation product, resorufin, which was monitored at 37ºC (excitation 550 nm; emission 580 nm), allowing the monitoring of H_2O_2 production/release. After a washing step with Na^+ medium (containing 140 mM NaCl, 5 mM KCl, 1 mM $CaCl_2$, 1 mM $MgCl_2$, 10 mM Glucose, 10 mM Hepes, pH 7.4/NaOH), H_2O_2 was measured in 10 µM Amplex® Red plus 0.5 units/mL of horseradish peroxidase during 20 min using a microplate reader Spectrofluorometer Gemini EM (Molecular Devices, USA). Nitric oxide (NO) and general redox changes were measured using DAF2-DA (10 µM) and H_2DCFDA (20 µM), respectively. Briefly, cells were incubated for 30 min, at 33°C, in Na^+ medium (described above). NO and redox modifications were measured by following DAF2 (491 nm excitation, 513 nm emission) and DCF (488 nm excitation, 530 nm emission) fluorescence, respectively at 33°C, continuously, for 20 min, using a Microplate Spectrofluorometer Gemini EM.

2.11. MITOCHONDRIAL FUNCTION ANALYSIS

2.11.1 OXYGEN CONSUMPTION RATE

Oxygen consumption rate (OCR) in striatal cells was measured using a Seahorse XFe-24 flux analyzer (Seahorse Bioscience, Billerica, MA, USA), following the manufacturer's instructions. Striatal cells were seeded in XF24 cell culture microplates at a density of 25,000 (Q7)/35,000 (Q111) cells per well. Prior to the experiments, cells were washed and culture medium was replaced by assay medium DMEM-5030, supplemented with 25 mM glucose and 2 mM glutamine, pH 7.4. Experiments were performed at 37ºC and four baseline measurements of OCR were sampled prior to sequential injection of mitochondrial complex V inhibitor oligomycin (1 μM), protonophore FCCP (1 μM) and antimycin A plus rotenone (1 μM each) to completely inhibit mitochondrial respiration. Mitochondrial basal respiration, maximal respiration and ATP production were calculated and recorded by the Seahorse software. Data were normalized for protein levels.

2.11.2. MITOSOX FLUORESCENCE

Twenty-four h after transfection with GFP or GFP+Y527F (see section 2.5), striatal cell lines or primary striatal neurons were incubated in experimental media (in mM: 132 NaCl, 4 KCl, 1 $CaCl_2$, 1.2 $NaH_2PO_4.H_2O$, 1.4 $MgCl_2$, 6 Glucose, 10 HEPES, pH 7.4) plus 1 μM MitoSOX red (Thermo Fisher Sci. , #M36008) for 25 min at 33^oC or 37^oC, respectively. Cells were then washed with experimental medium and the experiment was recorded in experimental media using an Axio Observer Z1 system, a fully motorized inverted widefield microscope (Zeiss, Jena, Germany) equipped with a large stage incubator for temperature and humidity control and EC plan-neofluar/1.3NA 40x lens. MitoSOX fluorescence along time was imaged at 510 nm excitation and 580 nm emission. Fluorescence intensities were calculated using Fiji software.

2.11.3 TMRM FLUORESCENCE

Striatal cells and primary striatal neurons were transfected with GFP or GFP+Y527F for 24h (see section 2.5). Then, cells were incubated in experimental media with 10 nM tetramethylrhodamine, methyl ester ($TMRM^+$, Thermo Fisher Sci., #T668), a concentration sufficient low to avoid quenching of the fluorescent signal in the mitochondrial matrix, for 30 min at 33°C or 37°C in the cells line or in neurons, respectively. Coverslips were washed twice with PBS and mounted in a pre-warmed insert in experimental media plus 10 nM $TMRM^+$. $TMRM^+$ fluorescence was monitored in a controlled temperature by excitation at 543 nm and emission at 458 nm using an LCI PlanNeofluar/1.3NA 63x lens on a Carl Zeiss Axio Observed Z1 inverted confocal microscope with the CSU-X1M spinning disc technology. Three images were collected every 10 sec in the basal condition using Zen Black 2012 software (Zeiss, Jena, Germany). Cells were exposed to 2 μM FCCP to induce $TMRM^+$ release from mitochondria and 3 images more were collected every 1 min after FCCP exposure. Fluorescence intensity at each time point was analyzed in Fiji software using the time series analyzer plugin (v 3.0) developed by Balaji J. (2007) at Dept. of Neurobiology, UCLA.

2.11.4. MITOCHONDRIAL NETWORK AND CO-LOCALIZATION STUDIES

MitoDsRed- and GFP/Y527F-transfected striatal cells were fixed with 4% paraformaldehyde (pre-warmed at 37°C) for 20 min, permeabilized in 0.1% Triton X-100 in PBS for 2 min and blocked for 1 hour, at room temperature in 3% (w/v) BSA in PBS. Nuclei were labelled with 4 μg/mL Hoechst 33342 for 15 min and coverslips were mounted using Mowiol 40-88. Confocal images were obtained using a Plan-Apochromat/1.4NA 63x lens on an Axio Observer.Z1 confocal microscope (Zeiss Microscopy, Germany) with Zeiss LSM 710 software. Mitochondrial morphology and protein co-localization analysis were achieved using Macros in Fiji designed in our Lab by Dr. Jorge Valero (currently at Institute for Neuroscience of Castilla y León, University of Salamanca, Spain). Briefly, image background was normalized using the function Subtract Background, included in Fiji. Mitochondria-targeting MitoDsRed images were extracted to

grayscale. FindFoci function was then used to allow the identification of peak intensity regions (Herbert et al., 2014) in order to show mitochondria-specific fluorescence. A threshold was applied to optimally resolve individual mitochondria. Mitochondrial outlines were traced through the Analyze Particles function. Aspect ratio (the ratio between the major and minor axis of mitochondria) was used as an index of mitochondrial length alongside, or Roundness (a relation between the area of mitochondria and its major axis). To obtain information about protein co-localization with mitochondria, a selection of mitochondrial ROIs was done, and the respective protein Integrated Density inside the ROIs was considered. Y527F+GFP and GFP were analyzed in the same way, considering also the value of Integrated Density. Each value derived represents a single cell.

2.12. ELECTROPHYSIOLOGICAL RECORDINGS

NMDA-induced currents were recorded in transfected primary striatal neurons (DIV 11) at −60 mV by whole-cell patch clamping using an AxonPatch 200B amplifier (Molecular Devices, USA). The borosilicate glass micropipettes used had a resistance of 4–6 MΩ and were filled with the following internal solution (in mM): $CsMeSO_4$ 130, CsCl 10, $CaCl_2$ 0.5, EGTA 5, HEPES 10, and NaCl 10 (pH 7.3 adjusted with CsOH). Cells were perfused with extracellular solution containing 140 mM NaCl, 2.5 mM KCl, 1.8 mM $CaCl_2$, 10 mM HEPES and 15 mM glucose supplemented with 10 μM glycine (pH 7.4 adjusted with NaOH). NMDA (100 μM) was diluted in the extracellular solution and rapidly perfused with a six channel perfusion valve control system VC-77SP/perfusion fast-step SF-77B (Warner Instruments, USA). All experiments were performed at RT (22–25 °C). The currents were filtered at 1 kHz (4-pole low-pass Bessel filter) and digitized at a sampling rate of 10 kHz to a personal computer and analyzed with pClamp 10.7 software (Molecular Devices, USA).

2.13. MEASUREMENT OF INTRACELLULAR CALCIUM LEVELS

Twenty-four hours after transfection with empty or empty+ SKF Y527F, primary striatal neurons were incubated in experimental media (in mM: 132 NaCl, 4 KCl, 1 $CaCl_2$, 1.2 $NaH_2PO_4.H_2O$, 1.4 $MgCl_2$, 6 Glucose, 10 HEPES, pH 7.4) plus 2 μM Fluo4-AM (Thermo Fisher Sci., #F14201) for 45 min, at 37°C. Cells were then washed and the experiment was recorded in experimental media, without Mg^{2+} and supplemented with glycine (20 μM) and serine (30 μM). Fluo4 fluorescence was monitored before and after exposure to 100 μM NMDA, in primary striatal neurons from WT and YAC128 mice, using an Axio Observer Z1 system, a fully motorized inverted widefield microscope equipped with a large stage incubator for temperature and humidity control and EC plan-neofluar/1.3NA 63x lens. Fluo4 fluorescence was imaged along time at 494 nm excitation and 506 nm emission, respectively. Fluorescence intensities were calculated using Fiji software.

2.14. STATISTICAL ANALYSES

Data were analyzed by using Excel (Microsoft, Seattle, WA, USA) and GraphPad Prism 8 (GraphPad Software, San Diego, CA, USA) softwares, and are expressed as the mean ± S.E.M. of the number of independent experiments or cells indicated in figure legends. Comparisons among multiple groups were performed by one-way ANOVA followed by the Bonferroni or Dunnett's nonparametric Multiple Comparison post-hoc tests or by two-way ANOVA, followed by Sidak's Multiple Comparison as post hoc test. Unpaired non-parametric Mann Whitney test was also performed for comparison between two Gaussian populations, when applicable, as described in figure legends. Significance was defined as $p<0.05$.

CHAPTER III

c-SRC REGULATES NRF2 ACTIVITY THROUGH PKCδ AFTER OXIDANT STIMULUS*

* Based on the following published manuscript: (Fão et al., 2019a)

3.1. SUMMARY

Nrf2 is the main transcription factor involved in expression of cell defense enzymes, which is altered in several oxidant-related disorders. Cytosolic Nrf2 activation is modulated through phosphorylation by PKCδ, an enzyme controlled by Src tyrosine kinases. Of relevance, Src family members are involved in numerous cellular processes and regulated by H_2O_2. In this study we analysed the activation of cell survival-related signaling proteins, c-Src and Nrf2, and the influence of c-Src kinase on Nrf2 regulation after exposure to H_2O_2. Acute exposure of HT22 mouse hippocampal neural cells to H_2O_2 increased c-Src and Nrf2 phosphorylation/activation at Tyr416 and Ser40, respectively. Nrf2 phosphorylation at Ser40, its nuclear accumulation and transcriptional activity involving HO-1 expression were dependent on c-Src kinase activation. Moreover, modulation of Nrf2 activity by c-Src occurred through PKCδ phosphorylation at Tyr311. We demonstrate, for the first time, c-Src-mediated regulation of Nrf2 transcriptional activity, via PKCδ activation, following an acute H_2O_2 stimulus. This work supports that the c-Src/PKCδ/Nrf2 pathway may constitute a novel signaling pathway stimulated by H_2O_2 and a potential target for the treatment of diseases involving redox deregulation.

3.2. INTRODUCTION

ROS are largely produced as byproducts of oxygen metabolism (Imlay, 2008). Imbalance between formation and/or accumulation of ROS and the capability of cells to defend against oxidative damage initiate deregulation of redox status and related signaling pathways, leading to oxidative stress. Indeed, increased levels of reactive oxidants cause several adverse effects on crucial biomolecules, such as proteins, nucleic acids and lipids, and cellular structures (Pizzino et al., 2017). This process has been related with the onset and/or progression of several diseases, such as neurodegenerative disorders, cancer, cardiovascular diseases, diabetes, atherosclerosis or metabolic diseases (Moris et al., 2017; Pizzino et al., 2017; Rodic and Vincent, 2017). H_2O_2 is a non-radical and relatively stable ROS that functions as a cellular signaling molecule (Obuobi et al., 2016), showing a rapid but limited permeation across biomembranes (Bienert et al., 2006); however, it may cause several harmful effects and alteration of cellular homeostasis, since it can be converted into highly reactive hydroxyl radical through the Fenton reaction (Grant, 2011).

Nrf2 is a transcription factor generally considered as an adaptive cell-response molecule and the central player in the inducible expression of cell defense enzymes to endogenous and environmental oxidative stress (Suzuki and Yamamoto, 2017). Thus, by binding a cis-regulatory element sequence named ARE in the promoter of target genes (Smith et al., 2016; Stępkowski and Kruszewski, 2011), Nrf2 mediates the expression of a high number of oxidative stress-related genes that encode for antioxidant proteins, detoxifying enzymes, transport proteins, proteasome subunits, chaperones, growth factors and their receptors, and other transcription factors (Basak et al., 2017). Nrf2 is ubiquitously expressed in most eukaryotic cells and is maintained, under normal conditions, at low levels in the cytosol due to its binding to Keap1 and constant targeting for poly-ubiquitination and proteasomal degradation (Kansanen et al., 2013; Nguyen et al., 2003). In the presence of an oxidant stimulus, Keap1 cysteine residues are oxidized, leading to conformational changes in Keap1 through modifications of its cysteine residues and release of Nrf2, allowing Nrf2 cytosolic accumulation and

subsequent migration to the nucleus (Kobayashi et al., 2004). Specifically, Nrf2 phosphorylation at Ser40 residue, mediated by PKCδ, disrupts Nrf2 and Keap1 association, promoting the translocation of Nrf2 to the nucleus (Huang et al., 2002; Niture et al., 2009; Numazawa et al., 2003).

SKF is a family of non-receptor tyrosine kinases composed by eleven members, namely Src, Yes, Fyn, Fgr, Frk, Srm, Lyn, Hck, Lck, Brk and Blk, wherein only c-Src, Yes and Fyn are expressed ubiquitously (Espada and Martín-Pérez, 2017; Roskoski, 2015). Several reports refer that SKF is involved in numerous processes, namely cell growth, differentiation, metabolism, signal transduction and neuronal ion channel and receptor regulation (Roskoski, 2015; Wang et al., 2005). c-Src has been found to be located at several subcellular compartments, namely the cytosol, plasma membrane, nucleus, rough endoplasmic reticulum, mitochondria, endosomes, lysosomes, phagosomes and the Golgi apparatus (Espada and Martín-Pérez, 2017; Sandilands and Frame, 2008). All SKF members share the same structure, composed of six functional regions, only differing in a unique domain that is characteristic of each element of the Src family (Chojnacka and Mruk, 2015). Src kinases activity is regulated by phosphorylation and dephosphorylation of its tyrosine residues, mainly Tyr527 and Tyr416, which cause structural changes by intramolecular interactions (Roskoski, 2015). As such, phosphorylation at Tyr527 closes Src proteins conformation and blocks its interaction with substrates, whereas Tyr416 phosphorylation opens Src proteins conformation and allows SKF activation (Chojnacka and Mruk, 2015). Importantly, Src proteins are redox-sensitive and can be directly or indirectly activated by H_2O_2 through the inhibition of tyrosine phosphatases, which can be downregulated by reactive oxidants due to the oxidation of their SH groups (Chojnacka and Mruk, 2015).

Previous studies showed that different pathways involving c-Src kinase are upregulated after specific stimulus, resulting in Nrf2 activation and increased HO-1 expression (Cheng et al., 2010; Lin et al., 2017; Yang et al., 2015). Furthermore, Fyn, a member of SFKs, is implicated in nuclear Nrf2 export and degradation (Culbreth et al., 2017; Li et al., 2017). However, whether cytosolic c-Src can regulate Nrf2 activity after an oxidant stimulus and whether c-Src kinase-mediated Nrf2 regulation improves cell response remains poorly understood. Thus, in this work, we aimed to define whether acute H_2O_2 exposure act as a

regulator of c-Src and Nrf2 phosphorylation, as well as the influence of c-Src activation on Nrf2 regulation. We show that Nrf2 phosphorylation, nuclear migration and activation is dependent on c-Src cytosolic activation, after an acute H_2O_2 stimulus. Furthermore, we give evidence that c-Src-mediated Nrf2 activity occurs through PKCδ.

3.3. RESULTS

3.3.1. ALTERED C-SRC PROTEIN LEVELS AND ACTIVATION IN CYTOPLASM AND NUCLEUS OF HT22 CELLS AFTER AN ACUTE EXPOSURE TO H_2O_2

c-Src has been reported to act as redox-sensitive Tyr kinase, regulated by H_2O_2. In order to determine the activation of c-Src by H_2O_2 in HT22 mouse hippocampal cell line, we measured the levels of total and Tyr416 phosphorylated c-Src in the cytoplasm and nucleus. Firstly, we evaluated dose-dependent effects of H_2O_2 (for 30 min-incubation) on c-Src total and phosphorylated protein levels in cytoplasmic (**Figure 3.1A-C**) and nuclear extracts (**Figure 3.1D-F**), derived from HT22 cells. As depicted in **Figure 3.1A-F**, 1 mM H_2O_2 for 30 min was the H_2O_2 concentration that consistently induced increased c-Src protein total levels and p(Tyr416)Src kinase levels, in both cytoplasmic and nuclear fractions, as great variability was observed after exposure to 100 or 500 μM.

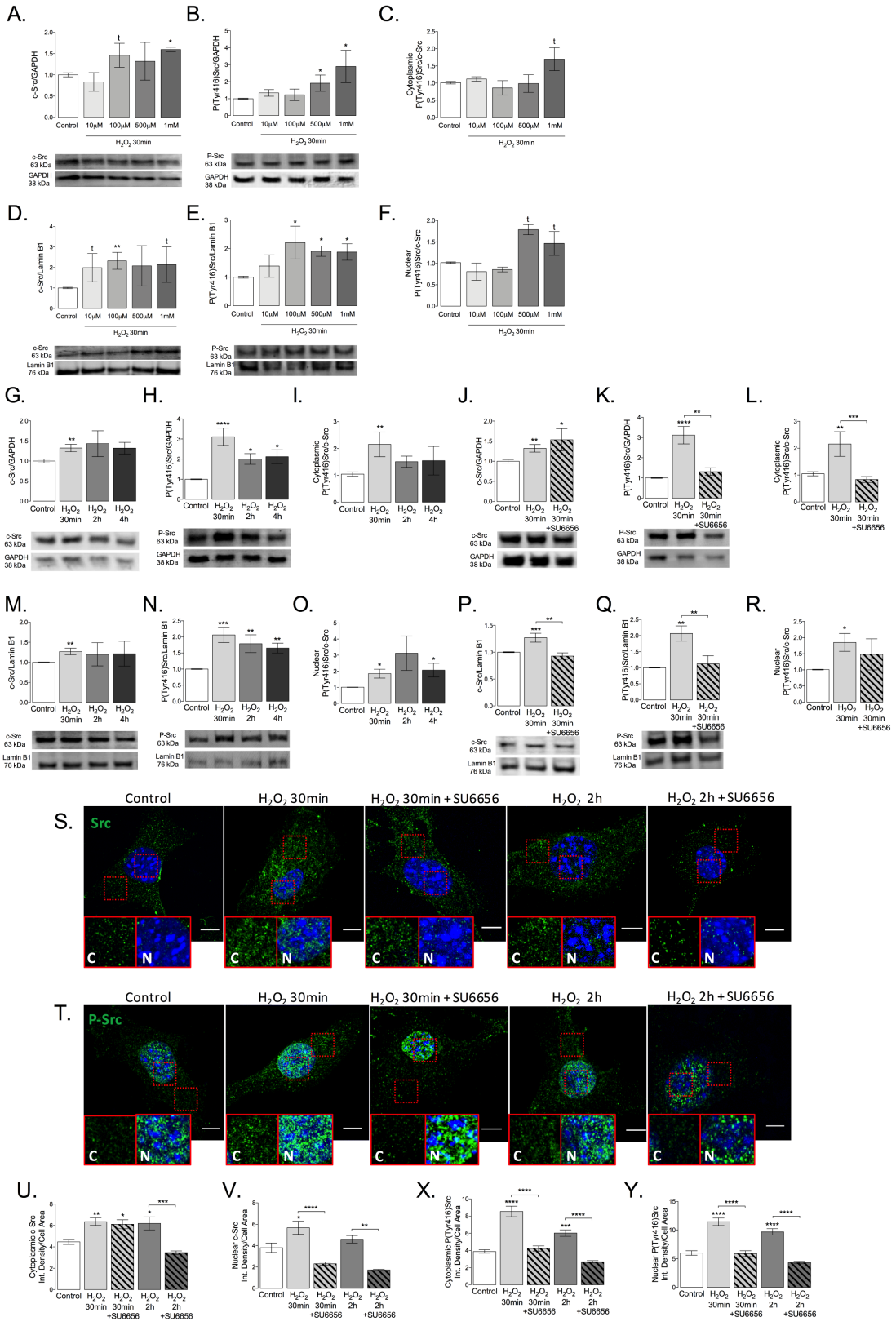

Figure 3.1 | Cytoplasmic and Nuclear c-Src Total and Phosphorylated levels in HT22 cells after H2O2 exposure. HT22 cells were incubated with 10 μM, 100 μM, 500 μM and 1 mM H2O2 for 30 min. The levels of c-Src/GAPDH (A), P(Tyr416)Src/GAPDH (B) and P(Tyr416)Src/c-Src (C) were evaluated by Western blotting in cytoplasmic-enriched fractions from HT22 cells. Levels of c-Src/Lamin B1 (D), P(Tyr416)Src/Lamin B1 (E) and P(Tyr416)Src/c-Src (F) were determined by Western blotting in nuclear-enriched

fractions from HT22 cells. Data are expressed in arbitrary units relative to GAPDH or Lamin B1 as the mean ± SEM of n=4 independent experiments. HT22 cells were further incubated with 1 mM H2O2 for 30 min, 2 or 4 h and the levels of c-Src/GAPDH (G,J), P(Tyr416)Src/GAPDH (H,K) and P(Tyr416)Src/c-Src (I,L) were evaluated by Western blotting in cytoplasmic-enriched fractions from HT22 cells. The effect of SU6656 (5 μM) were also analysed in cells exposed to H2O2, for 30 min (J-L). Data are expressed in arbitrary units relative to GAPDH as the mean ± SEM of n=4 to 11 independent experiments. Levels of c-Src/Lamin B1 (M,P), P(Tyr416)Src/Lamin B1 (N,Q) and P(Tyr416)Src/c-Src (O,R) were evaluated by Western blotting in nuclear-enriched fractions from HT22 cells, and the effect of SU6656 (5 μM) was also analysed (P-R). Data are expressed in arbitrary units relative to Lamin B1 as the mean ± SEM of n=6 to 11 independent experiments. c-Src (U,V) and p(Tyr416)Src (X,Y) cytoplasmic and nuclear levels were analysed by immunocytochemistry using confocal microscope and Image J software. Confocal images (S,T) were obtained with a 63x objective in confocal microscope Zeiss LSM 710 (scale bar: 10 μm). Inserts show at higher magnification the images indicated by boxes of cytoplasmic (C) and nucleus (N) labelling. Data are presented as the mean ± SEM of 3 to 5 independent experiments considering ~15 cells/condition. Statistical analysis: (A-R) *p <0.05, **p < 0.01, ***p < 0.001 and ****p < 0.0001 versus Control/untreated or versus H2O2 30 min+SU6656 (in K,L,P,Q) (nonparametric Kruskal-Wallis one-way ANOVA test, followed by Dunnett's Multiple Comparison as post hoc test); tp <0.05 versus Control (Student's t-test followed by nonparametric Mann Whitney as post hoc test). (U-Y) *p <0.05, **p < 0.01, ***p < 0.001 and ****p < 0.0001 between different groups, as depicted in each graph (one-way ANOVA, followed by Bonferroni's Multiple Comparison as post hoc test).

Prolonged exposure to 1 mM H_2O_2 has been described to cause oxidative stress and cause toxicity (Sies, 2017; Wang et al., 2003), while H_2O_2 extracellular concentration is more than 100-fold higher when compared to intracellular H_2O_2 concentration (Sies, 2017). Since we aimed to study c-Src modulation and response after an acute oxidant stimulus, we analyse time-dependent cytotoxicity induced by 1 mM H_2O_2 extracellular concentration. Cell death induced by 1 mM H_2O_2 over time, as well as time-dependent effects of 1 mM H_2O_2 incubation on cell proliferation were analysed by propidium iodide plus Hoechst labelling, the MTT assay and cell counting (**Figure 3.2A-D**). Data showed that 1 mM H_2O_2 for 30 min is not cytotoxic in HT22 cell line.

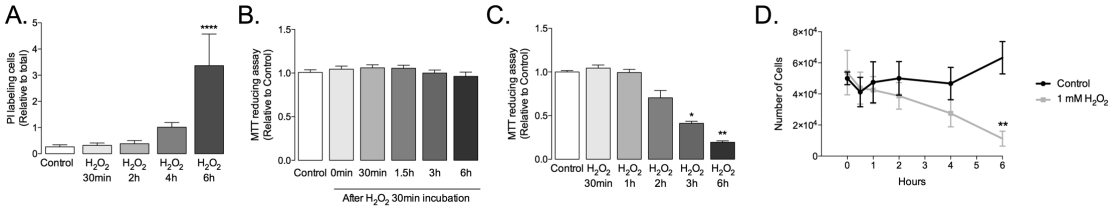

Figure 3.2 | Cytotoxicity in HT22 cells after H2O2 exposure. (A) HT22 cells were incubated with 1 mM H_2O_2 for 30min, 2, 4 and 6 h and cell death was evaluated by propidium iodide (PI) and Hoechst staining. (B) HT22 cells were incubated with 1 mM H_2O_2 for 30 min and

the medium was replaced by fresh culture medium for 30 min, 1.5, 3 and 6 h for analysis by the MTT assay. (C) HT22 cells were incubated with 1 mM H_2O_2 for 30 min, 1, 2, 3 and 6 h and cytotoxicity was evaluated by the MTT assay. (D) HT22 cells were incubated with 1 mM H_2O_2 for 30 min, 1, 2, 4 and 6 h and the time-dependent effects of 1 mM H_2O_2 incubation on cell proliferation were evaluated. The number of cells were counted at each time point, 1 mM H_2O_2 vs. Control. Data are presented as the mean ± SEM of 4 to 6 independent experiments, in (A) considering ~6 fields/condition. Statistical analysis: *p <0.05, **p < 0.01 and ****p < 0.0001 *versus* Control (nonparametric Kruskal-Wallis one-way ANOVA test, followed by Dunnett's Multiple Comparison as post hoc test).

Time-dependent changes in c-Src protein total levels after incubation with 1 mM H_2O_2 was also determined in the cytoplasm of HT22 cells. We observed a significant increase in c-Src total levels in the cytoplasm of HT22 cells after 30 min exposure to H_2O_2 (**Figure 3.1G**); similar results were observed in p(Tyr416)Src levels, which decreased after 2 and 4 h exposure to the oxidant stimulus (**Figure 3.1H,I**). Pre-treatment with SU6656 (5 μM), a selective Src inhibitor (Blake et al., 2000), markedly inhibited c-Src phosphorylation (**Figure 3.1K,L**), without altering total levels of c-Src protein levels (**Figure 3.1J**) , showing reversible modulation of c-Src activation after acute exposure to H_2O_2. In nuclear fractions, data showed a significant increase in c-Src protein levels after 30 min exposure to H_2O_2 (**Figure 3.1M**), as well as increased p(Tyr416)Src after 30 min, 2 and 4 h (**Figure 3.1N,O**). Interestingly, pre-treatment with SU6656 not only decreased nuclear c-Src Tyr416 activation/phosphorylation (**Figure 3.1Q,R**), but also decreased nuclear c-Src protein levels (**Figure 3.1P**), suggesting a possible role of c-Src protein phosphorylation on its translocation to the nucleus after an acute oxidant stimulus. In HT22 total cell extracts, H_2O_2 induced c-Src activation after 30 min exposure (**Figure 3.3-A,B**), which was effectively inhibited by SU6656 and the Src family-selective tyrosine kinase inhibitor, PP2 (Hanke et al., 1996) (10 μM) (**Figure 3.3,F,G**).

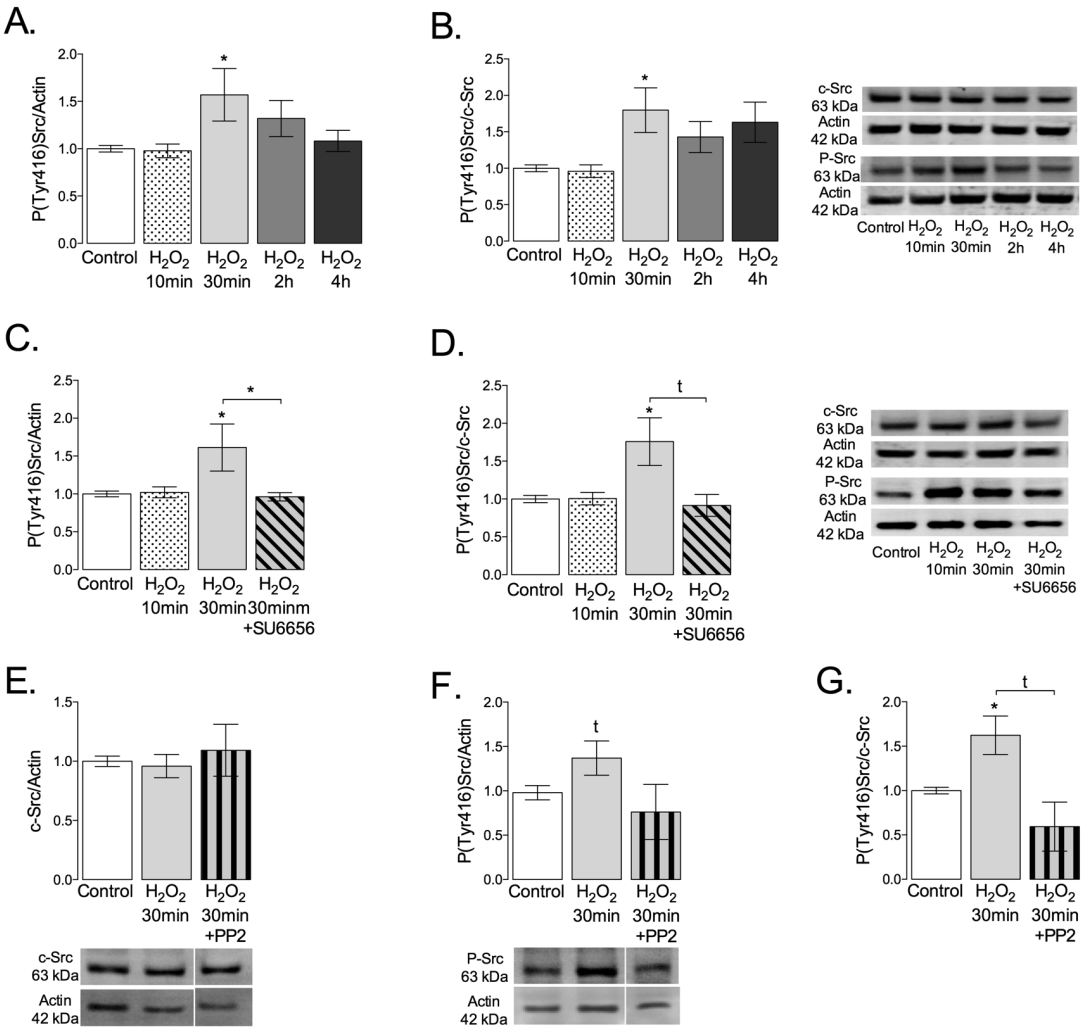

Figure 3.3 | c-Src total and phosphorylated protein levels in HT22 cells after H2O2 exposure. HT22 cells were incubated with 1 mM H_2O_2 for 10 min, 30 min, 2 and 4 h and the levels of P(Tyr416)Src family/actin (A), P(Tyr416)Src/Src (B) were evaluated by Western blotting. The effect of SU6656 (5 μM) and PP2 (10 μM) were also analysed in cells exposed to H_2O_2, for 30 min (C-G). Data are expressed in arbitrary units relative to actin as the mean ± SEM of n=4 to 10 independent experiments. Statistical analysis: *p <0.05 *versus* Control/untreated (nonparametric Kruskal-Wallis one-way ANOVA test, followed by Dunnett's Multiple Comparison as post hoc test); (D) ^{t}p <0.05 H_2O_2 30 min *versus* H_2O_2 30 min+SU6656; (F) ^{t}p <0.05 H_2O_2 30 min versus Control; (G) ^{t}p <0.05 H_2O_2 30 min *versus* H_2O_2 30 min+PP2; (Student's t-test followed by non-parametric Mann Whitney as post hoc test).

Nuclear (N) and cytoplasmic (C) levels of c-Src protein were also evaluated by immunocytochemistry in H_2O_2-treated HT22 cells, as depicted in **Figure 3.1S-Y**. Similarly to what was observed by Western blotting, total and phosphorylated levels of c-Src were increased in the cytoplasm (**Figure 3.1U,X**) and nucleus (**Figure 3.1V,Y**) after exposure for 30 min and 2 h to H_2O_2 (1 mM). Pre-treatment with 5 μM SU6656 inhibited H_2O_2-induced c-Src activation/phosphorylation in both nucleus and cytoplasm (**Figure 3.1U-Y**).

3.3.2 ACUTE H_2O_2 EXPOSURE CAUSES INCREASED NRF2 PROTEIN LEVELS AND PHOSPHORYLATION IN A C-SRC-DEPENDENT MANNER

The transcription factor Nrf2 is known to be activated by H_2O_2. Moreover, c-Src was shown to participate in Nrf2 nuclear accumulation (Cheng et al., 2010; Lin et al., 2017; Yang et al., 2015). However, the involvement of c-Src on Nrf2 regulation, through its phosphorylation at Ser40 residue, remains unknown. As shown in **Figure 3.4**, we analysed H_2O_2 dose-dependent effects on Nrf2 total and phosphorylated levels after incubation for 30 min in HT22 cytoplasmic and nuclear fractions.

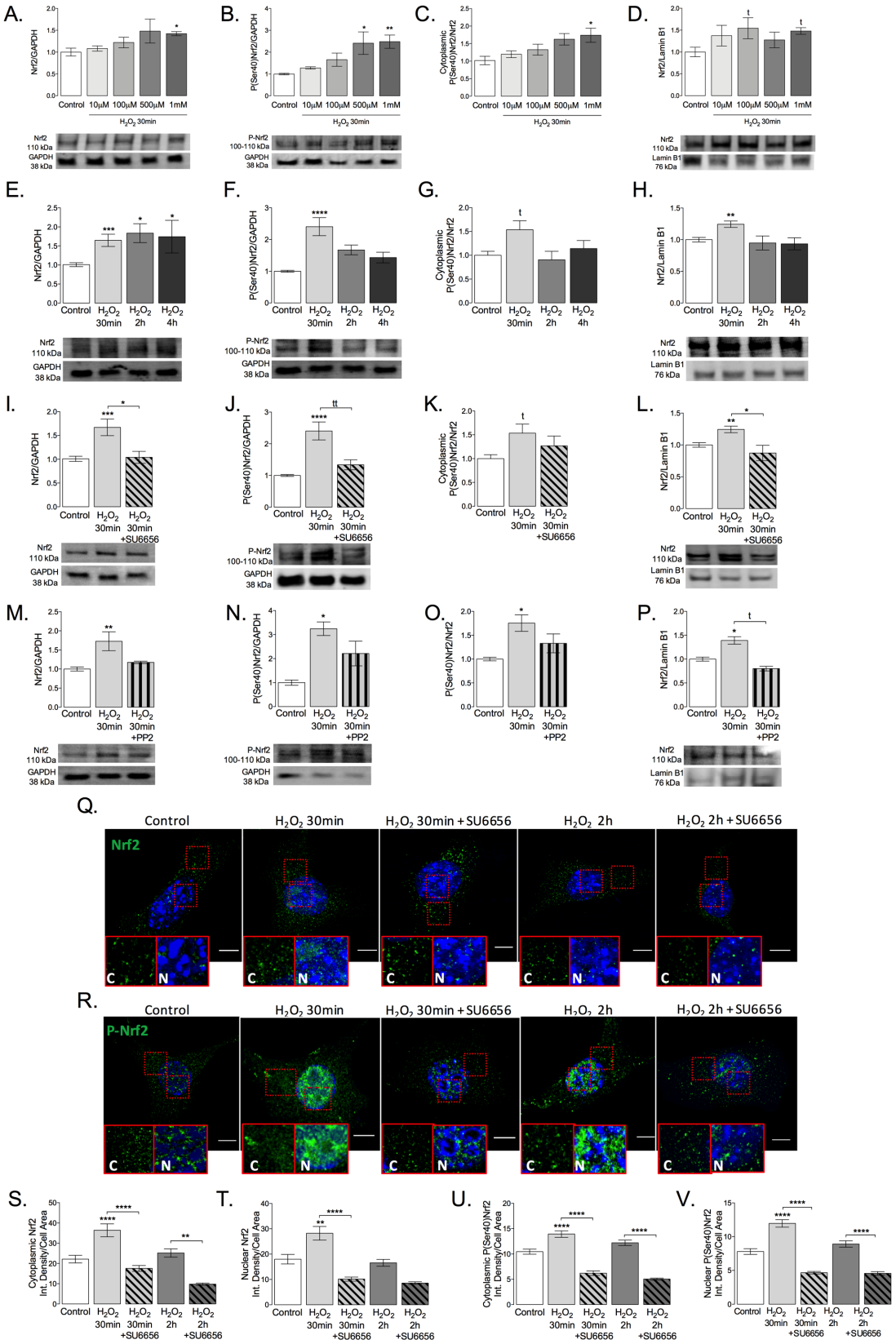

Figure 3.4 | Cytoplasmic and Nuclear Nrf2 Total and Phosphorylated levels in HT22 cells after H2O2 exposure. HT22 cells were incubated with 10 μM, 100 μM, 500 μM and 1 mM H_2O_2 for 30 min. Levels of Nrf2/GAPDH (A), P(Ser40)Nrf2/GAPDH (B) and P(Ser40)Nrf2/Nrf2 (C) were evaluated by Western blotting in cytoplasmic-enriched fractions from HT22 cells. Levels of Nrf2/Lamin B1 (D) were determined by Western

blotting in nuclear-enriched fractions from HT22 cells. Data are expressed in arbitrary units relative to Lamin B1 or GAPDH as the mean ± SEM of n=4 independent experiments. HT22 cells were incubated with 1 mM H_2O_2 for 30 min, 2 and 4 h and the levels of Nrf2/GAPDH (E,I,M) and P(Ser40)Nrf2/GAPDH (F,J,N) and P(Ser40)Nrf2/Nrf2 (G,K,O) were evaluated by Western blotting in cytoplasmic-enriched fractions from HT22 cells. The effect of SU6656 (5 μM) and PP2 (10 μM) were also evaluated in the cytoplasm of cells exposed to H_2O_2, for 30 min (I-K,M-O). Data are expressed in arbitrary units relative to GAPDH as the mean ± SEM of n=4 to 12 independent experiments. Levels of Nrf2/Lamin B1 (H,L,P) were determined by Western blotting in nuclear-enriched fractions from HT22 cells, and the effect of SU6656 (5 μM) and PP2 (10 μM) were also evaluated (L,P). Data are expressed in arbitrary units relative to Lamin B1 as the mean ± SEM of n=5 to 9 experiments. Nrf2 (S,T) and p(Ser40)Nrf2 (U,V) cytoplasmic (S,U) and nuclear (T,V) levels were analysed by immunocytochemistry using confocal microscope Image J software. Representative confocal images (Q,R) were obtained with a 63x objective in confocal microscope Zeiss LSM 710 (scale bar: 10 μm). Inserts show at higher magnification the images indicated by boxes of cytoplasmic (C) and nucleus (N) labelling. Data are presented as the mean ± SEM of 3 to 4 independent experiments considering ~15 cells/condition. Statistical analysis: (D,G,K) $^{t}p < 0.05$ *versus* Control, (J) $^{tt}p < 0.01$ H_2O_2 30 min *versus* H_2O_2 30 min+SU6656 and (P) $^{tt}p < 0.01$ H_2O_2 30 min *versus* H_2O_2 30 min+PP2 (Student's t-test followed by nonparametric Mann Whitney as post hoc test); *p <0.05, **p < 0.01 and ***p < 0.001 *versus* Control/untreated or *versus* H_2O_2 30 min+SU6656 (nonparametric Kruskal-Wallis one-way ANOVA test, followed by Dunnett's Multiple Comparison as post hoc test); (S-V) **p < 0.01 and ****p < 0.0001 between different groups, as depicted in each graph (one-way ANOVA, followed by Bonferroni's Multiple Comparison as post hoc test).

As depicted in **Figure 3.4A-D**, Nrf2 and P(Ser40)Nrf2 levels increased significantly and consistently in the presence of 1 mM H_2O_2 exposure, in both the cytoplasm and nucleus of HT22 cells. We further determined the time-dependent changes and investigated the relationship between c-Src and Nrf2, by analysing Nrf2 levels in cytoplasmic and nuclear extracts of HT22 cells treated with 1 mM H_2O_2 (**Figure 3.4E-P**). Nrf2 cytoplasmic levels were significantly increased after 30 min, 2 and 4 h of H_2O_2 treatment (**Figure 3.4E**). Phosphorylation of Nrf2 at Ser40 residue was reported as a signal for Nrf2 translocation from the cytosol to the nucleus (Niture et al., 2009). Importantly, we observed a significant increase in cytoplasmic p(Ser40)Nrf2 after 30 min exposure to H_2O_2, which was not sustained after 2 and 4 h in the cytoplasm (**Figure 3.4F,G**). Concordantly, nuclear Nrf2 increased largely after 30 min exposure to 1 mM H_2O_2 (**Figure 3.4H**). Interestingly, H_2O_2-induced total and phosphorylated Nrf2 levels in the cytoplasm were decreased after pre-treatment with the Src inhibitors SU6656 (**Figure 3.4I.K**) and PP2 (Figure **3.4M-O**). Similar results were observed in total cellular extracts, as depicted in **Figure 3.5**.

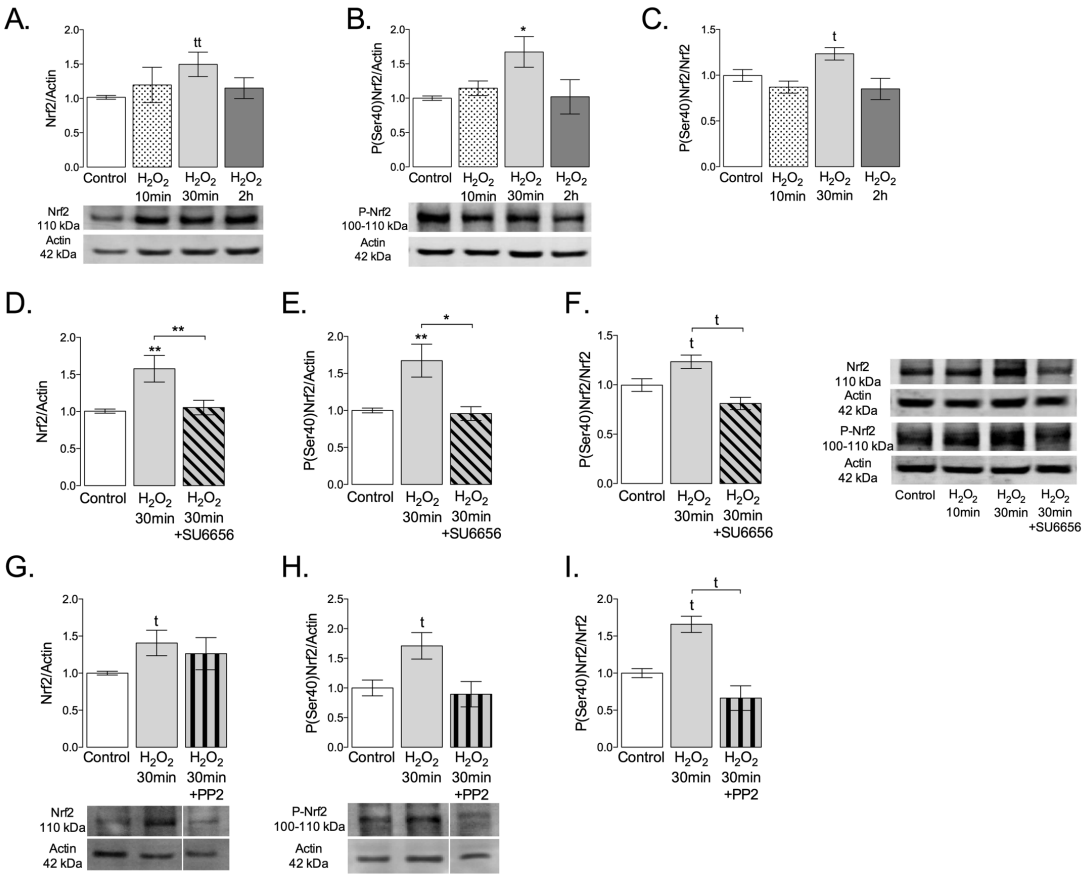

Figure 3.5 | Nrf2 total and phosphorylated protein levels in HT22 cells after H2O2 exposure. HT22 cells were incubated with 1 mM H_2O_2 for 10 min, 30 min and 2 h and the levels of Nrf2/actin (A), P(Ser40)Nrf2/actin (B) and P(Ser40)Nrf2/Nrf2 (C) were evaluated by Western blotting. The effect of SU6656 (5 μM) and PP2 (10 μM) were also evaluated in cells exposed to H_2O_2, for 30 min (D-I). Data are expressed in arbitrary units relative to actin as the mean ± SEM of n=4 to 9 independent experiments. Statistical analysis: *p <0.05 and **p <0.01 *versus* Control/untreated or *versus* H_2O_2 30'+SU6656 (nonparametric Kruskal-Wallis one-way ANOVA test, followed by Dunnett's Multiple Comparison as post hoc test). ^{t}p <0.05 Control versus H_2O_2 30 min, or H_2O_2 30 min *versus* H_2O_2 30 min +SU6656 or H_2O_2 30 min *versus* H_2O_2 30 min +PP2 (Student's t-test followed by non-parametric Mann Whitney as post hoc test).

Enhanced nuclear Nrf2 following incubation with 1 mM H_2O_2 for 30 min was also prevented by SU6656 and PP2 (**Figure 3.4L,P**). Thus, our results demonstrate, for the first time, the involvement of c-Src on Nrf2 cytoplasmic regulation, through its phosphorylation at Ser40, following an acute oxidant stimulus. The same experimental conditions were evaluated by immunocytochemistry. In agreement with previous results, data depicted in **Figure 3.4Q-V** showed that both cytoplasmic (C) and nuclear (N), total and phosphorylated Nrf2 levels were

increased after 30 min exposure to 1 mM H_2O_2. Here again, SU6656 pre-treatment decreased both Nrf2 total and phosphorylated levels in the cytoplasm and nucleus.

3.3.3. INDUCTION OF NRF2 TRANSCRIPTIONAL ACTIVITY IS MODULATED BY C-SRC

Since H_2O_2-mediated increase in nuclear Nrf2 levels could be modulated by c-Src, we further analysed whether c-Src could regulate Nrf2 transcriptional activity (**Figure 3.6**). For this purpose, HT22 cells were transfected with an ARE-driven luciferase reporter and incubated with H_2O_2 for 30 min. Luciferase activity was then assessed 1.5 h after H_2O_2 treatment. Results depicted in Figure 3A evidenced a significant increase in luciferase activity after H_2O_2 treatment, indicating an increase in Nrf2-ARE transcriptional activity. Importantly, an inhibitory effect of SU6656 pre-treatment on Nrf2 transcriptional activity (**Figure 3.6A**) was also observed, suggesting the involvement of c-Src on modulation of Nrf2 activity.

Nrf2 can regulate the transcription of several cytoprotective genes, including HO-1, SOD1 or peroxiredoxin-1 (Prdx-1) (Loboda et al., 2016; Ooi et al., 2017). Thus, the activity of Nrf2 was also assessed by analysing the expression of these Nrf2 target genes by quantitative real-time PCR, after 30 min incubation with H_2O_2 (1 mM) plus 30 min, 1.5, 3, 6, 12 and 24 h post-incubation (**Figure 3.6B-E**). Our data showed a significant increase in HO-1 mRNA levels after 1.5 and 3 h post-incubation (**Figure 3.6D**). An increase in Prdx1 mRNA levels was only detected after 6 h post-incubation (**Figure 3.6C**), whereas no significant differences were observed in SOD1 mRNA levels up to 24 h (**Figure 3.6B**). Notably, SU6656 pre-treatment decreased HO-1 mRNA levels, revealing the involvement of c-Src on the expression of HO-1 (**Figure 3.6E**). Data suggest that Nrf2 nuclear accumulation and transcriptional activity associated with enhanced HO-1 mRNA levels is dependent on c-Src activation.

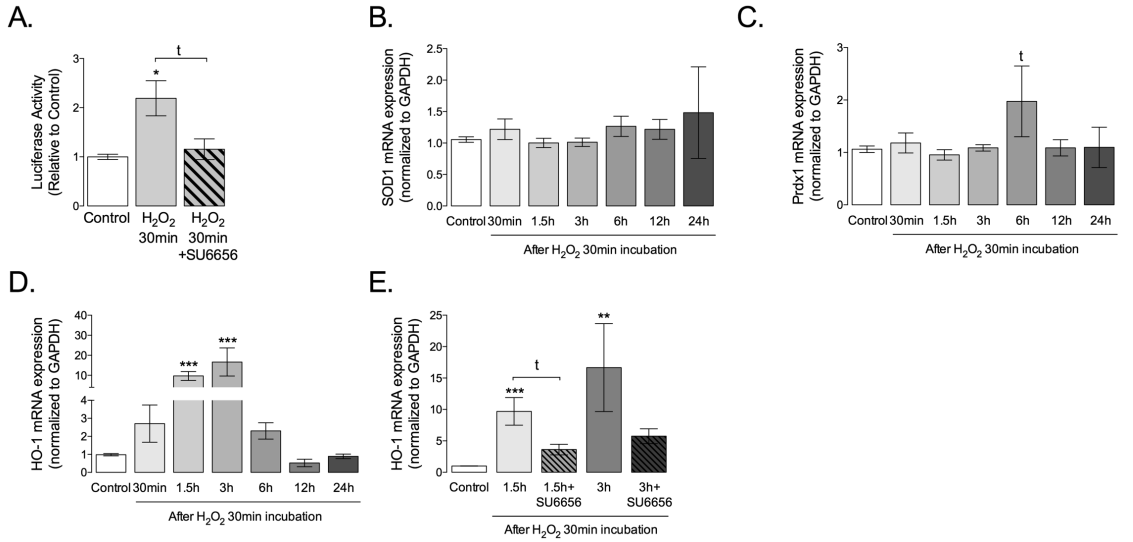

Figure 3.6 | Nrf2/ARE transcriptional activity in HT22 cells after H2O2 exposure. HT22 cells were incubated with 1 mM H_2O_2 for 30 min, in the absence or presence of SU6656 (5 μM). In (A) 1.5 h after H_2O_2 stimulus Nrf2/ARE transcriptional activity was measured by relative luciferase activity in total-enriched protein fractions. Data are presented as the mean ± SEM of 5 independent experiments. (B-E) After H_2O_2 treatment (30 min), medium was replaced by fresh culture medium for 30 min, 1.5, 3, 6, 12 and 24 h and mRNA levels of SOD1, Prdx-1 and HO-1 were analyzed by real-time qPCR. Data are presented as the mean ± SEM of 3 to 6 independent experiments. Statistical analysis: *p <0.05, **p <0.01 and ***p <0.001 *versus* Control/untreated condition (nonparametric Kruskal-Wallis one-way ANOVA test, followed by Dunnett's Multiple Comparison as post hoc test); ^{t}p <0.05 H_2O_2 30 min *versus* H_2O_2 30 min+SU6656 (A), Control *versus* H_2O_2 30 min+6 h (C) or H_2O_2 30 min+1.5 h *versus* H_2O_2 30 min+1.5 h+SU6656 (E) (Student's t-test followed by nonparametric Mann Whitney as post hoc test).

3.3.4 INVOLVEMENT OF PKCδ ON NRF2 REGULATION BY c-SRC

Our results evidenced the positive cytoplasmic regulation of Nrf2 by c-Src kinase. However, since c-Src is a tyrosine kinase, the phosphorylation of Nrf2 at residue Ser40 implicated an intermediary protein. In this sense, we hypothesized that PKC, a serine/threonine protein kinase family that mediates a considerable number of cellular signalling responses, could be involved in cytoplasmic Src/Nrf2 regulation pathway. Indeed, activation of PKCδ isoform in a redox-dependent mechanism requires c-Src dependent tyrosine phosphorylation at Tyr311 (Konishi et al., 2001; Rybin et al., 2004; Steinberg, 2015). Moreover, considering that PKCδ may phosphorylate Nrf2 at Ser40 residue (Niture et al., 2009), we postulated that Nrf2 regulation, in a Src-dependent manner, might occur through PKCδ. Thus, we analysed PKCδ total and phosphorylated levels, after 30 min

H_2O_2 exposure, in the absence or presence of SU6656, PP2 or rottlerin (1 μM), the latter a PKCδ inhibitor at low concentrations (Gschwendt et al., 1994) (**Figure 3.7**).

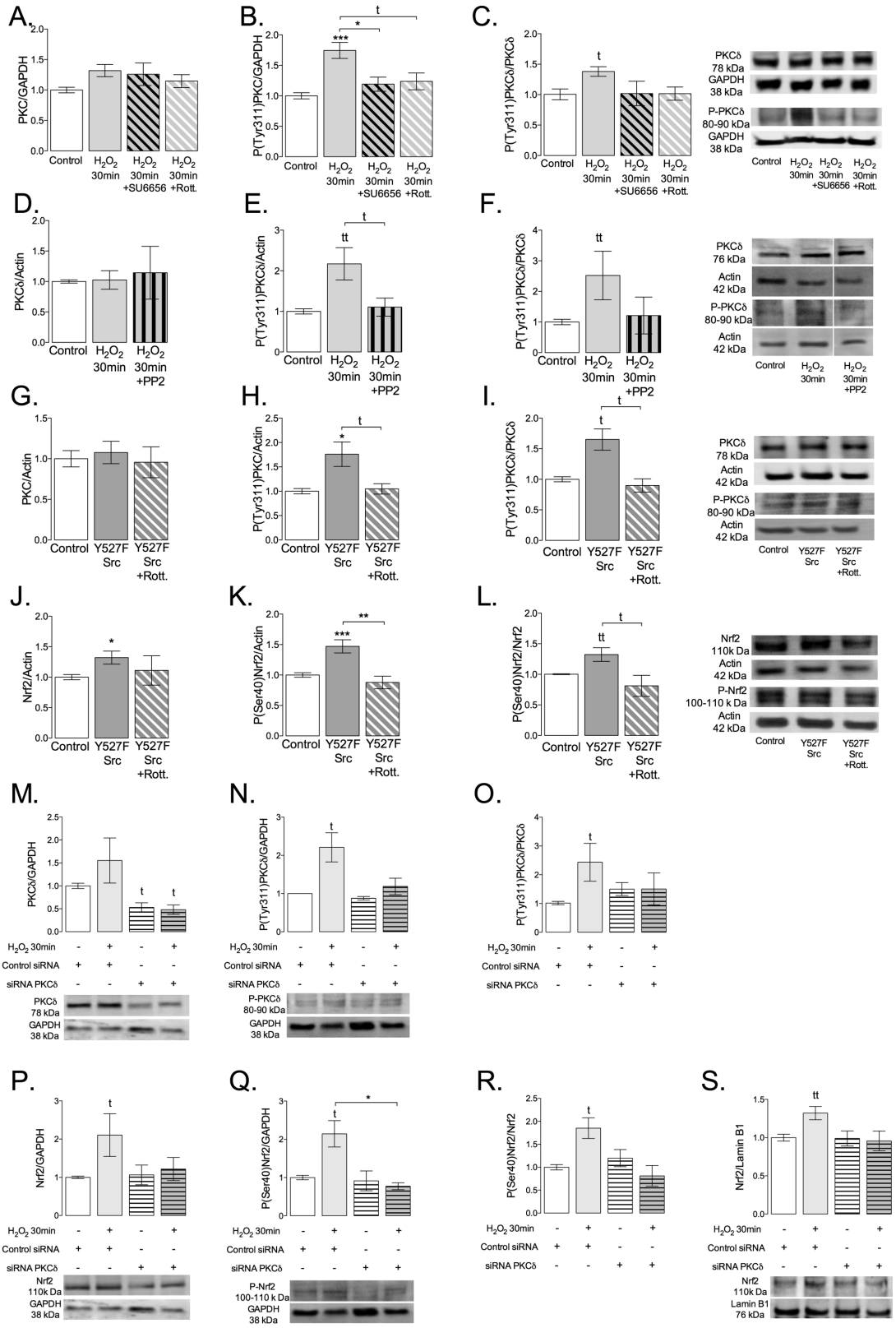

Figure 3.7 | Total and phosphorylated PKCδ and Nrf2 levels in HT22 cells subjected to H2O2 exposure, overexpression of an active form of Src or PKCδ silencing. (A-C) HT22 cells were incubated with 1 mM H_2O_2 for 30 min and the levels of PKCδ/GAPDH (A), P(Tyr311)PKCδ/GAPDH (B) and P(Tyr311)PKCδ/PKCδ (C) were evaluated by Western blotting in cytoplasmic-enriched fractions from HT22 cells. The effect of SU6656 (5 μM) and rottlerin (1 μM, a PKC inhibitor), were also evaluated. Data are expressed in arbitrary units relative to GAPDH as the mean ± SEM of n=3 to 10 independent experiments. (D-F) HT22 cells were incubated with 1 mM H_2O_2 for 30 min and the levels of PKCδ/actin (D), P(Tyr311)PKCδ/actin (E) and P(Tyr311)PKCδ/PKCδ (F) were analysed by Western blotting in total fractions from HT22 cells treated with PP2 (10 μM). Data are expressed in arbitrary units relative to actin as the mean ± SEM of n=3 to 4 independent experiments. (G-L) HT22 cells were transfected with plasmid constructs codifying for the constitutively active form of Src (Y527F SKF) and treated with rottlerin (1 μM) when indicated. Expression of plasmids was allowed for 24 h and levels of PKCδ/actin (G), P(Tyr311)PKCδ/actin (H), P(Tyr311)PKCδ/PKCδ (I), Nrf2/actin (J), P(Ser40)Nrf2/Actin (K) and P(Ser40)Nrf2/Nrf2 (L) were assessed by Western blotting in total fractions from HT22 cells. Data are expressed in arbitrary units relative to actin as the mean ± SEM of n=4 to 13 independent experiments. (M-S) HT22 cells were transfected with PKCδ specific siRNA or Control siRNA for 24h, and incubated with 1 mM H_2O_2 for 30 min; the levels of PKCδ/GAPDH (M), P(Tyr311)PKCδ/GAPDH (N), P(Tyr311)PKCδ (O), Nrf2/GAPDH (P), P(Ser40)Nrf2/GAPDH (Q) and P(Ser40)Nrf2/Nrf2 (R) were evaluated by Western blotting in cytoplasmic-enriched fractions from HT22 cells. Levels of Nrf2/Lamin B1 (S) were determined by Western blotting in nuclear-enriched fractions from HT22 cells. Data are expressed in arbitrary units relative to GAPDH or Lamin B1 as the mean ± SEM of n=3 to 5 experiments. Statistical analysis: (A-L) *p <0.05, **p < 0.01 and ***p < 0.001 *versus* Control/untreated or *versus* H_2O_2 30min+SU6656 (nonparametric Kruskal-Wallis one-way ANOVA test, followed by Dunnett's Multiple Comparison as post hoc test); ^{t}p <0.05 and ^{tt}p <0.01 *versus* Control or H_2O_2 30 min *versus* H_2O_2 30 min+Rott. or Y527F SKF *versus* Y527F SKF +Rottlerin (Student's t-test followed by nonparametric Mann Whitney as post hoc test). (M-S) *p <0.05 Control siRNA+H_2O_2 30 min *versus* PKCδ siRNA+H_2O_2 30 min (nonparametric Kruskal-Wallis one-way ANOVA test, followed by Dunnett's Multiple Comparison as post hoc test); ^{t}p <0.05 and ^{tt}p <0.01 *versus* Control siRNA (Student's t-test followed by nonparametric Mann Whitney as post hoc test).

Our results showed no significant differences in PKCδ total levels after exposure to H_2O_2 (**Figure 3.7A**); however, phosphorylation levels of PKCδ [p(Tyr311)PKCδ] were significantly increased after 30 min exposure to 1 mM H_2O_2 (**Figure 3.7B,C**). Importantly, this increase was inhibited by SU6656 (**Figure 3.7B,C**), as evaluated in cytoplasmic fractions, and by PP2 (**Figure 3.7E,F**), as determined in total extracts from HT22 cells, evidencing the role of c-Src activation on PKCδ phosphorylation/activation. As a control, cells were treated with rottlerin, a PKCδ inhibitor, which was shown to significantly reduce p(Tyr311)PKCδ (**Figure 3.7A-C**). PKCδ inhibition significantly decreased Nrf2 cytoplasmic levels and its phosphorylation at Ser40 following exposure to H_2O_2 in HT22 cells, as well as Nrf2 accumulation in the nucleus, confirming the role of PKCδ (**Figure 3.8,A-D**). P(Tyr416)Src levels were not significantly affected by

24h preincubation with rottlerin in cells exposed to 1 mM H_2O_2 for 30 min (data not shown).

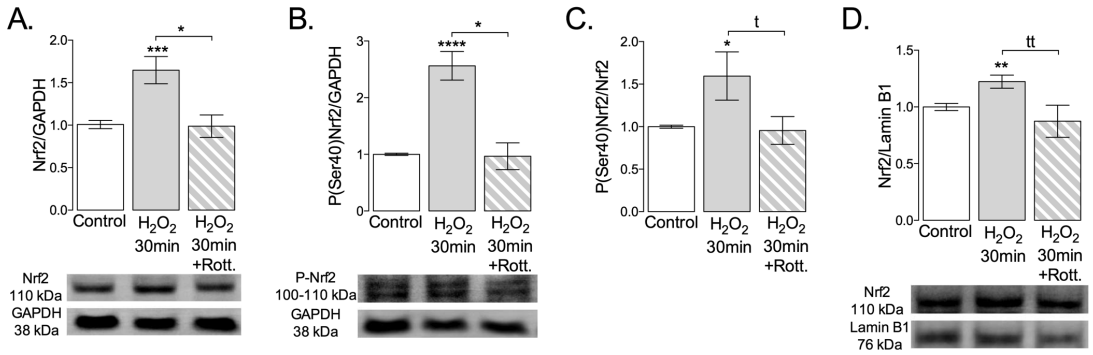

Figure 3.8 | Nrf2 total and phosphorylated protein levels in HT22 cells after H2O2 exposure. HT22 cells were incubated with 1 mM H_2O_2 for 30 min and the levels of Nrf2/GAPDH (A), P(Ser40)Nrf2/GAPDH (B), P(Ser40)Nrf2/Nrf2 (C) and Nrf2/Lamin B1 (D) were evaluated by Western blotting in cytoplasmic or nuclear-enriched fractions from HT22 cells. The effect of rottlerin (1 μM), a PKC inhibitor, was also evaluated. Data are expressed in arbitrary units relative to GAPDH or Lamin B1 as the mean ± SEM of n=4 to 13 independent experiments. Statistical analysis: (A-C) *p <0.05, **p < 0.01, ***p < 0.001 and ****p < 0.0001 *versus* Control or *versus* H_2O_2 30 min+Rott. (one-way ANOVA, followed by Dunnett's nonparametric Multiple Comparison as post hoc test); ^{t}p <0.05 and ^{tt}p <0.01 H_2O_2 30 min *versus* H_2O_2 30 min+Rott (Student's t-test followed by nonparametric Mann Whitney as post hoc test).

To affirm the role of c-Src on PKCδ and Nrf2 activation, we further analysed these proteins in total extracts of HT22 cells transfected with a constitutively active form of Src, Y527F SKF, in the absence or presence of rottlerin (**Figure 3.7G-L**). Expression of Y527F SKF caused a significant increase in phosphorylated PKCδ levels at Tyr311, which was inhibited by rottlerin (**Figure 3.7H,I**), indicating that c-Src activation positively influences PKCδ activation. Importantly, expression of an active form of c-Src caused a significant increase in Nrf2 levels (**Figure 3.7J**) and p(Ser40)Nrf2 (**Figure 3.7K,L**) in HT22 cells, the latter being reduced by the PKCδ inhibitor, rottlerin. No significant differences in p(Tyr416)Src, Nrf2 or p(Ser40)Nrf2 levels were observed in cells transfected with the empty vector (**Figure 3.9A-D**).

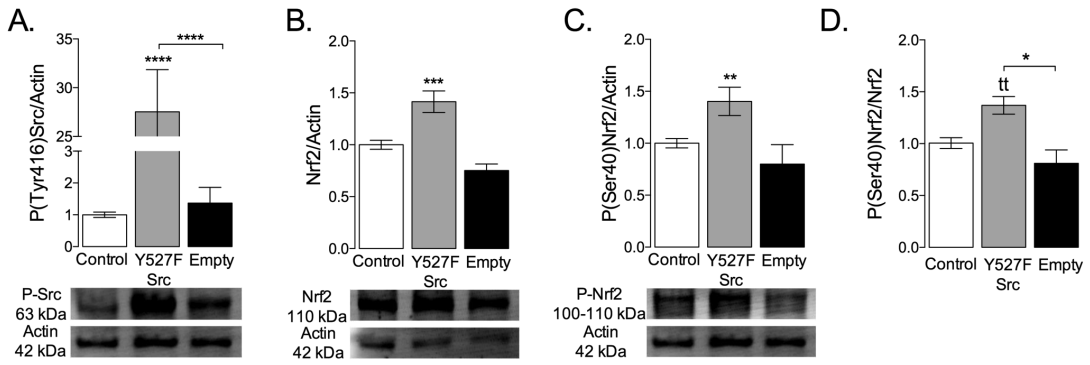

Figure 3.9 | c-Src and Nrf2 total and phosphorylated protein levels in HT22 cells overexpressing a constitutive active form of Src. HT22 cells were transfected with plasmid constructs codifying for the constitutively active form of Src (Y527F SKF) or the empty vector (empty). The levels of P(Tyr416)Src/actin (A), Nrf2/actin (B), P(Ser40)Nrf2/actin (C) and P(Ser40)Nrf2/Nrf2 (D) were evaluated by Western blotting. Data are expressed in arbitrary units relative to actin as the mean ± SEM of n=5 to 8 independent experiments. Statistical analysis: *p < 0.05, **p < 0.01, ***p < 0.001 and ****p < 0.0001 *versus* Control or *versus* Empty vector (one-way ANOVA, followed by Dunnett's nonparametric Multiple Comparison as post hoc test); ^{tt}p <0.01 Control *versus* Y527F SKF (Student's t-test followed by nonparametric Mann Whitney as post hoc test).

In order to confirm PKCδ involvement in the novel c-Src/PKCδ/Nrf2 pathway stimulated by acute H_2O_2 stimulus, we further tested the effect of PKCδ knock-down. HT22 cells were transfected with PKCδ specific siRNA or Control siRNA, in the presence or absence of 1 mM H_2O_2, for 30 min (**Figure 3.7M-S** and **3.10**). Data presented in Figure 4M and 6S,A, shows significantly reduced PKCδ levels (50-60% reduction, relatively to Control siRNA) in HT22 cytoplasmic fractions in the presence of PKCδ siRNA, confirming PKCδ silencing. p(Tyr311)PKCδ levels were significantly increased after incubation with 1 mM H_2O_2 in cells transfected with Control siRNA (**Figure 3.7N,O** and **3.10B,C**), but not after selective PKCδ knockdown. PKCδ siRNA did not alter c-Src total or phosphorylated levels, both in cytoplasmic or nuclear fractions, or in total extracts (**Figure 3.10G-O**). Additionally, increased total Nrf2 and P(Ser40)Nrf2 levels, in cytoplasm and nucleus of HT22 cells, were observed in the presence of Control siRNA in cells exposed to 1 mM H_2O_2 (30 min), but not after PKCδ selective knockdown (**Figure 3.7P-S**). Thus, p(Ser40)Nrf2 levels were significantly reduced after diminished PKCδ expression and exposure to 1 mM H_2O_2, confirming Nrf2 phosphorylation at Ser40 by PKCδ. Concordantly, H_2O_2-mediated increase in Nrf2 levels in the

nucleus of HT22 cells was abrogated by PKCδ specific siRNA. Similar results were obtained in HT22 total cell extracts (**Figure 3.10D-F**). Data indicate an indirect regulation of Nrf2 cytoplasmic activation by c-Src through the intermediate activation of PKCδ.

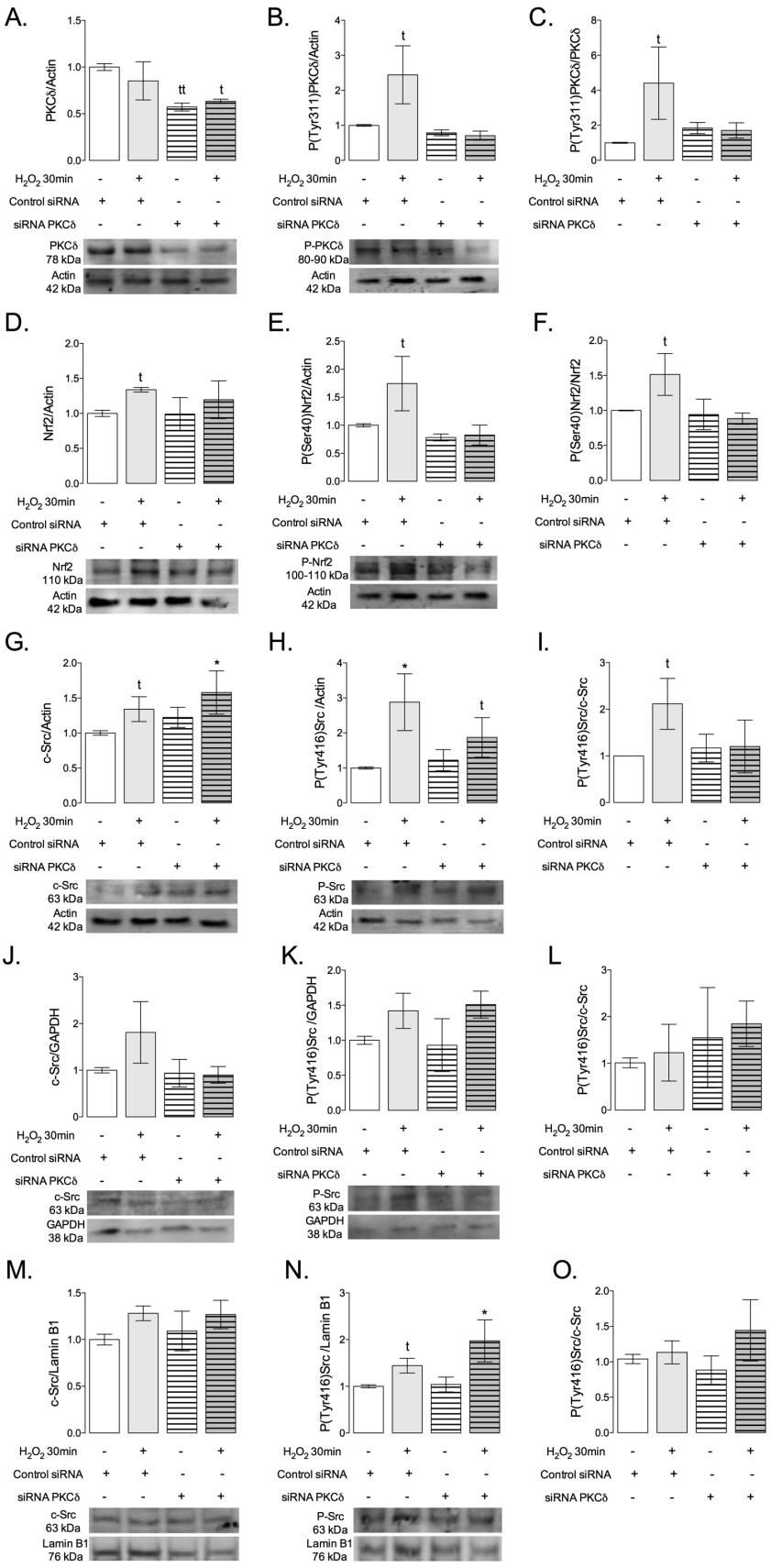

Figure 3.10 | Total and phosphorylated PKCδ, Nrf2 and Src levels in HT22 cells submitted to H2O2 exposure and PKCδ silencing. HT22 cells were transfected with PKCδ specific siRNA or Control siRNA and, 24h after transfection, cells were incubated with 1 mM H_2O_2

for 30 min and the levels of PKCδ/Actin (A), P(Tyr311)PKCδ/Actin (B), P(Tyr311)PKCδ/PKCδ (C), Nrf2/actin (D), P(Ser40)Nrf2/Actin (E), P(Ser40)Nrf2/Nrf2 (F), c-Src/Actin (G), P(Tyr416)Src/Actin (H) and P(Tyr416)Src/c-Src (I) were evaluated by Western blotting in total fractions from HT22 cells. Data are expressed in arbitrary units relative to actin as the mean ± SEM of n=3 to 5 independent experiments. Levels of c-Src/GAPDH (J), P(Tyr416)Src/GAPDH (K), P(Tyr416)Src/c-Src (L), c-Src/Lamin B1 (M), P(Tyr416)Src/Lamin B1 (N) and P(Tyr416)Src/c-Src (O) were determined by Western blotting in cytoplasmic (J-L) and nuclear (M-O) -enriched fractions from HT22 cells, respectively. Data are expressed in arbitrary units relative to GAPDH or Lamin B1 as the mean ± SEM of n=3 to 5 experiments. Statistical analysis: *p <0.05 *versus* Control siRNA (nonparametric Kruskal-Wallis one-way ANOVA test, followed by Dunnett's Multiple Comparison as post hoc test); ^{t}p <0.05 and ^{tt}p <0.01 *versus* Control siRNA (Student's t-test followed by nonparametric Mann Whitney as post hoc test).

To further confirm the results obtained by Western Blotting, we analysed the levels of c-Src and Nrf2 by immunocytochemistry, as well as their subcellular distribution in HT22 cells co-transfected with the constitutive active form of c-Src (Y527F SKF) and GFP, in the absence or presence of rottlerin (**Figure 3.11**). Results evidenced an enhancement in p(Tyr416)Src in the cytoplasm (C) and nucleus (N) of Y527F SKF transfected HT22 cells, which were unchanged in the presence of rottlerin (**Figure 3.11A,D**). Of relevance, results evidenced a significant increase in total cytoplasmic Nrf2 and p(Ser40)Nrf2 (**Figure 3.11B,C**), as well as an increase in nuclear Nrf2 total levels following Y527F SKF expression, when compared to control cells (GFP expression alone) in the cytoplasm and nucleus; these effects exerted by expression of Y527F SKF were inhibited by rottlerin (**Figure 3.11B,C,E**).

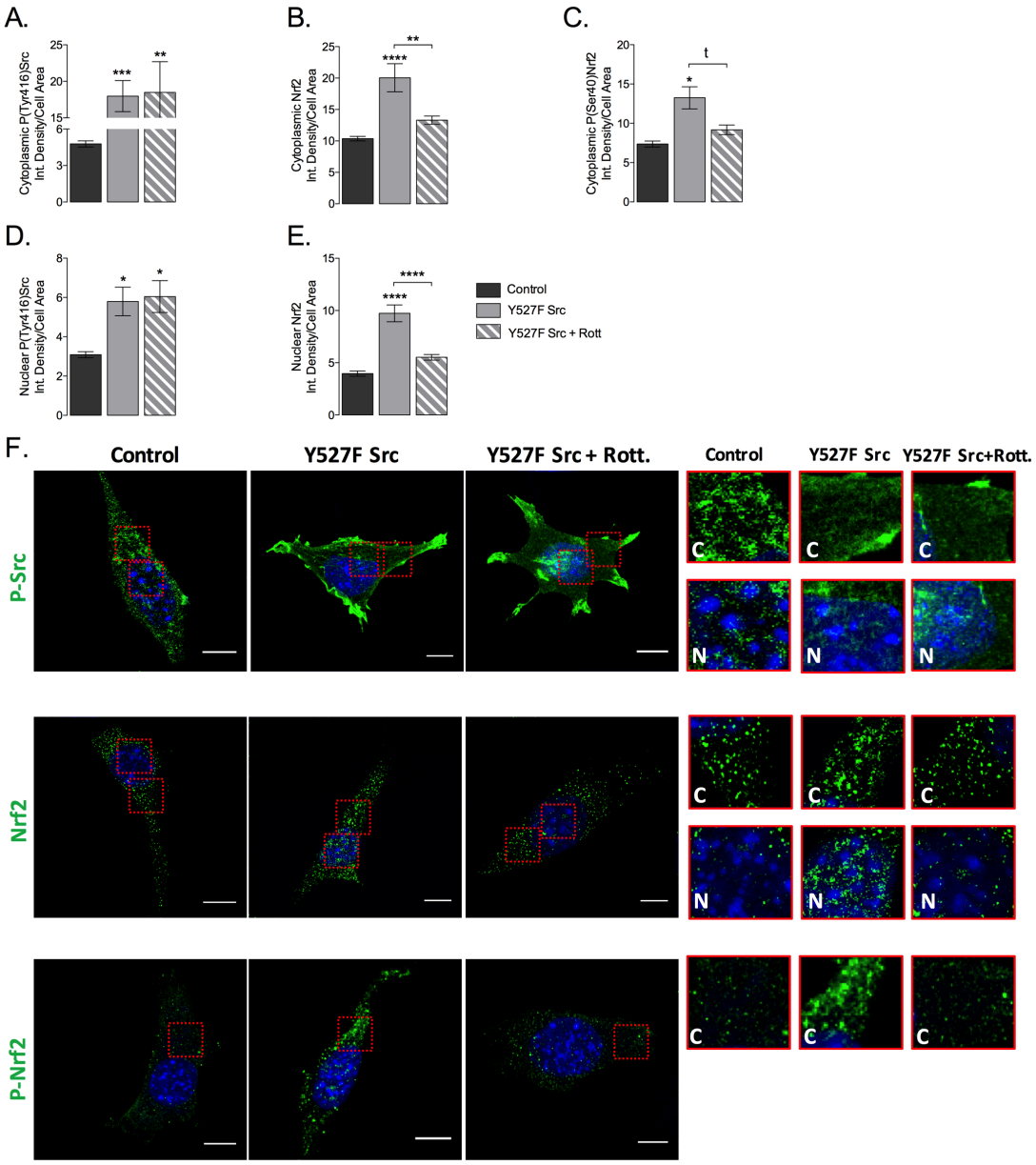

Figure 3.11 | Total and phosphorylated Nrf2 and Src Kinases levels in cells overexpressing an active form of Src. HT22 cells were co-transfected with GFP (Control) and Y527F SKF +GFP (Y527F SKF), for 24 h, and P(Tyr416)Src Family (A,D), Nrf2 (B,E) and P(Ser40)Nrf2 (C) cytoplasmic and nuclear levels were evaluated by immunocytochemistry using confocal microscope and Image J software. The effect of rottlerin (1 µM) was also evaluated. Confocal images were obtained with a 63x objective (F) (scale bar: 10 µm). Inserts show at higher magnification the images indicated by boxes of cytoplasmic (C) and nucleus (N) labelling. Data are presented as the mean ± SEM of 3 to 5 independent experiments considering ~12 cells/condition. Statistical analysis: *$p < 0.05$, **$p < 0.01$, ***$p < 0.001$ and ****$p < 0.0001$ between different groups (one-way ANOVA, followed by Tukeys's Multiple Comparison as post hoc test); (C) $^{t}p < 0.05$ Y527F SKF *versus* Y527F SKF + Rottlerin (Student's t-test followed by parametric and unpaired test).

Altogether, data strongly suggest that H_2O_2-elicited c-Src activation leads to PKCδ activation through its phosphorylation at residue Tyr311, which regulates cytosolic phosphorylation of Nrf2 at residue Ser40 and its translocation to the nucleus, resulting in enhanced Nrf2 transcriptional activity (c-Src/PKCδ/Nrf2 pathway) and increased HO-1 mRNA levels, as represented in **Figure 3.12**.

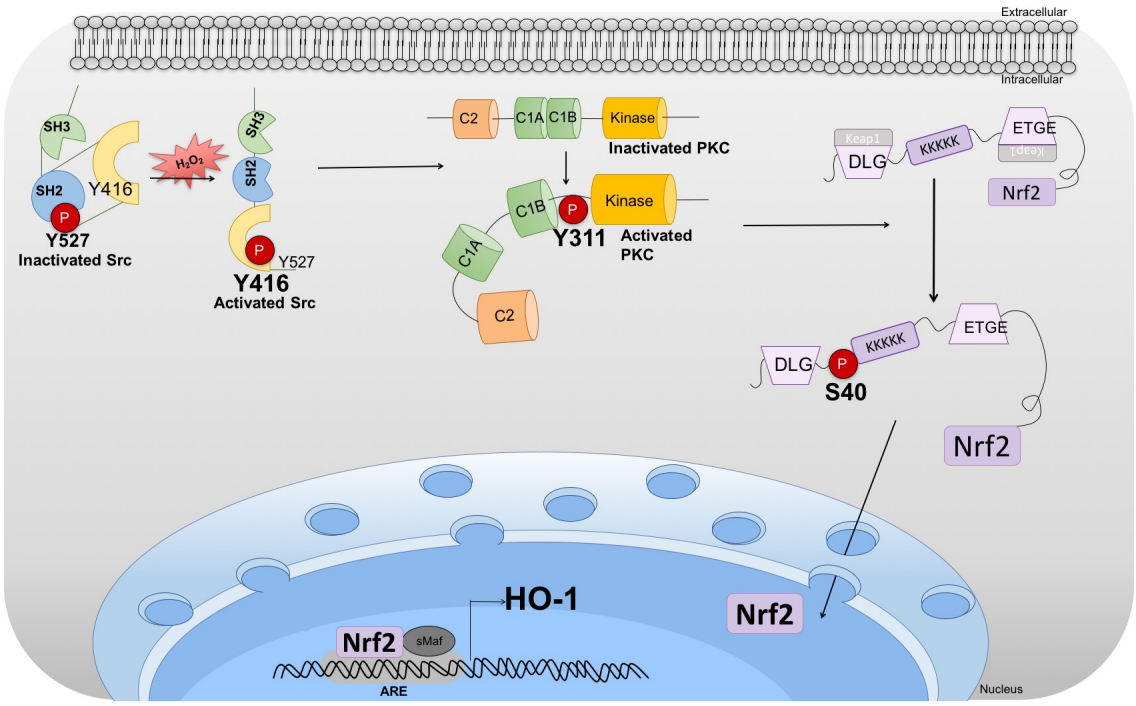

Figure 3.12 | Schematic representation of Src/PKCδ/Nrf2 signaling pathway involved in HO-1 expression after H2O2 exposure in HT22 cells. After H_2O_2 exposure, Src kinases are activated through Tyr416 phosphorylation. Src kinases-dependent phosphorylation of PKCδ Tyr 311 residue in the cytoplasm induces the activation of the protein, which can further phosphorylate Nrf2 at Ser40. Once phosphorylated, Nrf2 migrates to the nucleus, binds to the ARE element in genes promotor and regulates the transcription of target genes, namely HO-1.

3.4 DISCUSSION

The role of Nrf2 in triggering the expression of antioxidant proteins and detoxifying enzymes during mild oxidant conditions has been extensively studied (Moris et al., 2017; Pizzino et al., 2017; Rodic and Vincent, 2017). In the present study, we demonstrate that exposure of HT22 cells to H_2O_2 (used as an non-toxic acute oxidant stimulus) evokes Nrf2 cytoplasmic phosphorylation, its nuclear migration and accumulation in a process that is regulated by c-Src through activation of PKCδ.

c-Src levels have been described to be altered in several disease models, such as human tumor cells (Tsygankov and Shore, 2004; Turro et al., 2016), rat cardiomyocytes in cardiac hypertrophy (Chen et al., 2013) and pancreatic rat β-cells associated to diabetes (Weaver and Taylor-Fishwick, 2013; Zhang et al., 2006). Furthermore, we previously demonstrated reduced c-Src activity in the hippocampus of a mouse model of Alzheimer's disease, the 3xTg-AD mice, at 3 months of age (Mota et al., 2014b). c-Src is a redox-sensitive protein that can be activated by H_2O_2, resulting in its phosphorylation at Tyr416 residue. At the same time, tyrosine-phosphatase proteins, which modulate c-Src phosphorylation, are also sensitive to H_2O_2, favoring c-Src kinase activation (Espada and Martín-Pérez, 2017). In our experimental model, we confirmed cytoplasmic and nuclear c-Src activation in HT22 cell line exposed to H_2O_2.

There are several evidences for altered levels of the transcription factor Nrf2 (e.g. its upregulation) in distinct neurodegenerative diseases (Mota et al., 2015), ischemia and heart failure (Strom and Chen, 2017), cancer (Jeddi et al., 2018) or diabetes mellitus (Uruno et al., 2013), revealing the importance of understanding Nrf2 regulation. In the current study, we observed H_2O_2-mediated increase in total and p(Ser40)Nrf2 levels in the cytoplasm of HT22 cells. Previous data from Huang et al, 2002 (Huang et al., 2002), showed that there are no differences concerning ARE-binding of P(Ser40)Nrf2 or non-P(Ser40)Nrf2. The main effect of Nrf2 phosphorylation at Ser40 appears to be the dissociation from Keap1, and consequent nuclear migration, but once in the nucleus they appear to be both effective for ARE-mediated transcription, and Nrf2 in the nucleus is a more appropriate measure, concerning Nrf2 activation. Concordantly, H_2O_2-mediated increase in total and p(Ser40)Nrf2 levels in the cytoplasm was

associated with its nuclear migration and increased Nrf2 transcriptional activity, as shown by the augmented levels of HO-1 (at earlier time points) and Prdx-1 mRNA following H_2O_2 treatment. Our results do not evidence changes in SOD1 mRNA, suggesting a selective effect of oxidant-mediated Nrf2 transcription in HT22 cells. Indeed, stress-induced HO-1 gene expression has been shown to be largely controlled by Nrf2 activation (Alam et al., 1999, 1995, 1994), whereas SOD1 and Prdx-1 mRNA levels are also controlled by other transcription factors (Milani et al., 2011; Rhee and Kil, 2017). Interestingly, the Src inhibitor, SU6656, significantly reduced HO-1 mRNA levels, confirming that c-Src-mediated activity is involved in Nrf2-mediated transcription.

Nrf2 accumulation and its nuclear activity are regulated by several chemical and molecular mechanisms, depending on cell environment. Apart from Keap1-dependent regulation, Nrf2 activation is also influenced by different kinase proteins, such as PKC, MAPK, GSK-3β, PI3K/Akt, among others, favoring Nrf2 serine or threonine phosphorylation (Bryan et al., 2013; Jaramillo and Zhang, 2013). PKC, a family of signal-regulated enzymes, is responsible for modulating numerous physiological responses; it was the first protein family described to regulate Nrf2 phosphorylation at Ser40, modulating its cytosolic and nuclear accumulation (Huang et al., 2002). Later, Niture and colleagues (Niture et al., 2009), followed by others (Bang et al., 2017), described the PKCδ isoform as the main kinase responsible for this phosphorylation. Moreover, a possible relationship between c-Src and Nrf2 nuclear accumulation has been reported in few studies. Lee and colleagues demonstrated that lipoteichoic acid (a major constituent of the cell wall of gram-positive bacteria), which has a protective role in the pathogenesis of inflammatory responses, leads to enhanced Nrf2 levels and activity in human tracheal smooth muscle cells (HTSMCs) in a c-Src-dependent pathway (Lee et al., 2008). A similar work was developed by Cheng and colleagues, who demonstrated, using cigarette smoke particle-phase extract, that the activation of HO-1 *via* increased Nrf2 activity was dependent on c-Src activation (Cheng et al., 2010). Both data evidenced NADPH oxidase protein as the intermediate between c-Src and Nrf2, describing that c-Src-dependent NADPH oxidase activation could further lead to Nrf2 nuclear accumulation. Recently, two other studies described two different pathways of Nrf2 modulation by c-Src. Yang and colleagues, used the transition metal carbonyl compound

carbon monoxide-releasing molecule-2 (CORM-2) to induce HO-1 expression in HTSMCs cells (Yang et al., 2015). These authors described that CORM-2 activates c-Src, leading to its phosphorylation at residue Tyr139, which in turn activates the membrane epidermal growth factor receptor (EGFR) leading to PI3K/Akt pathway activation and consequent JNK1/2 and p38 MAPK phosphorylation, favoring Nrf2 activity (Yang et al., 2015). On other hand, Lin and co-workers used arachidonic acid (AA), a polyunsaturated fatty acid that causes ROS generation through NADPH oxidase activation, to study HO-1 expression in rat brain astrocytes (Lin et al., 2017); the authors evidenced a pathway in which AA-induced ROS cause c-Src phosphorylation and subsequent activation of Pyk2 tyrosine kinase. Pyk2 further activates the platelet-derived growth factor receptor linking to PI3K/Akt/ERK1/2 activation, which results in HO-1 augmented expression (Lin et al., 2017). Importantly, our findings evidenced that both increased Nrf2 total and phosphorylated levels in the cytoplasm and nucleus of HT22 cells, as well as Nrf2 transcriptional activity, were inhibited by SU6656, a selective Src kinase inhibitor. These results suggested that phosphorylation of Nrf2 at Ser40 occurred in a c-Src-dependent manner, as confirmed using a constitutive active form of Src (Y527F SKF). Considering that such interaction could only occur indirectly, here we demonstrate the involvement c-Src-dependent PKCδ activation on Nrf2 modulation. Indeed, both PKCδ inhibition by rottlerin and a PKCδ specific siRNA reduced Nrf2 total and phosphorylated levels in cytoplasm, as well as Nrf2 nuclear accumulation in HT22 cells exposed to H_2O_2.

Importantly, different authors described the link between c-Src and PKCδ proteins. Indeed, and as described above, c-Src can be activated by H_2O_2, which in turn, promotes the PKCδ-Src complex formation, leading to Src-dependent PKCδ tyrosine phosphorylation at Tyr311, and resulting in enhanced PKCδ catalytic activity (Konishi et al., 2001; Rybin et al., 2004; Steinberg, 2015). Concordantly, we show that PKCδ phosphorylation at Tyr311 increases after H_2O_2 exposure, in a c-Src-dependent manner, in the cytoplasm of HT22 cells. Data do not support the reciprocal interaction, PKCδ-mediated Src activation, because silencing of PKCδ did not alter c-Src total or phosphorylated levels. Thus, considering our results, H_2O_2-induced Nrf2 enhanced accumulation and

activity may occur through PKCδ phosphorylation via c-Src activation. Indeed, the constitutive active form of Src (Y527F SKF) enhanced Nrf2 phosphorylation through the intermediate phosphorylation of PKCδ at Tyr311 residue, leading to Nrf2 cytoplasmic and nuclear and accumulation, which potentially increased Nrf2 transcriptional activity and HO-1 and later Prdx1 expression.

Our data provide strong evidence that acute H_2O_2 exposure results in increased c-Src activation in HT22 cells, which in turn upregulates PKCδ phosphorylation, subsequently increasing Nrf2 phosphorylation at Ser40 residue; under these conditions, Nrf2 shows enhanced accumulation in the nucleus and Nrf2/ARE transcriptional activity, testified through increased HO-1 mRNA levels (Figure 6). To our knowledge, our study provides the first evidence that c-Src can serve as Nrf2 co-activator via PKCδ, after acute oxidant stimulus induced by H_2O_2. In this way, c-Src may constitute an essential protein in regulating Nrf2 nuclear activity after short exposure to a high concentration of H_2O_2, which may occur locally in cells. Considering that increased oxidant conditions are a common feature in several diseases, our study provides the first evidence that c-Src is a key protein in Nrf2 regulation after an oxidant stimulus, highlighting the c-Src/PKCδ/Nrf2 pathway as a possible novel target for ameliorating pathologies linked to redox deregulation.

CHAPTER IV

RESTORATION OF c-SRC/FYN PROTEINS RESCUES MITOCHONDRIAL DYSFUNCTION IN HUNTINGTON'S DISEASE*

* Based on the following published manuscript: (Fão et al., 2022)

4.1. SUMMARY

HD is an autosomal-dominant neurodegenerative disorder with no effective therapies. mHTT, the main HD proteinaceous hallmark, has been linked to ROS formation and mitochondrial dysfunction, among other pathological mechanisms. Importantly, Src-related kinases, c-Src and Fyn, are activated by ROS and regulate mitochondrial activity. However, c-Src/Fyn involvement in HD is largely unexplored. Thus, in this study we aimed to explore changes in Src/Fyn proteins in HD models and their role in defining altered mitochondrial function and dynamics and redox regulation.

We show, for the first time, that c-Src/Fyn phosphorylation/activation and proteins levels are decreased in several human and mouse HD models mainly due to autophagy degradation, concomitantly with mHtt-expressing cells showing enhanced TFEB-mediated autophagy induction and autophagy flux. c-Src/Fyn co-localization with mitochondria is also reduced. Importantly, expression of constitutive active c-Src/Fyn to restore active SKF levels improves mitochondrial morphology and function, namely through improved mitochondrial transmembrane potential, mitochondrial basal respiration and ATP production, but did not affect mitophagy. Additionally, constitutive active c-Src/Fyn expression diminishes the levels of reactive species in cells expressing mHTT.

c-Src/Fyn restoration in HD improves mitochondrial morphology and function, precluding the rise in oxidant species and cell death. This work supports a relevant role for c-Src/Fyn proteins in controlling mitochondrial function and redox regulation in HD, revealing a potential HD therapeutic target

4.2. INTRODUCTION

HD is an autosomal-dominantly inherited neurodegenerative disorder for which there is no cure. HD is caused by an abnormal expansion of CAG triplets encoding for an abnormally long polyQ tract (Finkbeiner, 2011) in the coding region of the ubiquitously expressed *HTT* gene, encoding for mHTT (Morreale, 2015). Clinically, HD symptoms include psychiatric and behavioural disturbances, cognitive dysfunction, involuntary motor movement, and progressive dementia (Morreale, 2015; Ross and Tabrizi, 2011). Neuropathologically, HD is characterized by selective neurodegeneration of MSNs in striatum (caudate and putamen), with a dorsomedial to ventrolateral direction (Sieradzan and Mann, 2001). HTT aggregates intracellularly and causes cytotoxicity, associated to protein clearance pathways inhibition, mitochondrial and synaptic dysfunction, altered Ca^{2+} handling, ER stress, impaired gene transcription and translation, among other defective pathways (Finkbeiner, 2011).

Mitochondrial dysfunction is one of the major early relevant pathogenic mechanisms in HD. Several studies reported ultrastructural defects in mitochondria isolated from *postmortem* HD cortical tissue and compromised oxidative function and ATP synthesis in pre-symptomatic HD carriers (e.g. Saft et al., 2005). Moreover, decreased activity of mitochondrial complexes II-IV was observed in HD patient's *postmortem* striata, human peripheral cells and animal brains (Pandey et al., 2008). In accordance, isolated brain mitochondria from caudate nucleus of HD patients (Yano et al., 2014) and different HD cellular (e.g. human neuroblastoma cells and platelets, mouse striatal ST*Hdh*$^{Q111/Q111}$ cells) and animal models (Hdh(CAG)150 knock-in mouse) showed HTT fragments in close contact with mitochondria (Choo, 2004; Orr et al., 2008; Silva et al., 2013b), supporting a direct effect of mHTT on mitochondrial function.

Autophagy is an essential catabolic mechanism in neuronal homeostasis and survival (e.g. Komatsu et al., 2006). Several HD models showed dysfunctional autophagy, suggesting that macroautophagy dysregulation contributes to neurotoxicity. Martinez-Vicente and colleagues evidenced an increase in the number of autophagic vacuoles in several HD models (e.g.

primary neurons, striatal cell lines and fibroblasts) that did not undergo autophagy-mediated degradation mainly due to deficient cargo recognition (Martinez-Vicente et al., 2010).

Fyn and c-Src, two members of the SKF, are involved in several cellular processes, specifically regulation of neuronal ion channels activity, cell differentiation, signal transduction and general metabolism (Roskoski, 2015; Wang et al., 2005). SKF proteins can be directly and indirectly activated by H_2O_2, since they are redox-sensitive (Chojnacka and Mruk, 2015). Interestingly, c-Src/Fyn kinases were identified in the intermembrane space of highly purified rat brain mitochondria (Salvi et al., 2002). Moreover, c-Src/Fyn modulated brain mitochondrial respiration through phosphorylation of complexes I, III and IV (Ogura et al., 2012).

Indeed, increased ROS production and mitochondrial dysfunction are important features of HD ethiopatogenesis, while c-Src and Fyn proteins have several important roles in mitochondrial normal function and can be activated by ROS. However, the involvement of Src/Fyn in HD pathogenesis is still largely unexplored. In the context of mHTT expression, a previous study described the role of Src in Tyr phosphorylation of GluN2B subunits only (Song et al., 2003). Herein, we determined the changes in c-Src/Fyn total and activated/phosphorylated protein levels in several HD models, analysed their degradation process and determined the role of Src/Fyn kinases in HD-associated mitochondrial impairment. Our results evidence a decrease in Src and Fyn levels in HD due to autophagy degradation; this coincides with altered mitochondrial morphology and impaired function, and enhanced ROS levels. Importantly, data point out the therapeutic potential of modulating Src/Fyn activation/levels to alleviate HD cytopathological features.

4.3. RESULTS

4.3.1. ENHANCED SRC AND FYN PROTEIN DEGRADATION IN DIFFERENT HD MODELS

The SKF members have not been thoroughly explored before in the context of HD. Therefore, we first analysed c-Src and Fyn total and activated levels, the later using an anti-P-Tyr416-SKF antibody, in several models of HD by Western blotting and immunocytochemistry. *Postmortem* human caudate from HD patients presented reduced c-Src and Fyn total levels, when compared to control individuals (**Figure 4.1A,B**).

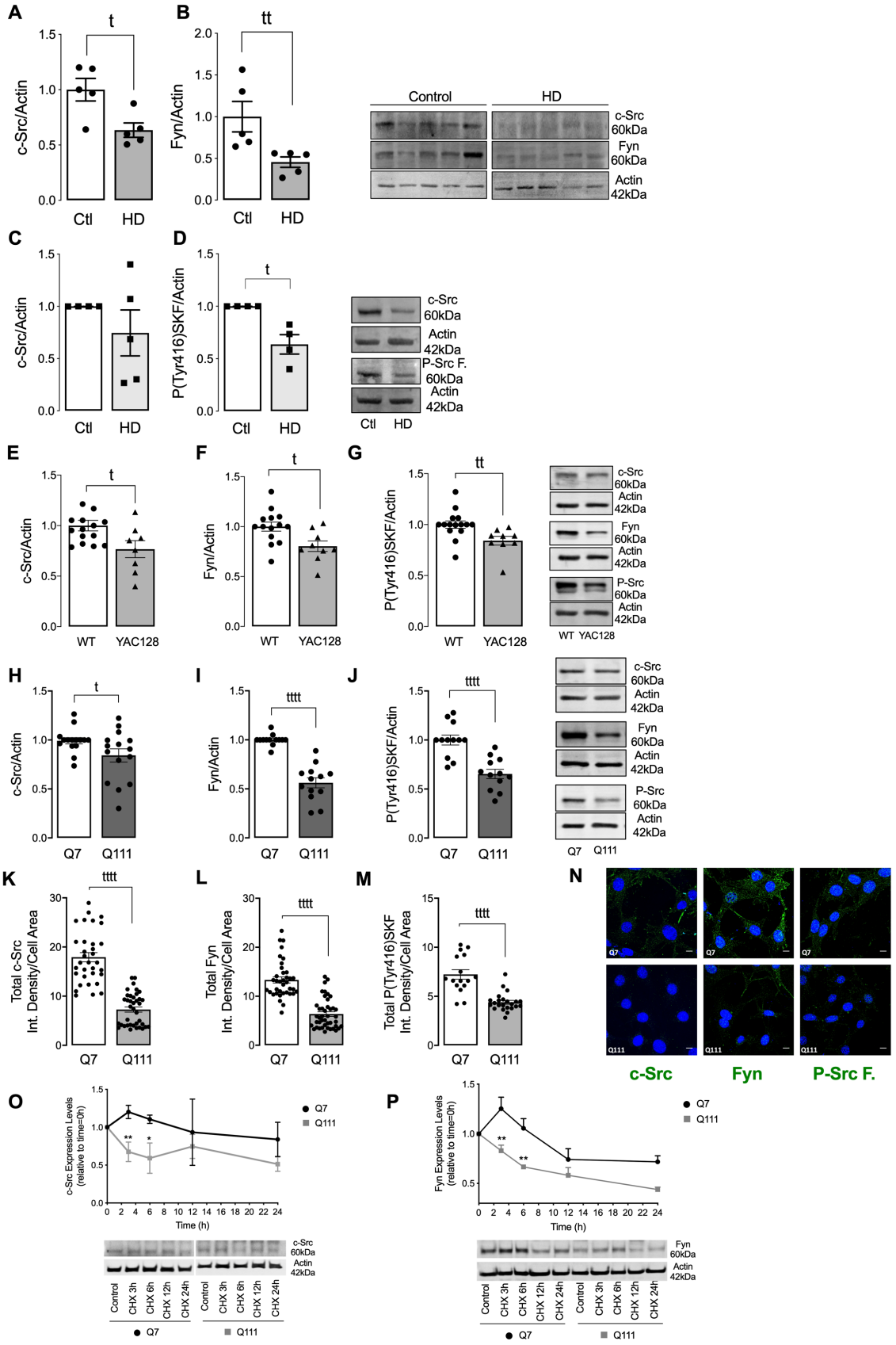

Figure 4.1 | c-Src and Fyn Total and Phosphorylated levels are reduced in different HD models. c-Src/Actin (A,C,E,H), Fyn/Actin (B,F,I) and P(Tyr416)SKF/Actin (D,G,J) were analysed by western blotting in total extracts from postmortem human caudate brain samples from control and HD patients (grade II-III, A,B), total extracts from human

heterozygous HD lymphoblasts expressing 42 to 49 CAG repeats in *HTT* gene (C,D), total extracts of primary striatal neurons obtained from the yeast artificial chromosome (YAC) bearing 128 CAG repeats in the human *HTT* gene (E-G), total extracts from Q7 vs. Q111 striatal cells (H-J). Data are expressed in arbitrary units relative to Actin as the mean ± SEM of 4 to 10 independent experiments. The levels of c-Src (K), Fyn (L) and P(Tyr416)SKF (M) were also evaluated by immunocytochemistry using confocal microscope and Image J software in Q7 vs. Q111 cells. Confocal images were obtained with a 63× objective in confocal microscope Zeiss LSM 710 (N, scale bar: 10 μm). Data are presented as the mean ± SEM of 4 independent experiments considering ~8 cells/condition. In (O-P) Q7 and Q111 cells were incubated with 350 μM cycloheximide for 3, 6, 12 or 24 h and the levels of c-Src/Actin (O) and Fyn/Actin (P) were evaluated by Western blotting in total extracts. Data are expressed in arbitrary units relative to Actin as the mean ± SEM of 3 to 4 independent experiments. Statistical analysis: (A–M) $^{t}p < 0.05$, $^{tt}p < 0.01$, and $^{tttt}p < 0.0001$ versus control conditions (nonparametric Mann Whitney test). (O,P) *p < 0.05, **p < 0.01 *versus* untreated Q7 cells (two-way ANOVA, followed by Sidak's Multiple Comparison as post hoc test).

No significant changes were observed in *postmortem* human parietal cortex from HD patients (**Figure 4.2A,B**). Moreover, in peripheral cells, namely lymphoblasts derived from HD affected patients containing heterozygous expansion mutation, we observed a significant decrease in the levels of P-Tyr416-SKF when compared with unaffected voluntary control siblings, suggesting reduced activated Src and Fyn, and a trend for decreased total c-Src protein levels (**Figure 4.1C,D**).

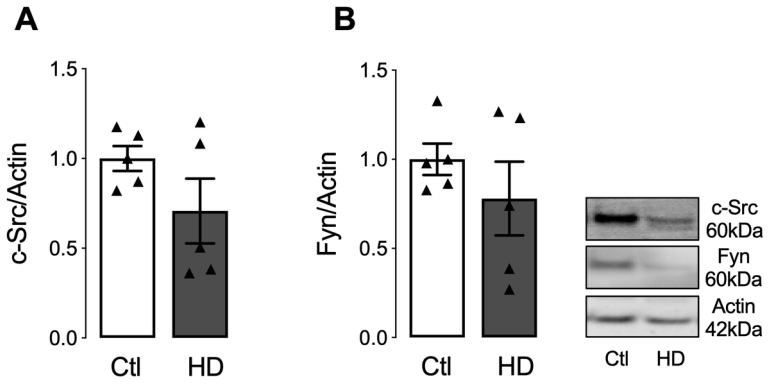

Figure 4.2 | c-Src and Fyn Total levels in HD human parietal cortex postmortem tissue. c-Src/Actin (A) and Fyn/Actin (B) were determined by western blotting in total extracts from parietal cortex human postmortem brain samples derived from control individuals and HD patients (grades II-III). Data are expressed in arbitrary units relative to Actin as the mean ± SEM of 5 independent analyses.

Primary striatal neurons from YAC128 transgenic mice (**Figure 4.1E-G**) also evidenced decreased in both c-Src and Fyn total and phosphorylated/active protein levels. Similar results were observed in knock-in striatal ST*Hdh*$^{Q111/Q111}$ cells (hereafter Q111 cells) by Western blotting (**Figure 4.1H-J**), and immunocytochemistry (**Figure 4.1K-N**), when compared to Q7/control cells. Moreover, striatal and cortical tissue isolated from 3 month-old YAC128 transgenic mice, at early-symptomatic stage, presented reduced total and phosphorylated Fyn levels (**Figure 4.3A-F**). Altogether, data indicate diminished c-Src/Fyn total levels and activation consistently across different human and mouse HD models.

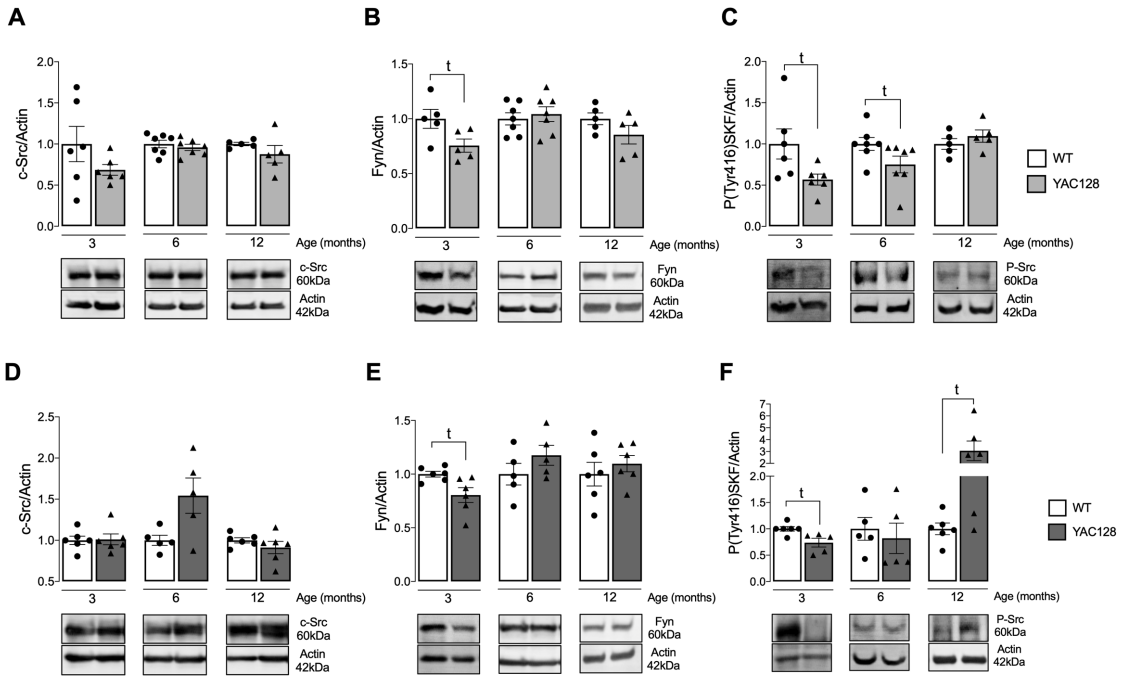

Figure 4.3 | Total Fyn and phosphorylated SKF levels are reduced in striatal and cortical total extracts from 3 month-old YAC128 mice. c-Src/Actin (A,D), Fyn/Actin (B, E) and p(Tyr416)SKF/Actin (C,F) levels were analysed by western blotting in total extracts from striatal (A-C) and cortical (D-F) tissue from WT and YAC128 mouse brain. Data are expressed in arbitrary units relative to Actin as the mean ± SEM of 5 to 7 animals through independent determinations. Statistical analysis: $^{t}p < 0.05$ versus WT (nonparametric Mann Whitney test).

SKF members have been reported to act as redox-sensitive Tyr kinase, regulated by H_2O_2. Considering that our results evidence an impairment in c-Src/Fyn activation in HD models, we evaluated c-Src/Fyn response to oxidative stress in Q7/Q111 cells (**Figure 4.4**). Cells were exposed to 100 μM H_2O_2 for 30 min and

1 hour and levels of total and Tyr416 phosphorylated c-Src/Fyn were measured in total extracts. Our results evidence significant increased total Fyn and phosphorylated SKF levels after H_2O_2 exposure (1 hour) in Q7 cells, while no differences were disclosed in Q111 cells, reinforcing the idea of an impairment in the activation pathway of SKF in this model.

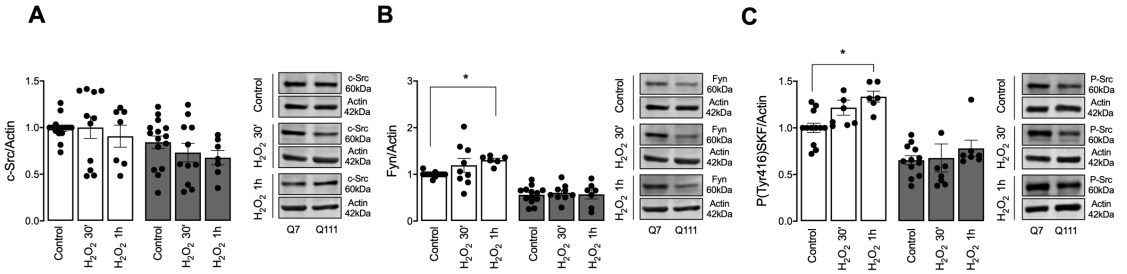

Figure 4.4 | Total Fyn and phosphorylated SKF levels are increased only in Q7 cells after exposure to H202. c-Src/Actin (A), Fyn/Actin (B) and p(Tyr416)SKF/Actin (C) levels were determined by Western blotting in total extracts from Q7 vs. Q111 cells after H2O2 exposure (100 μM) for 30 min and 1 h. Data are expressed in arbitrary units relative to Actin as the mean ± SEM of 7-9 independent analyses. Statistical analysis: *p < 0.05 versus Q7 cells without treatment (two-way ANOVA, followed by Sidak's Multiple Comparison as post hoc test).

To assess whether reduced c-Src/Fyn protein levels in HD models are related to decreased gene expression, we evaluated c-Src and Fyn mRNA levels. No differences between Q7 and Q111 cells or between YAC128 and WT primary striatal neurons were observed regarding c-Src and Fyn mRNA levels (**Figure 4.5**), indicating that decreased SKF levels is unrelated with altered gene transcription. Therefore, we then assessed c-Src/Fyn protein degradation kinetics using the cycloheximide (CHX, a protein synthesis inhibitor) chase assay (**Figure 4.1O,P**). Our results show a significant decrease in c-Src and Fyn total levels in Q111, when compared to Q7 cells, after 3 and 6 hours CHX treatment, which is maintained thereafter, indicating increased c-Src/Fyn protein degradation in mutant/Q111 cells.

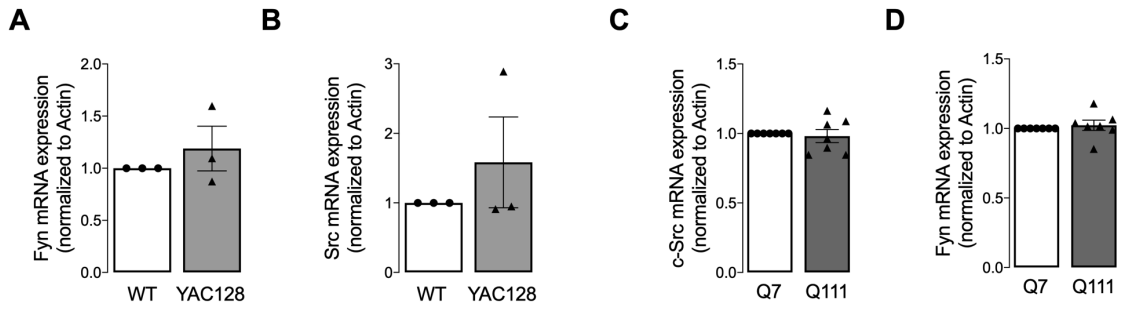

Figure 4.5 | c-Src and Fyn mRNA levels in primary striatal neurons from WT and YAC128 mice and Q7 and Q111 cells. mRNA levels of c-Src and Fyn were analysed by real-time qPCR, in primary neurons from WT and YAC128 mice (A,B), as well as in Q7 and Q111 striatal cells (C,D). Data are presented as the mean ± SEM of at least 3 independent experiments.

4.3.2. FYN AND c-SRC PROTEINS ARE DEGRADED DUE TO ENHANCED AUTOPHAGY IN CELLS EXPRESSING MHTT

Since our data evidenced higher c-Src/Fyn protein degradation in Q111 cells, we further analysed the involvement of protein degradation systems, namely endo-lysosomal, autophagy pathway and ubiquitin-proteasome system (UPS).

In **Figure 4.6A,B**, epoxomicin (selective UPS inhibitor) was used to assess the role of UPS in c-Src/Fyn degradation. Our results show that UPS seems to be involved in kinases degradation in Q7 cells only. In Q111 cells, UPS does not seem to be involved in kinases degradation, since no significant increase in protein accumulation was observed in the presence of epoxomicin (**Figure 4.6A,B**).

Autophagy pathway activation was evaluated at early and late phases. Early phase was assessed using 3-MA, which inhibits autophagy by blocking autophagosome formation via the inhibition of class III PI3K (**Figure 4.6C,D**), while late phase was analysed using bafilomycin A1, a lysosome proton pump inhibitor that prevents maturation of autophagic vacuoles by inhibiting fusion between autophagosomes and lysosomes (**Figure 4.6E,F**). c-Src protein levels are significantly increased in Q111 cells after incubation with 3-MA or bafilomycin A1, while no changes were observed in Q7 cells, suggesting autophagy-related degradation of Src in HD model (**Figure 4.6C,E**). Our results also evidence increased degradation of Fyn by autophagy pathway in Q111 cells (**Figure**

4.6D,F). Because Fyn levels are also increased after bafilomycin A1 exposure in Q7 cells, we calculated the fold change over the respective control (**Figure 4.6G**), confirming that Fyn protein is more degraded in Q111 cells by autophagy. Concordantly, treatment with rapamycin, which increase cellular autophagy through the inhibition of mTOR, reduced the protein levels of c-Src (**Figure 4.6H**) and Fyn (**Figure 4.6I**) in Q111 cells only, confirming the role of autophagy in the degradation of these two protein kinases in HD striatal cell model. Interestingly, in striatal primary neurons from WT and YAC128 mice treated with bafilomycin A1, the increase in c-Src and Fyn levels was only significant in YAC128 striatal neurons (**Figure 4.6L,M**); however, this was not observed after 3-MA treatment (**Figure 4.6J,K),** suggesting that degradation of these kinases in HD cells is favored at the late phase of autophagy, by lysosomes. These results may explain the decrease in c-Src and Fyn total and phosphorylated levels in HD cell models, namely in striatal Q111 cells and YAC128 mouse primary neurons.

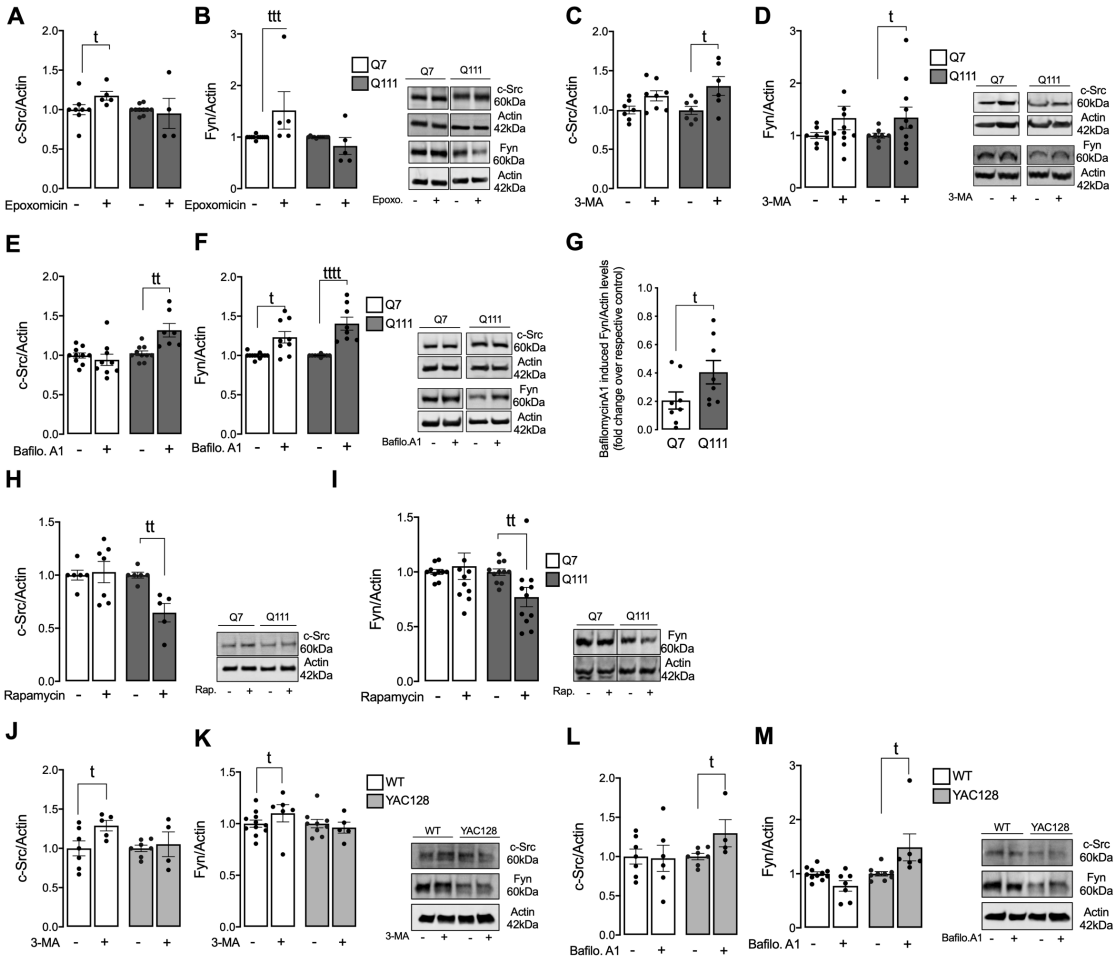

Figure 4.6 | Autophagy is implicated in c-Src and Fyn degradation in HD cell models. Q7

and Q111 cells were incubated with 200 nM epoxomicin for 24 h (A,B), 5 mM 3-MA for 4 h (C,D), 50 nM bafilomycin A1 for 24 h (E,F,G) and 200 nM rapamycin for 4 h (H,I) and the levels of c-Src/Actin (A,C,E,H) and Fyn/Actin (B,D,F,I) were evaluated by Western blotting in total extracts from Q7 vs. Q111 cells. Data are expressed in arbitrary units relative to Actin as the mean ± SEM of n = 3 to 8 independent experiments. (G) shows the fold change over respective control of Fyn/Actin levels after bafilomicyn A1 incubation. Primary striatal neurons from WT and YAC128 mice were incubated with 5 mM 3-MA for 4 h (J,K), 50 nM bafilomycin A1 for 24 h (L,M) and the levels of c-Src/Actin (J,L) and Fyn/Actin (K,M) were analysed by Western blotting in total cell extracts. Data are expressed in arbitrary units relative to Actin as the mean ± SEM of 3 to 5 independent experiments. Statistical analysis: $^{t}p < 0.05$, $^{tt}p < 0.01$, and $^{tttt}p < 0.0001$ versus Q7 cells or WT primary striatal neurons (nonparametric Mann Whitney test).

In order to confirm our hypothesis of enhanced degradation of c-Src/Fyn through autophagy, we further analysed some key proteins in the autophagy process. Cytosolic LC3-I is recruited to autophagosomal membranes, where is conjugated to phosphatidylethanolamine forming LC3-II. p62 is a selective autophagy receptor with an ubiquitin-binding domain, able to recognize ubiquitinated cargo designated for degradation. Q111 cells showed augmented levels of LC3-II/LC3-I and significantly reduced levels of p62 protein, which accumulated in the presence of bafilomycin A1 (**Figure 4.7A-D**), suggesting increased induction of autophagy in mutant striatal cells. Regarding Beclin-1, which acts during the initiation phase of autophagy by forming the isolation membrane, no significant differences were found between Q7 and Q111 cells (**Figure 4.7E,F**), suggesting that expression of mHtt does not impose changes in the initial steps of autophagosome formation. Furthermore, we analysed lysosomal biogenesis in HD cells. TFEB is an important mediator of autophagy regulation (Sardiello et al., 2009). Translocation of TFEB into the nucleus occurs in situations of stress in order to induce the expression of genes needed to activate and/or restore the autophagy-lysosomal pathway (Settembre et al., 2012). Our data show an increase in total and nuclear TFEB levels in Q111 cells (**Figure 4.7G-I**), which suggests augmented TFEB activation in cells expressing mHtt. Additionally, we measured LAMP1 levels, a lysosome-associated membrane protein, which correlates with the number of lysosomes and can be used as a marker of lysosomal biogenesis, a process regulated by TFEB. Consistent with TFEB data, LAMP1 levels were also found to be augmented in Q111 cells (**Figure 4.7J,K**). TFEB is activated by dephosphorylation and translocates to the nucleus where it promotes the transcription of several genes involved in the autophagy-lysosomal

pathway (Settembre et al., 2011), namely lysosomal cathepsin D (CTSD) and ATP6v0A1. Q111 cells show increased CTSD mRNA levels (**Figure 4.7L**), consistent with our data, showing augmented autophagy induction and increased c-Src/Fyn autophagy-dependent degradation. Concordantly with these data, we further show that autophagic flux is increased in Q111 cells (**Figure 4.7N,O**).

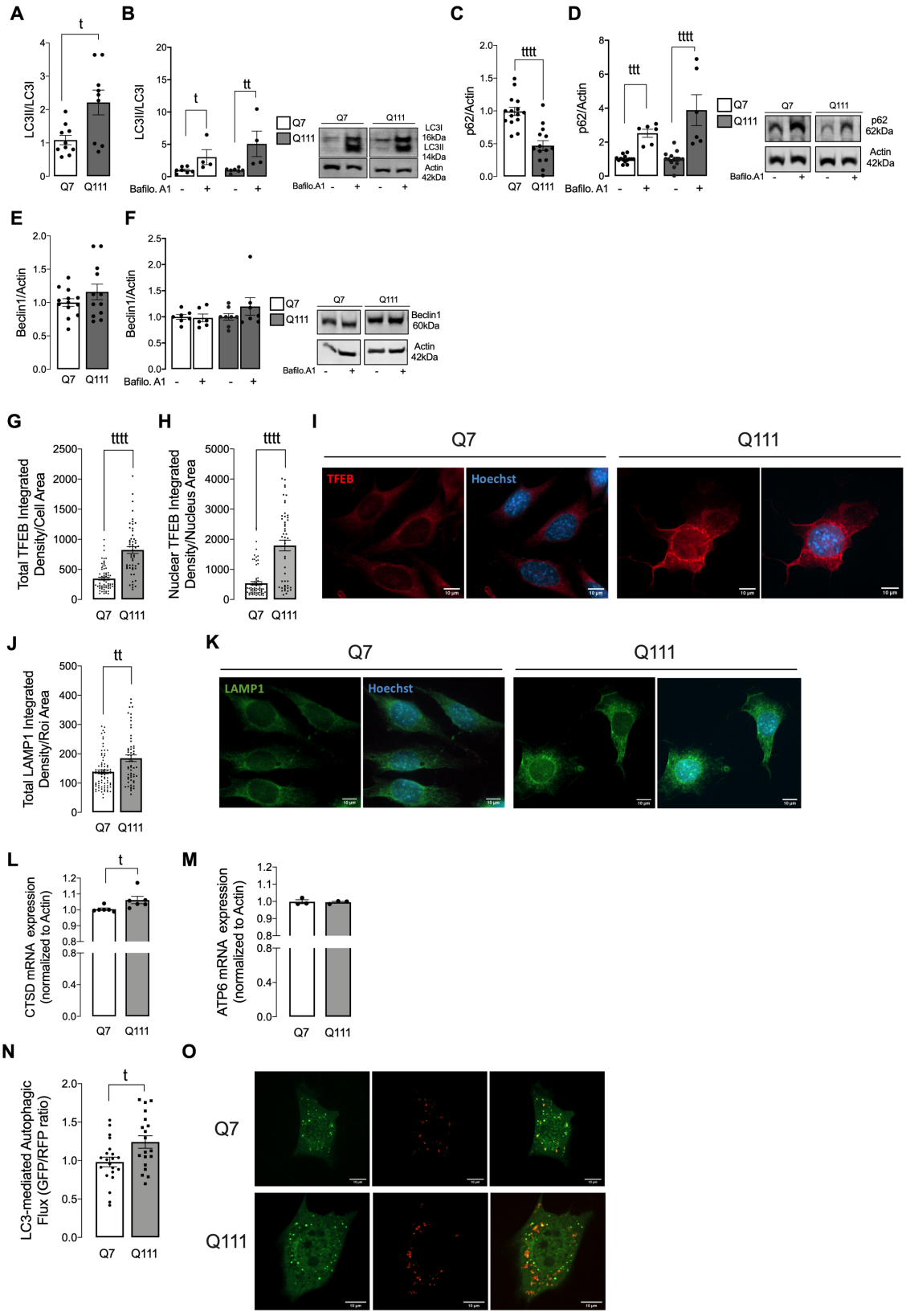

Figure 4.7 | Analysis of autophagy pathways in Q7 and Q111 cells. Q7 and Q111 cells were incubated with 50 nM bafilomycin A1 for 24 h when indicated (B,D,F) and the levels of LC3II/LC3I (A,B) and p62/Actin (C,D) and beclin/Actin (E,F) were evaluated by Western blotting in total extracts from Q7 vs. Q111 cells. Data are expressed in arbitrary units relative to Actin as the mean ± SEM of 4 to 12 independent experiments. Nuclear (H) and total (G) TFEB levels and total LAMP1 levels (J,K) were analysed by

immunocytochemistry using confocal microscope and Image J software in Q7 vs. Q111 cells. Images were obtained with a 63× objective in Zeiss LSM 710 confocal microscope (I,K, scale bar: 10 μm). Data are presented as the mean ± SEM of 4 independent experiments considering ~10 cells/condition. mRNA levels of CTSD and ATP6 were analysed by real-time qPCR, in Q7 and Q111 cells (L,M). Data are presented as the mean ± SEM of at least 3 independent experiments. (N,O) Q7 and Q111 cells were transfected with a specific plasmid (mRFP-EGFP-LC3) which allows the estimation of the autophagic flux as well as LC3 autophagy degradation rate. The GFP/RFP ratio represents the autophagic flux. Images were obtained with a 63× objective in Zeiss LSM 710 confocal microscope (O, scale bar: 10 μm). Data are presented as the mean ± SEM of 3 independent experiments considering ~6 cells/condition. Statistical analysis: $^{t}p < 0.05$, $^{tt}p < 0.01$ and $^{tttt}p < 0.0001$ *versus* control (nonparametric Mann Whitney test).

4.3.3. TOTAL AND PHOSPHORYLATED FYN LEVELS ARE DECREASED IN HD MITOCHONDRIA

c-Src/Fyn were previously shown to be located in mitochondria and their activity at complex I, III, and IV is crucial to maintain normal mitochondrial respiration and cell survival (Arachiche et al., 2008; Ogura et al., 2012).

Because our results evidence a consistent decrease of Fyn protein levels in several HD models, we analysed Fyn protein and phosphorylated SKF levels co-localization with mitochondria in Q7/Q111 cells and primary striatal neurons from WT and YAC128 mice, as well as in isolated mitochondria from WT and YAC128 mouse brain striata (**Figure 4.8**). Results show a significant decrease in Fyn and phosphorylated co-localization with mitochondria in Q111 cells (**Figure 4.8A-C**), YAC128 striatal primary neurons (**Figure 4.8D-F**) and in mitochondria isolated from 3 month-old YAC128 mouse striatum (**Figure 4.8G,H**), when compared with the respective controls.

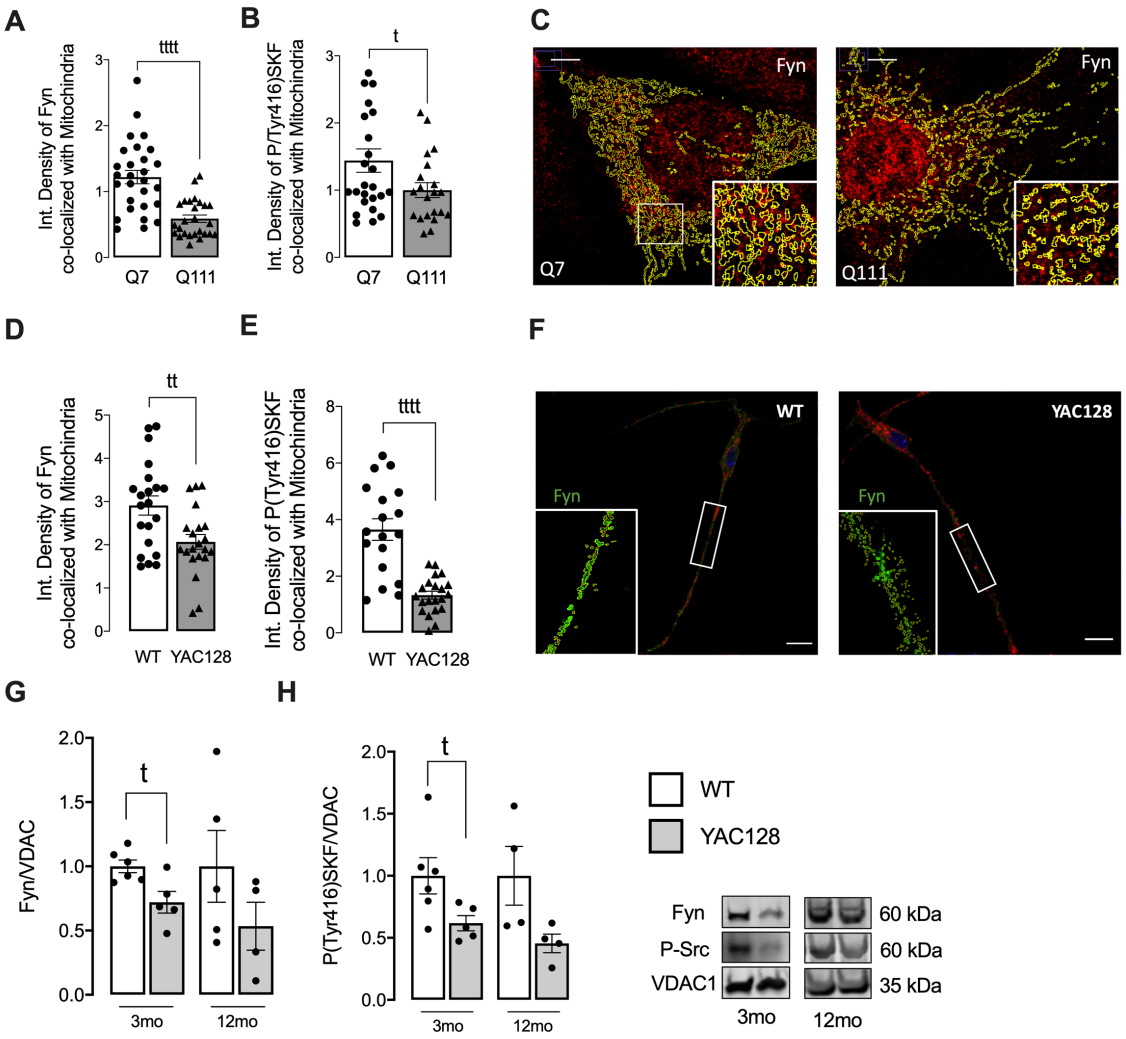

Figure 4.8 | Fyn total and phosphorylated levels co-localized with mitochondria are reduced in HD cells and in isolated striatal mitochondria. Fyn(A,D) and P(Tyr416)SKF (B,E) co-localization with mitochondria was analysed by immunocytochemistry using confocal microscope and Image J software in Q7 vs. Q111 cells (A-C) and primary striatal neurons from WT and YAC128 mice (D-F). Mitochondria were labeled after transfection with MitoDsRed plasmid. Images were obtained with a 63× objective in Zeiss LSM 710 confocal microscope (C,F, scale bar: 10 µm). Data are presented as the mean ± SEM of 4 independent experiments considering ~6 to 12 cells/condition. Fyn/VDAC1 (G) and P(Tyr416)SKF/VDAC (H) levels were determined by Western blotting in isolated mitochondrial extracts from striatal brain tissue of WT and YAC128 mice. Data are expressed in arbitrary units relative to VDAC as the mean ± SEM of 5 to 7 independent experiments. Statistical analysis: $^{t}p < 0.05$, and $^{tttt}p < 0.0001$ versus Q7 cells or WT primary striatal neurons (nonparametric Mann Whitney test).

4.3.4. CONSTITUTIVE ACTIVE SKF AMELIORATES MITOCHONDRIAL MORPHOLOGY INDEPENDENTLY OF MITOPHAGY IN HD CELLS

Considering our data showing reduced levels of Fyn associated with mitochondria, the fact that mHTT affects mitochondrial morphology and trafficking in different HD models (Naia et al., 2021; Napoli et al., 2013), as well as the involvement of SKF in regulating mitochondrial function (Arachiche et al., 2008; Ogura et al., 2012), we next evaluated the involvement of SKF proteins in mitochondrial morphology in HD cells (**Figure 4.9**).

HD mitochondrial morphology was assessed in Q7/Q111 cells (**Figure 4.9A-D**) and striatal primary neurons from WT and YAC128 mice (**Figure 4.9E-H**) following transfection with a constitutively active form of the SKF, Y527F. The Y527F mutation blocks the formation of the closed state of SKF proteins which is repressive, leading to a constitutive active form of these proteins (Irtegun et al., 2013). In accordance with previous published data, we observed a decrease in mitochondrial perimeter and in mitochondrial aspect ratio, accompanied by an increase in mitochondrial roundness in both Q111 cells and YAC128 striatal neurons, when compared to WT cells (**Figure 4.9**). Importantly, expression of Y527F SKF in Q111 cells restored mitochondrial perimeter (**Figure 4.9B**), roundness (**Figure 4.9C**) and aspect ratio (**Figure 4.9D).** Similar results were observed in mitochondria located at proximal neurites in YAC128 striatal neurons following expression of Y527F SKF, reestablishing mitochondrial perimeter (**Figure 4.9F_upper**), roundness (**Figure 4.9G_upper**) and aspect ratio (**Figure 4.9H_upper**). In distal neurites, the ameliorated effect of Y527F SKF in YAC128 neurons was only significant when assessing mitochondrial roundness (**Figure 4.9G_lower**). In this way, enhanced levels of SKF active form positively influence mitochondrial morphology in striatal cells expressing mHTT.

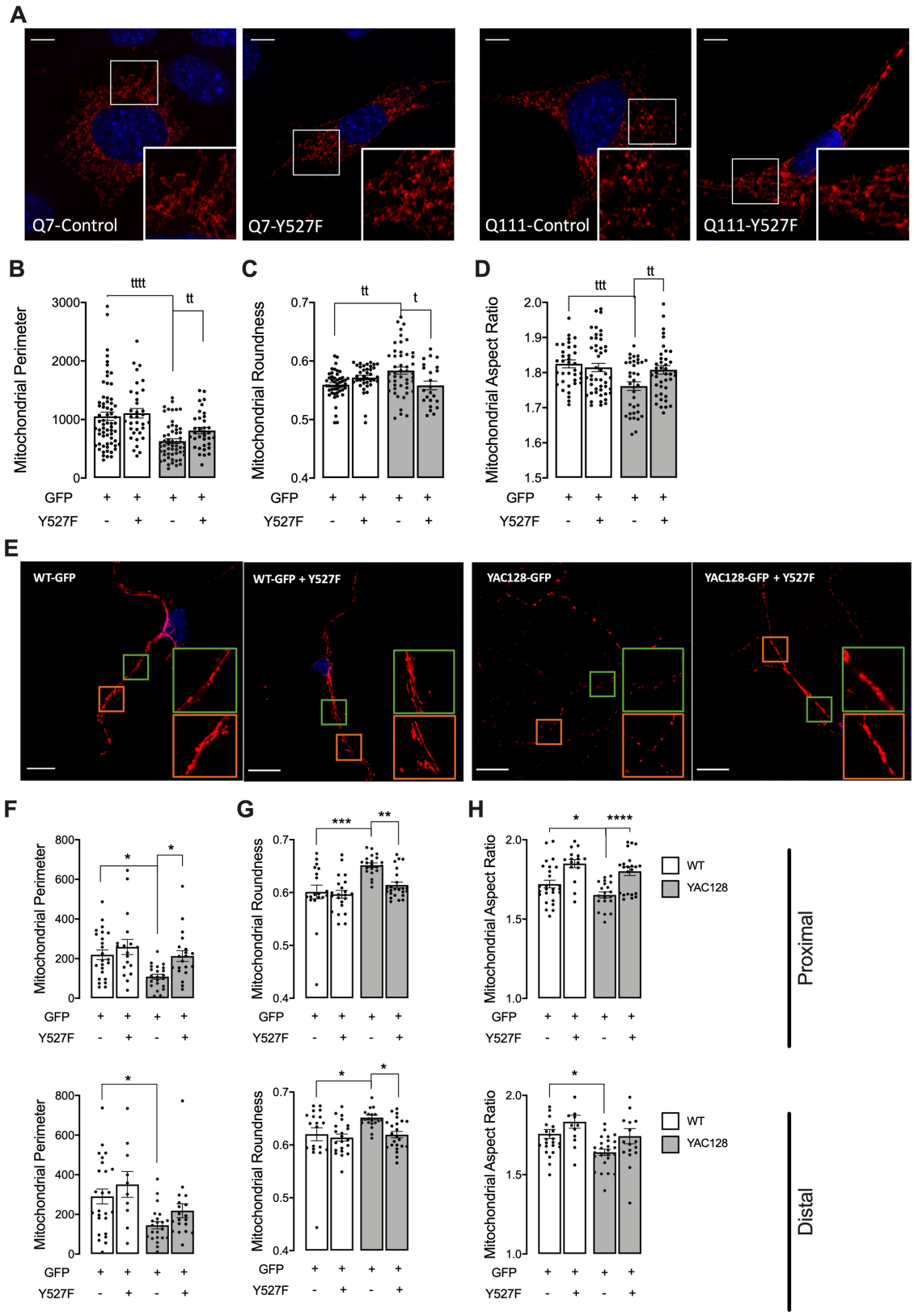

Figure 4.9 | Overexpression of activated SKF restores mitochondrial morphology in HD cell models. Mitochondrial perimeter (B,F), roundness (C,G) and aspect ratio (D,H) were analysed for categorization of mitochondrial morphology by immunocytochemistry using confocal microscope and Image J software in Q7 vs. Q111 cells (A-D) and striatal neurons from WT and YAC128 mice (E-H). Mitochondria were labeled using targeted MitoDsRed. Confocal images were obtained with a 63× objective in confocal microscope

Zeiss LSM 710 (A,E, scale bar: 10 μm). Data are presented as the mean ± SEM of 4 independent experiments considering ~6 to 12 cells/condition. Statistical analysis: $^{t}p < 0.05$, $^{tt}p < 0.01$, $^{ttt}p < 0.001$ and $^{tttt}p < 0.0001$ versus Q7 cells or Q111+GFP (nonparametric Mann Whitney test). *p < 0.05, **p < 0.01, ***p < 0.001, and ****p < 0.0001 versus WT primary striatal neurons or YAC128+GFP (two-way ANOVA, followed by Sidak's Multiple Comparison as post hoc test).

Since mitophagy is the primordial process for mitochondrial quality control and recycling, and it can be related to altered mitochondrial morphology (Twig and Shirihai, 2011), we analysed mitophagy in HD cells. The (PTEN)-induced putative kinase 1 (PINK1)/ Parkin (an E3 ligase)-dependent pathway is the most well characterized signalling cascade. PINK1 is stabilized in the MOM, and its auto-phosphorylation induces the recruitment of Parkin to the mitochondrial surface (Kazlauskaite et al., 2015). Once stabilized in the mitochondrial surface, Parkin ubiquitinates MOM proteins, promoting their degradation as well as their association with downstream autophagy adaptors, such as p62 and LC3-II (Narendra et al., 2008). Q111 cells showed increased levels of PINK1 (**Figure 4.10A**), Parkin (**Figure 4.10B**), LC3 (**Figure 4.10C**) and Ubiquitin (**Figure 4.10D**) in mitochondria, suggesting augmented mitophagy initiation in mHtt-expressing cells. To confirm this observation, we analysed MitoKeima red/green fluorescence, an index of mitophagic flux, as mitochondria that undergo degradation by the lysosome are red (Sun et al., 2017). Data show augmented mitophagy in Q111 cells, however, restoration of SKF levels did not affect mitophagy flux in both cells (**Figure 4.10E**), Q7 and Q111, which suggests that c-Src/Fyn-mediated mitochondrial changes are not regulated by mitophagy.

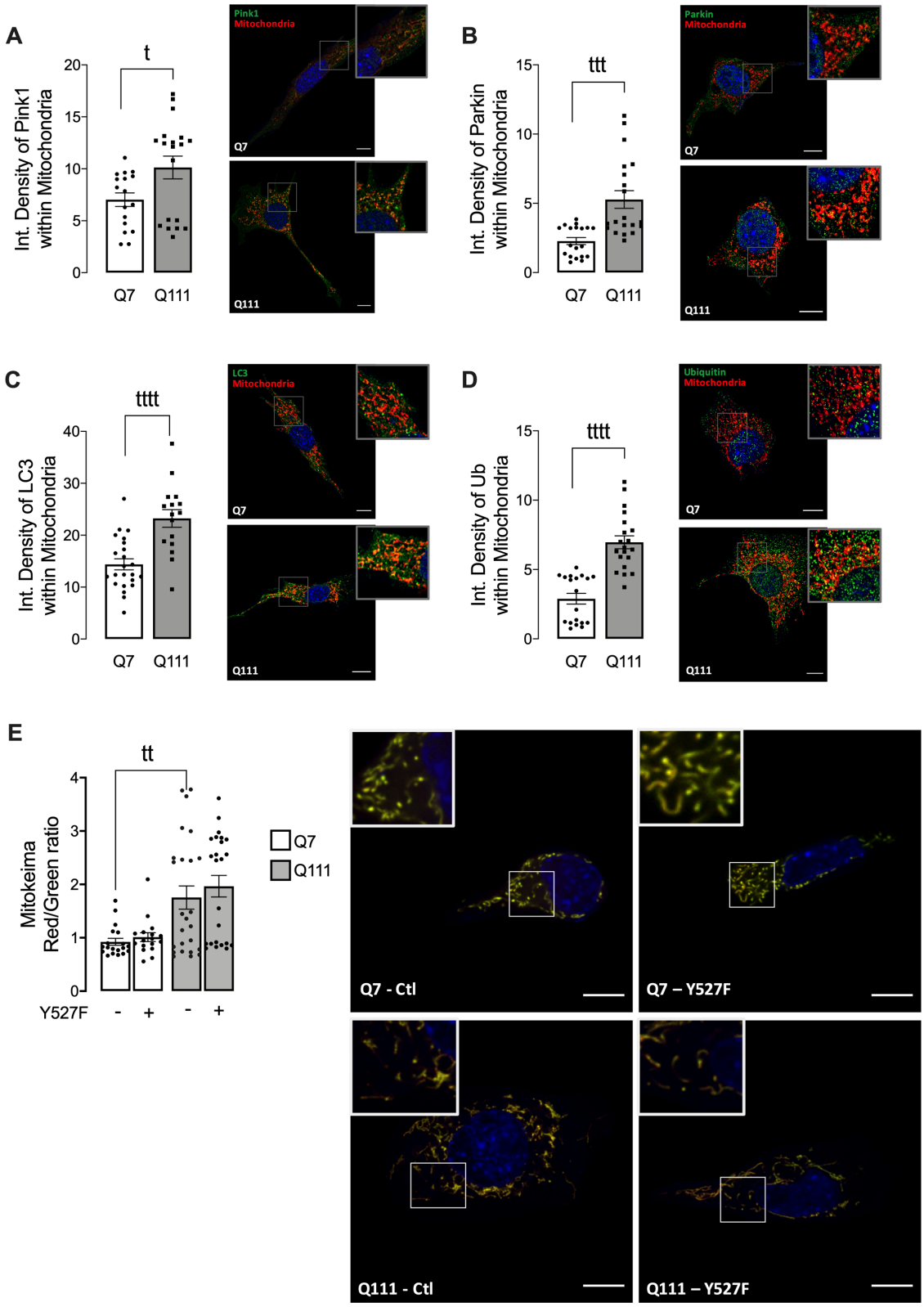

Figure 4.10 | Analysis of mitophagy in Q7 and Q111 cells. Mitochondrial levels of PINK1 (A), Parkin (B), LC3 (C) and Ubiquitin (D) were analysed by immunocytochemistry using confocal microscope and Image J software in Q7 vs. Q111 cells. Mitochondria were labeled after transfection with MitoDsRed plasmid. Images were obtained with a 63× objective in Zeiss LSM 710 confocal microscope (scale bar: 10 µm). Data are presented as the mean ± SEM of 3 independent experiments considering ~6 cells/condition. (E) Q7 and Q111 cells were transfected with a specific plasmid (pHAGE-mt-mKeima plasmid or

mito- Keima). Under neutral pH (in the cytosol), mitochondria are marked with green fluorescence, whereas under acidic pH (in the lysosomes), mitochondria are red. Images were obtained with a 63× objective in Zeiss LSM 710 confocal microscope (scale bar: 10 μm). Data are presented as the mean ± SEM of 4 independent experiments considering ~6 cells/condition. Statistical analysis: $^{t}p < 0.05$, $^{tt}p < 0.01$, $^{ttt}p < 0.001$ and $^{tttt}p < 0.0001$ versus control (nonparametric Mann Whitney test).

4.3.5. RESTORATION OF ACTIVE SKF ALLEVIATES HD MITOCHONDRIAL DYSFUNCTION

Our group has previously shown that Q111 cells exhibit mitochondrial depolarization and excessive levels of ROS. Thus, we next studied the influence of expression of constitutive active SKF on mitochondrial function in HD cell models.

Expression of Y527F SKF enhanced $TMRM^{+}$ mitochondrial accumulation, as evaluated after mitochondrial depolarization with FCCP, in both Q111 striatal cells (**Figure 4.11A**) and YAC128 striatal proximal neurites (**Figure 4.11B,C**), indicating a recovery in $\Delta\psi_m$ in mutant cells. As anticipated, decreased $\Delta\psi_m$ was accounted for by impaired mitochondrial basal and maximal respiration and ATP production, as observed in Q111 cells (**Figure 4.11E,F**). Y527F SKF expression slightly but significantly improved mitochondrial basal respiration and ATP production in Q111 striatal cells (**Figure 4.11E**). Interestingly, the SKF inhibitor SU6656 decreased mitochondrial basal and maximal respiration, as well as ATP production in Q7 cells, but not in Q111 cells (**Figure 4.11F**), indicating that SKF inactivation impairs mitochondrial function in control cells. These data reinforce the important role of SKF activation for normal mitochondrial function and the link between impaired mitochondrial function and reduced SKF levels associated with the organelle.

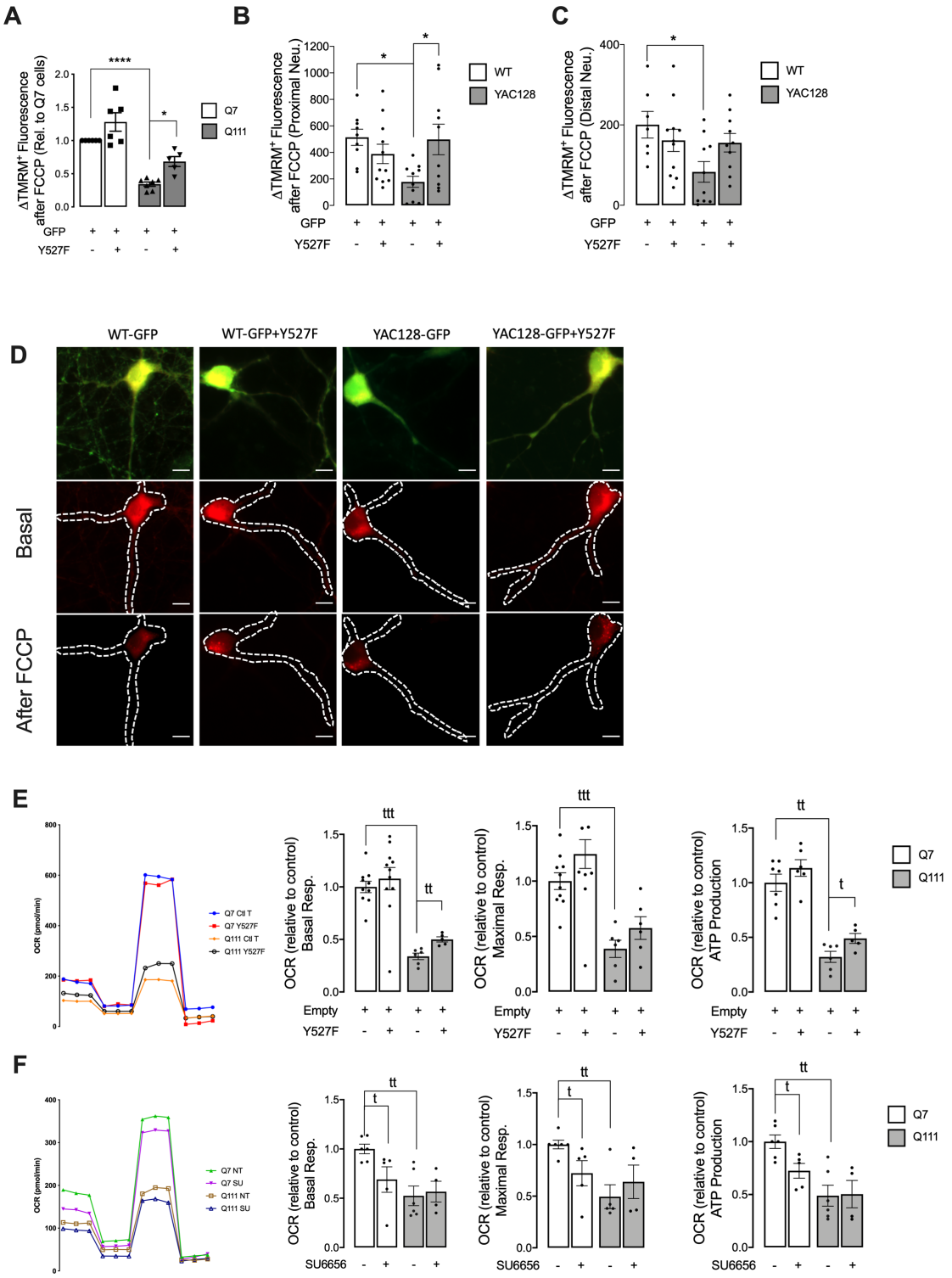

Figure 4.11 | Expression of constitutive active SKF improves mitochondrial function in HD models. Mitochondrial membrane potential was measured using TMRM+ under quenching (A) and non-quenching conditions (B-D). Units of fluorescence were monitored before and after exposure to 1 μM FCCP. In Q7 and Q111 cells (A) mitochondria membrane potential was evaluated by monitoring the fluorescence using a microplate reader Spectrofluorometer Gemini EM. In primary striatal neurons from WT and YAC128 mice, proximal (B) and distal (C) neurites mitochondria membrane potential was evaluated by monitoring the fluorescence using fluorescence microscopy. In D: representative images obtained in YAC128 and WT mouse neurons subjected to GFP

or Y527F SKF+GFP expression, where TMRM+ (in red) fluorescence was acquired before and 1 min after exposure to FCCP (2 μM, scale bar: 10 μm). Data are presented as the mean ± SEM of 3 independent experiments considering ~4 cells/condition. Oxygen consumption rate (OCR) was evaluated by Seahorse analyzer in Q7 and Q111 cells subjected to expression of activated/Y527F SKF (E) or in the presence of SU6656 (5 μM) (F). Basal respiration, maximal respiration and oligomycin-dependent ATP production were calculated relative to Q7 cells. Data are presented as the mean ± SEM of 4 independent experiments considering ~3 wells/condition. Statistical analysis: *p < 0.05, ****p < 0.0001 versus Q7 cells or WT primary striatal neurons (two-way ANOVA, followed by Sidak's Multiple Comparison as post hoc test); tp < 0.05, ttp < 0.01 and tttp < 0.001 versus Q7 cells (nonparametric Mann Whitney test).

4.3.6. EXPRESSION OF ACTIVE SKF DECREASES MITOCHONDRIAL AND TOTAL REACTIVE SPECIES LEVELS AND APOPTOSIS IN HD STRIATAL CELLS

Since oxidative stress and mitochondrial dysfunction are closely related in HD, we measured the specific mitochondrial $O_2^{\bullet-}$ in single cells using the fluorescent probe MitoSOX. Q111 cells (GFP transfected) exhibited increased $O_2^{\bullet-}$ levels when compared to Q7 cells (**Figure 4.12A,B**), as previously described by our group (Ribeiro et al., 2013). Importantly, expression of the constitutive active form of SKF (GFP plus Y527F SKF transfected cells) significantly reduced mitochondrial $O_2^{\bullet-}$ levels in Q111 cells. Similar results were observed in both proximal and distal neurites of YAC128 mouse striatal neurons subjected to Y527F SKF expression (**Figure 4.12C-E**). Concordantly, restoration of active/Y527F SKF levels decreased cellular generation of H_2O_2 in Q111 cells (**Figure 4.12F).**

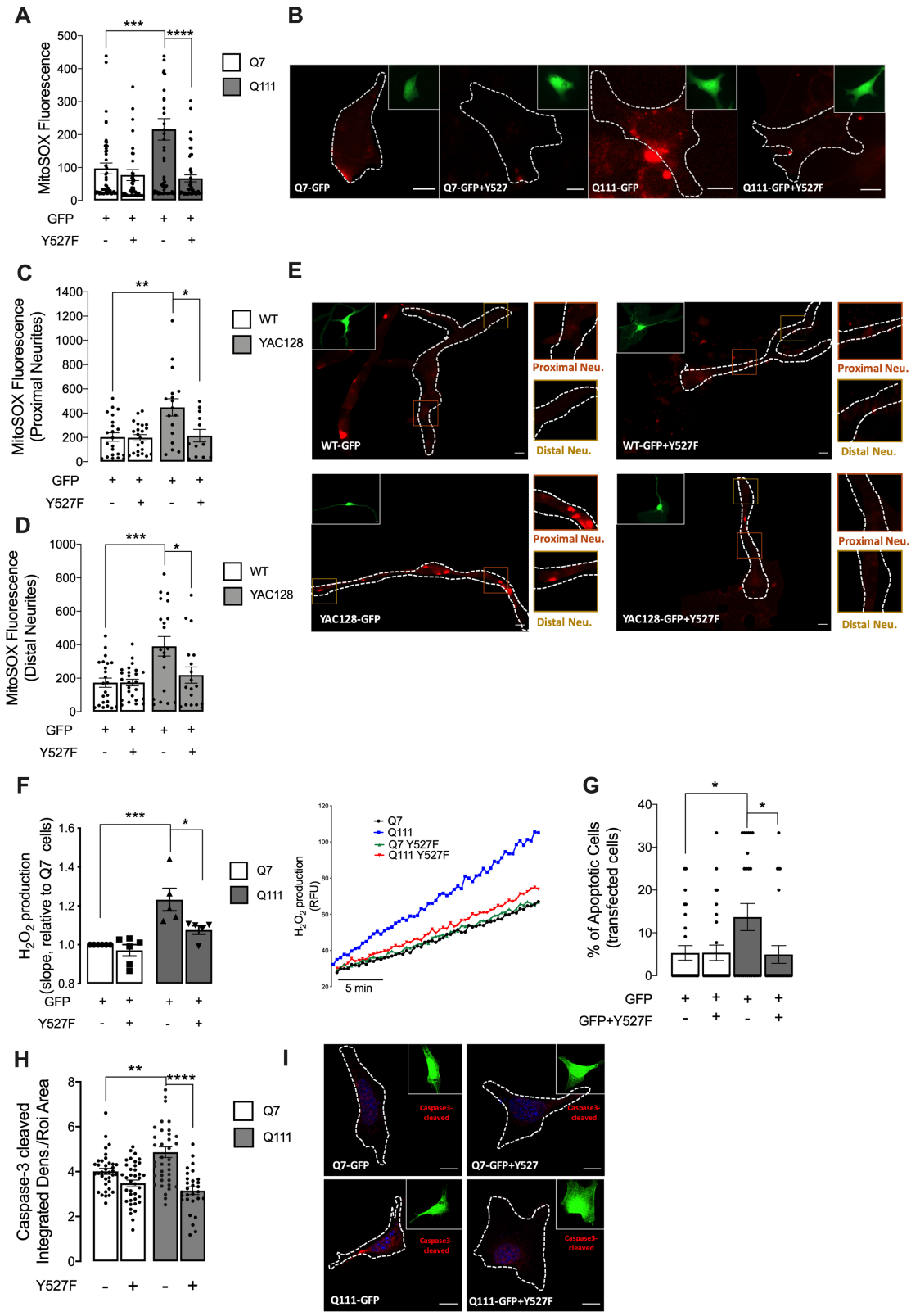

Figure 4.12 | Expression of activated SKF decreases mitochondrial and total ROS levels and reduces apoptosis in HD models. Single cell analysis of mitochondrial ROS was followed by MitoSox Red fluorescence in GFP and GFP+Y527F transfected striatal cells, namely Q7 and Q111 cells (A,B) and striatal neurons derived from WT and YAC128 mice (C-E); representative images are shown in B,E (scale bar: 10 μm). Data the mean ± SEM of 4 independent experiments considering ~4 to 8 cells/condition. H2O2 production was

analysed by monitoring the fluorescence of resorufin using AmplexRed (F) in Q7 and Q111 cells. Results were plotted as the slope differences relatively to control/GFP expressing Q7 cells; the graph in the right displays representative line charts of all experimental conditions. Data are expressed as the mean ± SEM of 5 to 6 experiments, run in quadruplicates. Analysis of Q7 and Q111 cells undergoing apoptosis (G) was determined by fluorescence microscopy following nuclei staining with Hoechst 33342. Caspase3-cleaved/activated levels (H) were analysed by immunocytochemistry using confocal microscope and Image J software in Q7 vs. Q111 cells. Images were obtained with a 63× objective in Zeiss LSM 710 confocal microscope (I, scale bar: 10 μm). Data are presented as the mean ± SEM of 3 independent experiments. Statistical analysis: *p < 0.05, **p < 0.01, ***p < 0.001 and ****p < 0.0001 versus Q7 cells or WT primary striatal neurons (two-way ANOVA, followed by Sidak's Multiple Comparison as post hoc test).

Furthermore, NO levels and overall redox changes were ameliorated after expression of constitutive active (Y527F) SKF (**Figure 4.13**). These data confirm augmented levels of reactive species in Q111/HD cells. Following SFK overexpression, we observed a tendency for a decrease in NO levels and a significant decrease in redox mechanisms, confirming the involvement of reduced c-Src/Fyn levels on redox signaling in HD.

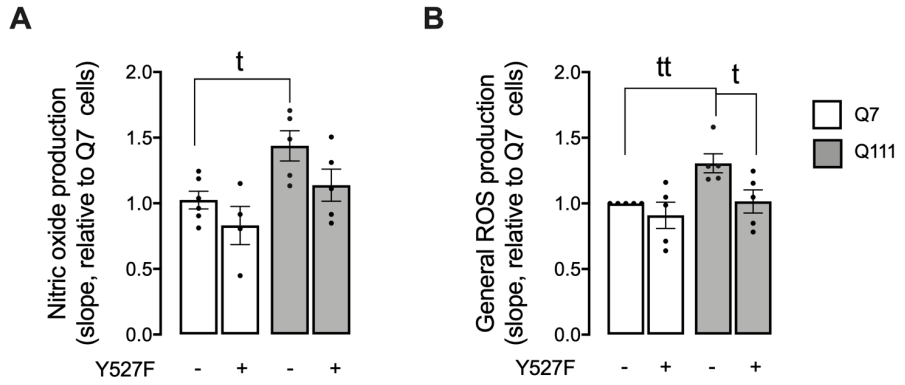

Figure 4.13 | Nitric oxide and redox modifications in Q7 and Q111 cells. NO levels (A) and redox changes (B) were analysed by monitoring the fluorescence of DAF2-DA and H_2DCFDA, respectively, in Q7 and Q111 cells. Results were plotted as the slope differences relatively to control/Q7 cells. Data are expressed as the mean ± SEM of 5 experiments, run in triplicates. Statistical analysis: $^{t}p < 0.05$ and $^{tt}p < 0.01$ versus Q7 Control or Q111 Y527F (nonparametric Mann Whitney test).

Significantly, Q111 cells expressing a constitutively active form of the SKF displayed a significant reduction in the number of apoptotic cells, as determined by nuclear condensation using Hoechst staining (**Figure 4.12G**), but there were no evidences of necrosis (**Figure 4.14**). Additionally, we validated apoptosis modulation following c-Src/Fyn restored levels in HD cells through decreased caspase3-cleaved/active levels (**Figure 4.12H,I**).

Altogether, these data evidence that SKF activation is essential for mitochondrial activity and cell survival in cells expressing mHTT/mHtt by ameliorating mitochondrial function and morphology, and limiting the levels of oxidant species.

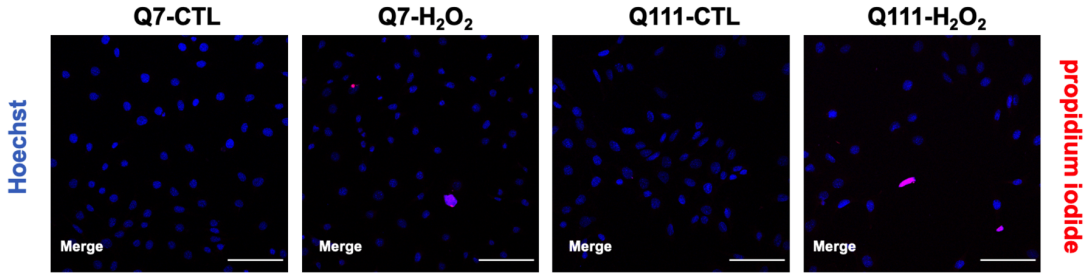

Figure 4.14 | H2O2 incubation is needed to induce necrosis in Q7 and Q111 cells. Q7 and Q111 cells were incubated with 150 μM H_2O_2 for 3 h, when indicated, and Hoechst and propidium iodide fluorescence were evaluated. Confocal images were obtained with a 20× objective in confocal microscope Zeiss LSM 710 (scale bar: 100 μm).

4.4. DISCUSSION

In the present study we provide evidence that two SKF members, c-Src and Fyn kinases, are reduced in several HD models, and that expression of constitutive active form of SKF is neuroprotective against mHTT-induced mitochondrial dysfunction and enhanced ROS levels. Indeed, we show a decrease in c-Src and Fyn protein levels, and in their activation in human brain caudate, YAC128 mouse brain striatum and cortex at early stages, YAC128 striatal neurons and Q111 striatal cell lines.

mHTT aggregates are ubiquitinated (DiFiglia et al., 1997), reflecting a generalized deficiency in UPS and decreased degradation of mHTT through this pathway. Indeed, different HD models show decreased UPS function, suggesting that proteasome sequestration by mHTT aggregates is responsible for altered UPS activity (Li and Li, 2011). To maintain normal proteostasis under conditions of UPS failure, autophagy can be upregulated (Pandey et al., 2007). Under normal conditions regulation of SKF protein levels occurs mainly through the proteasome (Harris et al., 1999), and we were able to confirm it in control/wild-type cells. Conversely, our results evidence a higher degradation of c-Src and Fyn proteins through (macro)autophagy pathway, as confirmed by using selective autophagy inhibitors, in cells expressing full-length mHTT, namely Q111 cells and YAC128 striatal neurons. In accordance, our data also show augmented TFEB-mediated autophagy induction, and autophagy flux linked to increased c-Src/Fyn autophagy-dependent degradation.

Fyn kinase was previously identified at the intermembrane space of highly purified rat brain mitochondria (Salvi et al., 2002), playing a key role in normal mitochondrial function (Ogura et al., 2012). In this study, we show, for the first time, that Fyn total and phosphorylated levels are reduced in YAC128 mouse striatal isolated mitochondria. We also show decreased co-localization of Fyn with mitochondria in striatal neurons or Q111 striatal cells. Since SKF do not contain a typical mitochondrial localization signal, adaptor proteins appear to be required for interaction with the organelle. Several studies revealed that two anchoring proteins of PKA, A Kinase Anchor Protein 121 (AKAP121) and Dok-4, can associate with Src both in the cytosol and mitochondria (Itoh et al., 2005; Alessandra Livigni et al., 2006). Moreover, AKAP121 was observed in the

mitochondrial inner membrane bound to SKF proteins (Sardanelli et al., 2006). However, AKAP121 or Dok-4 proteins have not been studied in the context of HD. Decreased co-localization of c-Src and Fyn protein with mitochondria might be related not only with increased autophagic degradation, but also with reduced interaction with mitochondrial proteins and/or mitochondrial translocation. This might occur similarly as described for the HD transgenic R6/2 mouse model showing defective protein import to mitochondria, as an early defect found in the forebrain, since mHTT interacts with TIM23 mitochondrial protein import complex (Yano et al., 2014). Additionally, although mitophagy is an important regulator of mitochondrial morphology (Twig and Shirihai, 2011) and our data suggest that mitophagy initiation is augmented in Q111 cells, c-Src/Fyn-mediated mitochondrial changes are not regulated by mitophagy.

Mitochondrial dysfunction and related oxidative stress is a well characterized early relevant HD pathogenic mechanism. Indeed, impaired OXPHOS, abnormal Δψm, oxidative stress, accompanied by modifications in mitochondrial morphology, favors the accumulation of damaged mitochondria in HD models, and ultimately extends to cell death. In this work we confirm mitochondrial morphology and function impairments as well as increased apoptosis in HD in *in vitro* models. Importantly, our findings evidence a restoration of mitochondrial morphology and function after the re-establishment of active SKF levels in both Q111 cells and YAC128 mouse striatal neurons. Of relevance, mitochondrial complexes are c-Src/Fyn substrates, and mitochondrial respiration is dependent on c-Src/Fyn-mediated phosphorylation of respiratory chain components, namely complex I, III, and IV (Arachiche et al., 2008; Ogura et al., 2012). Moreover, mitochondrial SKF activation is essential for cell survival (Arachiche et al., 2008; Ogura et al., 2012). Additionally, Fyn was associated with large complexes in mammalian mitochondria, including ribosomes and other translation components (Koc et al., 2017). The same authors showed that Fyn regulates mitochondrial translation by phosphorylation of its multiple components, and thus, stimulates energy generation in mammalian mitochondria (Koc et al., 2017). Our results are in accordance with these findings. Indeed, we show that active SKF expression restores mitochondrial morphology (mitochondrial perimeter, roundness and aspect ratio) and improves Δψm as well as mitochondrial respiratory through augmented basal respiration and ATP

production. Conversely, SKF inhibition is enough to induce HD-like mitochondrial phenotype, which evidence the mitochondrial-related SKF role under normal conditions. Moreover, expression of active SKF reduced mitochondrial ROS levels and augmented cell viability in cells expressing mHTT. The positive impact of SKF expression on mitochondrial reactive species and on decreased number of apoptotic cells and reduced caspase3-cleaved/active levels are probably due to its effect on mitochondrial function. Thus, this study discloses an essential role of SKF in regulating mitochondrial function in HD, potentially influencing disease progression (**Figure 4.15**).

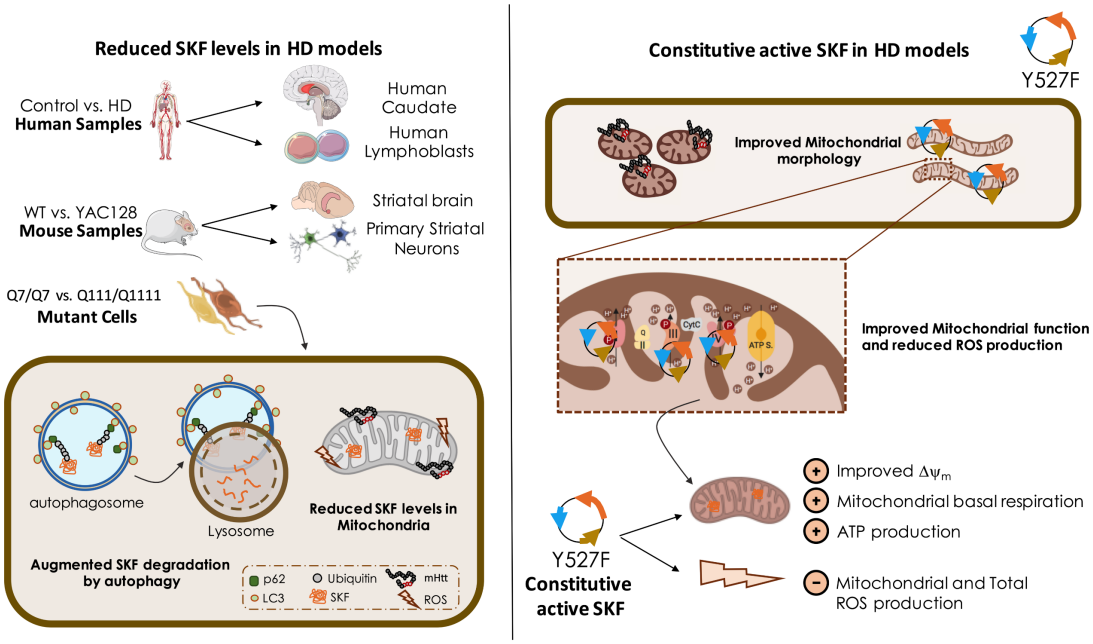

Figure 4.15 | Src kinase family proteins as important molecules in Huntington's Disease. SKF are reduced in several HD models, including in mitochondria, due to degradation through autophagy. Restauration of SKF constitutive active levels improves mitochondrial morphology and function, augmenting mitochondrial transmembrane potential, basal respiration and ATP production, as well as decreasing the levels of reactive/oxidant species, namely ROS.

Our study provides the first evidence that c-Src and Fyn proteins are reduced in HD models, including in HD mitochondria. c-Src and Fyn proteins are decreased in HD due to degradation through autophagy. Moreover, reduced c-Src and Fyn protein levels is accompanied by a decrease in c-Src/Fyn active form(s). Decreased Fyn mitochondrial co-localization correlates with HD-related mitochondrial dysfunction and altered morphology, and increased reactive/oxidant species levels. Importantly, restoration of active SKF levels

significantly alleviates mHTT-induced mitochondrial deregulation. Therefore, c-Src and Fyn may constitute essential proteins which deficits contribute for HD etiopathogenesis and thus should be considered as potential HD therapeutic target(s) (**Figure 4.15**).

CHAPTER V

RESTORED FYN LEVELS IN HUNTINGTON'S DISEASE CONTRIBUTES FOR ENHANCED SYNAPTIC GLUN2B-COMPOSED NMDA RECEPTORS AND CREB ACTIVITY

* Based on the submitted manuscript: Manuscript ID: cells-1925584

5.1. SUMMARY

NMDAR are important postsynaptic receptors that contribute to normal synaptic function and cell survival; however, when overactivated, as in HD, NMDARs cause excitotoxicity. HD-affected striatal neurons show altered NMDAR currents and augmented ratio of surface to internal GluN2B-containing NMDARs, with augmented accumulation at extrasynaptic sites. Fyn protein is a member of the SKF with an important role in NMDARs phosphorylation and synaptic localization and function; recently, we demonstrated that Fyn is reduced in several HD models. Thus, in this study, we aimed to explore the impact of HD-mediated altered Fyn levels at PSD, and their role in distorted NMDARs function and localization, and intracellular neuroprotective pathways in YAC128 mouse primary striatal neurons. We show that reduced synaptic Fyn levels and activity in HD mouse striatal neurons is related with decreased phosphorylation of synaptic GluN2B-composed NMDARs; this occurs concomitantly with augmented extrasynaptic NMDARs activity and currents and reduced CREB activation, along with induction of cell death pathways. Importantly, expression of a constitutive active form of SKF reestablishes NMDARs localization, phosphorylation and function at PSD in YAC128 mouse neurons. Enhanced SKF levels and activity also promotes CREB activation and reduces caspase-3 activation in YAC128 mouse striatal neurons. This work supports, for the first time, a relevant role for Fyn protein in PSD modulation, controlling NMDARs synaptic function in HD, and favoring neuroprotective pathways and cell survival. In this respect, Fyn Tyr kinase constitutes an important potential HD therapeutic target directly acting at PSD

5.2. INTRODUCTION

HD is an autosomal dominant progressive neurodegenerative disorder that affects mainly the striatum (caudate and putamen) and later the cortex (Sieradzan and Mann, 2001). HD is characterized by psychiatric and behavioral disturbances, such as motor impairment, psychiatric symptoms, like obsessive-compulsive disorder, depression and/or anxiety, cognitive decline and weight loss (Morreale, 2015; Ross and Tabrizi, 2011). HD is caused by an abnormal expansion of CAG repeat at the *HTT* gene, encoding for mHTT retaining a polyQ extension at the N-terminus (Finkbeiner, 2011). mHTT has been associated with protein conformational changes, aggregation and abnormal protein-protein interactions (Morreale, 2015), which cause cytotoxicity, evidenced through changes in gene transcription, synaptic dysfunction, NMDARs overactivation, decreased mitochondrial Ca^{2+} handling and organelle dysfunction, and increased oxidative events, leading to neuronal death (Finkbeiner, 2011). NMDARs involvement in HD pathogenesis is still not completely clear. HD-affected MSNs show altered NMDAR currents as well as augmented ratio of surface to internal GluN2B-containing NMDARs, with augmented accumulation at extrasynaptic sites (Milnerwood et al., 2010). Nonetheless, the mechanism underlying this altered NMDARs localization is largely unknown.

NMDARs are important postsynaptic receptors that contribute to normal synaptic function and cell survival. Activation of synaptic NMDARs is associated with augmented CREB-dependent gene expression. CREB is a signal-regulated transcription factor, important for neuronal survival with important roles in several processes, namely synaptic plasticity, neurogenesis, learning and memory. Conversely, extrasynaptic NMDARs activation promotes cell death pathways linked to dendritic blebbing, loss of mitochondrial membrane potential and CREB shut-off pathway, with blockade expression of BDNF, a neurotrophin relevant for survival of striatal neurons. Altered NMDAR function has been related to HD, as documented by previous studies. Milnerwood and colleagues showed that YAC128 HD mouse striatum presented increased extrasynaptic NMDAR

expression and currents and reduced nuclear CREB activation, which was reversed after NMDAR inhibition with memantine (Milnerwood et al., 2010).

Interestingly, intracellular mechanisms involved in HD pathogenesis, as altered striatal glutamatergic synapses and mitochondrial dysfunction linked to redox changes, are also relevant neuronal pathways modulated by c-Src and Fyn, two ubiquitous proteins belonging to the SKF, predominantly located in synaptic membranes (Goebel-Goody et al., 2009). c-Src and Fyn are broadly expressed in the Central Nervous System (CNS), being enriched in striatal neurons (Hattori et al., 2006), and have been implicated in brain neuronal development, transmission, synaptic activity and plasticity in mammalian CNS, being both kinases activated by H_2O_2 (Chojnacka and Mruk, 2015). Importantly, Fyn can be found in the PSD, concomitantly with components of the NMDAR complex (Brugge et al., 1985). Fyn interacts and phosphorylates NMDARs and postsynaptic scaffold proteins, as PSD95, to regulate synaptic transmission and plasticity (Brugge et al., 1985). Moreover, Fyn phosphorylates NMDAR GluN2B subunit at Tyr1472, increasing receptor retention at the synapse, thus controlling synaptic plasticity (Ai et al., 2013; Mota et al., 2014b). Several studies evidenced depressed synaptic transmission in HD. Importantly, there is a clear evidence for altered dendrite morphology in MSNs of HD patients, showing recurved endings and appendages, altered spine density and abnormalities in dendritic spine size and shape (Graveland et al., 1985). Moreover, Murmu and coworkers showed that mHTT in R6/2 mice causes a progressive loss of persistent-type spines, important for neuronal circuitry and long-term memory in the brain (Murmu et al., 2015, 2013). Recently, we showed that c-Src/Fyn activation and total protein levels are reduced in several human and mouse HD models mainly due to autophagy degradation (8). Moreover, restoration of active SKF levels improves mitochondrial morphology and function, namely through improved mitochondrial transmembrane potential, mitochondrial basal respiration and ATP production, diminishing ROS levels (Fão et al., 2022). Additionally, YAC128 mouse striatum revealed increased synaptic activity of STEP, correlating with decreased GluN2B phosphorylation at Tyr1472, reducing synaptic NMDARs by facilitating their movement to extrasynaptic sites (Gladding et al., 2012).

Based on these findings, in this study we aimed to explore the impact of HD-mediated altered Fyn levels on synaptic *versus* non-synaptic NMDARs

function and localization, as well as intracellular neuroprotective pathways. Our data reveal that SKF activation is important for normal synaptic function and neuronal survival in neurons expressing mHTT by contributing for synaptic NMDARs presence and function. Thus, synaptic modulation of Src/Fyn activation/levels may constitute a therapeutic potential target in HD.

5.3. RESULTS

5.3.1. SYNAPTIC AND EXTRASYNAPTIC GLUN2B-COMPOSED NMDAR ARE ALTERED IN EARLY HD STAGES

The two most common non-obligatory NMDAR subunits, GluN2B and GluN2A, predominate in the striatum (Landwehrmeyer et al., 2018) and have differential roles in synaptic plasticity and NMDARs function in adult cortex, as well as, different patterns of expression at PSD (Massey et al., 2004).

Thus, we initially determined the relative levels of GluN2B and GluN2A NMDARs in striatum from YAC128 mouse model at 3, 6 and 12 months of age (**Figure 5.1A-C**). Total GluN2A levels were significantly increased at 6 months of age, but not at 3 or 12 months of age in the striatum of YAC128 mice (**Figure 5.1A**), whereas total GluN2B levels were not significantly altered at 3-12 months of age (**Figure 5.1B**).

GluN2B phosphorylation at Tyr1472 by SKF is associated with enrichment of synaptic NMDAR (Goebel-Goody et al., 2009). We observed a significant decrease in Tyr1472 phosphorylation of GluN2B subunit in the striatum of 3 month-old YAC128 mice, a relative presymptomatic stage, when compared to WT mice (**Figure 5.1C**). Similar results were observed in primary striatal neurons from YAC128 mice (**Figure 5.1D-F**), which may suggest that in early HD stages NMDARs' retention at the synapse is altered, potentially contributing for modified synaptic function in HD.

To confirm these results we analyzed co-localization of total and phosphorylated levels of GluN2B-containing NMDARs with PSD or non-PSD sites (defined by co-localization or not with PSD-95, respectively) as described in (Milnerwood et al., 2010), from the soma to proximal (<50 μm) or distal neurites (<50 μm) in primary

striatal neurons, as identified in (Fão et al., 2022). In accordance with published data, YAC128 mouse striatal neurons showed reduced GluN2B-NMDARs levels at the synapse and augmented in the non-synaptic portion (**Figure 5.1G**), both in proximal and distal neurites. Tyr1472 phosphorylation of GluN2B subunit was reduced both in PSD and non-PSD compartments in HD neurons (**Figure 5.1H**), indicating that this NMDARs subunit is less phosphorylated. Additionally, primary striatal neurons showed reduced PSD-95 levels and puncta (Figure 1I), which suggests decreased PSD number and potential synaptic pruning in HD striatal neurons.

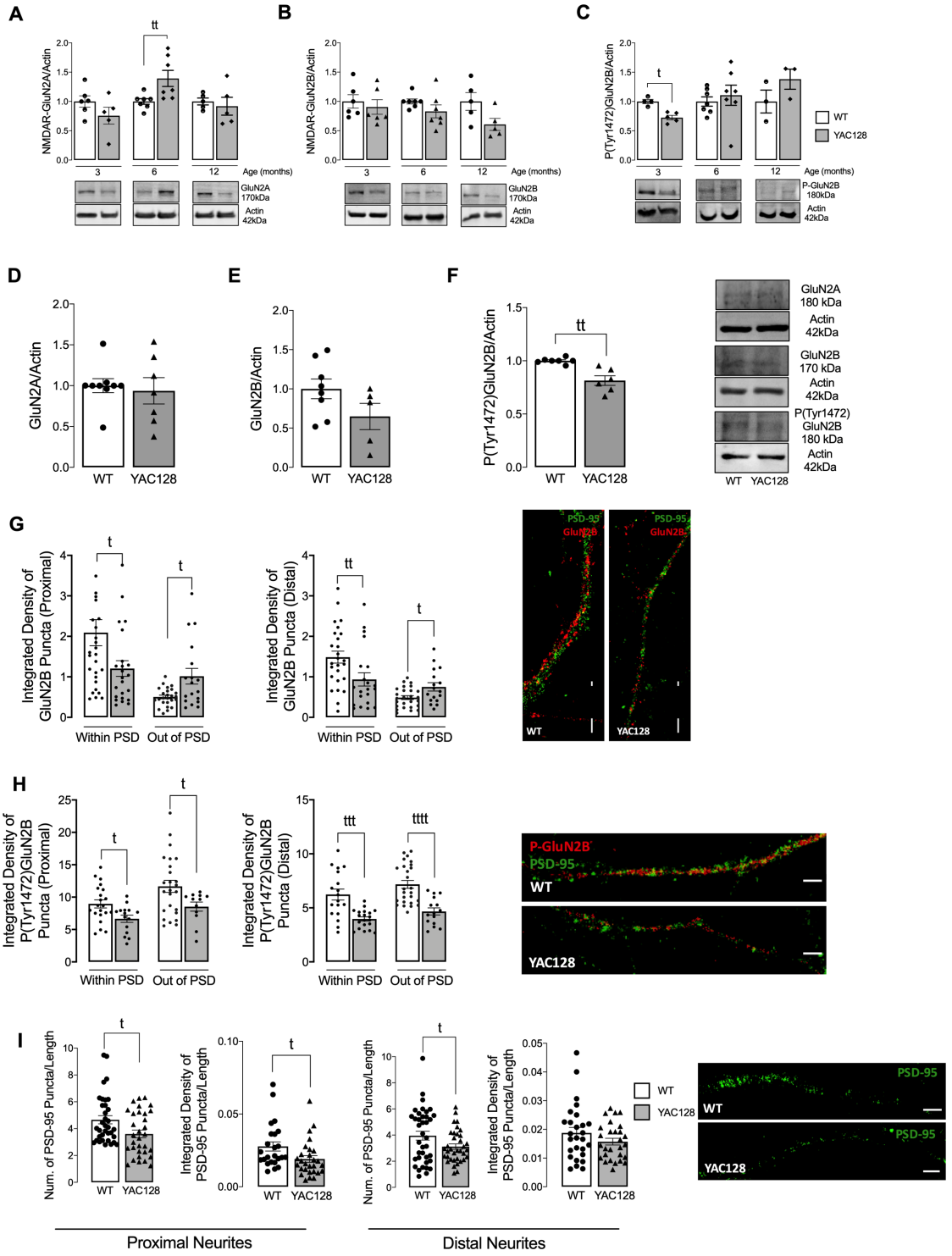

Figure 5.1 | Altered GluN2A- and GluN2B-composed NMDARs levels in HD models. GluN2A/Actin (A,D), GluN2B/Actin (B,E) and P(Tyr1472)GluN2B/Actin (C,F) were analysed by Western blotting in total extracts obtained from striatal tissue from WT and YAC128 mouse brain (A-C) and total extracts obtained from primary striatal mouse YAC128 and WT neurons (D-F). Data are expressed in arbitrary units relative to Actin as the mean ± SEM of 5 to 7 independent experiments. The levels of GluN2B (G) and P(Tyr1472)GluN2B (H) in co-localization with PSD-95, or out of PSD, as well as, the levels and number of puncta of PSD-95 (I), were evaluated by immunocytochemistry, in proximal (from soma to 50μm) and distal (more than 50μm) neurites, using confocal microscope and Image J software in YAC128 vs. WT striatal neurons. Confocal images

were obtained with a 63× objective in confocal microscope Zeiss LSM 710 (scale bar: 10 µm). Data are presented as the mean ± SEM of 4 independent experiments considering ~5 to 8 cells *per* condition *per* culture. Statistical analysis: $^{t}p < 0.05$, $^{tt}p < 0.01$, $^{ttt}p < 0.001$, and $^{tttt}p < 0.0001$ *versus* control conditions, by nonparametric Mann Whitney test.

5.3.2. FYN TOTAL AND PHOSPHORYLATED LEVELS ARE REDUCED IN PSD OF HD NEURONS

Fyn play a relevant role in regulating dendritic spine and synapse formation (Grant and Silva, 1994; Maness, 1992). Furthermore, Fyn regulates learning and memory through phosphorylation of NMDAR subunits, playing an important role in synaptic plasticity (Jiang et al., 2008). Considering that Fyn phosphorylation of GluN2B at Tyr1472 is associated with enrichment of synaptic NMDARs, when compared with extrasynaptic membrane receptors receptors (Goebel-Goody et al., 2009) and we recently observed diminished Fyn in several HD models (Fão et al., 2022), we further analyzed Fyn total and phosphorylated at Tyr416, the latter indicating SKF activation, since all the family members share the C-terminal. Firstly, we confirmed reduced Fyn total and phosphorylated/active levels in different neuronal sections, from soma to proximal and distal neurites in YAC128 primary striatal neurons (**Figure 5.2A,B**). Considering SKF role in NMDARs regulation, we further assessed Fyn total and phosphorylated levels in PSD and non-PSD portions in proximal and distal neurites of primary striatal neurons. As shown in **Figure 5.2C,D**, total and phosphorylated Fyn levels are significantly reduced in HD PSD. Considering that inhibition of SKF activity with PP2 decreased NMDAR subunits in synaptic and extrasynaptic membranes (Goebel-Goody et al., 2009), reduced Fyn levels and activity are apparently related with reduced synaptic GluN2B Tyr1472 phosphorylation (**Figure 5.1H**). These data suggest that Fyn reduced levels and activity in PSD may contribute to altered NMDARs phosphorylation and potentially their function.

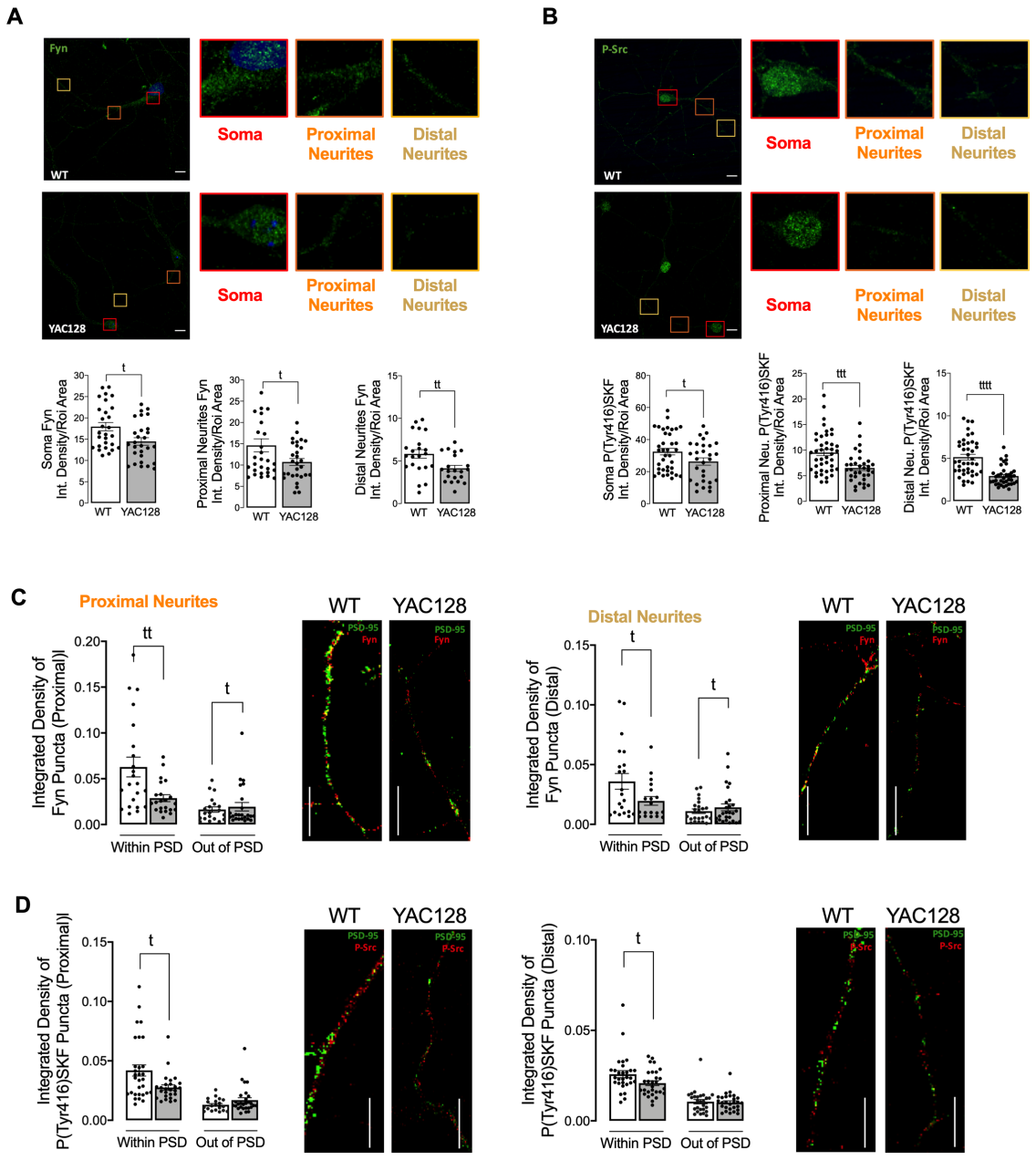

Figure 5.2 | Reduced total and phosphorylated Fyn levels in HD synapses. The total levels of Fyn (A) and P(Tyr416)SKF (B), as well as, the levels of Fyn (C) and P(Tyr416)SKF (D) in co-localization with PSD-95, or out of PSD were evaluated by immunocytochemistry, in proximal and distal neurites, using confocal microscope and Image J software in YAC128 *vs.* WT striatal neurons. Confocal images were obtained with a 63× objective in confocal microscope Zeiss LSM 710 (scale bar: 10 µm). Data are presented as the mean ± SEM of 4 independent experiments analyzing 5 to 8 cells *per* condition *per* culture. Statistical analysis: $^{t}p < 0.05$, $^{tt}p < 0.01$, $^{ttt}p < 0.001$, and $^{tttt}p < 0.0001$ *versus* control conditions (nonparametric Mann Whitney test).

5.3.3. CONSTITUTIVE ACTIVE SKF REESTABLISHES GLUN2B-COMPOSED NMDAR LEVELS AND ACTIVITY IN PSD

Considering reduced Fyn levels and activation within PSD and the observation that Fyn-mediated phosphorylation of GluN2B at Tyr1472 is related with enrichment of synaptic NMDARs (Goebel-Goody et al., 2009) next we evaluated the influence of SKF proteins on NMDARs localization and function in HD cells. GluN2B-composed NMDARs total and phosphorylated levels were assessed in striatal primary neurons from YAC128 and WT mice, both in PSD and non-PSD sites following transfection with a constitutively active form of the SKF, Y527F SKF (**Figure 5.3**). The Y527F SKF mutation enables a mutationally activated form by locking SKF proteins into the open conformation (Irtegun et al., 2013). Importantly, expression of Y527F SKF in YAC128 primary striatal neurons restored GluN2B Tyr1472 phosphorylated levels in both PSD and non-PSD compartments (**Figure 5.3E-H**) and GluN2B total levels in PSD, while decreasing GluN2B total levels in non-PSD compartment (**Figure 5.3A-D**) in proximal (**Figure 5.3A,B,E,F**) and distal (**Figure 5.3C,D,G,H**) neurites. These data indicate that augmented SKF activity is important for normal GluN2B phosphorylation and synaptic enrichment in HD.

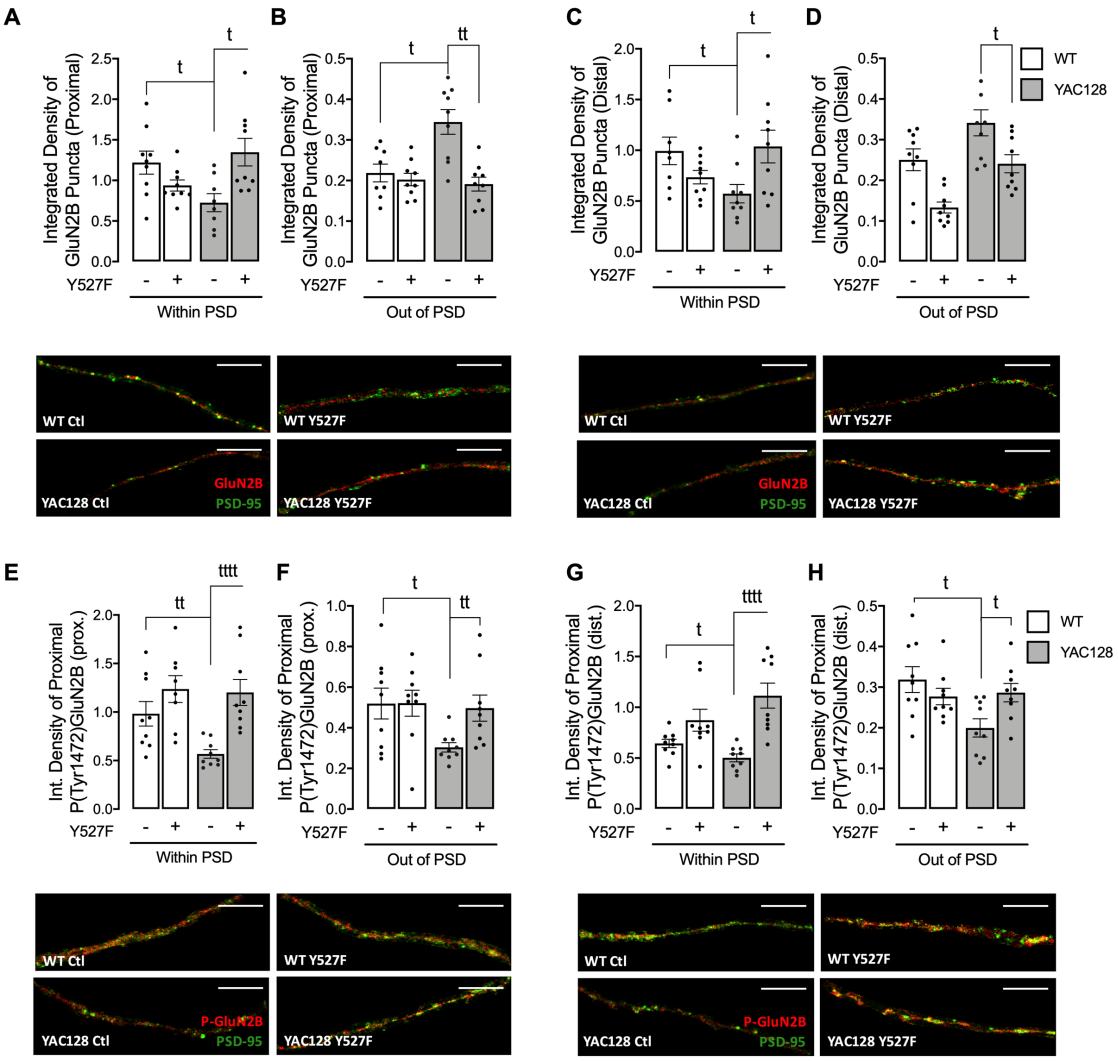

Figure 5.3 | Overexpression of activated SKF restores GluN2B-NMDARs total and phosphorylated levels in HD synapses. The levels of GluN2B (A-D) and P(Tyr1472)GluN2B (E-H) in colocalization with PSD-95, or out of PSD, were evaluated by immunocytochemistry, in proximal and distal neurites, using confocal microscope and Image J software in WT vs. YAC128 striatal neurons. Confocal images were obtained with a 63× objective in confocal microscope Zeiss LSM 710 (scale bar: 10 µm). Data are presented as the mean ± SEM of 4 independent experiments considering 5 to 8 cells *per* condition *per* condition. Statistical analysis: $^{t}p < 0.05$, $^{tt}p < 0.01$, and $^{tttt}p < 0.0001$ *versus* control conditions (nonparametric Mann Whitney test).

To support the hypothesis that HD-mediated SKF reduced levels influence the presence and function of NMDARs in the synapse, we evaluated the NMDARs function in soma, proximal and distal neurites (**Figure 5.4**). In accordance with previous published data (Milnerwood et al., 2010), we observed augmented NMDAR-mediated current density (**Figure 5.4A**), and activity, as observed by NMDAR-dependent Ca^{2+} entry (**Figure 5.4B**) in the soma of YAC128 striatal

neurons. This augmented NMDAR-mediated Ca^{2+}-entry were reduced after Y527F SKF transfection to levels similar to WT neurons, which suggests that augmented NMDARs occur due to augmented extrasynaptic NMDARs function. On other hand, in proximal (**Figure 5.4C**) and distal (**Figure 5.4D**) neurites, we observed reduced NMDARs activity in YAC128 striatal neurons, which was reestablished after expression of Y527F SKF, augmenting NMDA-induced Ca^{2+}-entry. Altogether, these data suggest that altered PSD number and reduced SKF levels and function in HD proximal and distal neurites may result in altered established synapses and reduced NMDARs activity. Of relevance, altered NMDARs activity in proximal and distal neurites can be restored by augmenting active SKF levels. As such, these results suggest that restoration of active SKF reduces extrasynaptic GluN2B-composed NMDARs, augmenting GluN2B-NMDARs at PSD and thus restoring normal NMDAR-dependent Ca^{2+} entry.

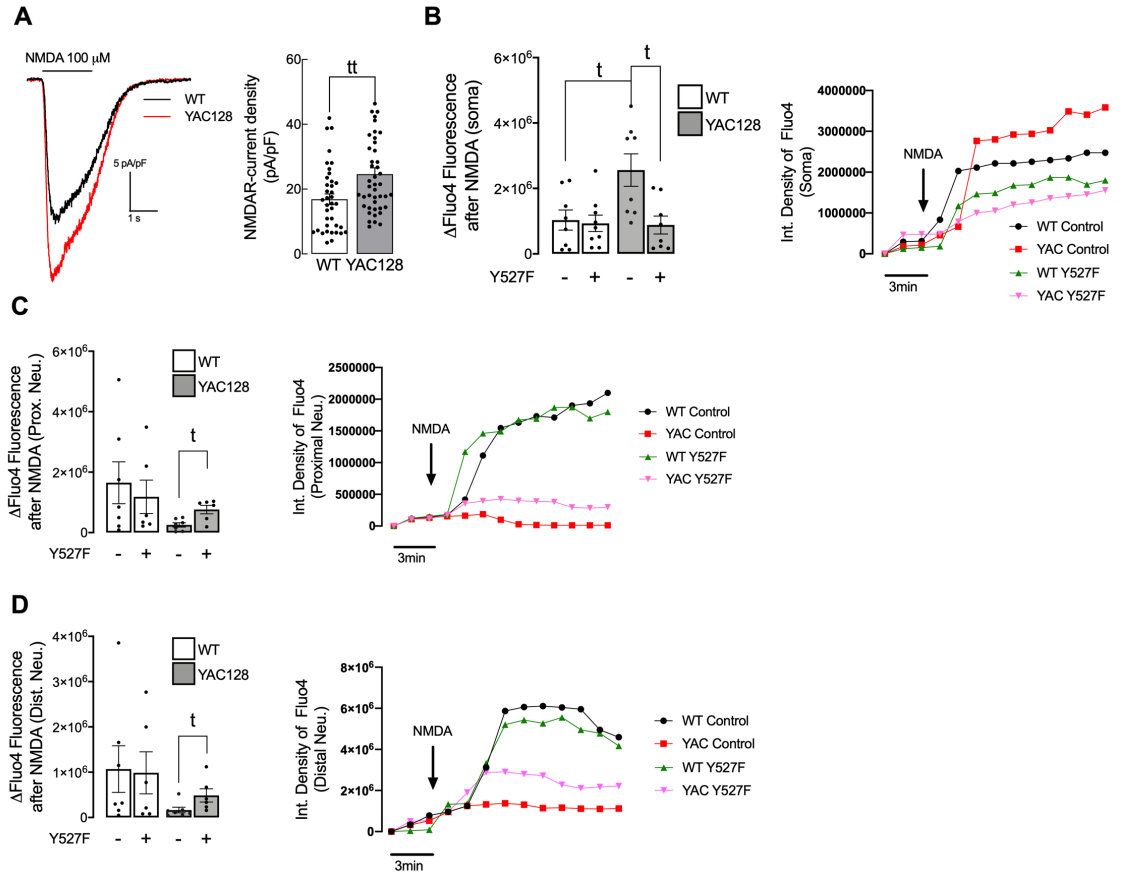

Figure 5.4 | Overexpression of activated SKF restores NMDARs currents levels in HD neurons. (A) Representative traces of NMDA (100 µM)-induced inward currents (-60 mV holding potential; with 10 µM glycine; without Mg^{2+}) in striatal neurons from wild-type (WT) and YAC128 mice showing a higher NMDA-induced current density in YAC128 mice-derived neurons *vs.* WT-derived neurons, as quantitatively summarized in the

histogram. Data are expressed as the mean ± SEM of peak NMDA-induced current density (pA/pF). $^{tt}p<0.01$ unpaired t-test. (B-D) Intracellular Ca^{2+} levels were measured using Fluo4 fluorescent dye, in soma (B), proximal neurites (C) and distal neurites (D). Units of fluorescence were monitored before and after exposure to 100 µM NMDA, in medium without Mg^{2+} and supplemented with glycine (20 µM) and serine (30 µM) in primary striatal neurons from WT and YAC128 mice, using fluorescence microscopy. Data are presented as the mean ± SEM of 4 independent experiments considering ~3 wells/condition. Statistical analysis: **p < 0.01 *versus* WT primary striatal neurons (two-way ANOVA, followed by Sidak's Multiple Comparison as post hoc test); $^{t}p < 0.05$, compared to WT control or YAC128 control (nonparametric Mann Whitney test).

5.3.4. RESTORATION OF ACTIVE SKF ENHANCES CREB ACTIVATION AND REDUCES APOPTOTIC PATHWAY ACTIVATION

Activated CREB promotes the expression of survival-related genes, including BDNF, which has neuroprotective properties and can rescue neurons from NMDAR blockade-induced neuronal death (Hansen et al., 2004). Additionally, several studies showed that extrasynaptic NMDAR's activation is associated with cell death pathways, whereas synaptic NMDAR function is associated to augmented CREB phosphorylation and activation, BDNF transcription, and improved antioxidant defenses (Hardingham et al., 2002). Considering restored synaptic NMDAR localization and function after expression of active form of SKF, we next evaluated CREB stimulation and apoptotic pathway activation (**Figure 5.5**). As expected, and in accordance with previous published data, we observed reduced CREB protein levels and activation/phosphorylation at Ser133 in YAC128 striatal neuron nuclei (**Figure 5.5A-C**). After Y527F SKF expression, CREB protein levels and activation were restored in the nucleus of YAC128 striatal neurons.

Caspase-3 is a cytosolic effector caspase with a central role in apoptosis, specifically being involved in the progression of neurodegenerative disorders (Khan et al., 2015). Accordingly, our data showed augmented cleaved/active caspase-3 in YAC128 mouse neurons in soma (**Figure 5.5D**), proximal (**Figure 5.5E**) and distal (**Figure 5.5F**) neurites. Importantly, increased cleaved/active caspase-3 levels were reduced following Y527F SKF plasmid expression, which validates apoptosis modulation (**Figure 5.5D-F**).

These results suggest that reestablished SKF levels and activity influence NMDARs presence and function at synaptic membrane, which may activate pro-survival pathways through augmented CREB activation.

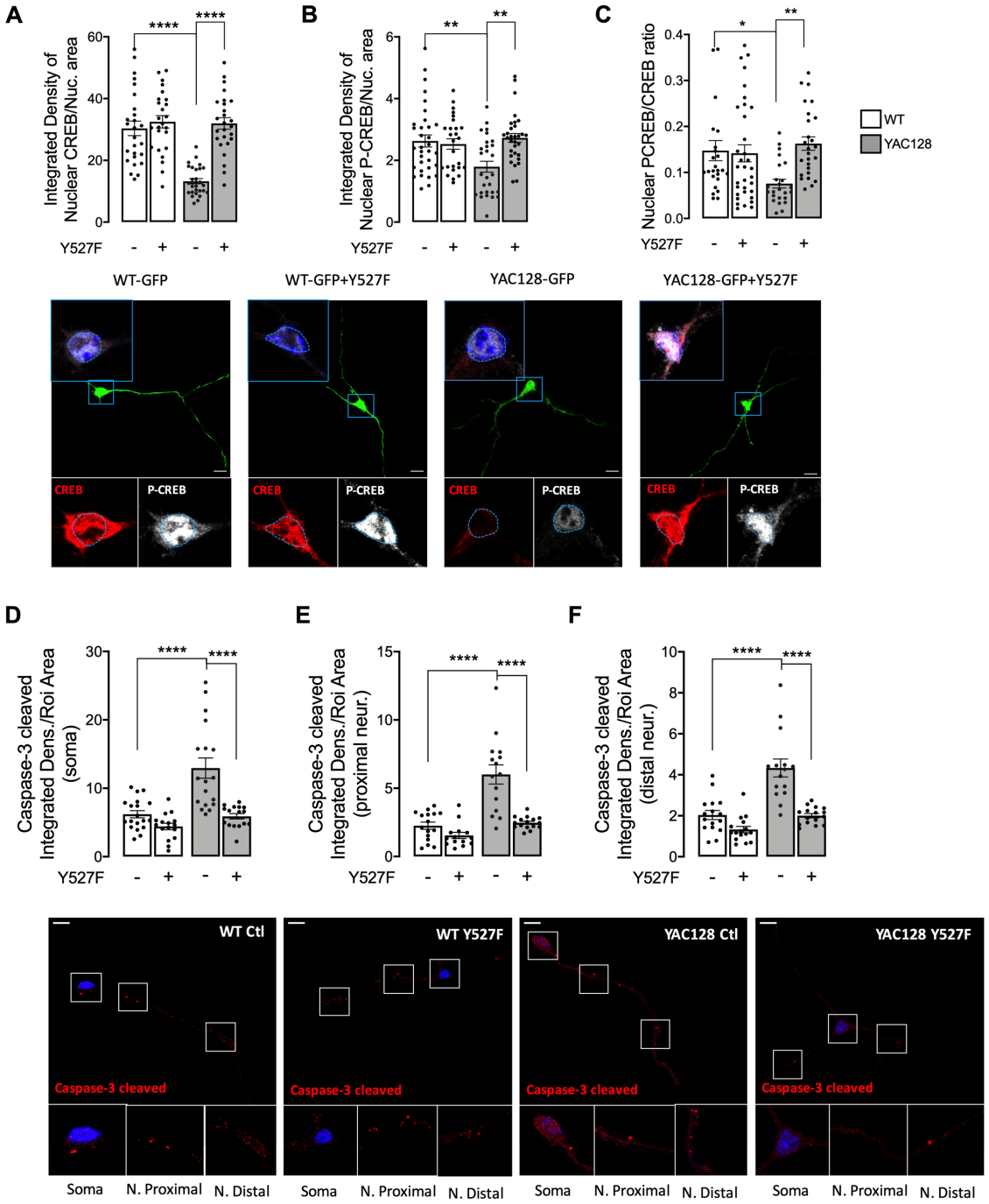

Figure 5.5 | Overexpression of activated SKF restores CREB activated levels and reduces caspase-3 levels in HD neurons. The nuclear levels of CREB (A), P(Ser133)CREB (B) and PCREB/CREB (C), as well as the levels of cleaved/active caspase-3 (D) in soma, proximal (E) and distal (F) neurites were evaluated by immunocytochemistry, using confocal microscope and Image J software in WT vs. YAC128 striatal neurons. Confocal images were obtained with a 63× objective in confocal microscope Zeiss LSM 710 (scale

bar: 10 µm). Data are presented as the mean ± SEM of 3 to 4 independent experiments considering ~6 wells/condition. Statistical analysis: **p < 0.01, and ****p < 0.0001 versus WT or YAC128 (two-way ANOVA, followed by Sidak's Multiple Comparison as post hoc test).

5.4. DISCUSSION

NMDARs are important synaptic receptors that contribute to normal synaptic function, cell survival, learning and memory (Bliss and Collingridge, 1993). Our study shows augmented extrasynaptic GluN2B-composed NMDARs in HD mouse neurons, while expression of a constitutive active form of SKF contributed to reestablish NMDARs localization and activity at PSD. Indeed, reduced Fyn activity in YAC128 PSDs contributes to reduced GluN2B phosphorylation at Tyr1472, which decreases synaptic NMDAR retention and may facilitate movement to extrasynaptic sites. Apart from restoring NMDARs phosphorylated levels at PSD, enhanced SKF levels and activity promote CREB activation and reduce apoptosis in YAC128 primary striatal neurons.

Previous studies showed that GluN2B-composed NMDARs function and trafficking are altered in HD (Chen et al., 1999; Fan et al., 2009, 2007; Milnerwood et al., 2010). Importantly, synaptic or extrasynaptic NMDARs activation are related to survival or apoptotis activation, respectively (Léveillé et al., 2008). Striatal neurons showed faster NMDAR trafficking to the surface membrane induced by mHTT (Fan et al., 2007), whereas this receptor accumulated at extrasynaptic sites of YAC128 mice at early age (Milnerwood et al., 2010). Concordantly, our results evidence a reduction in GluN2B-composed NMDARs levels in PSD, whereas these levels were augmented at extrasynaptic sites is YAC128 mouse striatal neurons. Moreover, in accordance with our data, other studies showed augmented NMDARs currents in HD mouse models (Milnerwood et al., 2010). However, this alteration is only measured in HD neuronal soma. In contrast, in proximal and distal neurites, altered PSD number, as well as reduced SKF levels and activity may result in abnormal synaptic function in HD, which may explain the reduction in NMDARs activity. Importantly, altered NMDARs function in proximal and distal neurites can be restored by augmenting active SKF levels.

Additionally, GluN2B Tyr1472 phosphorylation levels were decreased both in synaptic and extrasynaptic sites, which is in accordance with previous studies. Gladding and coworkers showed an increased synaptic STEP activity in YAC128 striatum, correlated with a decreased Tyr1472-GluN2B phosphorylation in YAC128 non-PSD and PSD fractions, similar to what we observed in the present

study, which facilitates NMDAR movement to extrasynaptic sites, reducing synaptic NMDAR retention (Gladding et al., 2012). Indeed, GluN2B-composed NMDAR Tyr1472 phosphorylation by SKF is associated with enrichment of synaptic NMDARs (Goebel-Goody et al., 2009), indicating that NMDAR lateral diffusion between synaptic and extrasynaptic sites is modulated by Tyr1472 phosphorylation. We previously showed that SKF members, specifically, c-Src and Fyn proteins are reduced in several HD models due to augmented degradation by autophagy (Fão et al., 2022). Concordantly with these data, here we show that Fyn total and phosphorylated levels are reduced at both PSD and non-PSD compartments, which may contribute to decrease Tyr1472-GluN2B phosphorylation at PSD and thus reduced synaptic NMDAR retention.

Fyn influence and fundamental role in PSD has long been recognized. Several studies have previously shown c-Src and Fyn roles in synapse development, plasticity, learning and memory (Grant and Silva, 1994; Maness, 1992). Takasu and colleagues showed that Ca^{2+} influx mediated by NMDARs activation upon its Tyr1472 phosphorylation by SKF resulted in gene transcription required for the remodeling of synaptic connections in excitatory synapses of primary cortical neurons (Takasu et al., 2002). In the present study we show, for the first time, that expression of a constitutive active form of SKF reestablishes NMDARs localization and function at PSD in YAC128 mouse striatal neurons, restoring neuronal function.

Decreased synaptic NMDARs and augmented extrasynaptic currents are associated with reduced nuclear CREB activation, reduced neuronal expression of the survival factor BDNF, and caused dysfunctional mitochondria, low energy levels and cell death in HD mouse striatum, before and after phenotype onset (Milnerwood et al., 2010). Extrasynaptic NMDARs activity is linked to cell death signaling cascades due to reduced phosphorylation/activation of CREB (Hardingham et al., 2002). Concordantly with previous studies showing decreased CREB activation in striatum of 1 and 4 months of age YAC128 mice (Milnerwood et al., 2010), our results show reduced nuclear CREB activation in YAC128 primary striatal neurons. Interestingly, decreased CREB activity and augmented active caspase-3 found in YAC128 striatal neurons were reversed following expression of the constitutive active form of SKF, Y527F SKF (Fig. 5),

previously shown by our group to be neuroprotective against mHTT-induced mitochondrial dysfunction and enhanced ROS levels (Fão et al., 2022).

Our study evidence, for the first time, that Fyn protein has an important role in synaptic GluN2B-composed NMDARs phosphorylation and activity, restoring CREB activation and decreasing caspase-3 levels, indicative of a decrease in cell death by apoptosis in HD. Decreased Fyn PSD co-localization correlates with HD-related reduced Tyr1472 GluN2B phosphorylation and augmented extrasynaptic NMDARs currents, as well as decreased CREB activation and cell death. Interestingly, reestablished active SKF levels restored NMDARs currents, NMDAR-dependent Ca^{2+} levels, CREB activation and reduced caspase-3 cleavage. Hence, we describe a potential mechanism, involving Fyn restored levels and activity that may constitute a potential HD therapeutic target to promote striatal glutamatergic synaptic function and survival.

CHAPTER VI

CONCLUSIONS AND PERSPECTIVES

HD is a multifaceted genetic neurodegenerative pathology with different dysfunctional mechanisms, namely ROS augmented production and defective elimination, dysfunctional protein degradation, mitochondrial dysfunction, deregulated autophagy, synaptic changes and malfunction and altered NMDAR activity and localization. SKF proteins can be located in several cellular compartments, such as the cytosol, mitochondria, endoplasmic reticulum, plasma membrane, nucleus, endosomes and lysosomes (Sandilands and Frame, 2008). c-Src/Fyn kinases, in particular, are highly brain expressed, specifically in the striatum, the most affected brain area in HD (Pascoli et al., 2011), are regulated by ROS, can influence NMDAR activity and localization, and are important proteins for normal mitochondrial function. Indeed, despite the different common pathways, the c-Src/Fyn involvement in HD was largely unexplored. Thus, we approached in this work, and for the first time, the fundamental role of SKF in HD ethiopathological mechanisms.

Nrf2 is the main transcription factor involved in expression of cell defense enzymes and its involvement in HD has been suggested in different works, as explored in section 1.2.2.2. Previously studies in our laboratory showed that ST*Hdh*$^{Q111/Q111}$ striatal cells presented increased ROS levels (e.g. Ribeiro et al., 2014; Oliveira et al., 2015), decreased Nrf2 levels and, despite augmented Nrf2 phosphorylation at Ser40 (Oliveira et al., 2015a), Nrf2 nuclear activity was reduced in HD cells, causing reduced antioxidant mRNA levels (Jin et al., 2013; Oliveira et al., 2015a). Since Nrf2 activation at cytosol is important for its consistent levels and activity in the nucleus, in this work we explored SKF involvement in Nrf2 modulation after an acute H_2O_2 (a ROS) exposure. Among other kinases, cytosolic Nrf2 activation occurs through PKCδ phosphorylation, which enables Nrf2 nuclear migration and activation (Huang et al., 2002). PKCδ phosphorylation is controlled by SKF (Konishi et al., 2001), which in turn are regulated by H_2O_2 (Akhand et al., 1999). Here we showed that acute H_2O_2 exposure resulted in augmented SKF members activation in HT22 cells, which in turn upregulated PKCδ phosphorylation at Tyr311, increasing Nrf2 phosphorylation at Ser40 residue (Fão et al., 2019b). In this way, in the presence of H_2O_2, Nrf2 increasingly accumulated in the nucleus, promoting Nrf2/ARE transcriptional activity, such as augmented HO-1 mRNA levels, in SKF-

dependent manner (Fão et al., 2019b). The SKF involvement in Nrf2 regulation had been demonstrated in other studies, as Fyn was implicated in nuclear Nrf2 export and degradation (Culbreth et al., 2017; Li et al., 2017); however, our work provided the first evidence that SKF can serve as Nrf2 co-activators via PKCδ after acute oxidant stimulus. Thus, we confirmed that SKF members are important proteins in Nrf2 nuclear activity regulation, after acute ROS production, which is a common feature in several neurodegenerative disorders, as HD. Considering that, we highlight the c-Src/PKCδ/Nrf2 pathway as a possible novel target for treating or ameliorating oxidative stress-associated diseases, like HD **(Figure 6.1A,D).**

We pursued the search for target organelles involved in HD pathogenesis and that are also related with ROS production and accumulation, which might be modulated by SKF. Mitochondria are one of the major relevant organelles early affected in HD, and SKF members, namely c-Src and Fyn, have important roles in normal mitochondrial function. Indeed, c-Src/Fyn kinases were identified in the intermembrane space of highly purified rat brain mitochondria (Salvi et al., 2002). Moreover, c-Src/Fyn modulated brain mitochondrial respiration through phosphorylation of complexes I, III and IV (Ogura et al., 2012). Concordantly, several studies described altered mitochondrial function in HD models, including decreased activity of mitochondrial complexes II-IV in HD patient's *postmortem* striata, human peripheral cells and animal brains (Pandey et al., 2008). In this way, we proposed to better understand SKF involvement in HD mitochondrial malfunction, in order to evaluate if SKF could be used as therapeutic targets for HD pathogenesis. We showed that c-Src and Fyn kinases total and activated levels were reduced in several HD models, including *postmortem* human brain caudate, YAC128 mouse brain striatum and cortex at early stages, YAC128 striatal neurons and ST*Hdh*$^{Q111/Q111}$ (or Q111) triatal cells lines, due to augmented degradation by autophagy. Under normal conditions regulation of SKF protein levels occurs mainly through the proteasome (Harris et al., 1999), however we discovered a higher degradation of c-Src and Fyn proteins through (macro)autophagy pathway in cells expressing full-length mouse mHtt and human mHTT, namely Q111 cells and YAC128 mouse striatal neurons, respectively (Fão et al., 2022). Moreover, we found reduced Fyn levels and activity in YAC128 mouse striatal isolated mitochondria, as well as in

mitochondria from striatal neurons or Q111 striatal cells. Considering that impaired OXPHOS, abnormal Δψm, augmented ROS levels, accompanied by modifications in mitochondrial morphology (e.g. Almeida et al., 2008; Ferreira et al., 2010; Naia et al., 2021) are well characterized HD features, we decided to explore the specific role of SKF in ameliorating HD mitochondrial function and ROS production. Our findings evidence a restoration of mitochondrial morphology (specifically mitochondrial perimeter, roundness and aspect ratio) and function after the re-establishment of active SKF levels in both Q111 cells and YAC128 mouse striatal neurons. Indeed, mitochondrial SKF activation was previously shown to be essential for cell survival (Arachiche et al., 2008; Ogura et al., 2012) and Fyn phosphorylation are important for the regulation of energy generation in mammalian mitochondria (Koc et al., 2017). Concordantly, in this work we proved that expression of active SKF improved mitochondrial function through augmented Δψm, basal respiration and ATP production **(Figure 6.1B)**. Conversely, SKF inhibition was enough to induce HD-like mitochondrial phenotype, suggesting SKF-dependent maintenance of mitochondrial function under normal conditions. Also, expression of active SKF reduced mitochondrial ROS levels and augmented cell viability in HD cells, namely by decreasing caspase3-cleaved/active levels **(Figure 6.1E).** Therefore, c-Src and Fyn appear to constitute essential proteins which deficits contribute for HD etiopathogenesis, such as mitochondrial dysfunction and ROS production, and thus should be considered as potential HD therapeutic targets.

The expression of mHTT in HD has been associated with protein conformational changes, aggregation and abnormal protein-protein interactions (Morreale, 2015), which has been associated with changes in gene transcription, synaptic dysfunction, NMDARs overactivation and increased oxidative events, leading to neuronal death (Finkbeiner, 2011, for review). Additionally, HD-affected MSNs show altered NMDAR currents as well as augmented ratio of surface to internal GluN2B-containing NMDARs, with augmented accumulation at extrasynaptic sites (Milnerwood et al., 2010). NMDARs are important postsynaptic receptors that contribute to normal synaptic function and cell survival (Finkbeiner, 2011) and the synaptic NMDARs activation is associated with augmented CREB-dependent gene expression, an important transcription factor for neuronal survival, synaptic plasticity, neurogenesis, learning and

memory (Hardingham et al., 2002). Moreover, Fyn can be found in the PSD and further phosphorylate NMDARs to regulate synaptic transmission and plasticity (e.g. Brugge et al., 1985). Fyn phosphorylates NMDAR GluN2B subunit at Tyr1472, increasing receptor retention at the synapse, thus controlling synaptic plasticity (Ai et al., 2013; Mota et al., 2014b). Because we showed (in the present study) that Fyn levels are reduced in several HD models, and considering its important role at the PSD, we decided to explore the impact of HD-mediated altered Fyn levels on synaptic *versus* non-synaptic NMDARs function and location, as well as intracellular neuroprotective pathways. We showed that extrasynaptic GluN2B-composed NMDARs protein levels are augmented in HD mouse neurons, while GluN2B Tyr1472 phosphorylation levels were decreased both in synaptic and extrasynaptic sites **(Figure 6.1C)**. As such, reduced Fyn activity in YAC128 mouse PSDs contributed for reduced GluN2B phosphorylation at Tyr1472, which decreased synaptic NMDAR retention and might have facilitated their movement to extrasynaptic sites. Interestingly, expression of the constitutive active form of SKF reestablished NMDARs localization and function at PSD in YAC128 mouse striatal neurons, restoring neuronal function. Extrasynaptic NMDARs activity was previously linked to cell death signaling cascades due to reduced phosphorylation/activation of CREB (Hardingham et al., 2002). Concordantly with previous studies showing decreased CREB activation in the striatum of 1 and 4 months of age YAC128 mice (Milnerwood et al., 2010), we showed reduced nuclear CREB activation in YAC128 mouse striatal neurons **(Figure 6.1C)**. Of relevance, restoration of SKF levels not only improved NMDARs phosphorylated levels at PSD, but also promoted CREB accumulation and nuclear activation, which reduced apoptosis in YAC128 mouse striatal neurons **(Figure 6.1F)**.

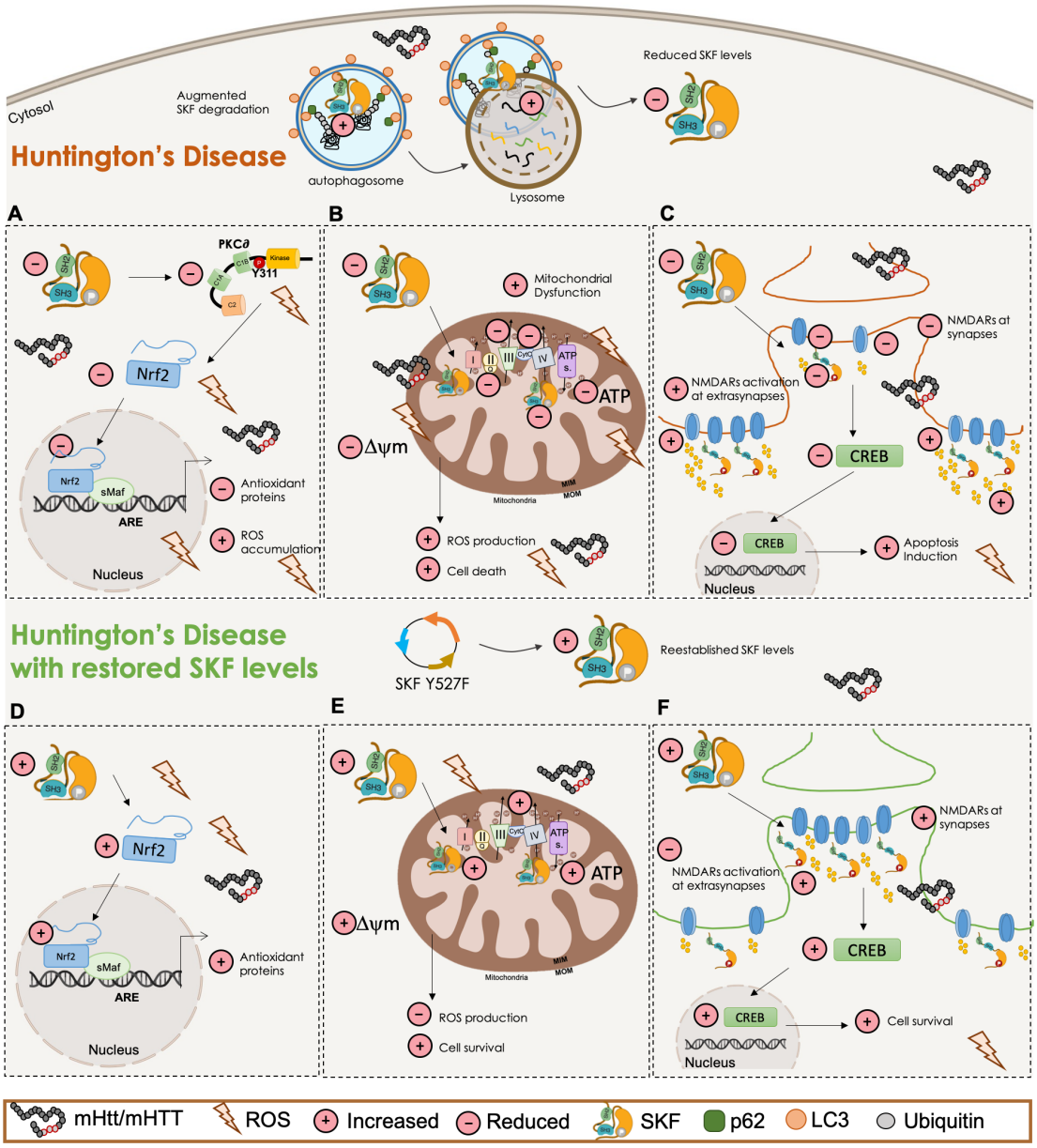

Figure 6.1 | Effects of SKF modulation in HD pathogenesis. In this work we showed that SKF levels are reduced in HD, in part due to augmented degradation by autophagy, and its modulation are neuroprotective in HD models expressing mHtt/mHTT: (A) Nrf2 is a transcription factor indirectly controlled by SKF, which was shown to be decreased in HD. We hypothesize that reduced SKF levels and activation contribute for reduced Nrf2 nuclear levels and activity and consequently decreasing the expression of antioxidant defense proteins in HD; (B) Reduced mitochondrial SKF levels induced mitochondrial dysfunction with reduced Δψm, mitochondrial respiratory through diminished basal respiration and ATP production, which resulted in augmented ROS production and induction of apoptosis. Also, in (C) SKF levels are reduced in PSD, contributing for reduced NMDARs synaptic function, augmented extrasynaptic NMDARs activity and diminished CREB activation, resulting in cell death. (D-F) After restoration of active SKF levels by expressing the constitutive active form of SKF (Y527F), we hypothesize that Nrf2 might be more active resulting in augmented antioxidant proteins expression (D); furthermore, current thesis work showed that SKF levels improves mitochondrial function and decreases ROS production (E), as well as increases CREB activation through augmented synaptic NMDARs activity, reducing cell death (F).

In conclusion, the present work shows that the expression of mHTT alters the protein degradation pathways, resulting in decreased SKF levels and activation, not only in the cytosol, but also in specific sites, such as the nucleus, mitochondria and neuronal synapses. Reduced mitochondrial SKF levels favor ROS production and mitochondrial dysfunction through altered morphology, Δψm, mitochondrial basal respiration and ATP production, which by adding the decrease in Nrf2 nuclear activity, favor increased ROS levels and accumulation due to reduced antioxidant defenses. Furthermore, decreased SKF levels and function at PSD participates in altered NMDAR phosphorylation and synaptic localization, augmenting extrasynaptic NMDARs function, which reduces CREB activation and induces cell death. Notably, restoration of SKF levels improved mitochondrial function, ROS levels, NMDARs phosphorylation and activation, CREB nuclear activation and cell survival. Taking into account all these SKF therapeutic roles, we strongly conceive that this PhD thesis brings out SKF as potential HD therapeutic targets to be considered in future studies and clinical trials.

In order to clarify whether increased expression c-Src/Fyn alleviates HD-related psychiatric and/or motor deficits, and contributes to alleviate disease progression, the next step of the present work would be to promote the expression of c-Src/Fyn (using adeno-associated virus) in HD and WT mouse striata (both hemispheres) and evaluate behavioral (e.g. depressive-like behavior and motor activity) and histological features at different time points. Once confirmed the positive influence of SKF modulation on HD progression in more than one HD animal model, new clinical trials might be designed considering different ways to increase SKF levels, namely by augmenting SKF expression and/or reducing SKF target(s) and selective autophagy degradation. Additionally, news strategies might be envisaged in order to increase SKF targeting to mitochondria, by augmenting Dok-4 (Itoh et al., 2005) or AKAP121 (A Livigni et al., 2006), the two described proteins shown to import SKF members to mitochondria.

CHAPTER VII

REFERENCES

Acevedo-Torres, K., Berríos, L., Rosario, N., Dufault, V., Skatchkov, S., Eaton, M.J., Torres-Ramos, C.A., Ayala-Torres, S., 2009. Mitochondrial DNA damage is a hallmark of chemically induced and the R6/2 transgenic model of Huntington's disease. DNA Repair (Amst). 8, 126–136. https://doi.org/10.1016/j.dnarep.2008.09.004

Ahlberg, J., Marzella, L., Glaumann, H., 1982. Uptake and degradation of proteins by isolated rat liver lysosomes. Suggestion of a microautophagic pathway of proteolysis. Lab. Investig.

Ai, H., Lu, W., Ye, M., Yang, W., 2013. Synaptic non-GluN2B-containing NMDA receptors regulate tyrosine phosphorylation of GluN2B 1472 tyrosine site in rat brain slices. Neurosci. Bull. 29, 614–620. https://doi.org/10.1007/s12264-013-1337-8

Akhand, A.A., Pu, M., Senga, T., Kato, M., Suzuki, H., Miyata, T., Hamaguchi, M., Nakashima, I., 1999. Nitric oxide controls Src kinase activity through a sulfhydryl group modification-mediated Tyr-527-independent and Tyr-416-linked mechanism. J. Biol. Chem. 274, 25821–25826. https://doi.org/10.1074/jbc.274.36.25821

Aladdin, A., Király, R., Boto, P., Regdon, Z., Tar, K., 2019. Juvenile Huntington's Disease Skin Fibroblasts Respond with Elevated Parkin Level and Increased Proteasome Activity as a Potential Mechanism to Counterbalance the Pathological Consequences of Mutant Huntingtin Protein. Int. J. Mol. Sci. 20, 5338. https://doi.org/10.3390/ijms20215338

Alam, J., Cai, J., Smith, A., 1994. Isolation and characterization of the mouse heme oxygenase-1 gene. Distal 5' sequences are required for induction by heme or heavy metals. J. Biol. Chem. 269, 1001–9.

Alam, J., Camhi, S., Choi, A.M.K., 1995. Identification of a second region upstream of the mouse heme oxygenase-1 gene that functions as a basal level and inducer-dependent transcription enhancer. J. Biol. Chem. 270, 11977–11984. https://doi.org/10.1074/jbc.270.20.11977

Alam, J., Stewart, D., Touchard, C., Boinapally, S., Choi, a M., Cook, J.L., 1999. Nrf2, a Cap'n'Collar transcription factor, regulates induction of the heme oxygenase-1 gene. J. Biol. Chem. 274, 26071–26078. https://doi.org/10.1074/jbc.274.37.26071

Alberini, C.M., 2009. Transcription factors in long-term memory and synaptic plasticity. Physiol. Rev. https://doi.org/10.1152/physrev.00017.2008

Albin, R.L., Reiner, A., Anderson, K.D., Penney, J.B., Young, A.B., 1990. Striatal and nigral neuron subpopulations in rigid Huntington's disease: Implications for the functional anatomy of chorea and rigidity-akinesia. Ann. Neurol. https://doi.org/10.1002/ana.410270403

Ali, D.W., Salter, M.W., 2001. NMDA receptor regulation by Src kinase signalling in excitatory synaptic transmission and plasticity. Curr. Opin. Neurobiol. 11, 336–342. https://doi.org/10.1016/S0959-4388(00)00216-6

Ali, N.J., Levine, M.S., 2006. Changes in expression of N-methyl-D-aspartate receptor subunits occur early in the R6/2 mouse model of Huntington's disease. Dev. Neurosci. https://doi.org/10.1159/000091921

Almeida, S., Sarmento-Ribeiro, A.B., Januário, C., Rego, A.C., Oliveira, C.R., 2008. Evidence of apoptosis and mitochondrial abnormalities in peripheral blood cells of Huntington's disease patients. Biochem. Biophys. Res. Commun. 374, 599–603. https://doi.org/10.1016/j.bbrc.2008.07.009

Alonso, G., Koegl, M., Mazurenko, N., Courtneidge, S.A., 1995. Sequence requirements for binding of Src family tyrosine kinases to activated growth factor receptors. J. Biol. Chem. https://doi.org/10.1074/jbc.270.17.9840

Anderson, G., Maes, M., 2014. Neurodegeneration in Parkinson's disease: Interactions of oxidative stress, tryptophan catabolites and depression with mitochondria and sirtuins. Mol. Neurobiol. https://doi.org/10.1007/s12035-013-8554-z

Anderson, S., Bankier, A.T., Barrell, B.G., De Bruijn, M.H.L., Coulson, A.R., Drouin, J., Eperon, I.C., Nierlich, D.P., Roe, B.A., Sanger, F., Schreier,

P.H., Smith, A.J.H., Staden, R., Young, I.G., 1981. Sequence and organization of the human mitochondrial genome. Nature. https://doi.org/10.1038/290457a0

André, V.M., Cepeda, C., Fisher, Y.E., Huynh, M., Bardakjian, N., Singh, S., Yang, X.W., Levine, M.S., 2011. Differential electrophysiological changes in striatal output neurons in Huntington's disease. J. Neurosci. https://doi.org/10.1523/JNEUROSCI.3539-10.2011

Anguita, E., Villalobo, A., 2017. Src-family tyrosine kinases and the Ca2 + signal. Biochim. Biophys. Acta - Mol. Cell Res. https://doi.org/10.1016/j.bbamcr.2016.10.022

Antonioli, M., Di Rienzo, M., Piacentini, M., Fimia, G.M., 2017. Emerging Mechanisms in Initiating and Terminating Autophagy. Trends Biochem. Sci. https://doi.org/10.1016/j.tibs.2016.09.008

Arachiche, A., Augereau, O., Decossas, M., Pertuiset, C., Gontier, E., Letellier, T., Dachary-Prigent, J., 2008. Localization of PTP-1B, SHP-2, and Src exclusively in rat brain mitochondria and functional consequences. J. Biol. Chem. 283, 24406–24411. https://doi.org/10.1074/jbc.M709217200

Ariano, M.A., Wagle, N., Grissell, A.E., 2005. Neuronal vulnerability in mouse models of Huntington's disease: Membrane channel protein changes. J. Neurosci. Res. https://doi.org/10.1002/jnr.20492

Ashkenazi, A., Bento, C.F., Ricketts, T., Vicinanza, M., Siddiqi, F., Pavel, M., Squitieri, F., Hardenberg, M.C., Imarisio, S., Menzies, F.M., Rubinsztein, D.C., 2017. Polyglutamine tracts regulate beclin 1-dependent autophagy. Nature. https://doi.org/10.1038/nature22078

Aslan, M., Ozben, T., 2004. Reactive oxygen and nitrogen species in Alzheimer's disease. Curr. Alzheimer Res. 1, 111–119. https://doi.org/10.2174/1567205043332162

Atwal, R.S., Xia, J., Pinchev, D., Taylor, J., Epand, R.M., Truant, R., 2007. Huntingtin has a membrane association signal that can modulate huntingtin

aggregation, nuclear entry and toxicity. Hum. Mol. Genet. https://doi.org/10.1093/hmg/ddm217

Augereau, O., Claverol, S., Boudes, N., Basurko, M.J., Bonneu, M., Rossignol, R., Mazat, J.P., Letellier, T., Dachary-Prigent, J., 2005. Identification of tyrosine-phosphorylated proteins of the mitochondrial oxidative phosphorylation machinery. Cell. Mol. Life Sci. 62, 1478–1488. https://doi.org/10.1007/s00018-005-5005-7

Axe, E.L., Walker, S.A., Manifava, M., Chandra, P., Roderick, H.L., Habermann, A., Griffiths, G., Ktistakis, N.T., 2008. Autophagosome formation from membrane compartments enriched in phosphatidylinositol 3-phosphate and dynamically connected to the endoplasmic reticulum. J. Cell Biol. https://doi.org/10.1083/jcb.200803137

Ayala-Peña, S., 2013. Role of oxidative DNA damage in mitochondrial dysfunction and Huntington's disease pathogenesis. Free Radic. Biol. Med. https://doi.org/10.1016/j.freeradbiomed.2013.04.017

Aylward, E.H., Codori, A.M., Barta, P.E., Pearlson, G.D., Harris, G.J., Brandt, J., 1996. Basal ganglia volume and proximity to onset in presymptomatic Huntington disease. Arch. Neurol. https://doi.org/10.1001/archneur.1996.00550120105023

Babus, L.W., Little, E.M., Keenoy, K.E., Minami, S.S., Chen, E., Song, J.M., Caviness, J., Koo, S.Y., Pak, D.T.S., Rebeck, G.W., Turner, R.S., Hoe, H.S., 2011. Decreased dendritic spine density and abnormal spine morphology in Fyn knockout mice. Brain Res. https://doi.org/10.1016/j.brainres.2011.07.059

Balu, M., Sangeetha, P., Haripriya, D., Panneerselvam, C., 2005. Rejuvenation of antioxidant system in central nervous system of aged rats by grape seed extract. Neurosci. Lett. https://doi.org/10.1016/j.neulet.2005.04.042

Bang, H.-Y., Park, S.-A., Saeidi, S., Na, H.-K., Surh, Y.-J., 2017. Docosahexaenoic Acid Induces Expression of Heme Oxygenase-1 and NAD(P)H:quinone Oxidoreductase through Activation of Nrf2 in Human

Mammary Epithelial Cells. Molecules 22, 969. https://doi.org/10.3390/molecules22060969

Barnham, K.J., Masters, C.L., Bush, A.I., 2004. Neurodegenerative diseases and oxidative stress. Nat. Rev. Drug Discov. 3, 205–214. https://doi.org/10.1038/nrd1330

Basak, P., Sadhukhan, P., Sarkar, P., Sil, P.C., 2017. Perspectives of the Nrf-2 signaling pathway in cancer progression and therapy. Toxicol. Reports 4, 306–318. https://doi.org/10.1016/j.toxrep.2017.06.002

Bates, G., 2003. Huntingtin aggregation and toxicity in Huntington's disease. Lancet (London, England) 361, 1642–4. https://doi.org/10.1016/S0140-6736(03)13304-1

Bates, G.P., Dorsey, R., Gusella, J.F., Hayden, M.R., Kay, C., Leavitt, B.R., Nance, M., Ross, C. a., Scahill, R.I., Wetzel, R., Wild, E.J., Tabrizi, S.J., 2015. Huntington disease. Nat. Rev. Dis. Prim. 15005. https://doi.org/10.1038/nrdp.2015.5

Bates, G.P., Mangiarini, L., Mahal, A., Davies, S.W., 1997. Transgenic models of Huntington's disease. Hum. Mol. Genet. https://doi.org/10.1093/hmg/6.10.1633

Bausewein, T., Mills, D.J., Langer, J.D., Nitschke, B., Nussberger, S., Kühlbrandt, W., 2017. Cryo-EM Structure of the TOM Core Complex from Neurospora crassa. Cell. https://doi.org/10.1016/j.cell.2017.07.012

Beal, M.F., Ferrante, R.J., Swartz, K.J., Kowall, N.W., 1991. Chronic quinolinic acid lesions in rats closely resemble Huntington's disease. J. Neurosci.

Ben M'Barek, K., Pla, P., Orvoen, S., Benstaali, C., Godin, J.D., Gardier, A.M., Saudou, F., David, D.J., Humbert, S., 2013. Huntingtin mediates anxiety/depression-related behaviors and hippocampal neurogenesis. J. Neurosci. https://doi.org/10.1523/JNEUROSCI.5110-12.2013

Benchoua, A., Trioulier, Y., Zala, D., Gaillard, M.C., Lefort, N., Dufour, N.,

Saudou, F., Elalouf, J.M., Hirsch, E., Hantraye, P., Déglon, N., Brouillet, E., 2006. Involvement of mitochondrial complex II defects in neuronal death produced by N-terminus fragment of mutated huntingtin. Mol. Biol. Cell. https://doi.org/10.1091/mbc.E05-07-0607

Bennett, E.J., Bence, N.F., Jayakumar, R., Kopito, R.R., 2005. Global impairment of the ubiquitin-proteasome system by nuclear or cytoplasmic protein aggregates precedes inclusion body formation. Mol. Cell. https://doi.org/10.1016/j.molcel.2004.12.021

Bennett, E.J., Shaler, T.A., Woodman, B., Ryu, K.Y., Zaitseva, T.S., Becker, C.H., Bates, G.P., Schulman, H., Kopito, R.R., 2007. Global changes to the ubiquitin system in Huntington's disease. Nature. https://doi.org/10.1038/nature06022

Berardelli, A., Noth, J., Thompson, P.D., Bollen, E.L.E.M., Currà, A., Deuschl, G., Van Dijk, J.G., Töpper, R., Schwarz, M., Roos, R.A.C., 1999. Pathophysiology of chorea and bradykinesia in Huntington's disease. Mov. Disord. https://doi.org/10.1002/1531-8257(199905)14:3<398::AID-MDS1003>3.0.CO;2-F

Beste, C., Konrad, C., Saft, C., Ukas, T., Andrich, J., Pfleiderer, B., Hausmann, M., Falkenstein, M., 2009. Alterations in voluntary movement execution in Huntington's disease are related to the dominant motor system - Evidence from event-related potentials. Exp. Neurol. https://doi.org/10.1016/j.expneurol.2008.11.018

Bienert, G.P., Schjoerring, J.K., Jahn, T.P., 2006. Membrane transport of hydrogen peroxide. Biochim. Biophys. Acta 1758, 994–1003. https://doi.org/10.1016/j.bbamem.2006.02.015

Birgisdottir, Å.B., Lamark, T., Johansen, T., 2013. The LIR motif - crucial for selective autophagy. J. Cell Sci. https://doi.org/10.1242/jcs.126128

Bjørkøy, G., Lamark, T., Brech, A., Outzen, H., Perander, M., Øvervatn, A., Stenmark, H., Johansen, T., 2005. p62/SQSTM1 forms protein aggregates degraded by autophagy and has a protective effect on huntingtin-induced

cell death. J. Cell Biol. https://doi.org/10.1083/jcb.200507002

Blake, R.A., Broome, M.A., Liu, X., Wu, J., Gishizky, M., Sun, L., Courtneidge, S.A., 2000. SU6656, a selective src family kinase inhibitor, used to probe growth factor signaling. Mol. Cell. Biol. 20, 9018–27. https://doi.org/10.1128/MCB.20.23.9018-9027.2000

Bliss, T.V.P., Collingridge, G.L., 1993. A synaptic model of memory: Long-term potentiation in the hippocampus. Nature. https://doi.org/10.1038/361031a0

Bloom, D.A., Jaiswal, A.K., 2003. Phosphorylation of Nrf2 at Ser40 by protein kinase C in response to antioxidants leads to the release of Nrf2 from INrf2, but is not required for Nrf2 stabilization/accumulation in the nucleus and transcriptional activation of antioxidant response element. J. Biol. Chem. 278, 44675–82. https://doi.org/10.1074/jbc.M307633200

Boehning, D., Patterson, R.L., Sedaghat, L., Glebova, N.O., Kurosaki, T., Snyder, S.H., 2003. Cytochrome c binds to inositol (1,4,5) trisphosphate receptors, amplifying calcium-dependent apoptosis. Nat. Cell Biol. https://doi.org/10.1038/ncb1063

Boerner, J.L., Demory, M.L., Silva, C., Parsons, S.J., 2004. Phosphorylation of Y845 on the epidermal growth factor receptor mediates binding to the mitochondrial protein cytochrome c oxidase subunit II. Mol. Cell. Biol. 24, 7059–71. https://doi.org/10.1128/MCB.24.16.7059-7071.2004

Bogdanov, M.B., Andreassen, O.A., Dedeoglu, A., Ferrante, R.J., Beal, M.F., 2001. Increased oxidative damage to DNA in a transgenic mouse model of Huntington's disease. J. Neurochem. 79, 1246–9. https://doi.org/10.1046/j.1471-4159.2001.00689.x

Bórquez, D.A., Urrutia, P.J., Wilson, C., Van Zundert, B., Núñez, M.T., González-Billault, C., 2016. Dissecting the role of redox signaling in neuronal development. J. Neurochem. 137, 506–517. https://doi.org/10.1111/jnc.13581

Brennan, W. a, Bird, E.D., Aprille, J.R., 1985. Regional mitochondrial respiratory

activity in Huntington's disease brain. J. Neurochem. 44, 1948–1950.

Brigman, J.L., Wright, T., Talani, G., Prasad-Mulcare, S., Jinde, S., Seabold, G.K., Mathur, P., Davis, M.I., Bock, R., Gustin, R.M., Colbran, R.J., Alvarez, V. a, Nakazawa, K., Delpire, E., Lovinger, D.M., Holmes, A., 2010. Loss of GluN2B-containing NMDA receptors in CA1 hippocampus and cortex impairs long-term depression, reduces dendritic spine density, and disrupts learning. J. Neurosci. 30, 4590–600. https://doi.org/10.1523/JNEUROSCI.0640-10.2010

Brouillet, E., Condé, F., Beal, M.F., Hantraye, P., 1999. Replicating Huntington's disease phenotype in experimental animals. Prog. Neurobiol. https://doi.org/10.1016/S0301-0082(99)00005-2

Brown, M.T., Cooper, J.A., 1996. Regulation, substrates and functions of src. Biochim. Biophys. Acta - Rev. Cancer. https://doi.org/10.1016/0304-419X(96)00003-0

Browne, S.E., 2008. Mitochondria and Huntington's disease pathogenesis: Insight from genetic and chemical models, in: Annals of the New York Academy of Sciences. https://doi.org/10.1196/annals.1427.018

Browne, S.E., Beal, M.F., 2006. Oxidative damage in Huntington's disease pathogenesis. Antioxid. Redox Signal. 8, 2061–73. https://doi.org/10.1089/ars.2006.8.2061

Browne, S.E., Bowling, A.C., MacGarvey, U., Baik, M.J., Berger, S.C., Muqit, M.M., Bird, E.D., Beal, M.F., 1997. Oxidative damage and metabolic dysfunction in Huntington's disease: Selective vulnerability of the basal ganglia. Ann. Neurol. 41, 646–53. https://doi.org/10.1002/ana.410410514

Browne, S.E., Ferrante, R.J., Beal, M.F., 1999. Oxidative stress in Huntington's disease. Brain Pathol. 9, 147–63.

Brugge, J.S., Cotton, P.C., Queral, A.E., Barrett, J.N., Nonner, D., Keane, R.W., 1985. Neurones express high levels of a structurally modified, activated form of pp60c-src. Nature. https://doi.org/10.1038/316554a0

Bryan, H.K., Olayanju, A., Goldring, C.E., Park, B.K., 2013. The Nrf2 cell defence pathway: Keap1-dependent and -independent mechanisms of regulation. Biochem. Pharmacol. https://doi.org/10.1016/j.bcp.2012.11.016

Busch, A., Engemann, S., Lurz, R., Okazawa, H., Lehrach, H., Wanker, E.E., 2003. Mutant Huntingtin Promotes the Fibrillogenesis of Wild-type Huntingtin. J. Biol. Chem. https://doi.org/10.1074/jbc.m303354200

Calabresi, P., Picconi, B., Tozzi, A., Ghiglieri, V., Di Filippo, M., 2014. Direct and indirect pathways of basal ganglia: A critical reappraisal. Nat. Neurosci. https://doi.org/10.1038/nn.3743

Calkins, M.J., Jakel, R.J., Johnson, D.A., Chan, K., Kan, Y.W., Johnson, J.A., 2005. Protection from mitochondrial complex II inhibition in vitro and in vivo by Nrf2-mediated transcription. Proc. Natl. Acad. Sci. U. S. A. 102, 244–9. https://doi.org/10.1073/pnas.0408487101

Calkins, M.J., Townsend, J.A., Johnson, D.A., Johnson, J.A., 2010. Cystamine protects from 3-nitropropionic acid lesioning via induction of nf-e2 related factor 2 mediated transcription. Exp. Neurol. https://doi.org/10.1016/j.expneurol.2010.04.008

Cao, Z., George, J., Baden, D.G., Murray, T.F., 2007. Brevetoxin-induced phosphorylation of Pyk2 and Src in murine neocortical neurons involves distinct signaling pathways. Brain Res. 1184, 17–27. https://doi.org/10.1016/j.brainres.2007.09.065

Cattaneo, E., Rigamonti, D., Goffredo, D., Zuccato, C., Squitieri, F., Sipione, S., 2001. Loss of normal huntingtin function: New developments in Huntington's disease research. Trends Neurosci. https://doi.org/10.1016/S0166-2236(00)01721-5

Caviston, J.P., Holzbaur, E.L.F., 2009. Huntingtin as an essential integrator of intracellular vesicular trafficking. Trends Cell Biol. https://doi.org/10.1016/j.tcb.2009.01.005

Cha, M.Y., Chen, H., Chan, D., 2018. Removal of the Mitochondrial Fission

Factor Mff Exacerbates Neuronal Loss and Neurological Phenotypes in a Huntington's Disease Mouse Model. PLoS Curr. https://doi.org/10.1371/currents.hd.a4e15b80c4915c828d39754942c6631f

Chan, H.Y.E., Warrick, J.M., Andriola, I., Merry, D., Bonini, N.M., 2002. Aggregated polyglutamine peptides delivered to nuclei are toxic to mammalian cells. Hum. Mol. Genet. https://doi.org/10.1093/hmg/11.23.2905

Chen, C.-M., Wu, Y.-R., Cheng, M.-L., Liu, J.-L., Lee, Y.-M., Lee, P.-W., Soong, B.-W., Chiu, D.T.-Y., 2007. Increased oxidative damage and mitochondrial abnormalities in the peripheral blood of Huntington's disease patients. Biochem. Biophys. Res. Commun. 359, 335–40. https://doi.org/10.1016/j.bbrc.2007.05.093

Chen, N., Luo, T., Wellington, C., Metzler, M., McCutcheon, K., Hayden, M.R., Raymond, L.A., 1999. Subtype-specific enhancement of NMDA receptor currents by mutant huntingtin. J. Neurochem. https://doi.org/10.1046/j.1471-4159.1999.0721890.x

Chen, P., Li, F., Xu, Z., Li, Z., Yi, X.P., 2013. Expression and distribution of Src in the nucleus of myocytes in cardiac hypertrophy. Int. J. Mol. Med. 32, 165–173. https://doi.org/10.3892/ijmm.2013.1382

Cheng, S.-E., Lee, I.-T., Lin, C.-C., Kou, Y.R., Yang, C.-M., 2010. Cigarette smoke particle-phase extract induces HO-1 expression in human tracheal smooth muscle cells: role of the c-Src/NADPH oxidase/MAPK/Nrf2 signaling pathway. Free Radic. Biol. Med. 48, 1410–1422. https://doi.org/10.1016/j.freeradbiomed.2010.02.026

Chojnacka, K., Mruk, D.D., 2015. The Src non-receptor tyrosine kinase paradigm: New insights into mammalian Sertoli cell biology. Mol. Cell. Endocrinol. 415, 133–142. https://doi.org/10.1016/j.mce.2015.08.012

Choo, Y.S., 2004. Mutant huntingtin directly increases susceptibility of mitochondria to the calcium-induced permeability transition and cytochrome c release. Hum. Mol. Genet. 13, 1407–1420.

https://doi.org/10.1093/hmg/ddh162

Chowdhry, S., Zhang, Y., McMahon, M., Sutherland, C., Cuadrado, A., Hayes, J.D., 2013. Nrf2 is controlled by two distinct β-TrCP recognition motifs in its Neh6 domain, one of which can be modulated by GSK-3 activity. Oncogene 32, 3765–81. https://doi.org/10.1038/onc.2012.388

Cisbani, G., Cicchetti, F., 2012. An in vitro perspective on the molecular mechanisms underlying mutant huntingtin protein toxicity. Cell Death Dis. https://doi.org/10.1038/cddis.2012.121

Colin, E., Zala, D., Liot, G., Rangone, H., Borrell-Pagès, M., Li, X.J., Saudou, F., Humbert, S., 2008. Huntingtin phosphorylation acts as a molecular switch for anterograde/retrograde transport in neurons. EMBO J. https://doi.org/10.1038/emboj.2008.133

Cooper, J.K., Schilling, G., Peters, M.F., Herring, W.J., Sharp, A.H., Kaminsky, Z., Masone, J., Khan, F.A., Delanoy, M., Borchelt, D.R., Dawson, V.L., Dawson, T.M., Ross, C.A., 1998. Truncated N-terminal fragments of huntingtin with expanded glutamine repeats form nuclear and cytoplasmic aggregates in cell culture. Hum. Mol. Genet. https://doi.org/10.1093/hmg/7.5.783

Cortes, C.J., La Spada, A.R., 2014. The many faces of autophagy dysfunction in Huntington's disease: From mechanism to therapy. Drug Discov. Today. https://doi.org/10.1016/j.drudis.2014.02.014

Costa, V., Giacomello, M., Hudec, R., Lopreiato, R., Ermak, G., Lim, D., Malorni, W., Davies, K.J.A., Carafoli, E., Scorrano, L., 2010. Mitochondrial fission and cristae disruption increase the response of cell models of Huntington's disease to apoptotic stimuli. EMBO Mol. Med. https://doi.org/10.1002/emmm.201000102

Cui, L., Jeong, H., Borovecki, F., Parkhurst, C.N., Tanese, N., Krainc, D., 2006. Transcriptional Repression of PGC-1α by Mutant Huntingtin Leads to Mitochondrial Dysfunction and Neurodegeneration. Cell. https://doi.org/10.1016/j.cell.2006.09.015

Culbreth, M., Zhang, Z., Aschner, M., 2017. Methylmercury augments Nrf2 activity by downregulation of the Src family kinase Fyn. Neurotoxicology 62, 200–206. https://doi.org/10.1016/j.neuro.2017.07.028

Culjkovic, B., Stojkovic, O., Vojvodic, N., Svetel, M., Rakic, L., Romac, S., Kostic, V., 1999. Correlation between triplet repeat expansion and computed tomography measures of caudate nuclei atrophy in Huntington's disease. J. Neurol. https://doi.org/10.1007/s004150050518

Cull-Candy, S., Brickley, S., Farrant, M., 2001. NMDA receptor subunits: diversity, development and disease. Curr Opin Neurobiol 11, 327–35. https://doi.org/S0959-4388(00)00215-4 [pii]

Davies, S.W., Turmaine, M., Cozens, B.A., DiFiglia, M., Sharp, A.H., Ross, C.A., Scherzinger, E., Wanker, E.E., Mangiarini, L., Bates, G.P., 1997. Formation of Neuronal Intranuclear Inclusions Underlies the Neurological Dysfunction in Mice Transgenic for the HD Mutation. Cell 90, 537–548. https://doi.org/10.1016/S0092-8674(00)80513-9

De La Monte, S.M., Vonsattel, J.P., Richardson, E.P., 1988. Morphometric demonstration of atrophic changes in the ceRebral cortex, white matter, and neostriatum in huntington's disease. J. Neuropathol. Exp. Neurol. https://doi.org/10.1097/00005072-198809000-00003

Deas, E., Plun-Favreau, H., Gandhi, S., Desmond, H., Kjaer, S., Loh, S.H.Y., Renton, A.E.M., Harvey, R.J., Whitworth, A.J., Martins, L.M., Abramov, A.Y., Wood, N.W., 2011. PINK1 cleavage at position A103 by the mitochondrial protease PARL. Hum. Mol. Genet. https://doi.org/10.1093/hmg/ddq526

Deng, Y.P., Wong, T., Bricker-Anthony, C., Deng, B., Reiner, A., 2013. Loss of corticostriatal and thalamostriatal synaptic terminals precedes striatal projection neuron pathology in heterozygous Q140 Huntington's disease mice. Neurobiol. Dis. https://doi.org/10.1016/j.nbd.2013.08.009

Deretic, V., Saitoh, T., Akira, S., 2013. Autophagy in infection, inflammation and immunity. Nat. Rev. Immunol. https://doi.org/10.1038/nri3532

Díaz-Hernández, M., Hernández, F., Martín-Aparicio, E., Gómez-Ramos, P., Morán, M.A., Castaño, J.G., Ferrer, I., Avila, J., Lucas, J.J., 2003. Neuronal Induction of the Immunoproteasome in Huntington's Disease. J. Neurosci. https://doi.org/10.1523/jneurosci.23-37-11653.2003

DiFiglia, M., Sapp, E., Chase, K., Schwarz, C., Meloni, A., Young, C., Martin, E., Vonsattel, J.P., Carraway, R., Reeves, S.A., Boyce, F.M., Aronin, N., 1995. Huntingtin is a cytoplasmic protein associated with vesicles in human and rat brain neurons. Neuron. https://doi.org/10.1016/0896-6273(95)90346-1

DiFiglia, M., Sapp, E., Chase, K.O., Davies, S.W., Bates, G.P., Vonsattel, J.P., Aronin, N., 1997. Aggregation of Huntingtin in Neuronal Intranuclear Inclusions and Dystrophic Neurites in Brain. Science (80-.). 277, 1990–1993. https://doi.org/10.1126/science.277.5334.1990

Ding, W.X., Ni, H.M., Li, M., Liao, Y., Chen, X., Stolz, D.B., Dorn, G.W., Yin, X.M., 2010. Nix is critical to two distinct phases of mitophagy, reactive oxygen species-mediated autophagy induction and Parkin-ubiquitin-p62-mediated mitochondrial priming. J. Biol. Chem. https://doi.org/10.1074/jbc.M110.119537

Doi, H., Mitsui, K., Kurosawa, M., MacHida, Y., Kuroiwa, Y., Nukina, N., 2004. Identification of ubiquitin-interacting proteins in purified polyglutamine aggregates. FEBS Lett. https://doi.org/10.1016/j.febslet.2004.06.077

Dooley, H.C., Razi, M., Polson, H.E.J., Girardin, S.E., Wilson, M.I., Tooze, S.A., 2014. WIPI2 Links LC3 Conjugation with PI3P, Autophagosome Formation, and Pathogen Clearance by Recruiting Atg12-5-16L1. Mol. Cell. https://doi.org/10.1016/j.molcel.2014.05.021

Droge, W., 2002. Free Radicals in the Physiological Control of Cell Function. Physiol Rev 82, 47–95.

Du, C.-P., Gao, J., Tai, J.-M., Liu, Y., Qi, J., Wang, W., Hou, X.-Y., 2009. Increased tyrosine phosphorylation of PSD-95 by Src family kinases after brain ischaemia. Biochem. J. 417, 277–85. https://doi.org/10.1042/BJ20080004

Dubé, L., Smith, A.D., Bolam, J.P., 1988. Identification of synaptic terminals of thalamic or cortical origin in contact with distinct medium-size spiny neurons in the rat neostriatum. J. Comp. Neurol. https://doi.org/10.1002/cne.902670402

Duyao, M.P., Auerbach, A.B., Ryan, A., Persichetti, F., Barnes, G.T., McNeil, S.M., Ge, P., Vonsattel, J.P., Gusella, J.F., Joyner, A.L., MacDonald, M.E., 1995. Inactivation of the mouse huntington's disease gene homolog Hdh. Science (80-.). https://doi.org/10.1126/science.7618107

Egan, D.F., Shackelford, D.B., Mihaylova, M.M., Gelino, S., Kohnz, R.A., Mair, W., Vasquez, D.S., Joshi, A., Gwinn, D.M., Taylor, R., Asara, J.M., Fitzpatrick, J., Dillin, A., Viollet, B., Kundu, M., Hansen, M., Shaw, R.J., 2011. Phosphorylation of ULK1 (hATG1) by AMP-activated protein kinase connects energy sensing to mitophagy. Science (80-.). https://doi.org/10.1126/science.1196371

Ehinger, Y., Morisot, N., Phamluong, K., Sakhai, S.A., Soneja, D., Adrover, M.F., Alvarez, V.A., Ron, D., 2021. cAMP-Fyn signaling in the dorsomedial striatum direct pathway drives excessive alcohol use. Neuropsychopharmacology. https://doi.org/10.1038/s41386-020-0712-1

Ellrichmann, G., Petrasch-Parwez, E., Lee, D.H., Reick, C., Arning, L., Saft, C., Gold, R., Linker, R.A., 2011. Efficacy of fumaric acid esters in the R6/2 and YAC128 models of huntington's disease. PLoS One 6. https://doi.org/10.1371/journal.pone.0016172

Espada, J., Martín-Pérez, J., 2017. An Update on Src Family of Nonreceptor Tyrosine Kinases Biology, in: International Review of Cell and Molecular Biology. pp. 83–122. https://doi.org/10.1016/bs.ircmb.2016.09.009

Esteban-Martínez, L., Boya, P., 2018. BNIP3L/NIX-dependent mitophagy regulates cell differentiation via metabolic reprogramming. Autophagy. https://doi.org/10.1080/15548627.2017.1332567

Estrada-Sánchez, A.M., Rebec, G. V., 2012. Corticostriatal dysfunction and glutamate transporter 1 (GLT1) in Huntington's disease: Interactions

between neurons and astrocytes. Basal Ganglia. https://doi.org/10.1016/j.baga.2012.04.029

Etcheberrigaray, R., Tan, M., Dewachter, I., Kuiperi, C., der Auwera, I. Van, Wera, S., Qiao, L., Bank, B., Nelson, T.J., Kozikowski, A.P., Leuven, F. Van, Alkon, D.L., 2004. Therapeutic effects of PKC activators in Alzheimer's disease transgenic mice. Proc. Natl. Acad. Sci. U. S. A. 101, 11141–11146. https://doi.org/10.1073/pnas.0403921101

Evans, S.J.W., Douglas, I., Rawlins, M.D., Wexler, N.S., Tabrizi, S.J., Smeeth, L., 2013. Prevalence of adult Huntington's disease in the UK based on diagnoses recorded in general practice records. J. Neurol. Neurosurg. Psychiatry 84, 1156–1160. https://doi.org/10.1136/jnnp-2012-304636

Faber, P.W., Barnes, G.T., Srinidhi, J., Chen, J., Gusella, J.F., MacDonald, M.E., 1998. Huntingtin interacts with a family of WW domain proteins. Hum. Mol. Genet. https://doi.org/10.1093/hmg/7.9.1463

Faideau, M., Kim, J., Cormier, K., Gilmore, R., Welch, M., Auregan, G., Dufour, N., Guillermier, M., Brouillet, E., Hantraye, P., DéGlon, N., Ferrante, R.J., Bonvento, G., 2010. In vivo expression of polyglutamine-expanded huntingtin by mouse striatal astrocytes impairs glutamate transport: A correlation with Huntington's disease subjects. Hum. Mol. Genet. https://doi.org/10.1093/hmg/ddq212

Fan, J., Cowan, C.M., Zhang, L.Y.J., Hayden, M.R., Raymond, L.A., 2009. Interaction of Postsynaptic Density Protein-95 with NMDA Receptors Influences Excitotoxicity in the Yeast Artificial Chromosome Mouse Model of Huntington's Disease. J. Neurosci. 29, 10928–10938. https://doi.org/10.1523/JNEUROSCI.2491-09.2009

Fan, M.M.Y., Fernandes, H.B., Zhang, L.Y.J., Hayden, M.R., Raymond, L.A., 2007. Altered NMDA Receptor Trafficking in a Yeast Artificial Chromosome Transgenic Mouse Model of Huntington's Disease. J. Neurosci. https://doi.org/10.1523/jneurosci.4356-06.2007

Fão, L., Coelho, P., Duarte, L., Vilaça, R., Hayden, M.R., Mota, S.I., Rego, A.C.,

2022. Restoration of c-Src/Fyn Proteins Rescues Mitochondrial Dysfunction in Huntington's Disease. Antioxid. Redox Signal. 1–21. https://doi.org/10.1089/ars.2022.0001

Fão, L., Mota, S.I., Rego, A.C., 2019a. Shaping the Nrf2-ARE-related pathways in Alzheimer's and Parkinson's diseases. Ageing Res. Rev. 54, 100942. https://doi.org/10.1016/j.arr.2019.100942

Fão, L., Mota, S.I., Rego, A.C., 2019b. c-Src regulates Nrf2 activity through PKCδ after oxidant stimulus. Biochim. Biophys. Acta - Mol. Cell Res. 1866, 686–698. https://doi.org/S0167488918302428

Fão, L., Rego, A.C., 2021. Mitochondrial and Redox-Based Therapeutic Strategies in Huntington's Disease. Antioxid. Redox Signal. 34, 650–673. https://doi.org/10.1089/ars.2019.8004

Farrer, L.A., Cupples, L.A., Wiater, P., Conneally, P.M., Gusella, J.F., Myers, R.H., 1993. The normal Huntington disease (HD) allele, or a closely linked gene, influences age at onset of HD. Am. J. Hum. Genet.

Feng, J., Lucchinetti, E., Enkavi, G., Wang, Y., Gehrig, P., Roschitzki, B., Schaub, M.C., Tajkhorshid, E., Zaugg, K., Zaugg, M., 2010. Tyrosine phosphorylation by Src within the cavity of the adenine nucleotide translocase 1 regulates ADP/ATP exchange in mitochondria. Am. J. Physiol. Cell Physiol. 298, C740–C748. https://doi.org/10.1152/ajpcell.00310.2009

Ferreira-Pinto, M.J., Ruder, L., Capelli, P., Arber, S., 2018. Connecting Circuits for Supraspinal Control of Locomotion. Neuron 100, 361–374. https://doi.org/10.1016/j.neuron.2018.09.015

Ferreira, I.L., Carmo, C., Naia, L., I. Mota, S., Cristina Rego, A., 2018. Assessing Mitochondrial Function in In Vitro and Ex Vivo Models of Huntington's Disease, in: Methods in Molecular Biology. pp. 415–442. https://doi.org/10.1007/978-1-4939-7825-0_19

Ferreira, I.L., Nascimento, M. V., Ribeiro, M., Almeida, S., Cardoso, S.M.,

Grazina, M., Pratas, J., Santos, M.J., Januário, C., Oliveira, C.R., Rego, A.C., 2010a. Mitochondrial-dependent apoptosis in Huntington's disease human cybrids. Exp. Neurol. 222, 243–255. https://doi.org/10.1016/j.expneurol.2010.01.002

Ferreira, I.L., Nascimento, M. V., Ribeiro, M., Almeida, S., Cardoso, S.M., Grazina, M., Pratas, J., Santos, M.J., Januário, C., Oliveira, C.R., Rego, A.C., 2010b. Mitochondrial-dependent apoptosis in Huntington's disease human cybrids. Exp. Neurol. 222, 243–255. https://doi.org/10.1016/j.expneurol.2010.01.002

Filimonenko, M., Isakson, P., Finley, K.D., Anderson, M., Jeong, H., Melia, T.J., Bartlett, B.J., Myers, K.M., Birkeland, H.C.G., Lamark, T., Krainc, D., Brech, A., Stenmark, H., Simonsen, A., Yamamoto, A., 2010. The Selective Macroautophagic Degradation of Aggregated Proteins Requires the PI3P-Binding Protein Alfy. Mol. Cell. https://doi.org/10.1016/j.molcel.2010.04.007

Finkbeiner, S., 2011. Huntington's Disease. Cold Spring Harb. Perspect. Biol. 3, a007476–a007476. https://doi.org/10.1101/cshperspect.a007476

Finley, D., 2009. Recognition and processing of ubiquitin-protein conjugates by the proteasome. Annu. Rev. Biochem. 78, 477–513. https://doi.org/10.1146/annurev.biochem.78.081507.101607

Flint Beal, M., Matson, W.R., Storey, E., Milbury, P., Ryan, E.A., Ogawa, T., Bird, E.D., 1992. Kynurenic acid concentrations are reduced in Huntington's disease cerebral cortex. J. Neurol. Sci. https://doi.org/10.1016/0022-510X(92)90191-M

Fox, J.H., Barber, D.S., Singh, B., Zucker, B., Swindell, M.K., Norflus, F., Buzescu, R., Chopra, R., Ferrante, R.J., Kazantsev, A., Hersch, S.M., 2004. Cystamine increases L-cysteine levels in Huntington's disease transgenic mouse brain and in a PC12 model of polyglutamine aggregation. J. Neurochem. https://doi.org/10.1111/j.1471-4159.2004.02726.x

Franco-Iborra, S., Plaza-Zabala, A., Montpeyo, M., Sebastian, D., Vila, M.,

Martinez-Vicente, M., 2020. Mutant HTT (huntingtin) impairs mitophagy in a cellular model of Huntington disease. Autophagy. https://doi.org/10.1080/15548627.2020.1728096

Fujita, N., Hayashi-Nishino, M., Fukumoto, H., Omori, H., Yamamoto, A., Noda, T., Yoshimori, T., 2008a. An Atg4B mutant hampers the lipidation of LC3 paralogues and causes defects in autophagosome closure. Mol. Biol. Cell. https://doi.org/10.1091/mbc.E08-03-0312

Fujita, N., Itoh, T., Omori, H., Fukuda, M., Noda, T., Yoshimori, T., 2008b. The Atg16L complex specifies the site of LC3 lipidation for membrane biogenesis in autophagy. Mol. Biol. Cell. https://doi.org/10.1091/mbc.E07-12-1257

Fukutomi, T., Takagi, K., Mizushima, T., Ohuchi, N., Yamamoto, M., 2014. Kinetic, Thermodynamic, and Structural Characterizations of the Association between Nrf2-DLGex Degron and Keap1. Mol. Cell. Biol. 34, 832–846. https://doi.org/10.1128/MCB.01191-13

Gadoth, N., and Goebel, H.H., 2011. Oxidative Stress and Free Radical Damage in Neurology, Oxidative Stress and Free Radical Damage in Neurology. Humana Press, Totowa, NJ. https://doi.org/10.1007/978-1-60327-514-9

Gan, L., Johnson, J.A., 2014. Oxidative damage and the Nrf2-ARE pathway in neurodegenerative diseases. Biochim. Biophys. Acta - Mol. Basis Dis. 1842, 1208–1218. https://doi.org/10.1016/j.bbadis.2013.12.011

Gao, Y., Chu, S.-F., Li, J.-P., Zuo, W., Wen, Z.-L., He, W.-B., Yan, J.-Q., Chen, N.-H., 2015. Do glial cells play an anti-oxidative role in Huntington's disease? Free Radic. Res. https://doi.org/10.3109/10715762.2014.936432

Garrido, J.L., Godoy, J.A., Alvarez, A., Bronfman, M., Inestrosa, N.C., 2002. Protein kinase C inhibits amyloid beta peptide neurotoxicity by acting on members of the Wnt pathway. FASEB J. 16, 1982–1984. https://doi.org/10.1096/fj.02-0327fje

Gemba, H., Kyuhou, S. ichi, Matsuzaki, R. ichi, Amino, Y., 1999. Oxidative damage to mitochondrial DNA in Huntington's disease parietal cortex. Neurosci. Lett. https://doi.org/10.1016/S0304-3940(99)00578-9

Gil, J.M., Rego, a C., 2008. Mechanisms of neurodegeneration in Huntington's disease. Eur.J.Neurosci. 27, 2803–2820. https://doi.org/10.1111/j.1460-9568.2008.06310.x

Gingrich, J.R., Pelkey, K.A., Fam, S.R., Huang, Y., Petralia, R.S., Wenthold, R.J., Salter, M.W., 2004. Unique domain anchoring of Src to synaptic NMDA receptors via the mitochondrial protein NADH dehydrogenase subunit 2. Proc. Natl. Acad. Sci. 101, 6237–6242. https://doi.org/10.1073/pnas.0401413101

Giralt, A., Brito, V., Chevy, Q., Simonnet, C., Otsu, Y., Cifuentes-Díaz, C., de Pins, B., Coura, R., Alberch, J., Ginés, S., Poncer, J.-C., Girault, J.-A., 2017. Pyk2 modulates hippocampal excitatory synapses and contributes to cognitive deficits in a Huntington's disease model. Nat. Commun. 8, 15592. https://doi.org/10.1038/ncomms15592

Gladding, C.M., Sepers, M.D., Xu, J., Zhang, L.Y.J., Milnerwood, A.J., Lombroso, P.J., Raymond, L.A., 2012. Calpain and STriatal-Enriched protein tyrosine Phosphatase (STEP) activation contribute to extrasynaptic NMDA receptor localization in a huntington's disease mouse model. Hum. Mol. Genet. https://doi.org/10.1093/hmg/dds154

Goebel-Goody, S.M., Davies, K.D., Alvestad Linger, R.M., Freund, R.K., Browning, M.D., 2009. Phospho-regulation of synaptic and extrasynaptic N-methyl-d-aspartate receptors in adult hippocampal slices. Neuroscience 158, 1446–1459. https://doi.org/10.1016/j.neuroscience.2008.11.006

Goffredo, D., Rigamonti, D., Tartari, M., De Micheli, A., Verderio, C., Matteoli, M., Zuccato, C., Cattaneo, E., 2002. Calcium-dependent cleavage of endogenous wild-type huntingtin in primary cortical neurons. J. Biol. Chem. https://doi.org/10.1074/jbc.C200353200

Goswami, A., Dikshit, P., Mishra, A., Mulherkar, S., Nukina, N., Jana, N.R.,

2006. Oxidative stress promotes mutant huntingtin aggregation and mutant huntingtin-dependent cell death by mimicking proteasomal malfunction. Biochem. Biophys. Res. Commun. 342, 184–190. https://doi.org/10.1016/j.bbrc.2006.01.136

Grant, C.M., 2011. Regulation of translation by hydrogen peroxide. Antioxid. Redox Signal. 15, 191–203. https://doi.org/10.1089/ars.2010.3699

Grant, S., Stein, P., Soriano, P., Kandel, E., Karl, K., O'Dell, T., 2006. Impaired long-term potentiation, spatial learning, and hippocampal development in fyn mutant mice. Science (80-.). 258, 1903–1910. https://doi.org/10.1126/science.1361685

Grant, S.G.N., Silva, A.J., 1994. Targeting learning. Trends Neurosci. https://doi.org/10.1016/0166-2236(94)90077-9

Graveland, G.A., Williams, R.S., Difiglia, M., 1985. Evidence for degenerative and regenerative changes in neostriatal spiny neurons in Huntington's disease. Science (80-.). https://doi.org/10.1126/science.3155875

Gray, M., Shirasaki, D.I., Cepeda, C., Andre, V.M., Wilburn, B., Lu, X.-H., Tao, J., Yamazaki, I., Li, S.-H., Sun, Y.E., Li, X.-J., Levine, M.S., Yang, X.W., 2008. Full-Length Human Mutant Huntingtin with a Stable Polyglutamine Repeat Can Elicit Progressive and Selective Neuropathogenesis in BACHD Mice. J. Neurosci. 28, 6182–6195. https://doi.org/10.1523/JNEUROSCI.0857-08.2008

Gschwendt, M., Müller, H.J., Kielbassa, K., Zang, R., Kittstein, W., Rincke, G., Marks, F., 1994. Rottlerin, a novel protein kinase inhibitor. Biochem. Biophys. Res. Commun. https://doi.org/10.1006/bbrc.1994.1199

Gu, M., Gash, M.T., Mann, V.M., Javoy-Agid, F., Cooper, J.M., Schapira, A.H. V, 1996. Mitochondrial defect in Huntington's disease caudate nucleus. Ann. Neurol. 39, 385–389. https://doi.org/10.1002/ana.410390317

Gutekunst, C.A., Li, S.H., Yi, H., Mulroy, J.S., Kuemmerle, S., Jones, R., Rye, D., Ferrante, R.J., Hersch, S.M., Li, X.J., 1999. Nuclear and neuropil

aggregates in Huntington's disease: Relationship to neuropathology. J. Neurosci. https://doi.org/10.1523/jneurosci.19-07-02522.1999

Halliday, G.M., McRitchie, D.A., Macdonald, V., Double, K.L., Trent, R.J., McCusker, E., 1998. Regional Specificity of Brain Atrophy in Huntington's Disease. Exp. Neurol. 154, 663–672. https://doi.org/10.1006/exnr.1998.6919

Hamasaki, M., Furuta, N., Matsuda, A., Nezu, A., Yamamoto, A., Fujita, N., Oomori, H., Noda, T., Haraguchi, T., Hiraoka, Y., Amano, A., Yoshimori, T., 2013. Autophagosomes form at ER-mitochondria contact sites. Nature. https://doi.org/10.1038/nature11910

Hamilton, J.M., 2004. Rate and correlates of weight change in Huntington's disease. J. Neurol. Neurosurg. Psychiatry 75, 209–212. https://doi.org/10.1136/jnnp.2003.017822

Han, Y.-S., Zheng, W.-H., Bastianetto, S., Chabot, J.-G., Quirion, R., 2004. Neuroprotective effects of resveratrol against beta-amyloid-induced neurotoxicity in rat hippocampal neurons: involvement of protein kinase C. Br. J. Pharmacol. 141, 997–1005. https://doi.org/10.1038/sj.bjp.0705688

Hands, S., Sajjad, M.U., Newton, M.J., Wyttenbach, A., 2011. In vitro and in vivo aggregation of a fragment of huntingtin protein directly causes free radical production. J. Biol. Chem. 286, 44512–44520. https://doi.org/10.1074/jbc.M111.307587

Hanke, J.H., Gardner, J.P., Dow, R.L., Changelian, P.S., Brissette, W.H., Weringer, E.J., Pollok, B.A., Connelly, P.A., 1996. Discovery of a novel, potent, and Src family-selective tyrosine kinase inhibitor: Study of Lck- and FynT-dependent T cell activation. J. Biol. Chem. https://doi.org/10.1074/jbc.271.2.695

Hansen, H.H., Briem, T., Dzietko, M., Sifringer, M., Voss, A., Rzeski, W., Zdzisinska, B., Thor, F., Heumann, R., Stepulak, A., Bittigau, P., Ikonomidou, C., 2004. Mechanisms leading to disseminated apoptosis following NMDA receptor blockade in the developing rat brain. Neurobiol.

Dis. https://doi.org/10.1016/j.nbd.2004.03.013

Harding, R.J., Tong, Y.F., 2018. Proteostasis in Huntington's disease: Disease mechanisms and therapeutic opportunities. Acta Pharmacol. Sin. https://doi.org/10.1038/aps.2018.11

Hardingham, G.E., Fukunaga, Y., Bading, H., 2002. Extrasynaptic NMDARs oppose synaptic NMDARs by triggering CREB shut-off and cell death pathways. Nat. Neurosci. https://doi.org/10.1038/nn835

Harris, K.F., Shoji, I., Cooper, E.M., Kumar, S., Oda, H., Howley, P.M., 1999. Ubiquitin-mediated degradation of active Src tyrosine kinase. Proc. Natl. Acad. Sci. 96, 13738–13743. https://doi.org/10.1073/pnas.96.24.13738

Harris, K.L., Armstrong, M., Swain, R., Erzinclioglu, S., Das, T., Burgess, N., Barker, R.A., Mason, S.L., 2019. Huntington's disease patients display progressive deficits in hippocampal-dependent cognition during a task of spatial memory. Cortex 119, 417–427. https://doi.org/10.1016/j.cortex.2019.07.014

Hassel, B., Tessler, S., Faull, R.L.M., Emson, P.C., 2008. Glutamate uptake is reduced in prefrontal cortex in Huntington's disease. Neurochem. Res. https://doi.org/10.1007/s11064-007-9463-1

Hattori, K., Uchino, S., Isosaka, T., Maekawa, M., Iyo, M., Sato, T., Kohsaka, S., Yagi, T., Yuasa, S., 2006. Fyn is required for haloperidol-induced catalepsy in mice. J. Biol. Chem. https://doi.org/10.1074/jbc.M511608200

Hayashi, T., Su, T.P., 2007. Sigma-1 Receptor Chaperones at the ER-Mitochondrion Interface Regulate Ca2+ Signaling and Cell Survival. Cell. https://doi.org/10.1016/j.cell.2007.08.036

Hebert-Chatelain, E., 2013. Src kinases are important regulators of mitochondrial functions. Int. J. Biochem. Cell Biol. https://doi.org/10.1016/j.biocel.2012.08.014

Hebert-Chatelain, E., Jose, C., Gutierrez Cortes, N., Dupuy, J.-W., Rocher, C.,

Dachary-Prigent, J., Letellier, T., 2012. Preservation of NADH ubiquinone-oxidoreductase activity by Src kinase-mediated phosphorylation of NDUFB10. Biochim. Biophys. Acta - Bioenerg. 1817, 718–725. https://doi.org/10.1016/j.bbabio.2012.01.014

Hébert Chatelain, E., Dupuy, J.-W., Letellier, T., Dachary-Prigent, J., 2011. Functional impact of PTP1B-mediated Src regulation on oxidative phosphorylation in rat brain mitochondria. Cell. Mol. Life Sci. 68, 2603–13. https://doi.org/10.1007/s00018-010-0573-6

Heinsen, H., Strik, M., Bauer, M., Luther, K., Ulmar, G., Gangnus, D., Jungkunz, G., Eisenmengers, W., Götz, M., 1994. Cortical and striatal neurone number in Huntington's disease. Acta Neuropathol. https://doi.org/10.1007/BF00310376

Heng, M.Y., Detloff, P.J., Albin, R.L., 2008. Rodent genetic models of Huntington disease. Neurobiol. Dis. https://doi.org/10.1016/j.nbd.2008.06.005

Heng, M.Y., Detloff, P.J., Wang, P.L., Tsien, J.Z., Albin, R.L., 2009. In Vivo Evidence for NMDA Receptor-Mediated Excitotoxicity in a Murine Genetic Model of Huntington Disease. J. Neurosci. https://doi.org/10.1523/jneurosci.5599-08.2009

Heng, M.Y., Tallaksen-Greene, S.J., Detloff, P.J., Albin, R.L., 2007. Longitudinal evaluation of the Hdh(CAG)150 knock-in murine model of Huntington's disease. J. Neurosci. https://doi.org/10.1523/JNEUROSCI.1830-07.2007

Herbert, A.D., Carr, A.M., Hoffmann, E., 2014. FindFoci: A Focus Detection Algorithm with Automated Parameter Training That Closely Matches Human Assignments, Reduces Human Inconsistencies and Increases Speed of Analysis. PLoS One 9, e114749. https://doi.org/10.1371/journal.pone.0114749

Hering, T., Birth, N., Taanman, J.W., Orth, M., 2015. Selective striatal mtDNA depletion in end-stage Huntington's disease R6/2 mice. Exp. Neurol. https://doi.org/10.1016/j.expneurol.2015.02.004

Hilditch-Maguire, P., Trettel, F., Passani, L.A., Auerbach, A., Persichetti, F., MacDonald, M.E., 2000. Huntingtin: An iron-regulated protein essential for normal nuclear and perinuclear organelles. Hum. Mol. Genet. https://doi.org/10.1093/hmg/9.19.2789

Hirotsu, Y., Katsuoka, F., Funayama, R., Nagashima, T., Nishida, Y., Nakayama, K., Douglas Engel, J., Yamamoto, M., 2012. Nrf2-MafG heterodimers contribute globally to antioxidant and metabolic networks. Nucleic Acids Res. 40, 10228–10239. https://doi.org/10.1093/nar/gks827

Hodges, A., Hughes, G., Brooks, S., Elliston, L., Holmans, P., Dunnett, S.B., Jones, L., 2008. Brain gene expression correlates with changes in behavior in the R6/1 mouse model of Huntington's disease. Genes, Brain Behav. https://doi.org/10.1111/j.1601-183X.2007.00350.x

Hodgson, J.G., Agopyan, N., Gutekunst, C.A., Leavitt, B.R., Lepiane, F., Singaraja, R., Smith, D.J., Bissada, N., McCutcheon, K., Nasir, J., Jamot, L., Xiao-Jiang, L., Stevens, M.E., Rosemond, E., Roder, J.C., Phillips, A.G., Rubin, E.M., Hersch, S.M., Hayden, M.R., 1999. A YAC mouse model for Huntington's disease with full-length mutant huntingtin, cytoplasmic toxicity, and selective striatal neurodegeneration. Neuron. https://doi.org/10.1016/S0896-6273(00)80764-3

Hosokawa, N., Hara, T., Kaizuka, T., Kishi, C., Takamura, A., Miura, Y., Iemura, S.I., Natsume, T., Takehana, K., Yamada, N., Guan, J.L., Oshiro, N., Mizushima, N., 2009. Nutrient-dependent mTORCl association with the ULK1-Atg13-FIP200 complex required for autophagy. Mol. Biol. Cell. https://doi.org/10.1091/mbc.E08-12-1248

Huang, H.-C., Nguyen, T., Pickett, C.B., 2002. Phosphorylation of Nrf2 at Ser-40 by Protein Kinase C Regulates Antioxidant Response Element-mediated Transcription. J. Biol. Chem. 277, 42769–42774. https://doi.org/10.1074/jbc.M206911200

Huang, K., Yanai, A., Kang, R., Arstikaitis, P., Singaraja, R.R., Metzler, M., Mullard, A., Haigh, B., Gauthier-Campbell, C., Gutekunst, C.A., Hayden,

M.R., El-Husseini, A., 2004. Huntingtin-interacting protein HIP14 is a palmitoyl transferase involved in palmitoylation and trafficking of multiple neuronal proteins. Neuron. https://doi.org/10.1016/j.neuron.2004.11.027

Huang, N., Erie, C., Lu, M.L., Wei, J., 2018. Aberrant subcellular localization of SQSTM1/p62 contributes to increased vulnerability to proteotoxic stress recovery in Huntington's disease. Mol. Cell. Neurosci. https://doi.org/10.1016/j.mcn.2017.12.005

Hubbs, A.F., Benkovic, S.A., Miller, D.B., O'Callaghan, J.P., Battelli, L., Schwegler-Berry, D., Ma, Q., 2007. Vacuolar leukoencephalopathy with widespread astrogliosis in mice lacking transcription factor Nrf2. Am. J. Pathol. 170, 2068–76. https://doi.org/10.2353/ajpath.2007.060898

Humbert, S., Bryson, E.A., Cordelières, F.P., Connors, N.C., Datta, S.R., Finkbeiner, S., Greenberg, M.E., Saudou, F., 2002. The IGF-1/Akt pathway is neuroprotective in Huntington's disease and involves huntingtin phosphorylation by Akt. Dev. Cell. https://doi.org/10.1016/S1534-5807(02)00188-0

Hyrskyluoto, A., Pulli, I., Törnqvist, K., Huu Ho, T., Korhonen, L., Lindholm, D., 2013. Sigma-1 receptor agonist PRE084 is protective against mutant huntingtin-induced cell degeneration: Involvement of calpastatin and the NF-κB pathway. Cell Death Dis. https://doi.org/10.1038/cddis.2013.170

Imlay, J.A., 2008. Cellular Defenses against Superoxide and Hydrogen Peroxide. Annu. Rev. Biochem. https://doi.org/10.1146/annurev.biochem.77.061606.161055

Irtegun, S., Wood, R.J., Ormsby, A.R., Mulhern, T.D., Hatters, D.M., 2013. Tyrosine 416 Is Phosphorylated in the Closed, Repressed Conformation of c-Src. PLoS One 8, e71035. https://doi.org/10.1371/journal.pone.0071035

Isagawa, T., Mukai, H., Oishi, K., Taniguchi, T., Hasegawa, H., Kawamata, T., Tanaka, C., Ono, Y., 2000. Dual effects of PKNalpha and protein kinase C on phosphorylation of tau protein by glycogen synthase kinase-3beta. Biochem. Biophys. Res. Commun. 273, 209–12.

https://doi.org/10.1006/bbrc.2000.2926

Isakson, P., Holland, P., Simonsen, A., 2013. The role of ALFY in selective autophagy. Cell Death Differ. https://doi.org/10.1038/cdd.2012.66

Ismailoglu, I., Chen, Q., Popowski, M., Yang, L., Gross, S.S., Brivanlou, A.H., 2014. Huntingtin protein is essential for mitochondrial metabolism, bioenergetics and structure in murine embryonic stem cells. Dev. Biol. https://doi.org/10.1016/j.ydbio.2014.04.005

Isosaka, T., Hattori, K., Kida, S., Kohno, T., Nakazawa, T., Yamamoto, T., Yagi, T., Yuasa, S., 2008. Activation of Fyn tyrosine kinase in the mouse dorsal hippocampus is essential for contextual fear conditioning. Eur. J. Neurosci. https://doi.org/10.1111/j.1460-9568.2008.06405.x

Itoh, K., Chiba, T., Takahashi, S., Ishii, T., Igarashi, K., Katoh, Y., Oyake, T., Hayashi, N., Satoh, K., Hatayama, I., Yamamoto, M., Nabeshima, Y., 1997. An Nrf2/Small Maf Heterodimer Mediates the Induction of Phase II Detoxifying Enzyme Genes through Antioxidant Response Elements. Biochem. Biophys. Res. Commun. 236, 313–322. https://doi.org/10.1006/bbrc.1997.6943

Itoh, K., Wakabayashi, N., Katoh, Y., Ishii, T., Igarashi, K., Engel, J.D., Yamamoto, M., 1999. Keap1 represses nuclear activation of antioxidant responsive elements by Nrf2 through binding to the amino-terminal Neh2 domain. Genes Dev. 13, 76–86. https://doi.org/10.1101/gad.13.1.76

Itoh, S., Lemay, S., Osawa, M., Che, W., Duan, Y., Tompkins, A., Brookes, P.S., Sheu, S.S., Abe, J., 2005. Mitochondrial Dok-4 recruits Src kinase and regulates NF-kappaB activation in endothelial cells. J. Biol. Chem. 280, 26383–26396. https://doi.org/M410262200 [pii]\n10.1074/jbc.M410262200

Jang, M., Cho, I.H., 2016. Sulforaphane Ameliorates 3-Nitropropionic Acid-Induced Striatal Toxicity by Activating the Keap1-Nrf2-ARE Pathway and Inhibiting the MAPKs and NF-κB Pathways. Mol. Neurobiol. 53, 2619–2635. https://doi.org/10.1007/s12035-015-9230-2

Jarabek, B.R., 2003. Regulation of proteins affecting NMDA receptor-induced excitotoxicity in a Huntington's mouse model. Brain 127, 505–516. https://doi.org/10.1093/brain/awh058

Jaramillo, M., Zhang, D., 2013. The emerging role of the Nrf2–Keap1 signaling pathway in cancer. Genes Dev. 27, 2179–2191. https://doi.org/10.1101/gad.225680.113.

Jech, R., Klempíř, J., Vymazal, J., Židovská, J., Klempířová, O., Růžička, E., Roth, J., 2007. Variation of selective gray and white matter atrophy in Huntington's disease. Mov. Disord. https://doi.org/10.1002/mds.21620

Jeddi, F., Soozangar, N., Sadeghi, M.R., Somi, M.H., Shirmohamadi, M., Eftekhar-Sadat, A.T., Samadi, N., 2018. Nrf2 overexpression is associated with P-glycoprotein upregulation in gastric cancer. Biomed. Pharmacother. 97, 286–292. https://doi.org/10.1016/j.biopha.2017.10.129

Jenner, P., 2003. Oxidative stress in Parkinson's disease. Ann. Neurol. 53 Suppl 3, S26-36; discussion S36–8. https://doi.org/10.1002/ana.10483

Jeong, H., Then, F., Melia, T.J., Mazzulli, J.R., Cui, L., Savas, J.N., Voisine, C., Paganetti, P., Tanese, N., Hart, A.C., Yamamoto, A., Krainc, D., 2009. Acetylation Targets Mutant Huntingtin to Autophagosomes for Degradation. Cell. https://doi.org/10.1016/j.cell.2009.03.018

Jiang, X., Mu, D., Biran, V., Faustino, J., Chang, S., Rincón, C.M., Sheldon, R.A., Ferriero, D.M., 2008. Activated Src kinases interact with the N-methyl-D-aspartate receptor after neonatal brain ischemia. Ann. Neurol. https://doi.org/10.1002/ana.21365

Jin, J., Gu, H., Anders, N.M., Ren, T., Jiang, M., Tao, M., Peng, Q., Rudek, M.A., Duan, W., 2016. Metformin Protects Cells from Mutant Huntingtin Toxicity Through Activation of AMPK and Modulation of Mitochondrial Dynamics. NeuroMolecular Med. https://doi.org/10.1007/s12017-016-8412-z

Jin, Y.N., Yu, Y. V., Gundemir, S., Jo, C., Cui, M., Tieu, K., Johnson, G.V.W.,

2013. Impaired Mitochondrial Dynamics and Nrf2 Signaling Contribute to Compromised Responses to Oxidative Stress in Striatal Cells Expressing Full-Length Mutant Huntingtin. PLoS One 8. https://doi.org/10.1371/journal.pone.0057932

Julien, C.L., Thompson, J.C., Wild, S., Yardumian, P., Snowden, J.S., Turner, G., Craufurd, D., 2007. Psychiatric disorders in preclinical Huntington's disease. J. Neurol. Neurosurg. Psychiatry. https://doi.org/10.1136/jnnp.2006.103309

Jung, Y.-S., Ryu, B.R., Lee, B.K., Mook-Jung, I., Kim, S.U., Lee, S.H., Baik, E.J., Moon, C.-H., 2004. Role for PKC-epsilon in neuronal death induced by oxidative stress. Biochem. Biophys. Res. Commun. 320, 789–94. https://doi.org/10.1016/j.bbrc.2004.05.217

Kabeya, Y., Mizushima, N., Yamamoto, A., Oshitani-Okamoto, S., Ohsumi, Y., Yoshimori, T., 2004. LC3, GABARAP and GATE16 localize to autophagosomal membrane depending on form-II formation. J. Cell Sci. https://doi.org/10.1242/jcs.01131

Kalkhoven, E., 2004. CBP and p300: HATs for different occasions, in: Biochemical Pharmacology. pp. 1145–1155. https://doi.org/10.1016/j.bcp.2004.03.045

Kamat, P.K., Kalani, A., Kyles, P., Tyagi, S.C., Tyagi, N., 2014. Autophagy of Mitochondria: A Promising Therapeutic Target for Neurodegenerative Disease. Cell Biochem. Biophys. https://doi.org/10.1007/s12013-014-0006-5

Kansanen, E., Kuosmanen, S.M., Leinonen, H., Levonenn, A.L., 2013. The Keap1-Nrf2 pathway: Mechanisms of activation and dysregulation in cancer. Redox Biol. 1, 45–49. https://doi.org/10.1016/j.redox.2012.10.001

Karl, K., McGarry, A., McDermott, M.P., Kayson, E., Walker, F., Goldstein, J., Hyson, C., Agarwal, P., Deppen, P., Fiedorowicz, J., Kostyk, S., Wright, A., Leavitt, B., Nance, M., LeDoux, M.S., Shannon, K.M., Siderowf, A., Cudkowicz, M., Rabinowitz, K., Ross, V., Watts, A., Tedroff, J., 2013. A

randomized, double-blind, placebo-controlled trial of pridopidine in Huntington's disease. Mov. Disord. https://doi.org/10.1002/mds.25362

Kaspar, J.W., Jaiswal, A.K., 2011. Tyrosine phosphorylation controls nuclear export of Fyn, allowing Nrf2 activation of cytoprotective gene expression. FASEB J. https://doi.org/10.1096/fj.10-171553

Katoh, Y., Itoh, K., Yoshida, E., Miyagishi, M., Fukamizu, A., Yamamoto, M., 2001. Two domains of Nrf2 cooperatively bind CBP, a CREB binding protein, and synergistically activate transcription. Genes to Cells 6, 857–868. https://doi.org/10.1046/j.1365-2443.2001.00469.x

Kaushik, S., Cuervo, A.M., 2012. Chaperone-mediated autophagy: A unique way to enter the lysosome world. Trends Cell Biol. https://doi.org/10.1016/j.tcb.2012.05.006

Kaushik, S., Massey, A.C., Mizushima, N., Cuervo, A.M., 2008. Constitutive activation of chaperone-mediated autophagy in cells with impaired macroautophagy. Mol. Biol. Cell. https://doi.org/10.1091/mbc.E07-11-1155

Kay, C., Collins, J.A., Miedzybrodzka, Z., Madore, S.J., Gordon, E.S., Gerry, N., Davidson, M., Slama, R.A., Hayden, M.R., 2016. Huntington disease reduced penetrance alleles occur at high frequency in the general population. Neurology 87, 282–288. https://doi.org/10.1212/WNL.0000000000002858

Kazlauskaite, A., Martínez-Torres, R.J., Wilkie, S., Kumar, A., Peltier, J., Gonzalez, A., Johnson, C., Zhang, J., Hope, A.G., Peggie, M., Trost, M., Aalten, D.M., Alessi, D.R., Prescott, A.R., Knebel, A., Walden, H., Muqit, M.M., 2015. Binding to serine 65-phosphorylated ubiquitin primes Parkin for optimal PINK 1-dependent phosphorylation and activation . EMBO Rep. https://doi.org/10.15252/embr.201540352

Kegel, K.B., Kim, M., Sapp, E., McIntyre, C., Castano, J.G., Aronin, N., DiFiglia, M., 2000. Huntingtin expression stimulates endosomal-lysosomal activity, endosome tubulation, and autophagy. J. Neurosci.

https://doi.org/10.1523/jneurosci.20-19-07268.2000

Keum, Y.S., Choi, B.Y., 2014. Molecular and chemical regulation of the keap1-Nrf2 signaling pathway. Molecules. https://doi.org/10.3390/molecules190710074

Khalil, B., El Fissi, N., Aouane, A., Cabirol-Pol, M.J., Rival, T., Liévens, J.C., 2015. PINK1-induced mitophagy promotes neuroprotection in Huntington's disease. Cell Death Dis. https://doi.org/10.1038/cddis.2014.581

Khan, S., Ahmad, K., Alshammari, E.M.A., Adnan, M., Baig, M.H., Lohani, M., Somvanshi, P., Haque, S., 2015. Implication of Caspase-3 as a Common Therapeutic Target for Multineurodegenerative Disorders and Its Inhibition Using Nonpeptidyl Natural Compounds. Biomed Res. Int. 2015, 1–9. https://doi.org/10.1155/2015/379817

Kim, J., Kundu, M., Viollet, B., Guan, K.L., 2011. AMPK and mTOR regulate autophagy through direct phosphorylation of Ulk1. Nat. Cell Biol. https://doi.org/10.1038/ncb2152

Kirisako, T., Ichimura, Y., Okada, H., Kabeya, Y., Mizushima, N., Yoshimori, T., Ohsumi, M., Takao, T., Noda, T., Ohsumi, Y., 2000. The reversible modification regulates the membrane-binding state of Apg8/Aut7 essential for autophagy and the cytoplasm to vacuole targeting pathway. J. Cell Biol. https://doi.org/10.1083/jcb.151.2.263

Klapstein, G.J., Fisher, R.S., Zanjani, H., Cepeda, C., Jokel, E.S., Chesselet, M.-F., Levine, M.S., 2017. Electrophysiological and Morphological Changes in Striatal Spiny Neurons in R6/2 Huntington's Disease Transgenic Mice. J. Neurophysiol. https://doi.org/10.1152/jn.2001.86.6.2667

Klepac, N., Relja, M., Klepac, R., Hećimović, S., Babić, T., Trkulja, V., 2007. Oxidative stress parameters in plasma of Huntington's disease patients, asymptomatic Huntington's disease gene carriers and healthy subjects: A cross-sectional study. J. Neurol. 254, 1676–1683. https://doi.org/10.1007/s00415-007-0611-y

Klionsky, D.J., 2007. Autophagy: From phenomenology to molecular understanding in less than a decade. Nat. Rev. Mol. Cell Biol. https://doi.org/10.1038/nrm2245

Klionsky, D.J., Emr, S.D., 2000. Autophagy as a regulated pathway of cellular degradation. Science (80-.). https://doi.org/10.1126/science.290.5497.1717

Knott, A.B., Perkins, G., Schwarzenbacher, R., Bossy-Wetzel, E., 2008. Mitochondrial fragmentation in neurodegeneration. Nat. Rev. Neurosci. https://doi.org/10.1038/nrn2417

Kobayashi, A., Kang, M.-I., Okawa, H., Ohtsuji, M., Zenke, Y., Chiba, T., Igarashi, K., Yamamoto, M., 2004. Oxidative stress sensor Keap1 functions as an adaptor for Cul3-based E3 ligase to regulate proteasomal degradation of Nrf2. Mol. Cell. Biol. 24, 7130–9. https://doi.org/10.1128/MCB.24.16.7130

Koc, E.C., Miller-Lee, J.L., Koc, H., 2017. Fyn kinase regulates translation in mammalian mitochondria. Biochim. Biophys. Acta - Gen. Subj. 1861, 533–540. https://doi.org/10.1016/j.bbagen.2016.12.004

Koentjoro, B., Park, J.S., Sue, C.M., 2017. Nix restores mitophagy and mitochondrial function to protect against PINK1/Parkin-related Parkinson's disease. Sci. Rep. https://doi.org/10.1038/srep44373

Koga, H., Martinez-Vicente, M., Arias, E., Kaushik, S., Sulzer, D., Cuervo, A.M., 2011. Constitutive upregulation of chaperone-mediated autophagy in Huntington's disease. J. Neurosci. https://doi.org/10.1523/JNEUROSCI.3219-11.2011

Köhr, G., Seeburg, P.H., 1996. Subtype-specific regulation of recombinant NMDA receptor-channels by protein tyrosine kinases of the src family. J. Physiol. 492 (Pt 2, 445–52.

Komatsu, M., Waguri, S., Chiba, T., Murata, S., Iwata, J., Tanida, I., Ueno, T., Koike, M., Uchiyama, Y., Kominami, E., Tanaka, K., 2006. Loss of

autophagy in the central nervous system causes neurodegeneration in mice. Nature 441, 880–884. https://doi.org/10.1038/nature04723

Kondapalli, C., Kazlauskaite, A., Zhang, N., Woodroof, H.I., Campbell, D.G., Gourlay, R., Burchell, L., Walden, H., MacArtney, T.J., Deak, M., Knebel, A., Alessi, D.R., Muqit, M.M.K., 2012. PINK1 is activated by mitochondrial membrane potential depolarization and stimulates Parkin E3 ligase activity by phosphorylating Serine 65. Open Biol. https://doi.org/10.1098/rsob.120080

Konishi, H., Yamauchi, E., Taniguchi, H., Yamamoto, T., Matsuzaki, H., Takemura, Y., Ohmae, K., Kikkawa, U., Nishizuka, Y., 2001. Phosphorylation sites of protein kinase C delta in H2O2-treated cells and its activation by tyrosine kinase in vitro. Proc. Natl. Acad. Sci. U. S. A. 98, 6587–92. https://doi.org/10.1073/pnas.111158798

Koppula, S., Kumar, H., Kim, I.S., Choi, D.K., 2012. Reactive oxygen species and inhibitors of inflammatory enzymes, NADPH oxidase, and iNOS in experimental models of parkinsons disease. Mediators Inflamm. https://doi.org/10.1155/2012/823902

Kumar, P., Kalonia, H., Kumar, A., 2010. Huntington's disease: pathogenesis to animal models. Pharmacol. Rep. 62, 1–14. https://doi.org/10.1016/S1734-1140(10)70238-3

Kurosawa, M., Matsumoto, G., Kino, Y., Okuno, M., Kurosawa-Yamada, M., Washizu, C., Taniguchi, H., Nakaso, K., Yanagawa, T., Warabi, E., Shimogori, T., Sakurai, T., Hattori, N., Nukina, N., 2015. Depletion of p62 reduces nuclear inclusions and paradoxically ameliorates disease phenotypes in Huntington's model mice. Hum. Mol. Genet. 24, 1092–1105. https://doi.org/10.1093/hmg/ddu522

Kwok, R.P., Lundblad, J.R., Chrivia, J.C., Richards, J.P., Bächinger, H.P., Brennan, R.G., Roberts, S.G., Green, M.R., Goodman, R.H., 1994. Nuclear protein CBP is a coactivator for the transcription factor CREB. Nature. https://doi.org/10.1038/370223a0

Lamark, T., Perander, M., Outzen, H., Kristiansen, K., Øvervatn, A., Michaelsen, E., BjØrkoy, G., Johansen, T., 2003. Interaction Codes within the Family of Mammalian Phox and Bem1p Domain-containing Proteins. J. Biol. Chem. https://doi.org/10.1074/jbc.M303221200

Lamb, C.A., Yoshimori, T., Tooze, S.A., 2013. The autophagosome: Origins unknown, biogenesis complex. Nat. Rev. Mol. Cell Biol. https://doi.org/10.1038/nrm3696

Landwehrmeyer, G., Standaert, D., Testa, C., Penney, J., Young, A., 2018. NMDA receptor subunit mRNA expression by projection neurons and interneurons in rat striatum. J. Neurosci. https://doi.org/10.1523/jneurosci.15-07-05297.1995

Langbehn, D.R., Brinkman, R.R., Falush, D., Paulsen, J.S., Hayden, M.R., 2004. A new model for prediction of the age of onset and penetrance for Huntington's disease based on CAG length. Clin. Genet. https://doi.org/10.1111/j.1399-0004.2004.00241.x

Lanska, D.J., 2000. George Huntington (1850-1916) and hereditary chorea. J. Hist. Neurosci. https://doi.org/10.1076/0964-704X(200004)9:1;1-2;FT076

Lapper, S.R., Bolam, J.P., 1992. Input from the frontal cortex and the parafascicular nucleus to cholinergic interneurons in the dorsal striatum of the rat. Neuroscience 51, 533–545. https://doi.org/10.1016/0306-4522(92)90293-B

Lau, L.F., Huganir, R.L., 1995. Differential tyrosine phosphorylation of N-methyl-D-aspartate receptor subunits. J Biol Chem 270, 20036–20041.

Lazarou, M., Jin, S.M., Kane, L.A., Youle, R.J., 2012. Role of PINK1 Binding to the TOM Complex and Alternate Intracellular Membranes in Recruitment and Activation of the E3 Ligase Parkin. Dev. Cell. https://doi.org/10.1016/j.devcel.2011.12.014

Lee, H., Noh, J.Y., Oh, Y., Kim, Y., Chang, J.W., Chung, C.W., Lee, S.T., Kim, M., Ryu, H., Jung, Y.K., 2012. IRE1 plays an essential role in ER stress-

mediated aggregation of mutant huntingtin via the inhibition of autophagy flux. Hum. Mol. Genet. https://doi.org/10.1093/hmg/ddr445

Lee, I.-T., Wang, S.-W., Lee, C.-W., Chang, C.-C., Lin, C.-C., Luo, S.-F., Yang, C.-M., 2008. Lipoteichoic acid induces HO-1 expression via the TLR2/MyD88/c-Src/NADPH oxidase pathway and Nrf2 in human tracheal smooth muscle cells. J. Immunol. 181, 5098–110. https://doi.org/181/7/5098 [pii]

Lee, J.-M., Gillis, T., Mysore, J.S., Ramos, E.M., Myers, R.H., Hayden, M.R., Morrison, P.J., Nance, M., Ross, C.A., Margolis, R.L., Squitieri, F., Griguoli, A., Di Donato, S., Gomez-Tortosa, E., Ayuso, C., Suchowersky, O., Trent, R.J., McCusker, E., Novelletto, A., Frontali, M., Jones, R., Ashizawa, T., Frank, S., Saint-Hilaire, M.-H., Hersch, S.M., Rosas, H.D., Lucente, D., Harrison, M.B., Zanko, A., Abramson, R.K., Marder, K., Sequeiros, J., MacDonald, M.E., Gusella, J.F., 2012. Common SNP-Based Haplotype Analysis of the 4p16.3 Huntington Disease Gene Region. Am. J. Hum. Genet. 90, 434–444. https://doi.org/10.1016/j.ajhg.2012.01.005

Lee, J.-M., Wheeler, V.C., Chao, M.J., Vonsattel, J.P.G., Pinto, R.M., Lucente, D., Abu-Elneel, K., Ramos, E.M., Mysore, J.S., Gillis, T., MacDonald, M.E., Gusella, J.F., Harold, D., Stone, T.C., Escott-Price, V., Han, J., Vedernikov, A., Holmans, P., Jones, L., Kwak, S., Mahmoudi, M., Orth, M., Landwehrmeyer, G.B., Paulsen, J.S., Dorsey, E.R., Shoulson, I., Myers, R.H., 2015. Identification of Genetic Factors that Modify Clinical Onset of Huntington's Disease. Cell 162, 516–526. https://doi.org/10.1016/j.cell.2015.07.003

Lee, J.M., Shih, A.Y., Murphy, T.H., Johnson, J.A., 2003. NF-E2-related factor-2 mediates neuroprotection against mitochondrial complex I inhibitors and increased concentrations of intracellular calcium in primary cortical neurons. J. Biol. Chem. 278, 37948–37956. https://doi.org/10.1074/jbc.M305204200

Lee, W., Boo, J.H., Jung, M.W., Park, S.D., Kim, Y.H., Kim, S.U., Mook-Jung, I., 2004. Amyloid beta peptide directly inhibits PKC activation. Mol. Cell.

Neurosci. 26, 222–231. https://doi.org/10.1016/j.mcn.2003.10.020

Leitman, J., Ulrich Hartl, F., Lederkremer, G.Z., 2013. Soluble forms of polyQ-expanded huntingtin rather than large aggregates cause endoplasmic reticulum stress. Nat. Commun. https://doi.org/10.1038/ncomms3753

Léveillé, F., gaamouch, F. El, Gouix, E., Lecocq, M., Lobner, D., Nicole, O., Buisson, A., 2008. Neuronal viability is controlled by a functional relation between synaptic and extrasynaptic NMDA receptors. FASEB J. https://doi.org/10.1096/fj.08-107268

Levinson, W.E., Varmus, H.E., Garapin, A.C., Bishop, J.M., 1972. DNA of Rous sarcoma virus: its nature and significance. Science. 175(4017), 76–78.

Li, L., Fan, M., Icton, C.D., Chen, N., Leavitt, B.R., Hayden, M.R., Murphy, T.H., Raymond, L.A., 2003. Role of NR2B-type NMDA receptors in selective neurodegeneration in Huntington disease, in: Neurobiology of Aging. https://doi.org/10.1016/j.neurobiolaging.2003.04.003

Li, Q., Niu, C., Zhang, X., Dong, M., 2017. Gastrodin and Isorhynchophylline Synergistically Inhibit MPP + -Induced Oxidative Stress in SH-SY5Y Cells by Targeting ERK1/2 and GSK-3β Pathways: Involvement of Nrf2 Nuclear Translocation. ACS Chem. Neurosci. acschemneuro.7b00247. https://doi.org/10.1021/acschemneuro.7b00247

Li, S.H., Cheng, A.L., Li, H., Li, X.J., 1999. Cellular defects and altered gene expression in PC12 cells stably expressing mutant huntingtin. J. Neurosci. https://doi.org/10.1523/jneurosci.19-13-05159.1999

Li, X.-J., Li, S., 2011. Proteasomal dysfunction in aging and Huntington disease. Neurobiol. Dis. 43, 4–8. https://doi.org/10.1016/j.nbd.2010.11.018

Li, X., Wang, C.E., Huang, S., Xu, X., Li, X.J., Li, H., Li, S., 2010. Inhibiting the ubiquitin-proteasome system leads to preferential accumulation of toxic N-terminal mutant huntingtin fragments. Hum. Mol. Genet. https://doi.org/10.1093/hmg/ddq127

Li, X., Zhang, D., Hannink, M., Beamer, L.J., 2004. Crystal structure of the Kelch domain of human Keap1. J. Biol. Chem. 279, 54750–54758. https://doi.org/10.1074/jbc.M410073200

Liddell, J., 2017. Are Astrocytes the Predominant Cell Type for Activation of Nrf2 in Aging and Neurodegeneration? Antioxidants. https://doi.org/10.3390/antiox6030065

Lin, C.-C., Yang, C.-C., Chen, Y.-W., Hsiao, L.-D., Yang, C.-M., 2017. Arachidonic Acid Induces ARE/Nrf2-Dependent Heme Oxygenase-1 Transcription in Rat Brain Astrocytes. Mol. Neurobiol. 1–16. https://doi.org/10.1007/s12035-017-0590-7

Lin, J., Wu, P.H., Tarr, P.T., Lindenberg, K.S., St-Pierre, J., Zhang, C.Y., Mootha, V.K., Jäger, S., Vianna, C.R., Reznick, R.M., Cui, L., Manieri, M., Donovan, M.X., Wu, Z., Cooper, M.P., Fan, M.C., Rohas, L.M., Zavacki, A.M., Cinti, S., Shulman, G.I., Lowell, B.B., Krainc, D., Spiegelman, B.M., 2004. Defects in adaptive energy metabolism with CNS-linked hyperactivity in PGC-1α null mice. Cell. https://doi.org/10.1016/j.cell.2004.09.013

Liu, C.S., Cheng, W.L., Kuo, S.J., Li, J.Y., Soong, B.W., Wei, Y.H., 2008. Depletion of mitochondrial DNA in leukocytes of patients with poly-Q diseases. J. Neurol. Sci. https://doi.org/10.1016/j.jns.2007.07.016

Liu, L., Feng, D., Chen, G., Chen, M., Zheng, Q., Song, P., Ma, Q., Zhu, C., Wang, R., Qi, W., Huang, L., Xue, P., Li, B., Wang, X., Jin, H., Wang, J., Yang, F., Liu, P., Zhu, Y., Sui, S., Chen, Q., 2012. Mitochondrial outer-membrane protein FUNDC1 mediates hypoxia-induced mitophagy in mammalian cells. Nat. Cell Biol. https://doi.org/10.1038/ncb2422

Liu, P., Li, Y., Yang, W., Liu, D., Ji, X., Chi, T., Guo, Z., Li, L., Zou, L., 2019. Prevention of Huntington's Disease-Like Behavioral Deficits in R6/1 Mouse by Tolfenamic Acid Is Associated with Decreases in Mutant Huntingtin and Oxidative Stress. Oxid. Med. Cell. Longev. 2019, 1–13. https://doi.org/10.1155/2019/4032428

Livigni, A., Scorziello, A., Agnese, S., Adornetto, A., Carlucci, A., Garbi, C.,

Castaldo, I., Annunziato, L., Avvedimento, E. V., Feliciello, A., 2006. Mitochondrial AKAP121 Links cAMP and src Signaling to Oxidative Metabolism. Mol. Biol. Cell 17, 263–271. https://doi.org/10.1091/mbc.e05-09-0827

Livigni, A., Scorziello, A., Agnese, S., Adornetto, A., Carlucci, A., Garbi, C., Castaldo, I., Annunziato, L., Avvedimento, E. V, Feliciello, A., 2006. Mitochondrial AKAP121 links cAMP and src signaling to oxidative metabolism. Mol Biol Cell 17, 263–271. https://doi.org/10.1091/mbc.E05-09-0827

Loboda, A., Damulewicz, M., Pyza, E., Jozkowicz, A., Dulak, J., 2016. Role of Nrf2/HO-1 system in development, oxidative stress response and diseases: an evolutionarily conserved mechanism. Cell. Mol. Life Sci. 73, 1–27. https://doi.org/10.1007/s00018-016-2223-0

Long, J.D., Matson, W.R., Juhl, A.R., Leavitt, B.R., Paulsen, J.S., 2012. 8OHdG as a marker for Huntington disease progression. Neurobiol. Dis. 46, 625–634. https://doi.org/10.1016/j.nbd.2012.02.012

Lopes, C., Aubert, S., Bourgois-Rocha, F., Barnat, M., Rego, A.C., Déglon, N., Perrier, A.L., Humbert, S., 2016. Dominant-Negative Effects of Adult-Onset Huntingtin Mutations Alter the Division of Human Embryonic Stem Cells-Derived Neural Cells. PLoS One 11, e0148680. https://doi.org/10.1371/journal.pone.0148680

Lu, K., Psakhye, I., Jentsch, S., 2014a. A new class of ubiquitin-Atg8 receptors involved in selective autophagy and polyQ protein clearance. Autophagy. https://doi.org/10.4161/15548627.2014.981919

Lu, K., Psakhye, I., Jentsch, S., 2014b. Autophagic clearance of PolyQ proteins mediated by ubiquitin-Atg8 adaptors of the conserved CUET protein family. Cell. https://doi.org/10.1016/j.cell.2014.05.048

Lundin, A., Dietrichs, E., Haghighi, S., Göller, M.L., Heiberg, A., Loutfi, G., Widner, H., Wiktorin, K., Wiklund, L., Svenningsson, A., Sonesson, C., Waters, N., Waters, S., Tedroff, J., 2010. Efficacy and safety of the

dopaminergic stabilizer pridopidine (ACR16) in patients with Huntington's disease. Clin. Neuropharmacol. https://doi.org/10.1097/WNF.0b013e3181ebb285

MacDermott, A.B., Mayer, M.L., Westbrook, G.L., Smith, S.J., Barker, J.L., 1986. NMDA-receptor activation increases cytoplasmic calcium concentration in cultured spinal cord neurones. Nature 321, 519–22. https://doi.org/10.1038/321519a0

MacDonald, M.E., Ambrose, C.M., Duyao, M.P., Myers, R.H., Lin, C., Srinidhi, L., Barnes, G., Taylor, S.A., James, M., Groot, N., MacFarlane, H., Jenkins, B., Anderson, M.A., Wexler, N.S., Gusella, J.F., Bates, G.P., Baxendale, S., Hummerich, H., Kirby, S., North, M., Youngman, S., Mott, R., Zehetner, G., Sedlacek, Z., Poustka, A., Frischauf, A.M., Lehrach, H., Buckler, A.J., Church, D., Doucette-Stamm, L., O'Donovan, M.C., Riba-Ramirez, L., Shah, M., Stanton, V.P., Strobel, S.A., Draths, K.M., Wales, J.L., Dervan, P., Housman, D.E., Altherr, M., Shiang, R., Thompson, L., Fielder, T., Wasmuth, J.J., Tagle, D., Valdes, J., Elmer, L., Allard, M., Castilla, L., Swaroop, M., Blanchard, K., Collins, F.S., Snell, R., Holloway, T., Gillespie, K., Datson, N., Shaw, D., Harper, P.S., 1993. A novel gene containing a trinucleotide repeat that is expanded and unstable on Huntington's disease chromosomes. Cell. https://doi.org/10.1016/0092-8674(93)90585-E

Magalhães, J.D., Fão, L., Vilaça, R., Cardoso, S.M., Rego, A.C., 2021. Macroautophagy and Mitophagy in Neurodegenerative Disorders: Focus on Therapeutic Interventions. Biomedicines 9, 1625. https://doi.org/10.3390/biomedicines9111625

Mai, A., Jung, S.K., Yonehara, S., 2004. hDKIR, a human homologue of the Drosophila kelch protein, involved in a ring-like structure. Exp. Cell Res. 300, 72–83. https://doi.org/10.1016/j.yexcr.2004.06.023

Maiuri, T., Woloshansky, T., Xia, J., Truant, R., 2013. The huntingtin N17 domain is a multifunctional CRM1 and ran-dependent nuclear and cilial export signal. Hum. Mol. Genet. https://doi.org/10.1093/hmg/dds554

Malhotra, D., Portales-Casamar, E., Singh, A., Srivastava, S., Arenillas, D., Happel, C., Shyr, C., Wakabayashi, N., Kensler, T.W., Wasserman, W.W., Biswal, S., 2010. Global mapping of binding sites for Nrf2 identifies novel targets in cell survival response through chip-seq profiling and network analysis. Nucleic Acids Res. 38, 5718–5734. https://doi.org/10.1093/nar/gkq212

Maness, P.F., 1992. Nonreceptor protein tyrosine kinases associated with neuronal development. Dev. Neurosci. https://doi.org/10.1159/000111670

Mangiarini, L., Sathasivam, K., Seller, M., Cozens, B., Harper, A., Hetherington, C., Lawton, M., Trottier, Y., Lehrach, H., Davies, S.W., Bates, G.P., 1996. Exon I of the HD gene with an expanded CAG repeat is sufficient to cause a progressive neurological phenotype in transgenic mice. Cell. https://doi.org/10.1016/S0092-8674(00)81369-0

Marder, K., Zhao, H., Eberly, S., Tanner, C.M., Oakes, D., Shoulson, I., 2009. Dietary intake in adults at risk for Huntington disease: Analysis of PHAROS Research Participants. Neurology. https://doi.org/10.1212/WNL.0b013e3181b04aa2

Marques Sousa, C., Humbert, S., 2013. Huntingtin: Here, there, everywhere! J. Huntingtons. Dis. https://doi.org/10.3233/JHD-130082

Martinez-Vicente, M., 2017. Neuronal mitophagy in neurodegenerative diseases. Front. Mol. Neurosci. https://doi.org/10.3389/fnmol.2017.00064

Martinez-Vicente, M., Talloczy, Z., Wong, E., Tang, G., Koga, H., Kaushik, S., de Vries, R., Arias, E., Harris, S., Sulzer, D., Cuervo, A.M., 2010. Cargo recognition failure is responsible for inefficient autophagy in Huntington's disease. Nat. Neurosci. 13, 567–576. https://doi.org/10.1038/nn.2528

Mason, R.P., Casu, M., Butler, N., Breda, C., Campesan, S., Clapp, J., Green, E.W., Dhulkhed, D., Kyriacou, C.P., Giorgini, F., 2013. Glutathione peroxidase activity is neuroprotective in models of Huntington's disease. Nat. Genet. 45, 1249–1254. https://doi.org/10.1038/ng.2732

Massey, P. V., Johnson, B.E., Moult, P.R., Auberson, Y.P., Brown, M.W., Molnar, E., Collingridge, G.L., Bashir, Z.I., 2004. Differential roles of NR2A and NR2B-containing NMDA receptors in cortical long-term potentiation and long-term depression. J. Neurosci. https://doi.org/10.1523/JNEUROSCI.1697-04.2004

Mealer, R.G., Murray, A.J., Shahani, N., Subramaniam, S., Snyder, S.H., 2014. Rhes, a Striatal-selective Protein Implicated in Huntington Disease, Binds Beclin-1 and activates autophagy. J. Biol. Chem. https://doi.org/10.1074/jbc.M113.536912

Menalled, L.B., Kudwa, A.E., Miller, S., Fitzpatrick, J., Watson-Johnson, J., Keating, N., Ruiz, M., Mushlin, R., Alosio, W., McConnell, K., Connor, D., Murphy, C., Oakeshott, S., Kwan, M., Beltran, J., Ghavami, A., Brunner, D., Park, L.C., Ramboz, S., Howland, D., 2012. Comprehensive Behavioral and Molecular Characterization of a New Knock-In Mouse Model of Huntington's Disease: ZQ175. PLoS One. https://doi.org/10.1371/journal.pone.0049838

Menalled, L.B., Sison, J.D., Dragatsis, I., Zeitlin, S., Chesselet, M.F., 2003. Time course of early motor and neuropathological anomalies in a knock-in mouse model of Huntington's disease with 140 CAG repeats. J. Comp. Neurol. https://doi.org/10.1002/cne.10776

Mercer, C.A., Kaliappan, A., Dennis, P.B., 2009. A novel, human Atg13 binding protein, Atg101, interacts with ULK1 and is essential for macroautophagy. Autophagy. https://doi.org/10.4161/auto.5.5.8249

Messa, M., Congia, S., Defranchi, E., Valtorta, F., Fassio, A., Onofri, F., Benfenati, F., 2010. Tyrosine phosphorylation of synapsin I by Src regulates synaptic-vesicle trafficking. J. Cell Sci. 123, 2256–2265. https://doi.org/10.1242/jcs.068445

Metzger, S., Saukko, M., Van Che, H., Tong, L., Puder, Y., Riess, O., Nguyen, H.P., 2010. Age at onset in Huntington's disease is modified by the autophagy pathway: Implication of the V471A polymorphism in Atg7. Hum.

Genet. https://doi.org/10.1007/s00439-010-0873-9

Milakovic, T., Quintanilla, R.A., Johnson, G.V.W., 2006. Mutant Huntingtin expression induces mitochondrial calcium handling defects in clonal striatal cells: Functional consequences. J. Biol. Chem. https://doi.org/10.1074/jbc.M603845200

Milani, P., Gagliardi, S., Cova, E., Cereda, C., 2011. SOD1 Transcriptional and Posttranscriptional Regulation and Its Potential Implications in ALS. Neurol. Res. Int. 2011, 1–9. https://doi.org/10.1155/2011/458427

Miller, B.R., Dorner, J.L., Bunner, K.D., Gaither, T.W., Klein, E.L., Barton, S.J., Rebec, G. V., 2012. Up-regulation of GLT1 reverses the deficit in cortically evoked striatal ascorbate efflux in the R6/2 mouse model of Huntington's disease. J. Neurochem. https://doi.org/10.1111/j.1471-4159.2012.07691.x

Milnerwood, A.J., Gladding, C.M., Pouladi, M.A., Kaufman, A.M., Hines, R.M., Boyd, J.D., Ko, R.W.Y., Vasuta, O.C., Graham, R.K., Hayden, M.R., Murphy, T.H., Raymond, L.A., 2010. Early Increase in Extrasynaptic NMDA Receptor Signaling and Expression Contributes to Phenotype Onset in Huntington's Disease Mice. Neuron. https://doi.org/10.1016/j.neuron.2010.01.008

Miyazaki, T., Tanaka, S., Sanjay, A., Baron, R., 2006. The role of c-Src kinase in the regulation of osteoclast function. Mod. Rheumatol. 16, 68–74. https://doi.org/10.1007/s10165-006-0460-z

Mizuno, M., Yamada, K., He, J., Nakajima, A., Nabeshima, T., 2003. Involvement of BDNF Receptor TrkB in Spatial Memory Formation. Learn. Mem. 10, 108–115. https://doi.org/10.1101/lm.56003

Mizushima, N., 2007. Autophagy: Process and function. Genes Dev. https://doi.org/10.1101/gad.1599207

Mizushima, N., Yamamoto, A., Hatano, M., Kobayashi, Y., Kabey, Y., Suzuki, K., Tokuhis, T., Ohsumi, Y., Yoshimori, T., 2001. Dissection of autophagosome formation using Apg5-deficient mouse embryonic stem

cells. J. Cell Biol. https://doi.org/10.1083/jcb.152.4.657

Mo, C., Hannan, A.J., Renoir, T., 2015. Environmental factors as modulators of neurodegeneration: Insights from gene–environment interactions in Huntington's disease. Neurosci. Biobehav. Rev. 52, 178–192. https://doi.org/10.1016/j.neubiorev.2015.03.003

Mokranjac, D., Neupert, W., 2010. The many faces of the mitochondrial TIM23 complex. Biochim. Biophys. Acta - Bioenerg. https://doi.org/10.1016/j.bbabio.2010.01.026

Monyer, H., Burnashev, N., Laurie, D.J., Sakmann, B., Seeburg, P.H., 1994. Developmental and regional expression in the rat brain and functional properties of four NMDA receptors. Neuron. https://doi.org/10.1016/0896-6273(94)90210-0

Mori, F., Tanji, K., Toyoshima, Y., Yoshida, M., Kakita, A., Takahashi, H., Wakabayashi, K., 2012. Optineurin immunoreactivity in neuronal nuclear inclusions of polyglutamine diseases (Huntington's, DRPLA, SCA2, SCA3) and intranuclear inclusion body disease. Acta Neuropathol. https://doi.org/10.1007/s00401-012-0956-x

Morimoto, B.H., Koshland, D.E., 1990. Induction and expression of long- and short-term neurosecretory potentiation in a neural cell line. Neuron 5, 875–880. https://doi.org/10.1016/0896-6273(90)90347-I

Moris, D., Spartalis, M., Tzatzaki, E., Spartalis, E., Karachaliou, G.-S., Triantafyllis, A.S., Karaolanis, G.I., Tsilimigras, D.I., Theocharis, S., 2017. The role of reactive oxygen species in myocardial redox signaling and regulation. Ann. Transl. Med. 5, 324–324. https://doi.org/10.21037/atm.2017.06.17

Morita, A., Yamashita, N., Sasaki, Y., Uchida, Y., Nakajima, O., Nakamura, F., Yagi, T., Taniguchi, M., Usui, H., Katoh-Semba, R., Takei, K., Goshima, Y., 2006. Regulation of dendritic branching and spine maturation by semaphorin3A-fyn signaling. J. Neurosci. https://doi.org/10.1523/JNEUROSCI.5453-05.2006

Morreale, M.K., 2015. Huntington's Disease: Looking Beyond the Movement Disorder, in: Advances in Psychosomatic Medicine. pp. 135–142. https://doi.org/10.1159/000369111

Morrison, P.J., 2012. Prevalence estimates of Huntington disease in Caucasian populations are gross underestimates. Mov. Disord. 27, 1707–1708. https://doi.org/10.1002/mds.25266

Morton, A.J., Lagan, M.A., Skepper, J.N., Dunnett, S.B., 2000. Progressive formation of inclusions in the striatum and hippocampus of mice transgenic for the human Huntington's disease mutation. J. Neurocytol. https://doi.org/10.1023/A:1010887421592

Mosmann, T., 1983. Rapid colorimetric assay for cellular growth and survival: Application to proliferation and cytotoxicity assays. J. Immunol. Methods. https://doi.org/10.1016/0022-1759(83)90303-4

Mota, S.I., Costa, R.O., Ferreira, I.L., Santana, I., Caldeira, G.L., Padovano, C., Fonseca, A.C., Baldeiras, I., Cunha, C., Letra, L., Oliveira, C.R., Pereira, C.M.F., Rego, A.C., 2015. Oxidative stress involving changes in Nrf2 and ER stress in early stages of Alzheimer's disease. Biochim. Biophys. Acta - Mol. Basis Dis. 1852, 1428–1441. https://doi.org/10.1016/j.bbadis.2015.03.015

Mota, S.I., Ferreira, I.L., Rego, A.C., 2014a. Dysfunctional synapse in Alzheimer's disease - A focus on NMDA receptors. Neuropharmacology. https://doi.org/10.1016/j.neuropharm.2013.08.013

Mota, S.I., Ferreira, I.L., Valero, J., Ferreiro, E., Carvalho, A.L., Oliveira, C.R., Rego, A.C., 2014b. Impaired Src signaling and post-synaptic actin polymerization in Alzheimer's disease mice hippocampus - Linking NMDA receptors and the reelin pathway. Exp. Neurol. 261, 698–709. https://doi.org/10.1016/j.expneurol.2014.07.023

Motohashi, H., Katsuoka, F., Engel, J.D., Yamamoto, M., 2004. Small Maf proteins serve as transcriptional cofactors for keratinocyte differentiation in the Keap1-Nrf2 regulatory pathway. Proc. Natl. Acad. Sci. U. S. A. 101,

6379–6384. https://doi.org/10.1073/pnas.0305902101

Müller, M., Schmidt, O., Angelova, M., Faserl, K., Weys, S., Kremser, L., Pfaffenwimmer, T., Dalik, T., Kraft, C., Trajanoski, Z., Lindner, H., Teis, D., 2015. The coordinated action of the MVB pathway and autophagy ensures cell survival during starvation. Elife. https://doi.org/10.7554/eLife.07736

Murmu, R.P., Li, W., Holtmaat, A., Li, J.-Y., 2013. Dendritic Spine Instability Leads to Progressive Neocortical Spine Loss in a Mouse Model of Huntington's Disease. J. Neurosci. https://doi.org/10.1523/jneurosci.5284-12.2013

Murmu, R.P., Li, W., Szepesi, Z., Li, J.-Y., 2015. Altered Sensory Experience Exacerbates Stable Dendritic Spine and Synapse Loss in a Mouse Model of Huntington's Disease. J. Neurosci. 35, 287–298. https://doi.org/10.1523/JNEUROSCI.0244-14.2015

Myers, R.H., 2004. Huntington's disease genetics. NeuroRX 1, 255–262. https://doi.org/10.1602/neurorx.1.2.255

Nagaoka, U., Kim, K., Nihar, R.J., Doi, H., Maruyama, M., Mitsui, K., Oyama, F., Nukina, N., 2004. Increased expression of p62 in expanded polyglutamine-expressing cells and its association with polyglutamine inclusions. J. Neurochem. https://doi.org/10.1111/j.1471-4159.2004.02692.x

Naia, L., Carmo, C., Campesan, S., Fão, L., Cotton, V.E., Valero, J., Lopes, C., Rosenstock, T.R., Giorgini, F., Rego, A.C., 2021. Mitochondrial SIRT3 confers neuroprotection in Huntington's disease by regulation of oxidative challenges and mitochondrial dynamics. Free Radic. Biol. Med. 163, 163–179. https://doi.org/10.1016/j.freeradbiomed.2020.11.031

Naia, L., Cunha-Oliveira, T., Rodrigues, J., Rosenstock, T.R., Oliveira, A., Ribeiro, M., Carmo, C., Oliveira-Sousa, S.I., Duarte, A.I., Hayden, M.R., Rego, A.C., 2017a. Histone deacetylase inhibitors protect against pyruvate dehydrogenase dysfunction in huntington's disease. J. Neurosci. https://doi.org/10.1523/JNEUROSCI.2006-14.2016

Naia, L., Ferreira, I.L., Cunha-Oliveira, T., Duarte, A.I., Ribeiro, M., Rosenstock, T.R., Laço, M.N., Ribeiro, M.J., Oliveira, C.R., Saudou, F., Humbert, S., Rego, A.C., 2014. Activation of IGF-1 and Insulin Signaling Pathways Ameliorate Mitochondrial Function and Energy Metabolism in Huntington's Disease Human Lymphoblasts. Mol. Neurobiol. https://doi.org/10.1007/s12035-014-8735-4

Naia, L., Rego, A.C., 2018. Isolation and Maintenance of Striatal Neurons. BIO-PROTOCOL 8. https://doi.org/10.21769/BioProtoc.2823

Naia, L., Ribeiro, M., Rodrigues, J., Duarte, A.I., Lopes, C., Rosenstock, T.R., Hayden, M.R., Rego, A.C., 2016. Insulin and IGF-1 regularize energy metabolites in neural cells expressing full-length mutant huntingtin. Neuropeptides. https://doi.org/10.1016/j.npep.2016.01.009

Naia, L., Ribeiro, M.J., Rego, A.C., 2011. Mitochondrial and metabolic-based protective strategies in Huntington's disease: the case of creatine and coenzyme Q. Rev. Neurosci. 23, 13–28. https://doi.org/10.1515/RNS.2011.060

Naia, L., Rosenstock, T.R., Oliveira, A.M., Oliveira-Sousa, S.I., Caldeira, G.L., Carmo, C., Laço, M.N., Hayden, M.R., Oliveira, C.R., Rego, A.C., 2017b. Comparative Mitochondrial-Based Protective Effects of Resveratrol and Nicotinamide in Huntington's Disease Models. Mol. Neurobiol. 54, 5385–5399. https://doi.org/10.1007/s12035-016-0048-3

Nance, M.A., Mathias-Hagen, V., Breningstall, G., Wick, M.J., McGlennen, R.C., 1999. Analysis of a very large trinucleotide repeat in a patient with juvenile Huntington's disease. Neurology. https://doi.org/10.1212/wnl.52.2.392

Nance, M.A., Myers, R.H., 2001. Juvenile onset Huntington's disease?clinical and research perspectives. Ment. Retard. Dev. Disabil. Res. Rev. 7, 153–157. https://doi.org/10.1002/mrdd.1022

Napoli, E., Wong, S., Hung, C., Ross-Inta, C., Bomdica, P., Giulivi, C., 2013. Defective mitochondrial disulfide relay system, altered mitochondrial morphology and function in Huntington's disease. Hum. Mol. Genet. 22,

989–1004. https://doi.org/10.1093/hmg/dds503

Narendra, D., Tanaka, A., Suen, D.F., Youle, R.J., 2008. Parkin is recruited selectively to impaired mitochondria and promotes their autophagy. J. Cell Biol. https://doi.org/10.1083/jcb.200809125

Nath, S., Munsie, L.N., Truant, R., 2015. A huntingtin-mediated fast stress response halting endosomal trafficking is defective in Huntington's disease. Hum. Mol. Genet. https://doi.org/10.1093/hmg/ddu460

Newpher, T.M., Ehlers, M.D., 2009. Spine microdomains for postsynaptic signaling and plasticity. Trends Cell Biol. https://doi.org/10.1016/j.tcb.2009.02.004

Nguyen, T., Sherratt, P.J., Huang, H.C., Yang, C.S., Pickett, C.B., 2003. Increased protein stability as a mechanism that enhances Nrf2-mediated transcriptional activation of the antioxidant response element: Degradation of Nrf2 by the 26 S proteasome. J. Biol. Chem. 278, 4536–4541. https://doi.org/10.1074/jbc.M207293200

Nioi, P., McMahon, M., Itoh, K., Yamamoto, M., Hayes, J.D., 2003. Identification of a novel Nrf2-regulated antioxidant response element (ARE) in the mouse NAD(P)H:quinone oxidoreductase 1 gene: reassessment of the ARE consensus sequence. Biochem. J. 374, 337–48. https://doi.org/10.1042/BJ20030754

Nioi, P., Nguyen, T., Sherratt, P.J., Pickett, C.B., 2005. The carboxy-terminal Neh3 domain of Nrf2 is required for transcriptional activation. Mol. Cell. Biol. 25, 10895–10906. https://doi.org/10.1128/MCB.25.24.10895-10906.2005

Niture, S.K., Jain, A.K., Jaiswal, A.K., 2009. Antioxidant-induced modification of INrf2 cysteine 151 and PKC-delta-mediated phosphorylation of Nrf2 serine 40 are both required for stabilization and nuclear translocation of Nrf2 and increased drug resistance. J. Cell Sci. 122, 4452–4464. https://doi.org/10.1242/jcs.074286

Numazawa, S., Ishikawa, M., Yoshida, A., Tanaka, S., Yoshida, T., 2003. Atypical protein kinase C mediates activation of NF-E2-related factor 2 in response to oxidative stress. Am. J. Physiol. Cell Physiol. 285, C334-42. https://doi.org/10.1152/ajpcell.00043.2003

Obeso, J.A., Rodríguez-Oroz, M.C., Benitez-Temino, B., Blesa, F.J., Guridi, J., Marin, C., Rodriguez, M., 2008. Functional organization of the basal ganglia: Therapeutic implications for Parkinson's disease. Mov. Disord. https://doi.org/10.1002/mds.22062

Obuobi, S., Karatayev, S., Chai, C.L.L., Ee, P.L.R., Mátyus, P., 2016. The role of modulation of antioxidant enzyme systems in the treatment of neurodegenerative diseases. J. Enzyme Inhib. Med. Chem. 6366, 1–11. https://doi.org/10.1080/14756366.2016.1205047

Ogura, M., Yamaki, J., Homma, M.K., Homma, Y., 2014. Phosphorylation of flotillin-1 by mitochondrial c-Src is required to prevent the production of reactive oxygen species. FEBS Lett. 588, 2837–2843. https://doi.org/10.1016/j.febslet.2014.06.044

Ogura, M., Yamaki, J., Homma, M.K., Homma, Y., 2012. Mitochondrial c-Src regulates cell survival through phosphorylation of respiratory chain components. Biochem. J. 447, 281–289. https://doi.org/10.1042/BJ20120509

Oguro, A., Kubota, H., Shimizu, M., Ishiura, S., Atomi, Y., 2011. Protective role of the ubiquitin binding protein Tollip against the toxicity of polyglutamine-expansion proteins. Neurosci. Lett. https://doi.org/10.1016/j.neulet.2011.08.043

Okamoto, K., 2014. Organellophagy: Eliminating cellular building blocks via selective autophagy. J. Cell Biol. https://doi.org/10.1083/jcb.201402054

Okita, S., Morigaki, R., Koizumi, H., Kaji, R., Nagahiro, S., Goto, S., 2012. Cell type-specific localization of optineurin in the striatal neurons of mice: Implications for neuronal vulnerability in Huntington's disease. Neuroscience. https://doi.org/10.1016/j.neuroscience.2011.11.059

Oliet, H.R., Papouin, T., 2014. Organization , control and function of extrasynaptic NMDA receptors. Philos. Trans. R. Soc. 18–21. https://doi.org/10.1098/rstb.2013.0601

Oliveira, A.M., Cardoso, S.M., Ribeiro, M., Seixas, R.S.G.R., Silva, A.M.S., Rego, A.C., 2015a. Protective effects of 3-alkyl luteolin derivatives are mediated by Nrf2 transcriptional activity and decreased oxidative stress in Huntington's disease mouse striatal cells. Neurochem. Int. 91, 1–12. https://doi.org/10.1016/j.neuint.2015.10.004

Oliveira, A.M., Cardoso, S.M., Ribeiro, M., Seixas, R.S.G.R., Silva, A.M.S., Rego, A.C., 2015b. Protective effects of 3-alkyl luteolin derivatives are mediated by Nrf2 transcriptional activity and decreased oxidative stress in Huntington's disease mouse striatal cells. Neurochem. Int. 91, 1–12. https://doi.org/10.1016/j.neuint.2015.10.004

Oliveira, J.M.A., Chen, S., Almeida, S., Riley, R., Goncalves, J., Oliveira, C.R., Hayden, M.R., Nicholls, D.G., Ellerby, L.M., Rego, A.C., 2006. Mitochondrial-Dependent Ca2+ Handling in Huntington's Disease Striatal Cells: Effect of Histone Deacetylase Inhibitors. J. Neurosci. 26, 11174–11186. https://doi.org/10.1523/JNEUROSCI.3004-06.2006

Oliveira, J.M.A., Jekabsons, M.B., Chen, S., Lin, A., Rego, A.C., Gonçalves, J., Ellerby, L.M., Nicholls, D.G., 2007. Mitochondrial dysfunction in Huntington's disease: The bioenergetics of isolated and in situ mitochondria from transgenic mice. J. Neurochem. https://doi.org/10.1111/j.1471-4159.2006.04361.x

Ooi, B., Goh, B., Yap, W., 2017. Oxidative Stress in Cardiovascular Diseases: Involvement of Nrf2 Antioxidant Redox Signaling in Macrophage Foam Cells Formation. Int. J. Mol. Sci. 18, 2336. https://doi.org/10.3390/ijms18112336

Orr, A.L., Li, S., Wang, C.-E., Li, H., Wang, J., Rong, J., Xu, X., Mastroberardino, P.G., Greenamyre, J.T., Li, X.-J., 2008. N-Terminal Mutant Huntingtin Associates with Mitochondria and Impairs Mitochondrial

Trafficking. J. Neurosci. 28, 2783–2792. https://doi.org/10.1523/JNEUROSCI.0106-08.2008

Orsi, A., Razi, M., Dooley, H.C., Robinson, D., Weston, A.E., Collinson, L.M., Tooze, S.A., 2012. Dynamic and transient interactions of Atg9 with autophagosomes, but not membrane integration, are required for autophagy. Mol. Biol. Cell. https://doi.org/10.1091/mbc.E11-09-0746

Palikaras, K., Tavernarakis, N., 2014. Mitochondrial homeostasis: The interplay between mitophagy and mitochondrial biogenesis. Exp. Gerontol. https://doi.org/10.1016/j.exger.2014.01.021

Palo, J., Somer, H., Ikonen, E., Karila, L., Peltonen, L., 1987. LOW PREVALENCE OF HUNTINGTON'S DISEASE IN FINLAND. Lancet 330, 805–806. https://doi.org/10.1016/S0140-6736(87)92545-1

Pandey, M., Varghese, M., Sindhu, K.M., Sreetama, S., Navneet, A.K., Mohanakumar, K.P., Usha, R., 2008. Mitochondrial NAD+-linked State 3 respiration and complex-I activity are compromised in the cerebral cortex of 3-nitropropionic acid-induced rat model of Huntington's disease. J. Neurochem. 104, 420–434. https://doi.org/10.1111/j.1471-4159.2007.04996.x

Pandey, U.B., Nie, Z., Batlevi, Y., McCray, B.A., Ritson, G.P., Nedelsky, N.B., Schwartz, S.L., DiProspero, N.A., Knight, M.A., Schuldiner, O., Padmanabhan, R., Hild, M., Berry, D.L., Garza, D., Hubbert, C.C., Yao, T.-P., Baehrecke, E.H., Taylor, J.P., 2007. HDAC6 rescues neurodegeneration and provides an essential link between autophagy and the UPS. Nature 447, 860–864. https://doi.org/10.1038/nature05853

Pankiv, S., Clausen, T.H., Lamark, T., Brech, A., Bruun, J.A., Outzen, H., Øvervatn, A., Bjørkøy, G., Johansen, T., 2007. p62/SQSTM1 binds directly to Atg8/LC3 to facilitate degradation of ubiquitinated protein aggregates by autophagy*[S]. J. Biol. Chem. https://doi.org/10.1074/jbc.M702824200

Panov, A. V., Gutekunst, C.A., Leavitt, B.R., Hayden, M.R., Burke, J.R., Strittmatter, W.J., Greenamyre, J.T., 2002. Early mitochondrial calcium

defects in Huntington's disease are a direct effect of polyglutamines. Nat. Neurosci. https://doi.org/10.1038/nn884

Papouin, T., Ladépêche, L., Ruel, J., Sacchi, S., Labasque, M., Hanini, M., Groc, L., Pollegioni, L., Mothet, J.P., Oliet, S.H.R., 2012. Synaptic and extrasynaptic NMDA receptors are gated by different endogenous coagonists. Cell 150, 633–646. https://doi.org/10.1016/j.cell.2012.06.029

Parsons, S.J., Parsons, J.T., 2004. Src family kinases, key regulators of signal transduction. Oncogene. https://doi.org/10.1038/sj.onc.1208160

Pascoli, V., Besnard, A., Herv, D., Pags, C., Heck, N., Girault, J.A., Caboche, J., Vanhoutte, P., 2011. Cyclic adenosine monophosphateindependent tyrosine phosphorylation of NR2B mediates cocaine-induced extracellular signal-regulated kinase activation. Biol. Psychiatry. https://doi.org/10.1016/j.biopsych.2010.08.031

Pellman, J.J., Hamilton, J., Brustovetsky, T., Brustovetsky, N., 2015. Ca^{2+} handling in isolated brain mitochondria and cultured neurons derived from the YAC128 mouse model of Huntington's disease. J. Neurochem. https://doi.org/10.1111/jnc.13165

Peña-Sánchez, M., Riverón-Forment, G., Zaldívar-Vaillant, T., Soto-Lavastida, A., Borrero-Sánchez, J., Lara-Fernández, G., Esteban-Hernández, E.M., Hernández-Díaz, Z., González-Quevedo, A., Fernández-Almirall, I., Pérez-López, C., Castillo-Casañas, Y., Martínez-Bonne, O., Cabrera-Rivero, A., Valdés-Ramos, L., Guerra-Badía, R., Fernández-Carriera, R., Menéndez-Sainz, M.C., González-García, S., 2015. Association of status redox with demographic, clinical and imaging parameters in patients with Huntington's disease. Clin. Biochem. https://doi.org/10.1016/j.clinbiochem.2015.06.014

Pérez-Severiano, F., Ríos, C., Segovia, J., 2000. Striatal oxidative damage parallels the expression of a neurological phenotype in mice transgenic for the mutation of Huntington's disease. Brain Res. https://doi.org/10.1016/S0006-8993(00)02082-5

Petersen, M.H., Budtz-Jørgensen, E., Sørensen, S.A., Nielsen, J.E., Hjermind,

L.E., Vinther-Jensen, T., Nielsen, S.M.B., Nørremølle, A., 2014. Reduction in mitochondrial DNA copy number in peripheral leukocytes after onset of Huntington's disease. Mitochondrion. https://doi.org/10.1016/j.mito.2014.05.001

Pickart, C.M., Cohen, R.E., 2004. Proteasomes and their kin: Proteases in the machine age. Nat. Rev. Mol. Cell Biol. https://doi.org/10.1038/nrm1336

Pickart, C.M., Fushman, D., 2004. Polyubiquitin chains: Polymeric protein signals. Curr. Opin. Chem. Biol. https://doi.org/10.1016/j.cbpa.2004.09.009

Pickel, V.M., Chan, J., Sesack, S.R., 1992. Cellular basis for interactions between catecholaminergic afferents and neurons containing leu-enkephalin-like immunoreactivity in rat caudate-putamen nuclei. J. Neurosci. Res. 31, 212–230. https://doi.org/10.1002/jnr.490310203

Pickles, S., Vigié, P., Youle, R.J., 2018. Mitophagy and Quality Control Mechanisms in Mitochondrial Maintenance. Curr. Biol. https://doi.org/10.1016/j.cub.2018.01.004

Pickrell, A.M., Fukui, H., Wang, X., Pinto, M., Moraes, C.T., 2011. The striatum is highly susceptible to mitochondrial oxidative phosphorylation dysfunctions. J. Neurosci. https://doi.org/10.1523/JNEUROSCI.6223-10.2011

Pickrell, A.M., Youle, R.J., 2015. The roles of PINK1, Parkin, and mitochondrial fidelity in parkinson's disease. Neuron. https://doi.org/10.1016/j.neuron.2014.12.007

Pitts, A., Dailey, K., Newington, J.T., Chien, A., Arseneault, R., Cann, T., Thompson, L.M., Cumming, R.C., 2012. Dithiol-based compounds maintain expression of antioxidant protein peroxiredoxin 1 that counteracts toxicity of mutant huntingtin. J. Biol. Chem. https://doi.org/10.1074/jbc.M111.334565

Pizzino, G., Irrera, N., Cucinotta, M., Pallio, G., Mannino, F., Arcoraci, V., Squadrito, F., Altavilla, D., Bitto, A., 2017. Oxidative Stress: Harms and Benefits for Human Health. Oxid. Med. Cell. Longev. 2017, 1–13.

https://doi.org/10.1155/2017/8416763

Polson, H.E.J., De Lartigue, J., Rigden, D.J., Reedijk, M., Urbé, S., Clague, M.J., Tooze, S.A., 2010. Mammalian Atg18 (WIPI2) localizes to omegasome-anchored phagophores and positively regulates LC3 lipidation. Autophagy. https://doi.org/10.4161/auto.6.4.11863

Ponten, H., Kullingsjö, J., Lagerkvist, S., Martin, P., Pettersson, F., Sonesson, C., Waters, S., Waters, N., 2010. In vivo pharmacology of the dopaminergic stabilizer pridopidine. Eur. J. Pharmacol. https://doi.org/10.1016/j.ejphar.2010.07.023

Portera-Cailliau, C., Price, D.L., Martin, L.J., 2010. N-Methyl-d-Aspartate Receptor Proteins NR2A and NR2B Are Differentially Distributed in the Developing Rat Central Nervous System as Revealed by Subunit-Specific Antibodies. J. Neurochem. https://doi.org/10.1046/j.1471-4159.1996.66020692.x

Qi, L., Zhang, X.D., Wu, J.C., Lin, F., Wang, J., DiFiglia, M., Qin, Z.H., 2012. The Role of Chaperone-Mediated Autophagy in Huntingtin Degradation. PLoS One. https://doi.org/10.1371/journal.pone.0046834

Rada, P., Rojo, A.I., Chowdhry, S., McMahon, M., Hayes, J.D., Cuadrado, A., 2011. SCF/{beta}-TrCP promotes glycogen synthase kinase 3-dependent degradation of the Nrf2 transcription factor in a Keap1-independent manner. Mol. Cell. Biol. 31, 1121–33. https://doi.org/10.1128/MCB.01204-10

Rada, P., Rojo, A.I., Evrard-Todeschi, N., Innamorato, N.G., Cotte, A., Jaworski, T., Tobón-Velasco, J.C., Devijver, H., García-Mayoral, M.F., Van Leuven, F., Hayes, J.D., Bertho, G., Cuadrado, A., Tobon-Velasco, J.C., Devijver, H., Garcia-Mayoral, M.F., Van Leuven, F., Hayes, J.D., Bertho, G., Cuadrado, A., 2012. Structural and functional characterization of Nrf2 degradation by the glycogen synthase kinase 3/β-TrCP axis. Mol. Cell. Biol. 32, 3486–99. https://doi.org/10.1128/MCB.00180-12

Ranen, N.G., Stine, O.C., Abbott, M.H., Sherr, M., Codori, A.M., Franz, M.L.,

Chao, N.I., Chung, A.S., Pleasant, N., Callahan, C., 1995. Anticipation and instability of IT-15 (CAG)n repeats in parent-offspring pairs with Huntington disease. Am. J. Hum. Genet. 57, 593–602.

Ratovitski, T., Chighladze, E., Arbez, N., Boronina, T., Herbrich, S., Cole, R.N., Ross, C.A., 2012. Huntingtin protein interactions altered by polyglutamine expansion as determined by quantitative proteomic analysis. Cell Cycle. https://doi.org/10.4161/cc.20423

Ravikumar, B., 2002. Aggregate-prone proteins with polyglutamine and polyalanine expansions are degraded by autophagy. Hum. Mol. Genet. https://doi.org/10.1093/hmg/11.9.1107

Ravikumar, B., Vacher, C., Berger, Z., Davies, J.E., Luo, S., Oroz, L.G., Scaravilli, F., Easton, D.F., Duden, R., O'Kane, C.J., Rubinsztein, D.C., 2004. Inhibition of mTOR induces autophagy and reduces toxicity of polyglutamine expansions in fly and mouse models of Huntington disease. Nat. Genet. https://doi.org/10.1038/ng1362

Rechsteiner, M., Hill, C.P., 2005. Mobilizing the proteolytic machine: Cell biological roles of proteasome activators and inhibitors. Trends Cell Biol. https://doi.org/10.1016/j.tcb.2004.11.003

Reddy, P.H., Shirendeb, U.P., 2012. Mutant huntingtin, abnormal mitochondrial dynamics, defective axonal transport of mitochondria, and selective synaptic degeneration in Huntington's disease. Biochim. Biophys. Acta - Mol. Basis Dis. 1822, 101–110. https://doi.org/10.1016/j.bbadis.2011.10.016

Reilmann, R., McGarry, A., Grachev, I.D., Savola, J.-M., Borowsky, B., Eyal, E., Gross, N., Langbehn, D., Schubert, R., Wickenberg, A.T., Papapetropoulos, S., Hayden, M., Squitieri, F., Kieburtz, K., Landwehrmeyer, G.B., Agarwal, P., Anderson, K.E., Aziz, N.A., Azulay, J.-P., Bachoud-Levi, A.C., Barker, R., Bebak, A., Beuth, M., Biglan, K., Blin, S., Bohlen, S., Bonelli, R., Caldwell, S., Calvas, F., Carlos, J., Castagliuolo, S., Chong, T., Chua, P., Coleman, A., Corey-Bloom, J., Cousins, R.,

Craufurd, D., Davison, J., Decorte, E., De Michele, G., Dornhege, L., Feigin, A., Gallehawk, S., Gauteul, P., Gonzales, C., Griffith, J., Gustov, A., Guttman, M., Heim, B., Heller, H., Hjermind, L., Illarioshkin, S., Ivanko, L., Jaynes, J., Jenckes, M., Kaminski, B., Kampstra, A., Konkel, A., Kopishinskaya, S., Krystkowiak, P., Komati, S.K., Kwako, A., Lakoning, S., Latipova, G., Leavitt, B., Loy, C., MacFarlane, C., Madsen, L., Marder, K., Mason, S., Mendis, N., Mendis, T., Nemeth, A., Nevitt, L., Norris, V., O'Neill, C., Olivier, A., Orth, M., Owens, A., Panegyres, P., Perlman, S., Preston, J., Priller, J., Puch, A., Quarrell, O., Ragosta, D., Rialland, A., Rickards, H., Romoli, A.M., Ross, C., Rosser, A., Rudzinska, M., Russo, C. V., Saft, C., Segro, V., Seppi, K., Shannon, B., Shprecher, D., Simonin, C., Skitt, Z., Slawek, J., Soliveri, P., Sorbi, S., Squitieri, F., Suski, V., Stepniak, I., Sungmee, P., Temirbaeva, S., Testa, C., Torvin-Moller, A., Uhl, S., Vangsted-Hansen, C., Verny, C., Wall, P., Walker, F., Wasserman, P., Witkowski, G., Wright, J., Zalyalova, Z., Zielonka, D., 2019. Safety and efficacy of pridopidine in patients with Huntington's disease (PRIDE-HD): a phase 2, randomised, placebo-controlled, multicentre, dose-ranging study. Lancet Neurol. 18, 165–176. https://doi.org/10.1016/S1474-4422(18)30391-0

Rhee, S.G., Kil, I.S., 2017. Multiple Functions and Regulation of Mammalian Peroxiredoxins. Annu. Rev. Biochem. 86, 749–775. https://doi.org/10.1146/annurev-biochem-060815-014431

Ribeiro, M., Rosenstock, T.R., Cunha-Oliveira, T., Ferreira, I.L., Oliveira, C.R., Rego, A.C., 2012. Glutathione redox cycle dysregulation in Huntington's disease knock-in striatal cells. Free Radic. Biol. Med. 53, 1857–1867. https://doi.org/10.1016/j.freeradbiomed.2012.09.004

Ribeiro, M., Rosenstock, T.R., Oliveira, A.M., Oliveira, C.R., Rego, A.C., 2014. Insulin and IGF-1 improve mitochondrial function in a PI-3K/Akt-dependent manner and reduce mitochondrial generation of reactive oxygen species in Huntington's disease knock-in striatal cells. Free Radic. Biol. Med. 74, 129–44. https://doi.org/10.1016/j.freeradbiomed.2014.06.023

Ribeiro, M., Silva, A.C., Rodrigues, J., Naia, L., Rego, A.C., 2013. Oxidizing Effects of Exogenous Stressors in Huntington's Disease Knock-in Striatal Cells—Protective Effect of Cystamine and Creatine. Toxicol. Sci. 136, 487–499. https://doi.org/10.1093/toxsci/kft199

Rigamonti, D., Bauer, J.H., De-Fraja, C., Conti, L., Sipione, S., Sciorati, C., Clementi, E., Hackam, A., Hayden, M.R., Li, Y., Cooper, J.K., Ross, C.A., Govoni, S., Vincenz, C., Cattaneo, E., 2000. Wild-type huntingtin protects from apoptosis upstream of caspase-3. J. Neurosci. https://doi.org/10.1523/jneurosci.20-10-03705.2000

Rockabrand, E., Slepko, N., Pantalone, A., Nukala, V.N., Kazantsev, A., Marsh, J.L., Sullivan, P.G., Steffan, J.S., Sensi, S.L., Thompson, L.M., 2007. The first 17 amino acids of Huntingtin modulate its sub-cellular localization, aggregation and effects on calcium homeostasis. Hum. Mol. Genet. https://doi.org/10.1093/hmg/ddl440

Rodic, S., Vincent, M.D., 2017. Reactive oxygen species (ROS) are a key determinant of cancer's metabolic phenotype. Int. J. Cancer. https://doi.org/10.1002/ijc.31069

Rojo, A.I., Innamorato, N.G., Martín-Moreno, A.M., De Ceballos, M.L., Yamamoto, M., Cuadrado, A., 2010. Nrf2 regulates microglial dynamics and neuroinflammation in experimental Parkinson's disease. Glia 58, 588–598. https://doi.org/10.1002/glia.20947

Rosas, H.D., Koroshetz, W.J., Chen, Y.I., Skeuse, C., Vangel, M., Cudkowicz, M.E., Caplan, K., Marek, K., Seidman, L.J., Makris, N., Jenkins, B.G., Goldstein, J.M., 2003. Evidence for more widespread cerebral pathology in early HD: An MRI-based morphometric analysis. Neurology. https://doi.org/10.1212/01.WNL.0000065888.88988.6E

Rosenblatt, A., Kumar, B. V., Mo, A., Welsh, C.S., Margolis, R.L., Ross, C.A., 2012. Age, CAG repeat length, and clinical progression in Huntington's disease. Mov. Disord. 27, 272–276. https://doi.org/10.1002/mds.24024

Rosenstock, T.R., De Brito, O.M., Lombardi, V., Louros, S., Ribeiro, M.,

Almeida, S., Ferreira, I.L., Oliveira, C.R., Rego, A.C., 2011. FK506 ameliorates cell death features in Huntington's disease striatal cell models. Neurochem. Int. https://doi.org/10.1016/j.neuint.2011.04.009

Roskoski, R., 2015. Src protein-tyrosine kinase structure, mechanism, and small molecule inhibitors. Pharmacol. Res. 94, 9–25. https://doi.org/10.1016/j.phrs.2015.01.003

Roskoski, R., 2004. Src protein-tyrosine kinase structure and regulation. Biochem. Biophys. Res. Commun. 324, 1155–1164. https://doi.org/10.1016/j.bbrc.2004.09.171

Ross, C.A., Aylward, E.H., Wild, E.J., Langbehn, D.R., Long, J.D., Warner, J.H., Scahill, R.I., Leavitt, B.R., Stout, J.C., Paulsen, J.S., Reilmann, R., Unschuld, P.G., Wexler, A., Margolis, R.L., Tabrizi, S.J., 2014a. Huntington disease: natural history, biomarkers and prospects for therapeutics. Nat. Rev. Neurol. 10, 204–216. https://doi.org/10.1038/nrneurol.2014.24

Ross, C.A., Pantelyat, A., Kogan, J., Brandt, J., 2014b. Determinants of functional disability in Huntington's disease: Role of cognitive and motor dysfunction. Mov. Disord. https://doi.org/10.1002/mds.26012

Ross, C.A., Tabrizi, S.J., 2011. Huntington's disease: from molecular pathogenesis to clinical treatment. Lancet Neurol. 10, 83–98. https://doi.org/10.1016/S1474-4422(10)70245-3

Rué, L., López-Soop, G., Gelpi, E., Martínez-Vicente, M., Alberch, J., Pérez-Navarro, E., 2013. Brain region- and age-dependent dysregulation of p62 and NBR1 in a mouse model of Huntington's disease. Neurobiol. Dis. https://doi.org/10.1016/j.nbd.2012.12.008

Rui, Y.N., Xu, Z., Patel, B., Chen, Z., Chen, D., Tito, A., David, G., Sun, Y., Stimming, E.F., Bellen, H.J., Cuervo, A.M., Zhang, S., 2015. Huntingtin functions as a scaffold for selective macroautophagy. Nat. Cell Biol. https://doi.org/10.1038/ncb3101

Russell, R.C., Tian, Y., Yuan, H., Park, H.W., Chang, Y.Y., Kim, J., Kim, H.,

Neufeld, T.P., Dillin, A., Guan, K.L., 2013. ULK1 induces autophagy by phosphorylating Beclin-1 and activating VPS34 lipid kinase. Nat. Cell Biol. https://doi.org/10.1038/ncb2757

Ryan, T.A., Tumbarello, D.A., 2018. Optineurin: A coordinator of membrane-associated cargo trafficking and autophagy. Front. Immunol. https://doi.org/10.3389/fimmu.2018.01024

Rybin, V.O., Guo, J., Sabri, A., Elouardighi, H., Schaefer, E., Steinberg, S.F., 2004. Stimulus-specific Differences in Protein Kinase Cδ Localization and Activation Mechanisms in Cardiomyocytes. J. Biol. Chem. 279, 19350–19361. https://doi.org/10.1074/jbc.M311096200

Sabharwal, S.S., Schumacker, P.T., 2014. Mitochondrial ROS in cancer: Initiators, amplifiers or an Achilles' heel? Nat. Rev. Cancer. https://doi.org/10.1038/nrc3803

Sadagurski, M., Cheng, Z., Rozzo, A., Palazzolo, I., Kelley, G.R., Dong, X., Krainc, D., White, M.F., 2011. IRS2 increases mitochondrial dysfunction and oxidative stress in a mouse model of Huntington disease. J. Clin. Invest. https://doi.org/10.1172/JCI46305

Saft, C., Zange, J., Andrich, J., Müller, K., Lindenberg, K., Landwehrmeyer, B., Vorgerd, M., Kraus, P.H., Przuntek, H., Schöls, L., 2005. Mitochondrial impairment in patients and asymptomatic mutation carriers of Huntington's disease. Mov. Disord. 20, 674–679. https://doi.org/10.1002/mds.20373

Sahlholm, K., Sijbesma, J.W.A., Maas, B., Kwizera, C., Marcellino, D., Ramakrishnan, N.K., Dierckx, R.A.J.O., Elsinga, P.H., Van Waarde, A., 2015. Pridopidine selectively occupies sigma-1 rather than dopamine D2 receptors at behaviorally active doses. Psychopharmacology (Berl). https://doi.org/10.1007/s00213-015-3997-8

Salter, M.W., Kalia, L. V, 2004. Src kinases: a hub for NMDA receptor regulation. Nat. Rev. Neurosci. 5, 317–328. https://doi.org/10.1038/nrn1368

Salvi, M., Brunati, A.M., Bordin, L., La Rocca, N., Clari, G., Toninello, A., 2002.

Characterization and location of Src-dependent tyrosine phosphorylation in rat brain mitochondria. Biochim. Biophys. Acta 1589, 181–195. https://doi.org/12007793

Salvi, M., Stringaro, A., Brunati, A.M., Agostinelli, E., Arancia, G., Clari, G., Toninello, A., 2004. Tyrosine phosphatase activity in mitochondria: Presence of Shp-2 phosphatase in mitochondria. Cell. Mol. Life Sci. 61, 2393–2404. https://doi.org/10.1007/s00018-004-4211-z

Sandhir, R., Sood, A., Mehrotra, A., Kamboj, S.S., 2012. N-acetylcysteine reverses mitochondrial dysfunctions and behavioral abnormalities in 3-nitropropionic acid-induced Huntington's disease. Neurodegener. Dis. https://doi.org/10.1159/000334273

Sandilands, E., Frame, M.C., 2008. Endosomal trafficking of Src tyrosine kinase. Trends Cell Biol. 18, 322–329. https://doi.org/10.1016/j.tcb.2008.05.004

Santamaría, A., Pérez-Severiano, F., Rodríguez-Martínez, E., Maldonado, P.D., Pedraza-Chaverri, J., Ríos, C., Segovia, J., 2001. Comparative analysis of superoxide dismutase activity between acute pharmacological models and a transgenic mouse model of Huntington's disease. Neurochem. Res. 26, 419–24. https://doi.org/10.1023/a:1010911417383

Sanz-Clemente, A., Matta, J.A., Isaac, J.T.R., Roche, K.W., 2010. Casein Kinase 2 Regulates the NR2 Subunit Composition of Synaptic NMDA Receptors. Neuron. https://doi.org/10.1016/j.neuron.2010.08.011

Sapp, E., Schwarz, C., Chase, K., Bhide, P.G., Young, A.B., Penney, J., Vonsattel, J.P., Aronin, N., DiFiglia, M., 1997. Huntingtin localization in brains of normal and Huntington's disease patients. Ann. Neurol. https://doi.org/10.1002/ana.410420411

Sardanelli, A.M., Signorile, A., Nuzzi, R., Rasmo, D. De, Technikova-Dobrova, Z., Drahota, Z., Occhiello, A., Pica, A., Papa, S., 2006. Occurrence of A-kinase anchor protein and associated cAMP-dependent protein kinase in the inner compartment of mammalian mitochondria. FEBS Lett. 580, 5690–

5696. https://doi.org/10.1016/j.febslet.2006.09.020

Sardiello, M., Palmieri, M., di Ronza, A., Medina, D.L., Valenza, M., Gennarino, V.A., Di Malta, C., Donaudy, F., Embrione, V., Polishchuk, R.S., Banfi, S., Parenti, G., Cattaneo, E., Ballabio, A., 2009. A Gene Network Regulating Lysosomal Biogenesis and Function. Science (80-.). 325, 473–477. https://doi.org/10.1126/science.1174447

Sathasivam, K., Hobbs, C., Turmaine, M., Mangiarini, L., Mahal, A., Bertaux, F., Wanker, E.E., Doherty, P., Davies, S.W., Bates, G.P., 1999. Formation of Polyglutamine Inclusions in Non-CNS Tissue. Hum. Mol. Genet. 8, 813–822. https://doi.org/10.1093/hmg/8.5.813

Sawiak, S.J., Wood, N.I., Williams, G.B., Morton, A.J., Carpenter, T.A., 2009. Use of magnetic resonance imaging for anatomical phenotyping of the R6/2 mouse model of Huntington's disease. Neurobiol. Dis. https://doi.org/10.1016/j.nbd.2008.09.017

Scherzinger, E., Lurz, R., Turmaine, M., Mangiarini, L., Hollenbach, B., Hasenbank, R., Bates, G.P., Davies, S.W., Lehrach, H., Wanker, E.E., 1997. Huntingtin-encoded polyglutamine expansions form amyloid-like protein aggregates in vitro and in vivo. Cell 90, 549–558. https://doi.org/10.1016/S0092-8674(00)80514-0

Schieber, M., Chandel, N.S., 2014. ROS function in redox signaling and oxidative stress. Curr. Biol. https://doi.org/10.1016/j.cub.2014.03.034

Schilling, B., Gafni, J., Torcassi, C., Cong, X., Row, R.H., LaFevre-Bernt, M.A., Cusack, M.P., Ratovitski, T., Hirschhorn, R., Ross, C.A., Gibson, B.W., Ellerby, L.M., 2006. Huntingtin phosphorylation sites mapped by mass spectrometry: Modulation of cleavage and toxicity. J. Biol. Chem. https://doi.org/10.1074/jbc.M513507200

Schilling, G., Becher, M.W., Sharp, A.H., Jinnah, H.A., Duan, K., Kotzuk, J.A., Slunt, H.H., Ratovitski, T., Cooper, J.K., Jenkins, N.A., Copeland, N.G., Price, D.L., Ross, C.A., Borchelt, D.R., 1999. Intranuclear inclusions and neuritic aggregates in transgenic mice expressing a mutant N-terminal

fragment of huntingtin. Hum. Mol. Genet.

Semaka, A., Collins, J.A., Hayden, M.R., 2009. Unstable familial transmissions of Huntington disease alleles with 27-35 CAG repeats (intermediate alleles). Am. J. Med. Genet. Part B Neuropsychiatr. Genet. 9999B, n/a-n/a. https://doi.org/10.1002/ajmg.b.30970

Settembre, C., Di Malta, C., Polito, V.A., Garcia Arencibia, M., Vetrini, F., Erdin, S., Erdin, S.U., Huynh, T., Medina, D., Colella, P., Sardiello, M., Rubinsztein, D.C., Ballabio, A., 2011. TFEB links autophagy to lysosomal biogenesis. Science 332, 1429–33. https://doi.org/10.1126/science.1204592

Settembre, C., Zoncu, R., Medina, D.L., Vetrini, F., Erdin, S., Erdin, S., Huynh, T., Ferron, M., Karsenty, G., Vellard, M.C., Facchinetti, V., Sabatini, D.M., Ballabio, A., 2012. A lysosome-to-nucleus signalling mechanism senses and regulates the lysosome via mTOR and TFEB. EMBO J. 31, 1095–1108. https://doi.org/10.1038/emboj.2012.32

Shefa, U., Jeong, N.Y., Song, I.O., Chung, H.J., Kim, D., Jung, J., Huh, Y., 2019. Mitophagy links oxidative stress conditions and neurodegenerative diseases. Neural Regen. Res. https://doi.org/10.4103/1673-5374.249218

Shen, W.C., Li, H.Y., Chen, G.C., Chern, Y., Tu, P.H., 2015. Mutations in the ubiquitin-binding domain of OPTN/optineurin interfere with autophagy-mediated degradation of misfolded proteins by a dominant-negative mechanism. Autophagy. https://doi.org/10.4161/auto.36098

Shibata, M., Lu, T., Furuya, T., Degterev, A., Mizushima, N., Yoshimori, T., MacDonald, M., Yankner, B., Yuan, J., 2006. Regulation of intracellular accumulation of mutant huntingtin by beclin 1. J. Biol. Chem. https://doi.org/10.1074/jbc.M600364200

Shirendeb, U., Reddy, A.P., Manczak, M., Calkins, M.J., Mao, P., Tagle, D.A., Reddy, P.H., 2011. Abnormal mitochondrial dynamics, mitochondrial loss and mutant huntingtin oligomers in Huntington's disease: Implications for selective neuronal damage. Hum. Mol. Genet. 20, 1438–1455.

https://doi.org/10.1093/hmg/ddr024

Shirendeb, U.P., Calkins, M.J., Manczak, M., Anekonda, V., Dufour, B., McBride, J.L., Mao, P., Reddy, P.H., 2012. Mutant Huntingtin's interaction with mitochondrial protein Drp1 impairs mitochondrial biogenesis and causes defective axonal transport and synaptic degeneration in Huntington's disease. Hum. Mol. Genet. https://doi.org/10.1093/hmg/ddr475

Siddiqui, A., Rivera-Sánchez, S., Castro, M.D.R., Acevedo-Torres, K., Rane, A., Torres-Ramos, C. a, Nicholls, D.G., Andersen, J.K., Ayala-Torres, S., 2012. Mitochondrial DNA damage is associated with reduced mitochondrial bioenergetics in Huntington's disease. Free Radic. Biol. Med. 53, 1478–88. https://doi.org/10.1016/j.freeradbiomed.2012.06.008

Sieradzan, K.A., Mann, D.M., 2001. The selective vulnerability of nerve cells in Huntington's disease. Neuropathol Appl Neurobiol 27, 1–21. https://doi.org/10.1046/j.0305-1846.2001.00299.x

Sies, H., 2017. Hydrogen peroxide as a central redox signaling molecule in physiological oxidative stress: Oxidative eustress. Redox Biol. https://doi.org/10.1016/j.redox.2016.12.035

Silva, A.C., Almeida, S., Laço, M., Duarte, A.I., Domingues, J., Oliveira, C.R., Januário, C., Rego, A.C., 2013a. Mitochondrial respiratory chain complex activity and bioenergetic alterations in human platelets derived from pre-symptomatic and symptomatic Huntington's disease carriers. Mitochondrion 13, 801–809. https://doi.org/10.1016/j.mito.2013.05.006

Silva, A.C., Almeida, S., Laço, M., Duarte, A.I., Domingues, J., Oliveira, C.R., Januário, C., Rego, A.C., 2013b. Mitochondrial respiratory chain complex activity and bioenergetic alterations in human platelets derived from pre-symptomatic and symptomatic huntington's disease carriers. Mitochondrion. https://doi.org/10.1016/j.mito.2013.05.006

Simonsen, A., Birkeland, H.C.G., Gillooly, D.J., Mizushima, N., Kuma, A., Yoshimori, T., Slagsvold, T., Brech, A., Stenmark, H., 2004. Alfy, a novel

FYVE-domain-containing protein associated with protein granules and autophagic membranes. J. Cell Sci. https://doi.org/10.1242/jcs.01287

Singaraja, R.R., 2002. HIP14, a novel ankyrin domain-containing protein, links huntingtin to intracellular trafficking and endocytosis. Hum. Mol. Genet. https://doi.org/10.1093/hmg/11.23.2815

Slow, E.J., 2003. Selective striatal neuronal loss in a YAC128 mouse model of Huntington disease. Hum. Mol. Genet. 12, 1555–1567. https://doi.org/10.1093/hmg/ddg169

Smith, D.M., Chang, S.C., Park, S., Finley, D., Cheng, Y., Goldberg, A.L., 2007. Docking of the Proteasomal ATPases' Carboxyl Termini in the 20S Proteasome's α Ring Opens the Gate for Substrate Entry. Mol. Cell. https://doi.org/10.1016/j.molcel.2007.06.033

Smith, R., Tran, K., Smith, C., McDonald, M., Shejwalkar, P., Hara, K., 2016. The Role of the Nrf2/ARE Antioxidant System in Preventing Cardiovascular Diseases. Diseases 4, 34. https://doi.org/10.3390/diseases4040034

Song, C., Zhang, Y., Parsons, C.G., Liu, Y.F., 2003. Expression of polyglutamine-expanded huntingtin induces tyrosine phosphorylation of N-methyl-D-aspartate receptors. J. Biol. Chem. 278, 33364–33369. https://doi.org/10.1074/jbc.M304240200

Song, W., Chen, J., Petrilli, A., Liot, G., Klinglmayr, E., Zhou, Y., Poquiz, P., Tjong, J., Pouladi, M.A., Hayden, M.R., Masliah, E., Ellisman, M., Rouiller, I., Schwarzenbacher, R., Bossy, B., Perkins, G., Bossy-Wetzel, E., 2011. Mutant huntingtin binds the mitochondrial fission GTPase dynamin-related protein-1 and increases its enzymatic activity. Nat. Med. https://doi.org/10.1038/nm.2313

Sorolla, M.A., Rodríguez-Colman, M.J., Tamarit, J., Ortega, Z., Lucas, J.J., Ferrer, I., Ros, J., Cabiscol, E., 2010. Protein oxidation in Huntington disease affects energy production and vitamin B6 metabolism. Free Radic. Biol. Med. https://doi.org/10.1016/j.freeradbiomed.2010.05.016

Sosa, V., Moliné, T., Somoza, R., Paciucci, R., Kondoh, H., LLeonart, M.E., 2013. Oxidative stress and cancer: An overview. Ageing Res. Rev. 12, 376–390. https://doi.org/10.1016/j.arr.2012.10.004

Squitieri, F., Almqvist, E.W., Cannella, M., Cislaghi, G., Hayden, M.R., 2003. Predictive testing for persons at risk for homozygosity for CAG expansion in the Huntington disease gene. Clin. Genet. 64, 524–525. https://doi.org/10.1046/j.1399-0004.2003.00155.x

Squitieri, F., Griguoli, A., Capelli, G., Porcellini, A., D'Alessio, B., 2016. Epidemiology of Huntington disease: first post- HTT gene analysis of prevalence in Italy. Clin. Genet. 89, 367–370. https://doi.org/10.1111/cge.12574

St-Pierre, J., Drori, S., Uldry, M., Silvaggi, J.M., Rhee, J., Jäger, S., Handschin, C., Zheng, K., Lin, J., Yang, W., Simon, D.K., Bachoo, R., Spiegelman, B.M., 2006. Suppression of Reactive Oxygen Species and Neurodegeneration by the PGC-1 Transcriptional Coactivators. Cell. https://doi.org/10.1016/j.cell.2006.09.024

Stack, C., Ho, D., Wille, E., Calingasan, N.Y., Williams, C., Liby, K., Sporn, M., Dumont, M., Beal, M.F., 2010. Triterpenoids CDDO-ethyl amide and CDDO-trifluoroethyl amide improve the behavioral phenotype and brain pathology in a transgenic mouse model of Huntington's disease. Free Radic. Biol. Med. https://doi.org/10.1016/j.freeradbiomed.2010.03.017

Starling, A.J., André, V.M., Cepeda, C., De Lima, M., Chandler, S.H., Levine, M.S., 2005. Alterations in N-methyl-D-aspartate receptor sensitivity and magnesium blockade occur early in development in the R6/2 mouse model of Huntington's disease. J. Neurosci. Res. https://doi.org/10.1002/jnr.20651

Stefanatos, R., Sanz, A., 2018. The role of mitochondrial ROS in the aging brain. FEBS Lett. https://doi.org/10.1002/1873-3468.12902

Steinberg, S.F., 2015. Mechanisms for redox-regulation of protein kinase C. Front. Pharmacol. 6, 1–9. https://doi.org/10.3389/fphar.2015.00128

Stępkowski, T.M., Kruszewski, M.K., 2011. Molecular cross-talk between the NRF2/KEAP1 signaling pathway, autophagy, and apoptosis. Free Radic. Biol. Med. 50, 1186–1195. https://doi.org/10.1016/j.freeradbiomed.2011.01.033

Stoy, N., Mackay, G.M., Forrest, C.M., Christofides, J., Egerton, M., Stone, T.W., Darlington, L.G., 2005. Tryptophan metabolism and oxidative stress in patients with Huntington's disease. J. Neurochem. 93, 611–623. https://doi.org/10.1111/j.1471-4159.2005.03070.x

Strom, J., Chen, Q.M., 2017. Loss of Nrf2 promotes rapid progression to heart failure following myocardial infarction. Toxicol. Appl. Pharmacol. 327, 52–58. https://doi.org/10.1016/j.taap.2017.03.025

Sun, N., Malide, D., Liu, J., Rovira, I.I., Combs, C.A., Finkel, T., 2017. A fluorescence-based imaging method to measure in vitro and in vivo mitophagy using mt-Keima. Nat. Protoc. https://doi.org/10.1038/nprot.2017.060

Sun, N., Yun, J., Liu, J., Malide, D., Liu, C., Rovira, I.I., Holmström, K.M., Fergusson, M.M., Yoo, Y.H., Combs, C.A., Finkel, T., 2015. Measuring In Vivo Mitophagy. Mol. Cell. https://doi.org/10.1016/j.molcel.2015.10.009

Suopanki, J., Götz, C., Lutsch, G., Schiller, J., Harjes, P., Herrmann, A., Wanker, E.E., 2006. Interaction of huntingtin fragments with brain membranes - Clues to early dysfunction in Huntington's disease. J. Neurochem. https://doi.org/10.1111/j.1471-4159.2005.03620.x

Suzuki, T., Okamuranoji, K., 1995. NMDA Receptor Subunits ϵ1 (NR2A) and ϵ2 (NR2B) Are Substrates for Fyn in the Postsynaptic Density Fraction Isolated from the Rat Brain. Biochem. Biophys. Res. Commun. https://doi.org/10.1006/bbrc.1995.2662

Suzuki, T., Yamamoto, M., 2017. Stress-sensing mechanisms and the physiological roles of the Keap1–Nrf2 system during cellular stress. J. Biol. Chem. 292, 16817–16824. https://doi.org/10.1074/jbc.R117.800169

Szabadkai, G., Bianchi, K., Várnai, P., De Stefani, D., Wieckowski, M.R., Cavagna, D., Nagy, A.I., Balla, T., Rizzuto, R., 2006. Chaperone-mediated coupling of endoplasmic reticulum and mitochondrial Ca2+ channels. J. Cell Biol. https://doi.org/10.1083/jcb.200608073

Taguchi-Atarashi, N., Hamasaki, M., Matsunaga, K., Omori, H., Ktistakis, N.T., Yoshimori, T., Noda, T., 2010. Modulation of local Ptdins3P levels by the PI phosphatase MTMR3 regulates constitutive autophagy. Traffic. https://doi.org/10.1111/j.1600-0854.2010.01034.x

Takasu, M.A., Dalva, M.B., Zigmond, R.E., Greenberg, M.E., 2002. Modulation of NMDA receptor - Dependent calcium influx and gene expression through EphB receptors. Science (80-.). https://doi.org/10.1126/science.1065983

Tang, T.-S., Slow, E., Lupu, V., Stavrovskaya, I.G., Sugimori, M., Llinas, R., Kristal, B.S., Hayden, M.R., Bezprozvanny, I., 2005. Disturbed Ca2+ signaling and apoptosis of medium spiny neurons in Huntington's disease. Proc. Natl. Acad. Sci. https://doi.org/10.1073/pnas.0409402102

Tang, T.S., Tu, H., Chan, E.Y.W., Maximov, A., Wang, Z., Wellington, C.L., Hayden, M.R., Bezprozvanny, I., 2003. Huntingtin and huntingtin-associated protein 1 influence neuronal calcium signaling mediated by inositol-(1,4,5) triphosphate receptor type 1. Neuron. https://doi.org/10.1016/S0896-6273(03)00366-0

Tellez-Nagel, I., Johnson, A.B., Terry, R.D., 1974. Studies on brain biopsies of patients with huntington's chorea. J. Neuropathol. Exp. Neurol. https://doi.org/10.1097/00005072-197404000-00008

Thompson, J.C., Harris, J., Sollom, A.C., Stopford, C.L., Howard, E., Snowden, J.S., Craufurd, D., 2012. Longitudinal evaluation of neuropsychiatric symptoms in Huntington's disease. J. Neuropsychiatry Clin. Neurosci. https://doi.org/10.1176/appi.neuropsych.11030057

Thompson, L.M., Aiken, C.T., Kaltenbach, L.S., Agrawal, N., Illes, K., Khoshnan, A., Martinez-Vincente, M., Arrasate, M., O'Rourke, J.G., Khashwji, H., Lukacsovich, T., Zhu, Y.Z., Lau, A.L., Massey, A., Hayden,

M.R., Zeitlin, S.O., Finkbeiner, S., Green, K.N., LaFerla, F.M., Bates, G., Huang, L., Patterson, P.H., Lo, D.C., Cuervo, A.M., Marsh, J.L., Steffan, J.S., 2009. IKK phosphorylates Huntingtin and targets it for degradation by the proteasome and lysosome. J. Cell Biol. https://doi.org/10.1083/jcb.200909067

THOMPSON, P.D., BERARDELLI, A., ROTHWELL, J.C., DAY, B.L., DICK, J.P.R., BENECKE, R., MARSDEN, C.D., 1988. THE COEXISTENCE OF BRADYKINESIA AND CHOREA IN HUNTINGTON'S DISEASE AND ITS IMPLICATIONS FOR THEORIES OF BASAL GANGLIA CONTROL OF MOVEMENT. Brain 111, 223–244. https://doi.org/10.1093/brain/111.2.223

Thrower, J.S., Hoffman, L., Rechsteiner, M., Pickart, C.M., 2000. Recognition of the polyubiquitin proteolytic signal. EMBO J. https://doi.org/10.1093/emboj/19.1.94

Tong, K.I., Katoh, Y., Kusunoki, H., Itoh, K., Tanaka, T., Yamamoto, M., 2006. Keap1 recruits Neh2 through binding to ETGE and DLG motifs: characterization of the two-site molecular recognition model. Mol. Cell. Biol. 26, 2887–900. https://doi.org/10.1128/MCB.26.8.2887-2900.2006

Tong, K.I., Kobayashi, A., Katsuoka, F., Yamamoto, M., 2006. Two-site substrate recognition model for the Keap1-Nrf2 system: A hinge and latch mechanism, in: Biological Chemistry. pp. 1311–1320. https://doi.org/10.1515/BC.2006.164

Trettel, F., 2000. Dominant phenotypes produced by the HD mutation in STHdhQ111 striatal cells. Hum. Mol. Genet. 9, 2799–2809. https://doi.org/10.1093/hmg/9.19.2799

Trinh, A.T., Kim, S.H., Chang, H.Y., Mastrocola, A.S., Tibbetts, R.S., 2013. Cyclin-dependent kinase 1-dependent phosphorylation of cAMP response element-binding protein decreases chromatin occupancy. J. Biol. Chem. https://doi.org/10.1074/jbc.M113.464057

Trushina, E., Dyer, R.B., Badger, J.D., Ure, D., Eide, L., Tran, D.D., Vrieze, B.T., Legendre-Guillemin, V., McPherson, P.S., Mandavilli, B.S., Van

Houten, B., Zeitlin, S., McNiven, M., Aebersold, R., Hayden, M., Parisi, J.E., Seeberg, E., Dragatsis, I., Doyle, K., Bender, A., Chacko, C., McMurray, C.T., 2004. Mutant Huntingtin Impairs Axonal Trafficking in Mammalian Neurons In Vivo and In Vitro. Mol. Cell. Biol. https://doi.org/10.1128/mcb.24.18.8195-8209.2004

Tsakiri, N., Kimber, I., Rothwell, N.J., Pinteaux, E., 2008. Interleukin-1-induced interleukin-6 synthesis is mediated by the neutral sphingomyelinase/Src kinase pathway in neurones. Br. J. Pharmacol. 153, 775–783. https://doi.org/10.1038/sj.bjp.0707610

Tsunemi, T., Ashe, T.D., Morrison, B.E., Soriano, K.R., Au, J., Roque, R.A.V., Lazarowski, E.R., Damian, V.A., Masliah, E., La Spada, A.R., 2012. PGC-1a rescues Huntington's disease proteotoxicity by preventing oxidative stress and promoting TFEB function. Sci. Transl. Med. https://doi.org/10.1126/scitranslmed.3003799

Tsygankov, A.Y., Shore, S.K., 2004. Src: regulation, role in human carcinogenesis and pharmacological inhibitors. Curr. Pharm. Des. 10, 1745–1756. https://doi.org/10.2174/1381612043384457

Turro, E., Greene, D., Wijgaerts, A., Thys, C., Lentaigne, C., Bariana, T.K., Westbury, S.K., Kelly, A.M., Selleslag, D., Stephens, J.C., Papadia, S., Simeoni, I., Penkett, C.J., Ashford, S., Attwood, A., Austin, S., Bakchoul, T., Collins, P., Deevi, S.V. V., Favier, R., Kostadima, M., Lambert, M.P., Mathias, M., Millar, C.M., Peerlinck, K., Perry, D.J., Schulman, S., Whitehorn, D., Wittevrongel, C., De Maeyer, M., Rendon, A., Gomez, K., Erber, W.N., Mumford, A.D., Nurden, P., Stirrups, K., Bradley, J.R., Lucy Raymond, F., Laffan, M.A., Van Geet, C., Richardson, S., Freson, K., Ouwehand, W.H., 2016. A dominant gain-of-function mutation in universal tyrosine kinase SRC causes thrombocytopenia, myelofibrosis, bleeding, and bone pathologies. Sci. Transl. Med. 8, 328ra30-328ra30. https://doi.org/10.1126/scitranslmed.aad7666

Twig, G., Shirihai, O.S., 2011. The interplay between mitochondrial dynamics and mitophagy. Antioxidants Redox Signal.

https://doi.org/10.1089/ars.2010.3779

Tyszkiewicz, J.P., Yan, Z., 2005. β-Amyloid Peptides Impair PKC-Dependent Functions of Metabotropic Glutamate Receptors in Prefrontal Cortical Neurons. J. Neurophysiol. 93, 3102–3111. https://doi.org/10.1152/jn.00939.2004

Uruno, A., Furusawa, Y., Yagishita, Y., Fukutomi, T., Muramatsu, H., Negishi, T., Sugawara, A., Kensler, T.W., Yamamoto, M., 2013. The Keap1-Nrf2 System Prevents Onset of Diabetes Mellitus. Mol. Cell. Biol. 33, 2996–3010. https://doi.org/10.1128/MCB.00225-13

Valencia, A., Sapp, E., Kimm, J.S., McClory, H., Reeves, P.B., Alexander, J., Ansong, K.A., Masso, N., Frosch, M.P., Kegel, K.B., Li, X., DiFiglia, M., 2013. Elevated NADPH oxidase activity contributes to oxidative stress and cell death in Huntington's disease. Hum. Mol. Genet. https://doi.org/10.1093/hmg/dds516

van der Burg, J.M., Björkqvist, M., Brundin, P., 2009. Beyond the brain: widespread pathology in Huntington's disease. Lancet Neurol. 8, 765–774. https://doi.org/10.1016/S1474-4422(09)70178-4

Van Raamsdonk, J.M., Gibson, W.T., Pearson, J., Murphy, Z., Lu, G., Leavitt, B.R., Hayden, M.R., 2006. Body weight is modulated by levels of full-length Huntingtin. Hum. Mol. Genet. https://doi.org/10.1093/hmg/ddl072

Van Raamsdonk, J.M., Pearson, J., Bailey, C.D.C., Rogers, D.A., Johnson, G.V.W., Hayden, M.R., Leavitt, B.R., 2005a. Cystamine treatment is neuroprotective in the YAC128 mouse model of Huntington disease. J. Neurochem. https://doi.org/10.1111/j.1471-4159.2005.03357.x

Van Raamsdonk, J.M., Pearson, J., Slow, E.J., Hossain, S.M., Leavitt, B.R., Hayden, M.R., 2005b. Cognitive dysfunction precedes neuropathology and motor abnormalities in the YAC128 mouse model of Huntington's disease. J. Neurosci. https://doi.org/10.1523/JNEUROSCI.0590-05.2005

Venkatraman, P., Wetzel, R., Tanaka, M., Nukina, N., Goldberg, A.L., 2004.

Eukaryotic proteasomes cannot digest polyglutamine sequences and release them during degradation of polyglutamine-containing proteins. Mol. Cell. https://doi.org/10.1016/S1097-2765(04)00151-0

Verfaillie, T., Rubio, N., Garg, A.D., Bultynck, G., Rizzuto, R., Decuypere, J.P., Piette, J., Linehan, C., Gupta, S., Samali, A., Agostinis, P., 2012. PERK is required at the ER-mitochondrial contact sites to convey apoptosis after ROS-based ER stress. Cell Death Differ. https://doi.org/10.1038/cdd.2012.74

Vonsattel, J.P., Myers, R.H., Stevens, T.J., Ferrante, R.J., Bird, E.D., Richardson, E.P., 1985. Neuropathological classification of huntington's disease. J. Neuropathol. Exp. Neurol. https://doi.org/10.1097/00005072-198511000-00003

Vonsattel, J.P.G., 2008. Huntington disease models and human neuropathology: Similarities and differences. Acta Neuropathol. https://doi.org/10.1007/s00401-007-0306-6

Vonsattel, J.P.G., DiFiglia, M., 1998. Huntington disease. J. Neuropathol. Exp. Neurol. https://doi.org/10.1097/00005072-199805000-00001

Vonsattel, J.P.G., Keller, C., Cortes Ramirez, E.P., 2011. Huntington's disease - neuropathology, Handbook of Clinical Neurology. https://doi.org/10.1016/B978-0-444-52014-2.00004-5

Wang, H., Liu, K., Geng, M., Gao, P., Wu, X., Hai, Y., Li, Y., Li, Y., Luo, L., Hayes, J.D., Wang, X.J., Tang, X., 2013. RXRα inhibits the NRF2-ARE signaling pathway through a direct interaction with the Neh7 domain of NRF2. Cancer Res. 73, 3097–3108. https://doi.org/10.1158/0008-5472.CAN-12-3386

Wang, H.Y., Pisano, M.R., Friedman, E., 1994. Attenuated protein kinase C activity and translocation in Alzheimer's disease brain. Neurobiol Aging 15, 293–298.

Wang, J., Wang, C.E., Orr, A., Tydlacka, S., Li, S.H., Li, X.J., 2008. Impaired

ubiquitin-proteasome system activity in the synapses of Huntington's disease mice. J. Cell Biol. https://doi.org/10.1083/jcb.200709080

Wang, J.Q., Chen, Q., Wang, X., Wang, Q.C., Wang, Y., Cheng, H.P., Guo, C., Sun, Q., Chen, Q., Tang, T.S., 2013. Dysregulation of mitochondrial calcium signaling and superoxide flashes cause mitochondrial genomic DNA damage in Huntington disease. J. Biol. Chem. 288, 3070–3084. https://doi.org/10.1074/jbc.M112.407726

Wang, J.Y., Shum, A.Y.C., Ho, Y.J., Wang, J.Y., 2003. Oxidative neurotoxicity in rat cerebral cortex neurons: Synergistic effects of H2O2 and NO on apoptosis involving activation of p38 mitogen-activated protein kinase and caspase-3. J. Neurosci. Res. https://doi.org/10.1002/jnr.10597

Wang, K., Hackett, J.T., Cox, M.E., Hoek, M. Van, Lindstrom, J.M., Parsons, S.J., Van Hoek, M., 2004. Regulation of the neuronal nicotinic acetylcholine receptor by SRC family tyrosine kinases. J. Biol. Chem. 279, 8779–86. https://doi.org/10.1074/jbc.M309652200

Wang, X., Sirianni, A., Pei, Z., Cormier, K., Smith, K., Jiang, J., Zhou, S., Wang, H., Zhao, R., Yano, H., Kim, J.E., Li, W., Kristal, B.S., Ferrante, R.J., Friedlander, R.M., 2011. The melatonin MT1 receptor axis modulates mutant Huntingtin-Mediated Toxicity. J. Neurosci. https://doi.org/10.1523/JNEUROSCI.3059-11.2011

Wang, Y., Botvinick, E.L., Zhao, Y., Berns, M.W., Usami, S., Tsien, R.Y., Chien, S., 2005. Visualizing the mechanical activation of Src. Nature 434, 1040–1045. https://doi.org/10.1038/nature03469

Watai, Y., Kobayashi, A., Nagase, H., Mizukami, M., Mcevoy, J., Singer, J.D., Itoh, K., Yamamoto, M., 2007. Subcellular localization and cytoplasmic complex status of endogenous Keap1. Genes to Cells 12, 1163–1178. https://doi.org/10.1111/j.1365-2443.2007.01118.x

Waters, S., Ponten, H., Klamer, D., Waters, N., 2014. Co-administration of the dopaminergic stabilizer pridopidine and tetrabenazine in rats. J. Huntingtons. Dis. https://doi.org/10.3233/JHD-140108

Watson, L.J., Alexander, K.M., Mohan, M.L., Bowman, A.L., Mangmool, S., Xiao, K., Naga Prasad, S. V., Rockman, H.A., 2016. Phosphorylation of Src by phosphoinositide 3-kinase regulates beta-adrenergic receptor-mediated EGFR transactivation. Cell. Signal. https://doi.org/10.1016/j.cellsig.2016.05.006

Weaver, J.R., Taylor-Fishwick, D.A., 2013. Regulation of NOX-1 expression in beta cells: A positive feedback loop involving the Src-kinase signaling pathway. Mol. Cell. Endocrinol. 369, 35–41. https://doi.org/10.1016/j.mce.2013.01.011

Weil, R., Laplantine, E., Curic, S., Génin, P., 2018. Role of optineurin in the mitochondrial dysfunction: Potential implications in neurodegenerative diseases and cancer. Front. Immunol. https://doi.org/10.3389/fimmu.2018.01243

Wen, A.Y., Sakamoto, K.M., Miller, L.S., 2010. The Role of the Transcription Factor CREB in Immune Function. J. Immunol. https://doi.org/10.4049/jimmunol.1001829

Weydt, P., Pineda, V. V., Torrence, A.E., Libby, R.T., Satterfield, T.F., Lazarowski, E.R.R., Gilbert, M.L., Morton, G.J., Bammler, T.K., Strand, A.D., Cui, L., Beyer, R.P., Easley, C.N., Smith, A.C., Krainc, D., Luquet, S., Sweet, I.R.R., Schwartz, M.W., La Spada, A.R., 2006. Thermoregulatory and metabolic defects in Huntington's disease transgenic mice implicate PGC-1α in Huntington's disease neurodegeneration. Cell Metab. https://doi.org/10.1016/j.cmet.2006.10.004

Weydt, P., Soyal, S.M., Landwehrmeyer, G.B., Patsch, W., 2014. A single nucleotide polymorphism in the coding region of PGC-1α is a male-specific modifier of Huntington disease age-at-onset in a large european cohort. BMC Neurol. https://doi.org/10.1186/1471-2377-14-1

Wheeler, V.C., Auerbach, W., White, J.K., Srinidhi, J., Auerbach, A., Ryan, A., Duyao, M.P., Vrbanac, V., Weaver, M., Gusella, J.F., Joyner, A.L., MacDonald, M.E., 1999. Length-dependent gametic CAG repeat instability

in the Huntington's disease knock-in mouse. Hum. Mol. Genet. https://doi.org/10.1093/hmg/8.1.115

Wild, P., McEwan, D.G., Dikic, I., 2014. The LC3 interactome at a glance. J. Cell Sci. https://doi.org/10.1242/jcs.140426

Wold, M.S., Lim, J., Lachance, V., Deng, Z., Yue, Z., 2016. ULK1-mediated phosphorylation of ATG14 promotes autophagy and is impaired in Huntington's disease models. Mol. Neurodegener. https://doi.org/10.1186/s13024-016-0141-0

Wong, Y.C., Holzbaur, E.L.F., 2014a. Optineurin is an autophagy receptor for damaged mitochondria in parkin-mediated mitophagy that is disrupted by an ALS-linked mutation. Proc. Natl. Acad. Sci. U. S. A. https://doi.org/10.1073/pnas.1405752111

Wong, Y.C., Holzbaur, E.L.F., 2014b. The regulation of autophagosome dynamics by huntingtin and HAP1 is disrupted by expression of mutant huntingtin, leading to defective cargo degradation. J. Neurosci. https://doi.org/10.1523/JNEUROSCI.1870-13.2014

Wyttenbach, A., Sauvageot, O., Carmichael, J., Diaz-Latoud, C., Arrigo, A.P., Rubinsztein, D.C., 2002. Heat shock protein 27 prevents cellular polyglutamine toxicity and suppresses the increase of reactive oxygen species caused by huntingtin. Hum. Mol. Genet. https://doi.org/10.1093/hmg/11.9.1137

Xu, P., Duong, D.M., Seyfried, N.T., Cheng, D., Xie, Y., Robert, J., Rush, J., Hochstrasser, M., Finley, D., Peng, J., 2009. Quantitative Proteomics Reveals the Function of Unconventional Ubiquitin Chains in Proteasomal Degradation. Cell. https://doi.org/10.1016/j.cell.2009.01.041

Yamazaki, H., Tanji, K., Wakabayashi, K., Matsuura, S., Itoh, K., 2015. Role of the Keap1/Nrf2 pathway in neurodegenerative diseases. Pathol. Int. 65, 210–219. https://doi.org/10.1111/pin.12261

Yang, C.-M., Lin, C.-C., Lee, I.-T., Hsu, C.-K., Tai, Y.-C., Hsieh, H.-L., Chi, P.-

L., Hsiao, L.-D., 2015. c-Src-dependent transactivation of EGFR mediates CORM-2-induced HO-1 expression in human tracheal smooth muscle cells. J. Cell. Physiol. 230, 2351–2361. https://doi.org/10.1002/jcp.24912

Yang, J.L., Weissman, L., Bohr, V.A., Mattson, M.P., 2008. Mitochondrial DNA damage and repair in neurodegenerative disorders. DNA Repair (Amst). https://doi.org/10.1016/j.dnarep.2008.03.012

Yano, H., Baranov, S. V., Baranova, O. V., Kim, J., Pan, Y., Yablonska, S., Carlisle, D.L., Ferrante, R.J., Kim, A.H., Friedlander, R.M., 2014. Inhibition of mitochondrial protein import by mutant huntingtin. Nat. Neurosci. 17, 822–831. https://doi.org/10.1038/nn.3721

Yeun, S.C., Mao, Z., Johnson, G.V.W., Lesort, M., 2005. Increased glutathione levels in cortical and striatal mitochondria of the R6/2 Huntington's disease mouse model. Neurosci. Lett. https://doi.org/10.1016/j.neulet.2005.05.065

Young, A.B., Greenamyre, J.T., Hollingsworth, Z., Albin, R., D'Amato, C., Shoulson, I., Penney, J.B., 1988. NMDA receptor losses in putamen from patients with Huntington's disease. Science (80-.). https://doi.org/10.1126/science.2841762

Young, J.C., Hoogenraad, N.J., Hartl, F.U., 2003. Molecular chaperones Hsp90 and Hsp70 deliver preproteins to the mitochondrial import receptor Tom70. Cell. https://doi.org/10.1016/S0092-8674(02)01250-3

Yu, S., Melia, T.J., 2017. The coordination of membrane fission and fusion at the end of autophagosome maturation. Curr. Opin. Cell Biol. https://doi.org/10.1016/j.ceb.2017.03.010

Yuan, Y., Zheng, Y., Zhang, X., Chen, Y., Wu, X., Wu, J., Shen, Z., Jiang, L., Wang, L., Yang, W., Luo, J., Qin, Z., Hu, W., Chen, Z., 2017. BNIP3L/NIX-mediated mitophagy protects against ischemic brain injury independent of PARK2. Autophagy. https://doi.org/10.1080/15548627.2017.1357792

Zachari, M., Ganley, I.G., 2017. The mammalian ULK1 complex and autophagy initiation. Essays Biochem. https://doi.org/10.1042/EBC20170021

Zeron, M.M., Chen, N., Moshaver, A., Ting-Chun Lee, A., Wellington, C.L., Hayden, M.R., Raymond, L.A., 2001. Mutant huntingtin enhances excitotoxic cell death. Mol. Cell. Neurosci. https://doi.org/10.1006/mcne.2000.0909

Zeron, M.M., Hansson, O., Chen, N., Wellington, C.L., Leavitt, B.R., Brundin, P., Hayden, M.R., Raymond, L.A., 2002. Increased sensitivity to N-methyl-D-aspartate receptor-mediated excitotoxicity in a mouse model of Huntington's disease. Neuron. https://doi.org/10.1016/S0896-6273(02)00615-3

Zhang, F., Zhang, Q., Tengholm, A., Sjöholm, A., 2006. Involvement of JAK2 and Src kinase tyrosine phosphorylation in human growth hormone-stimulated increases in cytosolic free Ca2+ and insulin secretion. Am. J. Physiol. Cell Physiol. 291, C466–C475. https://doi.org/10.1152/ajpcell.00418.2005

Zhang, Y., Li, P., Feng, J., Wu, M., 2016. Dysfunction of NMDA receptors in Alzheimer's disease. Neurol. Sci. 1–9. https://doi.org/10.1007/s10072-016-2546-5

Zhu, M., Fahl, W.E., 2001. Functional characterization of transcription regulators that interact with the electrophile response element. Biochem. Biophys. Res. Commun. 289, 212–9. https://doi.org/10.1006/bbrc.2001.5944

Zipper, L.M., Timothy Mulcahy, R., 2002. The Keap1 BTB/POZ dimerization function is required to sequester Nrf2 in cytoplasm. J. Biol. Chem. 277, 36544–36552. https://doi.org/10.1074/jbc.M206530200

Zuccato, C., Ciammola, A., Rigamonti, D., Leavitt, B.R., Goffredo, D., Conti, L., MacDonald, M.E., Friedlander, R.M., Silani, V., Hayden, M.R., Timmusk, T., Sipione, S., Cattaneo, E., 2001. Loss of huntingtin-mediated BDNF gene transcription in Huntington's disease. Science (80-.). https://doi.org/10.1126/science.1059581